

DESIGNING A DEWATERING PLAN FOR THE RUASHI MINE IN THE DEMOCRATIC REPUBLIC OF CONGO

Lordrif Chironga

Submitted in fulfilment of the degree

MSc in Geohydrology

in the

Faculty of Natural and Agricultural Sciences

Institute for Groundwater Studies

at the

University of the Free State

Study Leader: Prof G Steyl

BLOEMFONTEIN

September 2013



Declaration

I declare that the dissertation hereby handed in for the qualification Master of Science Geohydrology at the University of the Free State, is my own independent work and that I have not previously submitted the same work for a qualification at/in another University/Faculty.

I also concede copyright of the dissertation to the University of the Free State.



Lordrif Chironga

Acknowledgements

I would like to dedicate the success of this dissertation to the co-operation of several individuals and institutions. Special thanks to the following for their leading role and data availability:

- Ruashi Mining Company for allowing me to carry out the study in the mine concession area.
- KLM Consulting Services for appointing me as Project Site Hydrogeologist.
- Prof G. Steyl for his study leadership role.
- Mr Lukas for software availability.

I would like to extend my sincere gratitude to field technical assistants at Ruashi Mine and all the authorities without whose assistance this study could have been impossible. I would like to give special mention to Samuel Kasongo for working with me long days in the field and Peter Shankaya's role in data availability.

I gratefully acknowledge the support given by Ruashi Mine Senior Management without which this project would have been impossible to undertake. For detailed progress of the work, I acknowledge the invaluable support that was generously provided by Ruashi Mine Technical Services Manager, Mr John van Davies, Mineral Resources Manager, Mr Stuart Allen and Environmental Manager, Mr Yvon Mbayo. I also extend my special thanks to Mr Blessing Mudzingwa for teaching this researcher to calibrate the transient groundwater flow model.

Lastly I thank my wife (Abigail), daughter (Sandra), brothers and sisters for their patience during the time I committed long hours to this study. To my late parents Fabian and Francisca Chironga for teaching me to walk, talk and providing a strong education background.

INDEMNIFICATION CLAUSE

The recommendations or suggestions in this dissertation are based on information obtained from various sources, and the personnel of the Faculty of Natural and Agricultural Sciences and the University of the Free State can therefore not be held responsible for the correctness thereof.

It must also be stressed that, although the personnel of the Faculty of Natural and Agricultural Sciences, University of the Free State, act in good faith, it cannot be guaranteed that the recommendations or suggestions or any part thereof, will give the best, the only or any solution for any or all the problems identified in the dissertation or that such problems are indeed the only issues at site.

The decisions taken to implement or accept any or all the above-mentioned recommendations or suggestions and the risk involved in taking such a decision, therefore rests with the reader.

Table of Contents

LIST OF ACRONYMS	xiv
List of quantities and units	xv
Chapter 1: Introduction	1
1.1 Background	1
1.2 Brief history of the mine	1
1.3 The problem	2
1.4 Regional stress pattern	4
1.5 Study objectives	6
1.6 Summary	7
Chapter 2: Literature Review	8
2.1 Introduction	8
2.2 Case studies on groundwater flow problems	8
2.2.1 West Driefontein Underground Gold Mine, South Africa	8
2.2.2 Spontaneous inundation at Kombat Mine, Namibia	9
2.2.3 The Mufulira Disaster-Mufulira Underground Copper Mine, Zambia	9
2.2.4 Dorog Coal Mine, Hungary	9
2.3 Management of groundwater flow in mines	9
2.4 Sources of groundwater in mines	10
2.5 Groundwater flow systems in mines	12
2.6 Hydrogeological settings in mines	13
2.7 Mine hydrogeological investigations	14
2.7.1 Field Investigation	15
2.7.2 Mine water budget	17
2.7.3 Mine inflow pattern and source	17
2.7.4 Piezometry	18
2.7.5 Modelling of mine groundwater flow	18
2.8 Summary	21
Chapter 3: Study Area Characteristics	22
3.1 Location	22
3.2 Mine layout	22
3.3 Climate	23
3.4 Topography	24
3.5 Drainage	25
3.6 Brief Geology	25

3.6.1 Regional geology	25
3.7 Summary.....	26
Chapter 4: Field Data Collection Methodology.....	27
4.1 Overview of investigation	27
4.2 Hydrocensus	27
4.3 Drilling.....	29
4.3.1 Air percussion drilling method	29
4.3.2 Mud rotary drilling method	30
4.3.3 Initial drilling	30
4.3.4 Main drilling phase	34
4.3.5 Borehole drilling summary	40
4.4 Aquifer hydraulic testing	42
4.4.1 Introduction	42
4.4.2 Objectives	42
4.4.3 Methodology	42
4.4.4 Constant rate test and recovery.....	44
4.4.5 Aquifer hydraulic testing summary.....	46
4.5 Hydrochemical sampling	47
4.5.1 Introduction	47
4.5.2 Field measurements.....	47
4.5.3 Water quality summary.....	49
4.6 Groundwater levels	49
4.7 Groundwater abstraction	54
4.8 Field data collection summary	56
Chapter 5: Conceptual Hydrogeological Model.....	57
5.1 General.....	57
5.2 Geology	57
5.2.1 Drilling findings.....	57
5.2.2 Weathering and fracturing	58
5.2.3 Stratigraphy.....	58
5.2.4 Structure	59
5.3 Groundwater occurrence.....	60
5.3.1 General	60
5.3.2 Water strikes	60
5.3.3 Blow yield	61
5.4 Aquifer hydraulic parameters.....	63
5.4.1 Estimating aquifer hydraulic parameters.....	63

5.4.2	Groundwater flow phases deduced from aquifer hydraulic testing	64
5.4.3	Derivative flow characterisation	66
5.4.4	Aquifer diffusibility	67
5.5	Hydrostratigraphy	68
5.5.1	Aquifers	69
5.5.2	Aquiclude	71
5.5.3	Aquitard	72
5.6	Water levels	76
5.6.1	Water levels and topography	76
5.6.2	Groundwater gradient	76
5.6.3	Hydraulic continuity	77
5.6.4	Groundwater flow pattern as deduced from water temperature	79
5.7	Aquifer Recharge	80
5.7.1	Chloride mass balance method	80
5.7.2	Recharge from Tailings Dam	82
5.8	Water Quality	83
5.8.1	Groundwater classification	83
5.8.2	Distribution of groundwater types and facies	85
5.8.3	Groundwater portability	85
5.8.4	Aquifer vulnerability	86
5.9	Summary	86
Chapter 6: Numerical Groundwater Flow Model		87
6.1	Introduction	87
6.2	Numerical modelling objectives	88
6.3	Mine infrastructure	89
6.3.1	Open Cast Pits	89
6.3.2	Tailing Storage Facility (TSF)	89
6.3.3	Waste rock dump	90
6.3.4	Storm water dam (SWD)	90
6.4	Numerical modelling approach	90
6.4.1	Software selection	90
6.4.2	Model area	91
6.4.3	Hydrogeological boundaries	91
6.4.4	Model layers	92
6.4.5	Model properties	92
6.4.6	Aquifer transmissivity and hydraulic conductivity distribution	94
6.5	Model calibration	95
6.5.1	Steady state calibration	95

6.5.2 Steady state calibration results.....	95
6.5.3 Transient calibration.....	98
6.6 Numerical groundwater flow scenarios.....	100
6.6.1 Scenario 1- Sixteen (16) boreholes each pumping 500 m ³ /d plus existing boreholes.....	100
6.6.2 Scenario 2 - Sixteen (16) boreholes each pumping 1 000 m ³ /d plus existing boreholes.....	104
6.6.3 Scenario 3- Sixteen (16) boreholes each pumping 2 000 m ³ /d plus existing boreholes.....	107
6.7 Simulated flow through the inner and outer model boundary.....	110
6.8 Simulated pit inflows.....	111
6.8.1 Modelling methodology and simulation of pit inflows.....	111
6.8.2 Drawdown changes over 11 years of mining.....	114
6.9 Summary.....	116
Chapter 7: Dewatering Strategy.....	117
7.1 Introduction.....	117
7.2 Possible dewatering methods.....	117
7.2.1 Grouting.....	118
7.2.2 Storm water control.....	118
7.2.3 Vertical pit perimeter boreholes.....	118
7.2.4 In-pit vertical boreholes.....	118
7.2.5 Horizontal drain holes.....	119
7.2.6 Pit sumps.....	119
7.3 Pit 1 Dewatering.....	120
7.3.1 Flow response to preliminary pumping.....	120
7.3.2 Pit 1 Dewatering strategy.....	121
7.4 Pit 2 and Pit 3 Dewatering.....	127
7.4.1 Flow response to preliminary pumping.....	127
7.4.2 Pit 2 and Pit 3 Dewatering strategy.....	130
7.4.3 Pit sumps and drainage canal.....	134
7.5 Summary.....	135
Chapter 8: Conclusions and Recommendations.....	136
8.1 Conclusions.....	136
8.1.1 Field programme.....	136
8.1.2 Conceptual hydrogeological model.....	136
8.1.3 Numerical groundwater flow model.....	137
8.1.4 Dewatering strategy.....	138
8.1.5 Gap analysis.....	139

8.2 Recommendations	139
8.3 Main contribution of the dissertation	140

List of Figures

Figure 1-1: Location of Ruashi Mine (Adapted from www.maps.google.com).....	2
Figure 1-2: Rotational slide failure of Pit 2 walls at the mine site.	3
Figure 1-3: Groundwater flow into Pit 1 sump at Ruashi Mine	3
Figure 1-4: Patterns of stress and strain in Southern Africa (Modified after University of Karlsruhe 2008)	5
Figure 1-5: Ruashi hydrogeological study flow chart	6
Figure 2-1: The hydrological cycle (modified after Williams 1986).....	11
Figure 2-2: Potential mine locations with respect to local, intermediate, and regional groundwater systems (Modified after Williams 1986)	12
Figure 2-3: Geologic influence on groundwater flow systems (Modified after Williams 1986)	13
Figure 2-4: Surface water bodies as recharge boundaries (Modified after Williams 1986) ...	14
Figure 3-1: Location of Ruashi Mine showing the main pits and tailings infrastructure.....	22
Figure 3-2: Ruashi average monthly rainfall and temperature for year 2011.....	23
Figure 3-3: Ruashi Mine topography	24
Figure 4-1: Ruashi piezometric map.....	28
Figure 4-2: Air percussion drilling at dewatering borehole BH1-17 located in Pit 1. The foreground shows passage of groundwater through a V-notch.	30
Figure 4-3: Borehole BH3-39 lithological and construction log.....	33
Figure 4-4: Ruashi map showing positions of pumping borehole BH3-39 and monitoring boreholes.....	43
Figure 4-5: Step drawdown test plot of data recorded at borehole BH3-39	44
Figure 4-6: Constant rate test pumping drawdown at BH3-39	45
Figure 4-7: Recovery after constant rate pumping at BH3-39	45
Figure 4-8: Drawdown observed in monitoring boreholes during constant rate pumping of borehole BH3-39.....	46
Figure 4-9: Declining water levels in Pit 1.....	50
Figure 4-10 : Fluctuating groundwater levels in Pit 2	51
Figure 4-11 : Fluctuating groundwater levels in Pit 3	51
Figure 4-12: Fluctuating groundwater levels observed in boreholes located along TSF perimeter.....	52
Figure 4-13: Ruashi water levels with respect to pit floor levels-February 2012.....	53
Figure 4-14: Daily pumping volumes for Regideso Tank, Plant and Coffer dam delivery boreholes.....	55
Figure 5-1: Water strike frequency recorded during drilling campaign	61

Figure 5-2: Blow yield increase with depth recorded at BH2-4.....	62
Figure 5-3: Semi-log plot of drawdown (linear scale) against time (log scale) showing groundwater flow phases 1 to 5 described in the paragraphs below this caption.	65
Figure 5-5: Spread of cone of depression during test pumping at BH3-39.....	68
Figure 5-6: Pit 1 NE-SW cross section indicating the hydraulic conductivity zones.....	73
Figure 5-7: Pit 2 SW-NE cross section indicating the hydraulic conductivity zones.....	74
Figure 5-8: Pit 3 SW-NE cross section indicating the hydraulic conductivity zones.....	75
Figure 5-9: Ruashi water levels versus topography	76
Figure 5-10: Borehole BH3-39 temperature log	79
Figure 5-11: Canal from Tailings dam to Return Water Dam	83
Figure 5-12: Piper plot showing hydrochemical groups of boreholes at the mine.....	84
Figure 6-1: Ruashi finite element mesh showing refinement in the pits area.....	93
Figure 6-2: Ruashi initial heads map showing deep water level in the pits area due to pumping.....	94
Figure 6-3: Ruashi observed versus simulated hydraulic head.....	96
Figure 6-4: Groundwater flow in steady state showing water level flow from south western catchment and north eastern catchment towards the pits area.....	97
Figure 6-5: Ruashi modelled vs. observed head showing vertical and horizontal error bars	98
Figure 6-6: Observed vs. Simulated water level drawdown response at pumping well BH3-39	99
Figure 6-7: Observed vs. Simulated water level drawdown response at observation well MH3-6B located at 80 m south of pumping well BH3-39.....	99
Figure 6-8: Observed vs. Simulated water level drawdown response at observation well MH3-1 located at 40 m west of pumping well BH3-39	100
Figure 6-9: Simulated water level for Layers1 and 2 in Scenario 1 over operational time of 16 years.....	101
Figure 6-10: Simulated water level for Layer 1 in Scenario 2 over operational time of 16 years.....	104
Figure 6-11: Simulated water level for Layer1 in Scenario 3 over operational time of 16 years	107
Figure 6-12: Simulated flow into Ruashi open cast pit	113
Figure 6-13: Ruashi simulated versus observed water levels	115
Figure 7-1: Pit 1 declining groundwater levels	121
Figure 7-2: Positions of Pit 1 vertical boreholes.....	124
Figure 7-3: Black Ore Mineralised Zone showing weak and strong bands in Pit 1. The foreground shows ponding of groundwater adjacent to pit wall.....	126
Figure 7-4: Fluctuating groundwater levels in Pit 2	128

Figure 7-5: Fluctuating groundwater levels in Pit 3 cluster boreholes	128
Figure 7-6: Vertical boreholes plan for Pit 2.....	131
Figure 7-7: Vertical boreholes plan for Pit 3.....	132
Figure 7-8: Ruashi map showing positions of proposed dewatering boreholes.....	133
Figure 8-1: Flow chart illustrating important steps that can be followed in a mine hydrogeological investigation	141

List of Tables

Table 4-1 : Hydrogeological summary log for groundwater exploration borehole BH3-39	32
Table 4-2: Pumping and groundwater monitoring borehole information	34
Table 4-4: Groundwater monitoring boreholes	37
Table 4-5: Environmental monitoring boreholes	39
Table 4-6: Pictures of core recovered from geotechnical drilling	41
Table 4-7: Ruashi hydrochemistry (NB: Value of -1.00 denotes parameter was not analysed by laboratory)	48
Table 5-1: Ruashi stratigraphy	59
Table 5-2: Drawdown in boreholes along lithology strike	67
Table 5-3: Drawdown in boreholes across lithology strike	68
Table 5-4: Ruashi hydrostratigraphic units and hydraulic parameters.....	78
Table 6-1: Ruashi model layers	92
Table 6-2: Simulated groundwater flow through inner and outer model boundaries.....	110
Table 6-3: Simulated groundwater flow through model boundary conditions	110
Table 6-4: Predicted inflow into Ruashi open cast pits.....	112

List of Equations

Equation 2-1: Tracer velocity.....	16
Equation 2-2: Apparent interstitial tracer velocity.....	16
Equation 2-3: Residual drawdown.....	16
Equation 2-4: Cooper and Jacob (1946) aquifer transmissivity	17
Equation 2-5: Cooper and Jacob (1946) aquifer storativity(rearranged).....	17
Equation 2-6: Cooper and Jacob (1946) aquifer storativity(rearranged).....	17
Equation 2-7: Groundwater flux (Darcy velocity)	19
Equation 2-8: Groundwater flux (Darcy apparent velocity).....	19
Equation 2-9: Laplace steady state flux.....	19
Equation 2-10: Laplace steady state flux for homogenous aquifers	19
Equation 2-11: Laplace transient flux	19
Equation 2-12: Specific storage	19
Equation 2-13: Theis (1935) well equation	20
Equation 2-14: Theis (1935) well function	20
Equation 5-1: Cooper and Jacob (1946) aquifer transmissivity	63
Equation 5-2: Cooper and Jacob (1946) aquifer storativity	63
Equation 5-3: Aquifer Diffusibility.	67
Equation 5-4: Chloride mass balance.....	81
Equation 6-1: Groundwater flow	87
Equation 6-2: Groundwater flux (Laplace steady state)	87
Equation 6-3: Groundwater flux (Laplace transient state).....	87

LIST OF ACRONYMS

BOMZ	Black Ore Mineralised Zone
CMN	Calcareous Mineral Noirs
DRC	Democratic Republic of Congo
mamsl	meters above mean sea level
mbgl	meters below ground level
Ma	Million years
EC	Electrical Conductivity
FC	Flow Characteristics
TDS	Total Dissolved Solids
PHREEQC	PH reaction Equilibrium calculation
pH	Potential Hydrogen
RAT	Roches Argillaceous Talceus
RSC	Roches Siliceuses Cellulaires (<i>Siliceous Rocks with Cavities</i>)
RSF	Roches Siliceuses Feuilletées (<i>Foliated Siliceous Rocks</i>)
SDS	Shales Dolomitiques Superious Siliceuses (<i>Siliceous dolomitic Schist</i>)
TDS	Total Dissolved Solids
TSF	Tailings Storage Facility
WISH	Windows Interpretation System for Hydrogeologists

LIST OF QUANTITIES AND UNITS

Area (A)	meter squared (m^2)
Aquifer thickness (b)	m
Concentration	mg/l
Discharge (Q)	m^3/d
Drawdown (s)	m
Electrical conductivity (EC)	mS/m
Groundwater flux (q)	m^2/d
Groundwater velocity (v)	m/d
Hydraulic conductivity (K)	m/d
Transmissivity (T)	m^2/d

1 INTRODUCTION

1.1 Background

This researcher has been active in field data gathering during research and practical dewatering of open cast mines in Botswana, Democratic Republic of Congo (DRC) and South Africa. During the field experience, the researcher witnessed large volumes of water ingress into open cast pits and flooding at Ruashi Mine in DRC. The flooding of pits at Ruashi Mine was associated with collapse of pit walls. In order to dewater a mine, a groundwater study has to be carried out and develop a conceptual hydrogeological model that will guide in prediction of pit inflow volumes. This approach can be handy at Ruashi Mine which experiences pit inflows in excess of 15 000 cubic metres per day (m^3/d) during the rainy season.

A groundwater flow research was carried out at Ruashi Mine in DRC and the results are presented in this dissertation which comprises of 8 chapters:

Chapter 1 Introduction

Chapter 2 Literature review

Chapter 3 Study area characteristics

Chapter 4 Field data collection

Chapter 5 Conceptual hydrogeological model

Chapter 6 Numerical groundwater flow model

Chapter 7 Dewatering strategy

Chapter 8 Conclusions and recommendations

The dissertation ends in a list of references and appendices.

1.2 Brief history of the mine

Given the high-grade copper-cobalt mineralisation of the Central African Copperbelt and the scale of available ore bodies, the DRC and Zambia are fast becoming the global 'hotspots' for international mining investment and exploitation activities (Lydall and Auchterlonie 2011). Ruashi Mine (see location in Figure 1-1) is one the copper producers in the DRC. The mine, located in the Katanga Province, has a concession area of 15.7 square kilometres (km^2). Mining began in 2006 and is taking place in three pits from where copper ore is ferried to the

mine plant while cobalt ore is stockpiled for processing in Zambia. The three pits are expected to reach terminal depth of 180 metres below ground level (mbgl) by year 2024.



Figure 1-1: Location of Ruashi Mine (Adapted from www.maps.google.com)

1.3 The problem

Ever since the open pit mining began at Ruashi in 2006, the major operational problem has been the control of large inflows of groundwater into the pits. The rise in groundwater level contributes to increases in pore water pressure on pit walls which in some cases eventually collapse.

Figure 1-2 shows the collapse of pit walls at Ruashi Pit1. Figure 1-3 shows groundwater flow into Pit 1 sump at Ruashi Mine. The copper deposit occurs within the north east dipping layers of siliceous dolomitic schist in a local overturned syncline. Laterite deposits which cap the underlying formations at Ruashi form a variable weathered residual overburden (regolith) layer which varies in thickness. The collapse of pit walls is mostly associated with the weathered overburden and Laterite. The thickness of the regolith has an important effect on

the occurrence of groundwater in both the fractured zones and above basement formations (Acworth *et al.* 2001).

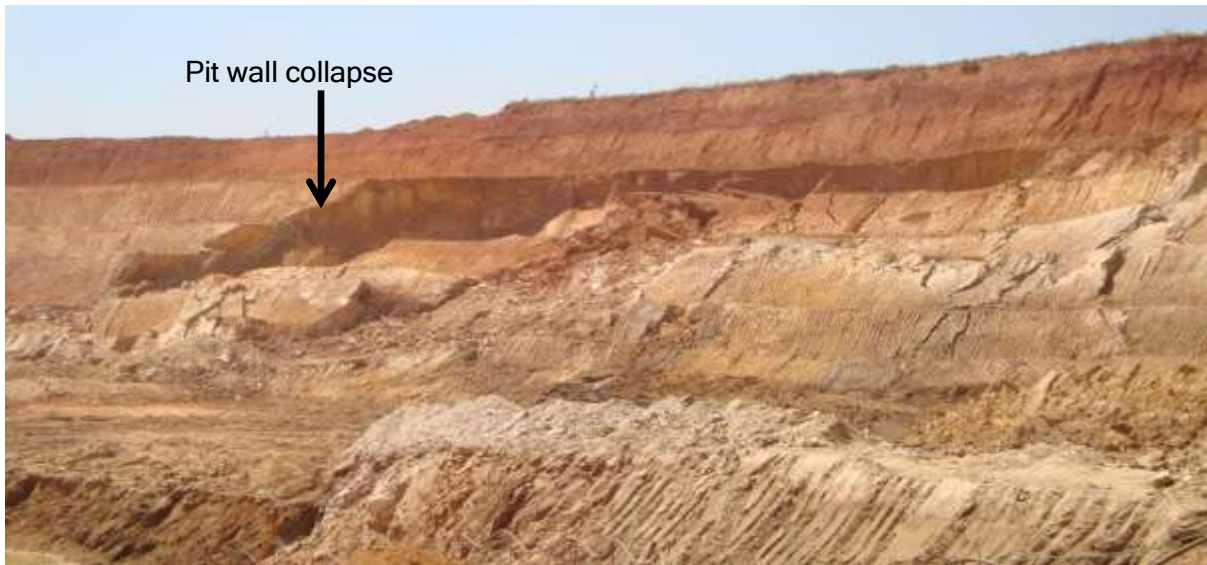


Figure 1-2: Rotational slide failure of Pit 2 walls at the mine site.



Figure 1-3: Groundwater flow into Pit 1 sump at Ruashi Mine

A number of mines in the region located along a “fold-and-thrust belt called the Lufilian Arc” like Mufulira in Zambia, Kinsenda and Tenge Fungurume Mine (TFM) in DRC experience the same problem of recurrent pit or shaft inflows and pit wall collapse. Groundwater occurrence in the region can be correlated to the regional stress pattern that created faulting and folding (Acworth *et al.* 2001) and this subject is discussed in the following section.

1.4 Regional stress pattern

The central African region had repeated episodes of compressive tectonism, involving at least four periods of wrench faulting separated by relaxation and dyke emplacement (Acworth *et al.* 2001). Most lineaments in the region are faults or tectonically related joints forming as planes of tectonic shearing and hence could be considered as compressive features at the time of inception. According to Bird *et al.* (2006), as expected in most stress domains, tension fractures must have formed contemporaneously with main planes of shearing parallel to the maximum principal stress. The stress map of Africa (Figure 1-4) shows tectonic regimes of normal faulting in the South Eastern DRC where Ruashi Mine is located.

According to Acworth *et al.* 2001, the stress orientation for the region is primarily in a NW-SE direction. The overturned syncline at Ruashi Mine has the same NW-SE strike orientation. Generally folding could have produced several sets of joints. Compression produce conjugate shear joints oblique to fold axis. Bending in folds produces tension joints which are parallel to the strike of the fold axis and dip joints parallel to the limb dip. Differences in temperatures at emplacement could have led to fracturing and creation of permeable zones which act as conduits for groundwater flow.

Groundwater flow in such deformed zones occurs both by matrix seepage and as fissure flow in discrete fracture channels, which could be part of an interconnected system. Open fractures below the water table surface have the capacity to store and channel water. According to Kellgren and Sander (2000), fractures that are under tensile and shear stresses are good targets for groundwater.

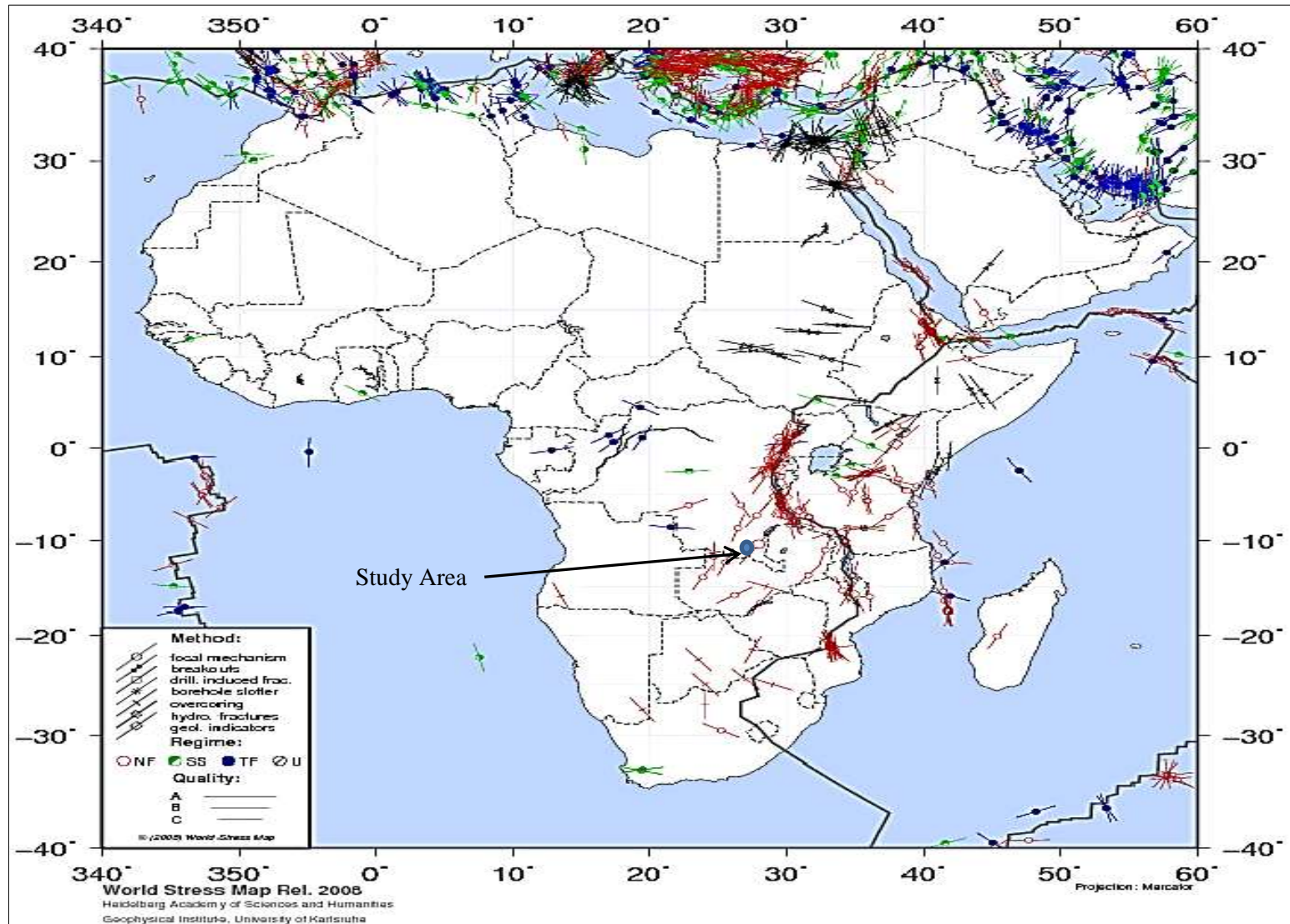


Figure 1-4: Patterns of stress and strain in Southern Africa (Modified after University of Karlsruhe 2008)

1.5 Study objectives

The main objective of the research was to construct a conceptual hydrogeological model that would act as framework for numerical groundwater flow modelling and feed into pit dewatering design for the mine site.

At the beginning of this research, the project was initially aimed at designing a dewatering plan for Ruashi Mine based on a thorough hydrogeological investigation. As the mine had very little data on the hydrogeology of the area, the focus was to characterise the rock units using drilling data, robust aquifer hydraulic testing and hydrochemical analysis. Drilling in the pits area and hydrochemistry work was thorough. However, due to limited budget, aquifer hydraulic testing was limited to one pumping well and packer testing was not performed. As a result the conceptual model was built using drilling data, preliminary pumping data, single well aquifer hydraulic testing data and information obtained from previous geotechnical and ore exploration drilling. It was therefore considered important to design the dewatering plan using numerical model results augmented by preliminary pumping observations.

The research method aimed at following the layout illustrated in the flow chart (Figure 1-5).

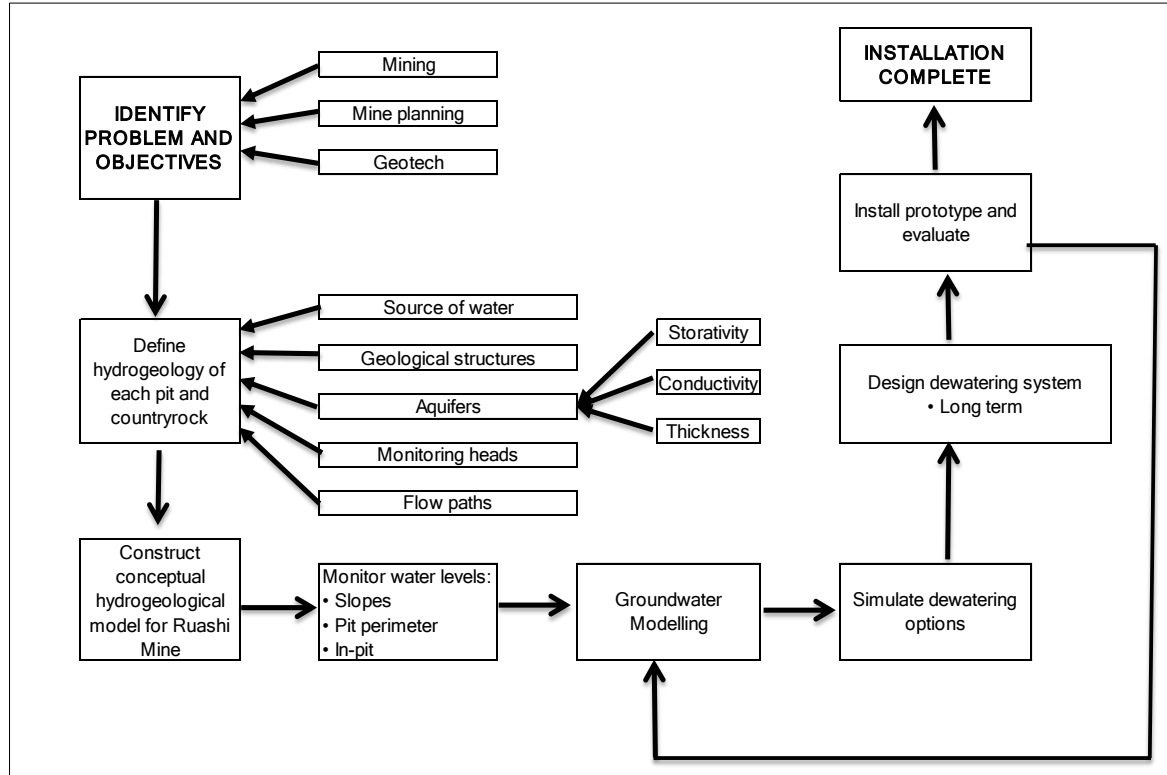


Figure 1-5: Ruashi hydrogeological study flow chart

The research focused on:

- The collection and collation of available regional geology information, climatological data (precipitation, temperatures, evapotranspiration, topography, surface water and soils) and mine plans.
- Hydrocensus to identify existing groundwater and surface water sample points at the mine. Water levels and pumping rates were recorded during the hydrocensus exercise.
- Hydrogeological logging of existing core in the Geotechnical Department.
- Drilling of groundwater monitoring and community supply wells that are also used for dewatering of the mine site.
- Drill cuttings recovered from wells were logged, as well as blow yields and water physicochemical parameters.
- Pumping test was carried out to obtain aquifer hydraulic parameters.

The information collected is used in characterising the aquifers and the influence of geological structures on groundwater occurrence at the Ruashi Mine. The results from the preceding section will be used to develop a greater understanding of the dominant hydrogeology factors at Ruashi Mine. This will afford a framework for numerical modelling, groundwater monitoring system and dewatering strategy for the mine site.

1.6 Summary

Chapter 1 gives the background information leading to the MSc research study. The main aim of the study was to investigate the hydrogeological properties of the rocks at Ruashi Mine and ultimately design a dewatering plan for the mine. The research carried out at Ruashi Mine focussed on contributing to ways of solving the problem of ingress of large volumes of groundwater into pits and the associated pit wall collapse.

Although regional hydrogeology information is important in solving groundwater flow in mines, site specific detailed studies provide a good platform for setting up dewatering strategies. The study site is located at Ruashi Mine which is situated about 6 km from the city of Lubumbashi, in the Katanga Province of the Democratic Republic of Congo.

The next chapter is literature review of typical mine settings, problems caused by groundwater flow into mines and mine hydrogeological investigation methods.

2 LITERATURE REVIEW

2.1 Introduction

This chapter reports relevant case histories of water ingress at international mine sites from both a surface water and groundwater perspective. A review on mine hydrogeological investigation methods is included. Solutions on the case histories on water ingress in mines and mine hydrogeological investigations will assist in the development of an effective dewatering strategy at the Ruashi Mine.

Groundwater flow problems have been witnessed in mines internationally. Application of the various methods of controlling groundwater flow into mine workings requires knowledge of the source and pathways of the portion of the aquifer that is hydraulically connected to the mine (Hargrave and Metesh 2003). According to Pardee and Schrader (1993), geoscientific methods use existing information, which can usually be obtained at low cost. Before going into the field, it is necessary to review the literature. The amount of geologic information about a particular area may vary greatly. Some mines with a great deal of development were never documented-neither in published materials nor in proprietary, unpublished materials. Mine maps are a great asset when they are available, but the level of detail varies greatly from mine to mine.

The information obtained at the mine guides in formulating a site-specific investigation method. The results of the field investigation determine the most appropriate and cost effective method of controlling groundwater flow into the mine. The control of groundwater flow into mine pits or shafts is often a long term and expensive task. This is due to the cost of pumping and increased equipment wear particularly if the mine workings become prone to acid mine drainage or silt formation.

2.2 Case studies on groundwater flow problems

2.2.1 West Driefontein Underground Gold Mine, South Africa

According to Singh and Vutukuri (2006), on 26 October 1968, the mine flooded following a water burst in one of the working tunnels. Although no lives were lost at that instance, almost four years before, in December 1962, much of the surface installation at West Driefontein disappeared into a huge sinkhole with the loss of 29 lives. The root cause of the accelerated mine subsidence was dewatering. Plugs were constructed to isolate the water inrush. Singh and Vutukuri (2006) highlighted that the incident at West Driefontein Mine highlighted that such large volumes of inflow can be curbed by a combination of sump pumping and drilling advanced boreholes.

2.2.2 Spontaneous inundation at Kombat Mine, Namibia

According to Singh and Vutukuri (2006) in the year 1988 there was major production interruption at Kombat Mine when a water bearing fissure was intersected during blasting. The rapid flow from the fissure to underground workings was estimated to be 5 000 m³/hr. The underground workings were flooded for 4 days. The problem was solved by drilling boreholes and grouting the water bearing fissure. The water level in the mine was lowered by active dewatering through vertical boreholes.

2.2.3 The Mufulira Disaster-Mufulira Underground Copper Mine, Zambia

According to MINESAFE Journal (1999) on 25 September 1970, eighty-nine (89) lives were lost as a result of 450 000 m³ of mud that slid into the underground workings. This is one of the mining worst disasters caused by mud and water ingress. Caving developed in some areas and produced a large sink hole on the surface under a tailings storage facility which caused an inrush of material at a point 500 metres below the surface. This caused all parts of the mine below the 434-580 m level to be flooded. The estimated inflow was 708 000 m³ of water. Much of the mine was recovered and restored to production.

2.2.4 Dorog Coal Mine, Hungary

According to Alliquander(2012) quoted through IMWA Paper (2012), Dorog Coal Mine as an example of mines that experienced problems of flooding. He stated that the mine is located in the karstic region in Hungary associated with frequent flooding of mines. Alliquander (2012) further stated that between 1980 and 2005 Dorog coal Mine experienced inflows in excess of 206 000 m³/d. The mine experienced water 18 inrush events between 1950 and 1970 leading to flooding leading to 40% lowering of the originally planned mining capacity. The mine had to stop ore extraction during episodes of flooding. The mine later installed an active dewatering system to lower the local water table.

2.3 Management of groundwater flow in mines

The presence of water in mining sites creates a range of operational and stability problems and requires drainage to be carried out from the mine workings in order to improve slope stability, avoid oxidation of metallic sulphides and reduce corrosion of mine plant and equipment (Rubio and Lorca 1993). Most mines in the world have coped by developing drainage and active dewatering systems.

Management of groundwater flow in mines is improving with new advanced investigation methods and better understanding of mine hydrogeology. According to Brawner (2006) the

amount of groundwater present, the rate at which it flows through the rock and the influence it will have on the economic development of the pit, depends on many factors. The cost of keeping dry working conditions should be compared to the cost of working a wet or dry mine.

A number of dewatering methods have been used in mines, and these include:

- a) Lowering the water table by means of a dewatering ring on the pit perimeter. This dewatering method was applied at Loy Yang Coal Open Pit, Victoria, Australia and Orapa Diamond Open Pit Mine in Botswana, Southern Africa (Bowell *et al.* 2002). In 2010, this researcher was actively involved in the installation of dewatering ring comprising of 16 vertical boreholes at AK6 Kimberlite Mine, Lethlakane, Botswana, Southern Africa. The diameter of the dewatering ring is about 500 m. Pumping of the boreholes induced a drawdown of 60 m after 30 days.
- b) Horizontal Drains is a technique which is commonly used to stabilise pit walls. According to Brawner (2006) holes 5 to 8 cm in diameter are drilled near the toe of the slope. These horizontal drain holes act as conduits through which passive flow will occur. Alternatively, adits can be constructed under the ore body and use the adit as drainage gallery from which water is pumped or drained by gravity.
- c) Grouting of highly permeable rock zones to reduce hydraulic conductivity and eliminate or reduce groundwater flow into an excavation. According to Daw and Pollard (2006) grouting methods include permeation grouting, hydrofracture grouting, squeeze grouting, void filling ground and combined techniques. In permeation grouting the grout material plugs the porous structure of the rock. Hydrofracture grouting involves deliberate overpressurisation to widen existing fractures or create new fissures. This creates access through low permeability ground to more permeable and treatable ground (Daw and Pollard 2006). Squeeze grouting is a technique by which grouts are used to apply high pressures to the ground to squeeze out excess pore water. Void filling involves filling cavities between the shaft or tunnel and the excavated profile. Cement grouting was successfully used by the cementation Company of America at four shafts in West Virginia (Daw and Pollard 2006).

2.4 Sources of groundwater in mines

In a mining environment, the sources of groundwater are:

- Precipitation.

- Surface water boundaries like water transmittal and storage bodies like rivers, lakes, dams and wetlands. Water percolates from these surface water bodies into the mine through transmissive weathered or fractured rocks.

In meteorology, groundwater is a component of the hydrologic cycle which is a consequence of the different forms of movement of water and changes of its physical state. The complete hydrologic cycle (see Figure 2-1) should be considered when carrying out a hydrogeological assessment in a mining environment.

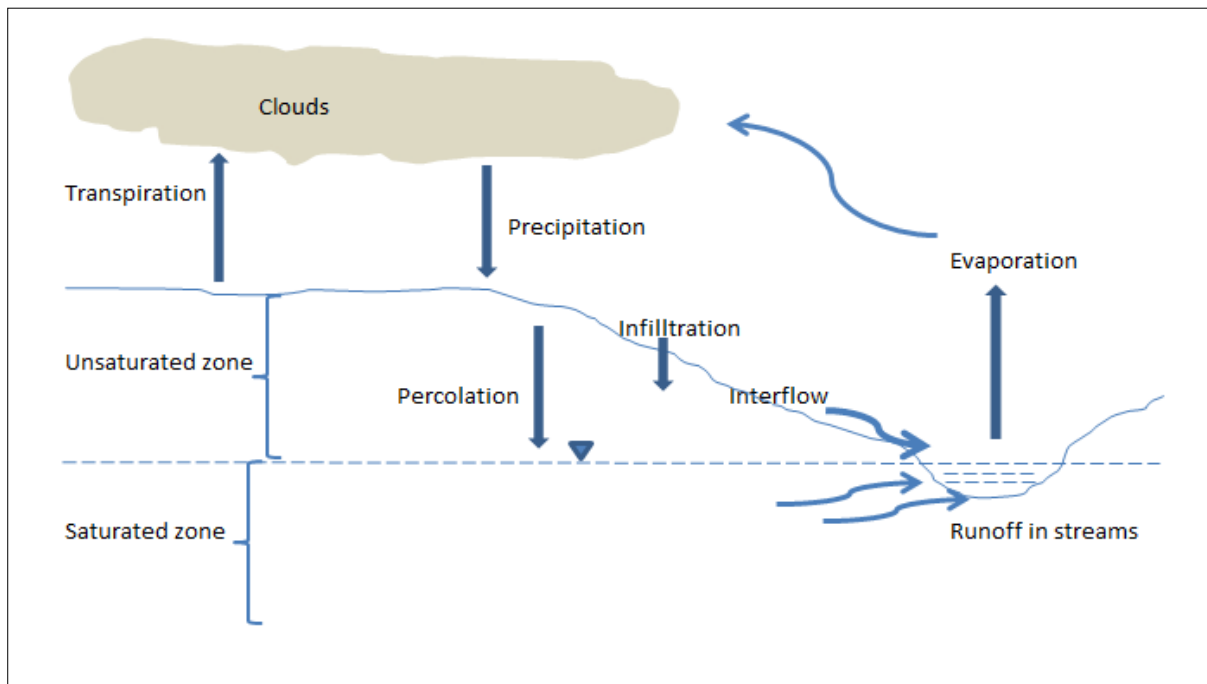


Figure 2-1: The hydrological cycle (modified after Williams 1986)

When precipitation reaches the ground, some of it infiltrates the unsaturated soil zone where it moves laterally as interflow to the surface water bodies. A high hydraulic head of the aquifers induces groundwater movement as baseflow to augment stream flow. According to Williams(1986) when the soil zone becomes saturated, excess precipitation moves as sheet flow towards low lying wetlands and surface water bodies. The transmissivity and storativity of the rock formations in the mine and evapotranspiration rates determine the proportion of precipitation that is fed to the groundwater system.

Other sources of groundwater flow into mines include:

- Abandoned mine workings
- Underground aquifers

2.5 Groundwater flow systems in mines

Groundwater flow is driven by the transmissivity of an aquifer system and the hydraulic gradient. According to Williams (1986), groundwater flows from a higher elevation and pressure head to a lower head. The recharge area, the unsaturated zone, saturated zone, interflow zone, baseflow zone and discharge area constitute a groundwater flow system.

A flow line defines the path that a water particle follows through the groundwater flow system. According to Williams (1986), groundwater flow systems are designated local, intermediate or regional (Figure 2-2). These systems should be well understood when assessing the impacts of mining in an environment. Williams (1986) defined these systems as follows:

- a) **Local System** - Recharge and discharge areas adjacent to each other at a topographic high and low respectively.
- b) **Intermediate System** - It has one or more topographic highs and lows located between its recharge and discharge areas that do not occupy the highest and lowest elevations in a basin.
- c) **Regional System** - Recharge and discharge areas occupying the highest and lowest elevations respectively in a basin.

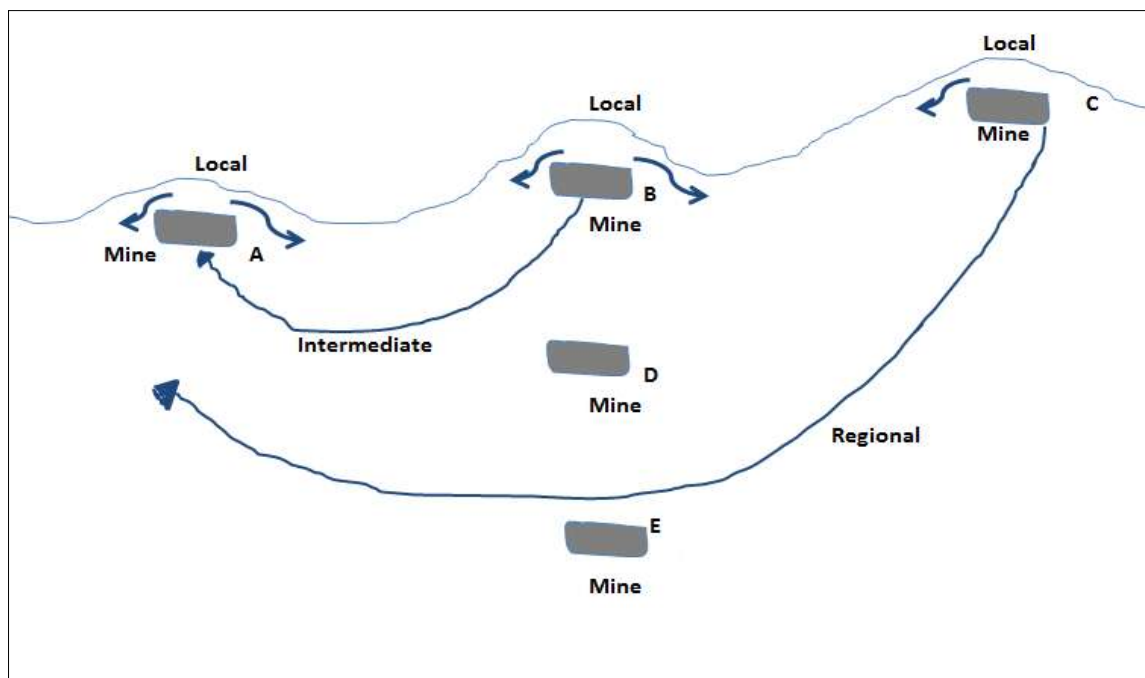


Figure 2-2: Potential mine locations with respect to local, intermediate, and regional groundwater systems (Modified after Williams 1986)

The concentration of dissolved constituents, pH, temperature and turbidity are to a large extent controlled by the pathways through which the water has passed. The mineralisation of groundwater is dependent on the time of contact of the water with soluble minerals in a porous medium and thus on velocity of movement and length of flow path (Williams 1986). Longer flow paths with low hydraulic conductivity produce high concentrations of dissolved solids in groundwater.

2.6 Hydrogeological settings in mines

Mines are located in aquifer settings which may be confined, semi-confined or unconfined. Different boundary conditions may exist and these can be either no flow or those boundaries which allow flow through them. Figure 2-3 illustrates the type of hydrogeological settings that can exist (Williams 1986). It is expected that hydrostratigraphic Unit 1 has high transmissivity and supports only local flow systems due to the influence of topography. Hydrostratigraphic Unit 2 and Unit 3 are expected to be fractured and weathered. As such, the two units support only shallow groundwater flow near the axis of the anticline. The influence of the fault is two-fold. The fault creates a high transmissive zone that transmits water from Unit 4 and discharges as a spring. The fault surface also creates a surface that blocks transverse flow.

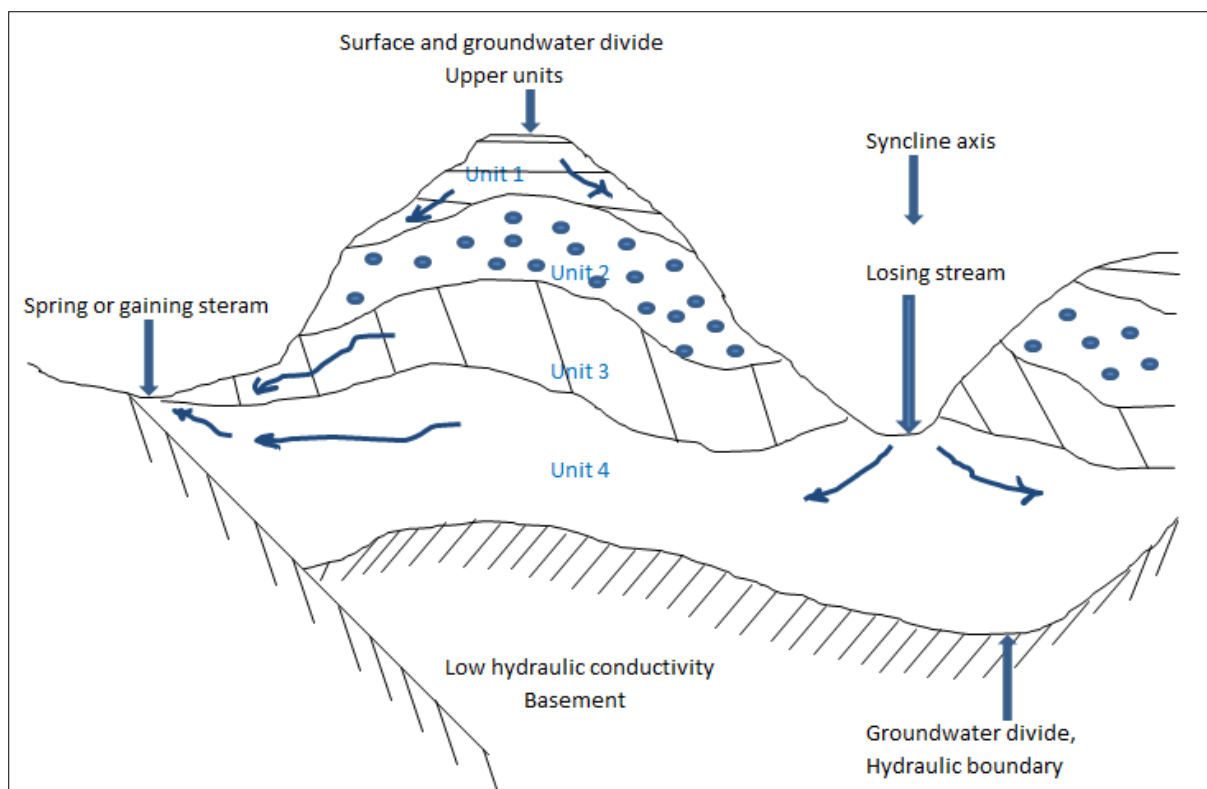


Figure 2-3: Geologic influence on groundwater flow systems (Modified after Williams 1986)

Brady and Brown (2002) stated that geological boundaries in groundwater flow regimes exist where there is a lateral discontinuity in hydraulic conductivity. A significant decrease in the hydraulic conductivity creates a barrier boundary across which little movement of groundwater can occur. Recharge boundaries are created where the aquifer unit intercepts surface water systems or geologic units with significantly higher storage capacity and hydraulic conductivity than the aquifer in question. Barrier boundaries can exist in various forms. According to Mandzic (1992) although faults in almost any rock can create transmissive zones, such zones can act as barriers blocking flow of groundwater.

Williams (1986) stated that recharge boundaries can occur when a hydrostratigraphic unit is in contact with a surface water body or a zone of high transmissivity. The recharge boundary can fully or partially penetrate the hydrostratigraphic unit as shown in Figure 2-4.

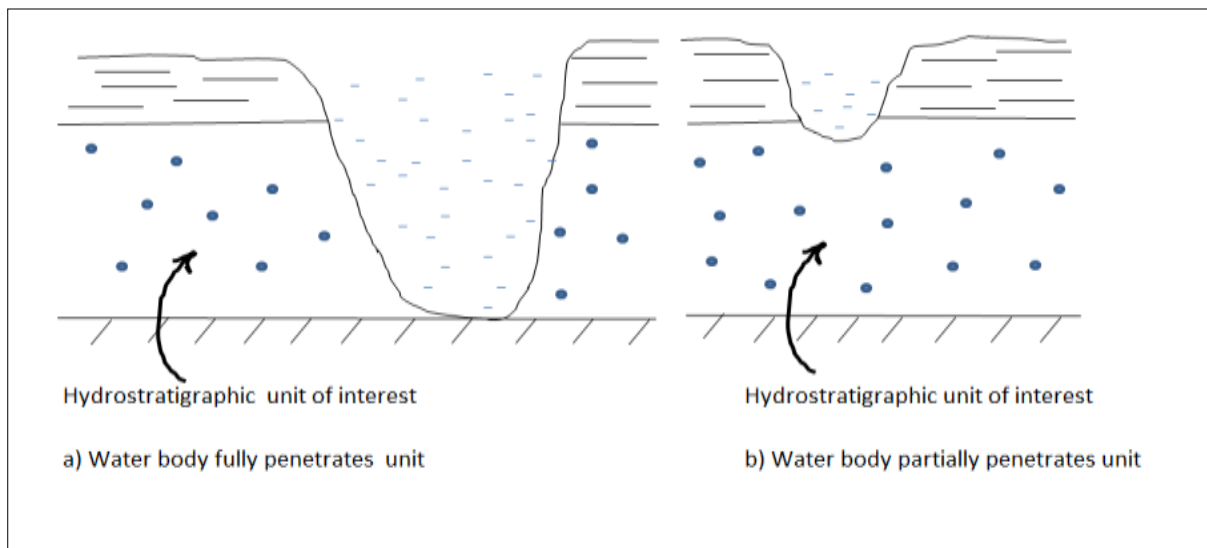


Figure 2-4: Surface water bodies as recharge boundaries (Modified after Williams 1986)

If mine drainage is higher than flow from aquifer storage, then the water levels in the mine will decline and mine flow will decline with time, the preferred condition for most mining activities. Conversely if the mine is in contact with constant head boundaries, the flow into the mine will increase with depth. Rubio and Lorca (1993) stated that an excellent example is Carbons de Berge underground coal mine in Spain, where coal seams are interbedded with Limestone and sandy carbonaceous Marl beds. The mine is in contact with Llogregat River which constantly supplies water to the aquifers.

2.7 Mine hydrogeological investigations

Mines around the world are located in unique hydrogeological settings. Therefore a carefully planned research plan should be site specific. Any research should preferably start with a

desk study complemented with a visit to the mine. Gap analysis should be done based on the results of the desk study and site visit. It is essential to understand the following parameters:

- Regional and local geological setting,
- hydrostratigraphy,
- geomorphologic setting
- regional and local surface hydrology,
- Longer term mine discharge records,
- Precipitation trend,
- Regional water table and local hydraulic heads,
- Regional groundwater flow direction,
- aquifer hydraulic parameters, and
- hydrochemistry.

2.7.1 Field investigation

The following parameters are critical in a hydrogeological investigation:

a) Regional and local geological setting

Conventional geophysical methods like electrical resistivity, electromagnetic, magnetic, gravity and seismic surveys can be used to delineate weathered zones and fracture systems. In addition to geophysical methods, structural geology mapping is essential to delineating fracture and fissure zones. By identifying the fracture zones, hydrogeological boundaries can be delineated. This enables the identification of preferred groundwater flow conduits.

b) Aquifer hydraulic parameters

Aquifer hydraulic parameters include transmissivity, hydraulic conductivity and storage coefficient. The most reliable and convenient method for estimating aquifer hydraulic parameters in mines is aquifer hydraulic test. Other methods include calculation from formulae, packer tests and tracer tests.

i) **Tracer tests:** Hydraulic conductivity can be estimated by measuring the time interval for a water tracer to travel between two test holes. For a tracer a dye, such as sodium fluorescein, or a salt, such as calcium chloride, is convenient, inexpensive, easy to detect, and safe (Hall 2005). As the tracer travels through the media with the average interstitial velocity(v_a), the velocity can be expressed as in Equation 2-1:

$$v_a = \frac{K}{\alpha} \times \frac{h}{L} \quad \text{(Equation 2-1)}$$

where, K = hydraulic conductivity, α = porosity, h = head difference between the point at which the tracer is added and at which the tracer is sampled, and L=distance between the point at which the tracer is added and at which it is sampled.

v_a can also be expressed by Equation 2-2:

$$v_a = L/t \quad \text{(Equation 2-2)}$$

where; t is the travel time interval of the tracer between the holes.

Despite the fact that tracer test method is practically simple, the limitations are as follows:

- The holes need to be close together; otherwise the tracer may entirely miss the observation hole.
- Multiple sampling holes may improve the reliability of the results, but these add to the cost of carrying out the test.
- The resultant hydraulic conductivity is not representative of all the aquifer units in a heterogeonous aquifer system.
- Chemical reactions occurring in the tracer are not factored in the resultant travel time.

ii) **Aquifer hydraulic tests:** Aquifer hydraulic tests can be carried out as slug tests, single drawdown-recovery tests or multiple drawdown-recovery tests. According to Theis (1935) the recovery method is the most reliable of obtaining representative values of transmissivity and hence hydraulic conductivity.

The recovery method was outlined by Theis (1935) as follows: After pumping a borehole at a constant rate, the borehole is shut. The rise of the water level is measured as residual drawdown “s”, (i.e. the difference between the original water level prior to pumping and the actual water level measured at a certain moment “t” since pumping stopped. Recovery is measured until the water level reaches the original water level.

Residual drawdown is given by Equation 2-3:

$$S = \frac{2.3Q}{4\pi T} \log \left(\frac{t+\Delta t}{\Delta t} \right) \quad \text{(Equation 2-3)}$$

Where, s =residual drawdown, $(h_0 - h_w)$, h_0 is the original piezometric head, h_w = piezometric head at a certain moment during recovery, Q = flow rate, T = transmissivity of the aquifer, and Δt is the time since the borehole was stopped.

The (Cooper and Jacob 1946) equation for calculating aquifer transmissivity is determined from the slope Δs and the discharge:

$$T = \frac{2.3Q}{4\pi\Delta s} \quad \text{(Equation 2-4)}$$

Where Δs = drawdown difference per log cycle.

When the multiple boreholes method is used, drawdown data are plotted as per standard drawdown plot. Using the Theis equation for unsteady state flow in a confined aquifer, the plot is then superimposed on a prepared plot of $W(u)$ vs. $(1/u)$ values (Krusemann and De Ridder 1994). The type curve is matched to the data plot while keeping both axes parallel. Values of $W(u)$, $1/u$, t , and s are read from match point on the plots and substituted into Equation 2-5:

$$T = \frac{Q}{4\pi s} W(u) \quad \text{(Equation 2-5)}$$

Where, T = transmissivity (L^2/T), Q = constant borehole discharge (L^3/T), s = drawdown in the observation well, and $W(u)$ = well function (dimensionless).

The storage coefficient can be obtained by substituting into Equation 2-6:

$$S = 4T (tr^2) u \quad \text{(Equation 2-6)}$$

Where, S = storage coefficient (dimensionless), t = time since pumping started, and r = distance from the pumping borehole to the observation borehole.

2.7.2 Mine water budget

The local water budget of an aquifer refers to the long term allocation of the available inflow water from precipitation, regional flow or recharge sources to components of natural or artificial discharge, for example, mine pumping (Driscoll 1995). Analysis of the local water budget helps in understanding the amount of water that is flowing into the aquifer system and the mine discharge.

2.7.3 Mine inflow pattern and source

Dissolved constituents in the water provide clues on its geologic history, the soil and rock masses through which it has passed, and its mode of origin within the hydrologic cycle.

Therefore, the source of water and its flow path can be traced using the water chemistry, provided the characters revealing this can be reliably discriminated (Freeze and Cherry 1979).

In a mine hydrochemical investigation, it is preferable to sample the entire mine in a limited period of time so as to provide a geochemical snapshot of the whole mining area. An informative hydrochemical analysis can be done by measuring dissolved solids, temperature, pH, conductivity, dissolved oxygen. Isotope and tracer analysis can augment the knowledge gained through the physicochemical parameter analysis. Radioactive isotopes, Tritium (^3H) and Carbon 14 (^{14}C) are used to determine the age of the water. Non-radioactive isotopes; Oxygen 18 (^{18}O) and Deuterium (^2H) serve mainly as indicators of groundwater source (Freeze and Cherry 1979).

2.7.4 Piezometry

The profile of the groundwater table should be understood. Water levels are measured through boreholes fitted with piezometric tubes and automatic water level recorders. The hydraulic gradient can be determined by manual or automatic water level measurements. It is important to relate water levels to the stratigraphy of the area as heterogeneous aquifers may give rise to an additional complexity of confined conditions.

2.7.5 Modelling of mine groundwater flow

When a reliable conceptual hydrogeological model has been built, groundwater flow can be simulated.

Aquifer hydraulic parameters, water budget and mine flows can be simulated using:

- a) Analytical methods
- b) Numerical methods

Although are based on simple groundwater flow formulae which are generally only suitable for simple flow problems involving homogenous hydraulic conductivity conditions. Complex conditions that characterise mine inflow problems cannot be described (Lloyd and Edwards 2000). Numerical methods can be used to simulate groundwater flow in three dimensions.

2.7.5.1 Analytical tools for estimating mine inflows

Groundwater flow can be approximated using a direct and simple application of Darcy's Law.

a) **Darcy's Law** (Equation 2-7) states that the flow rate (Q) is directly proportional to the cross-sectional area (A) through which flow is occurring, and directly proportional to the hydraulic gradient

$$Q = K \times A \times i \quad \text{(Equation 2-7)}$$

and apparent flow velocity (Equation 2-8),

$$V = \frac{Q}{A} = - (Ki) \quad \text{(Equation 2-8)}$$

where - (K*i*) indicates flow in the direction of reducing total head.

Darcy's Law is valid as long as the flow is laminar and can be used to estimate flow into a mine shaft or pit.

b) **Steady State Flow Equation:** The steady state flow describes a condition in which there is no change in head with time (i.e. $Q_{in} = Q_{out}$ and $\Delta Q = 0$). This is a situation where discharge is equal to recharge. The potential flow which describes the change in flux in response to a change in potential is given by Laplace Equation (Equation 2-9):

$$\Delta Q = [K_x \frac{\delta^2 h}{\delta x^2} + K_y \frac{\delta^2 h}{\delta y^2} + K_z \frac{\delta^2 z}{\delta z^2}] \delta x \cdot \delta y \cdot \delta z = 0 \quad \text{(Equation 2-9)}$$

where $\delta x \cdot \delta y \cdot \delta z$ = volume of ground. For homogenous and isotropic aquifer reduces to Equation 2-10:

$$\Delta Q = K \left[\frac{\delta^2 h}{\delta x^2} + \frac{\delta^2 h}{\delta y^2} + \frac{\delta^2 z}{\delta z^2} \right] \delta x \cdot \delta y \cdot \delta z = 0 \quad \text{(Equation 2-10)}$$

c) **Unsteady (Transient) State Flow Equation:** This is a groundwater flow condition in which there is a change in water level and thus hydraulic gradient changes with time, hence storage becomes involved as voids drain or fill. Discharge is in disequilibrium with recharge. The equation (Equation 2-11) for such flow through a saturated anisotropic porous medium is:

$$\Delta Q = \left[\frac{\delta \text{storage}}{\delta \text{time}} \right] \delta x \cdot \delta y \cdot \delta z = \left[K_x \frac{\delta^2 h}{\delta x^2} + K_y \frac{\delta^2 h}{\delta y^2} + K_z \frac{\delta^2 z}{\delta z^2} \right] \delta x \cdot \delta y \cdot \delta z \neq 0 \quad \text{(Equation 2-11)}$$

given that the $[Storage] \delta x \delta y \delta z = S_s$, where S_s = water released per unit volume of aquifer per unit change in total head. Thus within a column of aquifer of area ($\delta x \delta y$), the total volume capable of release in an aquifer of saturated thickness (b) is given by Equation 2-12:

$$S_s \cdot b = S \quad \text{(Equation 2-12)}$$

d) **Theis Well Equation:** The application of the Laplace equations for flow to non-steady radial flow towards a central sink was solved by Theis(1935) such that the basic relationship between drawdown, transmissivity, storage and discharge could be written as Equation 2-13 and Equation 2-14:

$$S = \frac{Q}{4\pi Kb} \times W(u) = \frac{Q}{4\pi T} \times W(u) \quad \text{(Equation 2-13)}$$

$$U = \frac{r^2 \times S}{4Tt} \quad \text{(Equation 2-14)}$$

where s = drawdown, Q = discharge, K= hydraulic conductivity, b = thickness, T = transmissivity, t = elapsed time, W (u) = well function where (W) = an exponential value and (u) its argument; where r = distance from pumping well to the observation hole where drawdown is measured or predicted, S = storage coefficient.

2.7.5.2 Numerical methods for estimating mine inflows

The main use of numerical models is to simulate physical processes occurring within the hydrogeological system, usually by digital computer. The main advantage of numerical methods over analytical methods lies in the ability to simulate three dimensional flow covering greater ground in a heterogenous aquifer system. This allows a more detailed representation of the groundwater system in the mine environment and leads to more accurate predictions (Lloyd and Edwards 2000).

A number of analytical methods have been applied in mining environments. However, the success was very low due to the complexity of the aquifer systems in mines. The major challenge in simulating groundwater flow in a mining environment is the dynamic nature of the groundwater system caused by mining. Some numerical modelling codes have been used successfully notably:

- UNSAT2. This package was used at a Uranium mine in New Mexico and Lead Mine in Missouri, USA (Williams 1986).
- Modflow: Used at the Dikuluwe-Mashamba copper- cobalt mines in the Kolwezi area, in The Democratic Republic of Congo, Central Africa (Straskraba 1991).
- Feflow: Used at a copper mine, Tenke Fungurume Mine, Fungurume, Democratic Republic of Congo, Central Africa. This researcher was active on this project in 1998.

A primary application of numerical models is simulation of drawdown changes over time and prediction of mine discharge. A bankable model depends on how well it represents the physical situation of the groundwater system. A detailed demonstration on how a numerical model can simulate a groundwater flow system is discussed in Chapter 6 of this dissertation.

2.8 Summary

Chapter 2 comprises of case studies of groundwater flooding of mines, mine hydrogeological settings, mine dewatering and water exclusion methods and mine hydrogeological investigation methods. Typically geology is the initial framework upon which the groundwater flow pattern and volumes of flow depend, the effects of mining activity forces the hydrogeological regime to change with time as well as with mining activity. For instance, the effects of rock blasting and extraction and their consequent effects of stress relief on the rock mass in a mine make the study of groundwater flow in a mine environment complicated. Hydrogeological boundaries that may have prevailed prior to the onset of mining may change after the commencement of mining. Thus, it was essential to establish a conceptual hydrogeological model for Ruashi Mine upon which the numerical groundwater flow model will be based.

The next chapter discusses the study area location, layout, climate, topography and brief regional geology.

3 STUDY AREA CHARACTERISTICS

3.1 Location

Ruashi Mine is located at approximately six kilometres (6 km) east of Luano Airport in Lubumbashi city in the Katanga Province of the Democratic Republic of Congo (DRC). The study area for the project is shown on the map of Africa in Figure 1-4.

3.2 Mine layout

The layout of Ruashi Mine site is presented in Figure 3.1.

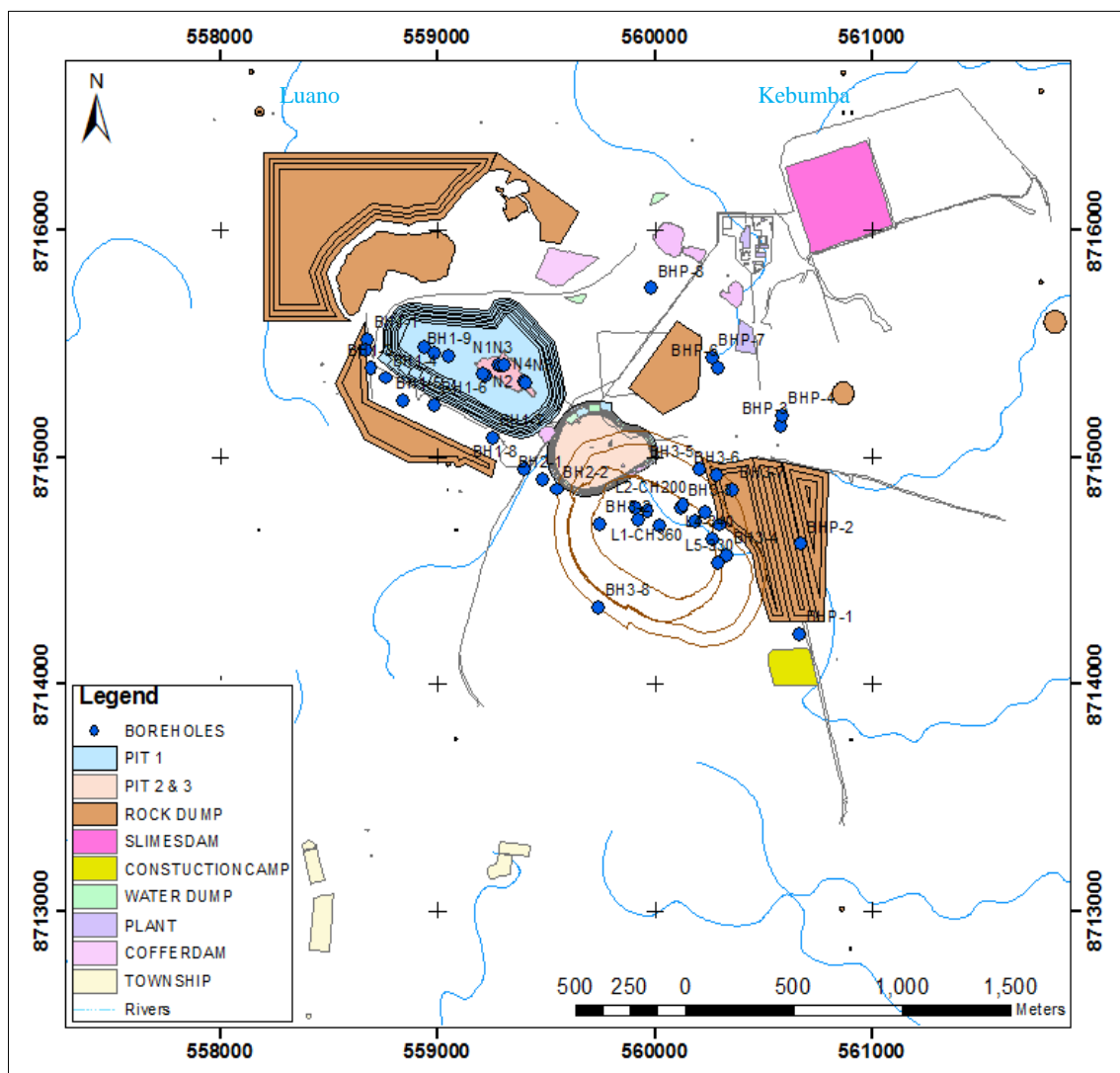


Figure 3-1: Location of Ruashi Mine showing the main pits and tailings infrastructure

In the central part of the mine are three pits located along the south east-north west (SE-NW) striking Roan series aquifer. There are three waste rock dumps to the south-east, north east

and north-west of the pits. The tailings storage facility (TSF) and Coffe dam are located in the north-east corner and north-west of the area respectively, underlain by predominantly less transmissive sandstones and shales of the Kundelungu formation. The processing plant and mine offices are located between the TSF and the north-eastern waste rock dump.

3.3 Climate

The study area climate is typical of sub-tropical to tropical rainforest characterised by warm winters and hot and humid summers. According to Straskraba (1991) temperature and humidity are high. Daily minimum and maximum temperatures vary from 15°C and 26°C (July) to 17°C and 36°C (October) respectively. The hottest months are September to November, when the mean daily temperature is typically in the region of 31°C to 32°C. Daytime temperatures can reach 36°C which can fall to 34°C at night. DRC straddles the equator hence the seasonal pattern of rainfall is affected. In the part of the country which lies north of the equator, the dry season which occurs from October to March corresponds to rainy season in the southern part of the country south of the equator. There is a great deal of variation, however, a number of places on either side of the equator have two wet and two dry seasons. Annual rainfall is highest in the heart of the Congo River basin and in the highlands towards the west of the country with some variation diminishing in direct relation to distance from these areas. The rainfall season stretches from late October to April. Figure 3-2 shows Ruashi Mine rainfall and temperature plots produced from data recorded at the mine.

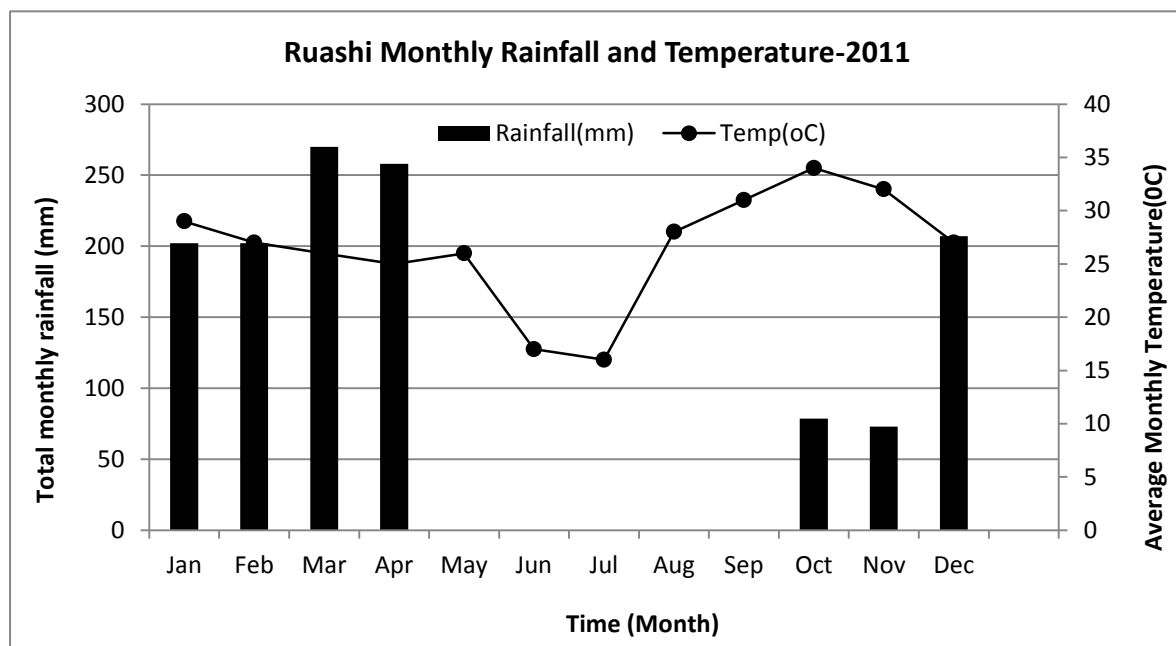


Figure 3-2: Ruashi average monthly rainfall and temperature for year 2011

According to Straskraba (1991) rainfall ranges from about 1 000 mm to 2 200 mm per annum but can have lower variations to 900 mm per annum. Humidity levels vary from a low of 40% during the winter to a peak of 90% at the start of the rainy season in October. Evaporation data obtained from Luano Airport Weather Station located in Lubumbashi, DRC indicate that the average daily evaporation rate during the rainfall season is 3 millimetres per day (mm/d), with a rate of 8 mm/d during the dry season. The prevailing wind direction in the dry season (July) is from the south east and is from the north-north-west in the wet season in January.

3.4 Topography

The study area is located just north of a north-west to south-east trending topographical high that acts as water divide. Topographic elevations (see Figure 3-3) range between 1 320 meters above mean sea level (mamsl) at the water divide, to 1 235 mamsl at the topographic low in the eastern river basin. In the vicinity of the mine site, the elevation is approximately 1 300 mamsl.

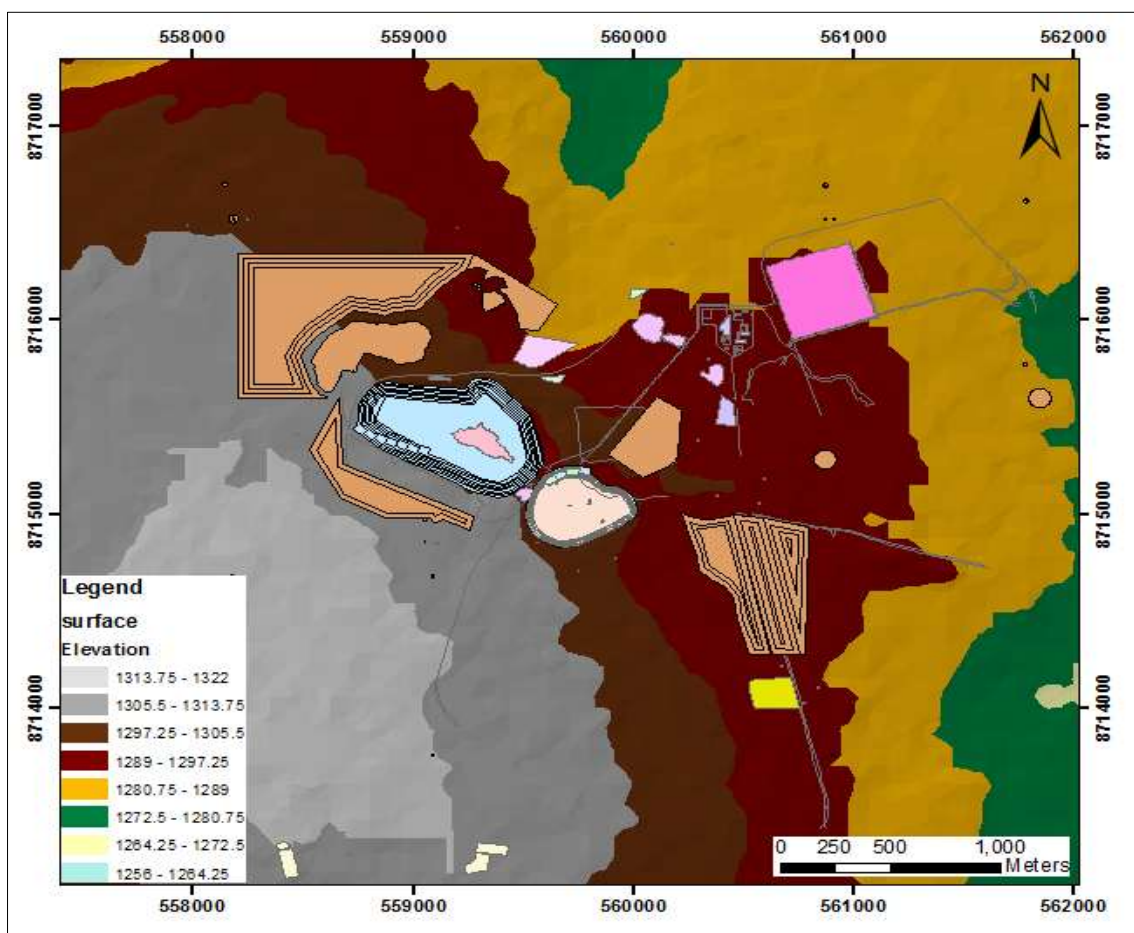


Figure 3-3: Ruashi Mine topography

3.5 Drainage

The study area drained by Luano River to the North West and Kebumba River to the North East (see Figure 3-1). Groundwater has a short residence time after recharge as it discharges as baseflow into surface water. This phenomenon is proven by immediate water level rises and decline during the rainfall season and dry season respectively. Ruashi Mine is situated in the upper reaches of the Luano River. The Luano River catchment contains the existing pit, existing plant and some of the roads leading to the mine. The catchment area of the Luano and Kebumba rivers is 5.1 square kilometers (km²).

A section of the Luano River in the Ruashi Mine concession was historically a low wet area of about 300 m wide but it was channelled by the previous mine owners. This resulted in the river flowing in a channel and significantly dried up. The reason for channelling of the flow was to divert the river away from the mining area. Kebumba River catchment is the main drainage that the Ruashi Mine smaller streams flow into. The river flows in a south-easterly direction and then south around the eastern side of the mine. The catchment area upstream coincides with the Luano River catchment that includes Luano Airport and Ruashi villages.

3.6 Brief Geology

3.6.1 Regional geology

According to Straskraba (1991) the Ruashi ore bodies are hosted by meta-sedimentary rocks of the 7 km thick Neoproterozoic Katanga System. The Ruashi Mine area sits on the south end of the Katangan Copperbelt which together with the Zambian Copperbelt are located within the deformed SE-NW trending syncline called the Lufilian Arc which stretches into Namibia. This Copperbelt is 600 km long extending from Luanshya (Zambia) in the south-east to Kolwezi (DRC) in the north-west.

In the DRC, the Katangan Supergroup is preserved both as tightly folded, but relatively intact sequences and as complexly deformed dolomitic rocks namely the Roan strata (Straskraba 1991). The Katangan system is composed of sedimentary rocks of the late Proterozoic era, a succession of interbedded Quartzites, Sandstones, Conglomerates, Shales, Siltstones, Dolomites, Limestones, Argillites and dolomitic Shales.

The Ruashi structural features are typically folded and brecciated, forming tight, steeply dipping synclinal and anticlinal structures. The vergence of the folds is variable; this is consistent with the interpretation of chaotic fragments within the breccia zone. The dip of the limbs is mainly steep from vertical to 85°, but also shallow down to 45° (GCS 2006). In some

places very shallow to sub horizontal dips occur. Fault displacements vary between 15 m and 45 m.

3.7 Summary

The study site is located in an area characterised by high humidity, high rainfall and highly transmissive dolomitic rocks. Study of the site geological history, stratigraphy, hydrostratigraphy, structure and its influence on the surface drainage pattern, would reveal potential major groundwater flow conduits and likely sources of recharge, and facilitate the delineation of hydrogeological boundaries. Hydrogeological boundaries are essential in defining the effective groundwater catchment and estimation of the water budget. Water level maps drawn using mine records give an insight into the behaviour of groundwater flow regime with time and mine level depth. Groundwater chemistry gives the means through which groundwater flow paths and patterns, and the overall nature of the flow regime could be defined and confirmed. The trends in modern world mining is to find ways of curbing inflows and thereby reduce the cost of pumping and in some cases eliminate the need of costly pumping altogether.

The next chapter discusses the research methodology. The methodology includes field investigation comprising of hydrocensus, borehole drilling and aquifer hydraulic testing. Data obtained from the field investigation programme is used to construct conceptual hydrogeological model for the mine.

4 FIELD DATA COLLECTION METHODOLOGY

The field programme was designed to provide information required to develop a conceptual hydrogeological model for the mine. Field investigations involved carrying out hydrocensus, drilling, aquifer hydraulic testing and water quality sampling.

4.1 Overview of investigation

The project initial phase included an initial hydrocensus, drilling of groundwater exploration boreholes, aquifer hydraulic testing, hydrochemical sampling and groundwater level monitoring. The initial phase was followed by the main field phase during which 14 plant and community supply/emergency dewatering boreholes and 34 groundwater monitoring boreholes were drilled.

A hydrocensus was carried out to identify existing groundwater supply and monitoring wells, surface water sources and mine infrastructure. After completion of hydrocensus, the following field activities were implemented:

- Desk study of mine plans and geophysical survey data to aid in confirming suitable drilling locations;
- Drilling a total of 34 in-pit and pit perimeter groundwater monitoring boreholes of variable depths;
- Drilling of one groundwater exploration borehole and 13 emergency pit dewatering and water supply boreholes to augment plant and community water supply;
- Controlled aquifer hydraulic testing to determine aquifer hydraulic parameters;
- Sampling of accessible water points for hydrochemical analysis.

4.2 Hydrocensus

A hydrocensus was carried out during the month of February 2010. Parameters that were collected during the hydrocensus include position of borehole; existing water supply equipment; borehole use; borehole status; reported yield; reported or measured borehole depth, static water level and photographs. The hydrocensus data was used in planning the next phase of the hydrogeological investigation, notably drilling, aquifer hydraulic testing and water quality sampling. A piezometric map (Figure 4-1) was constructed using water levels measured during the hydrocensus.

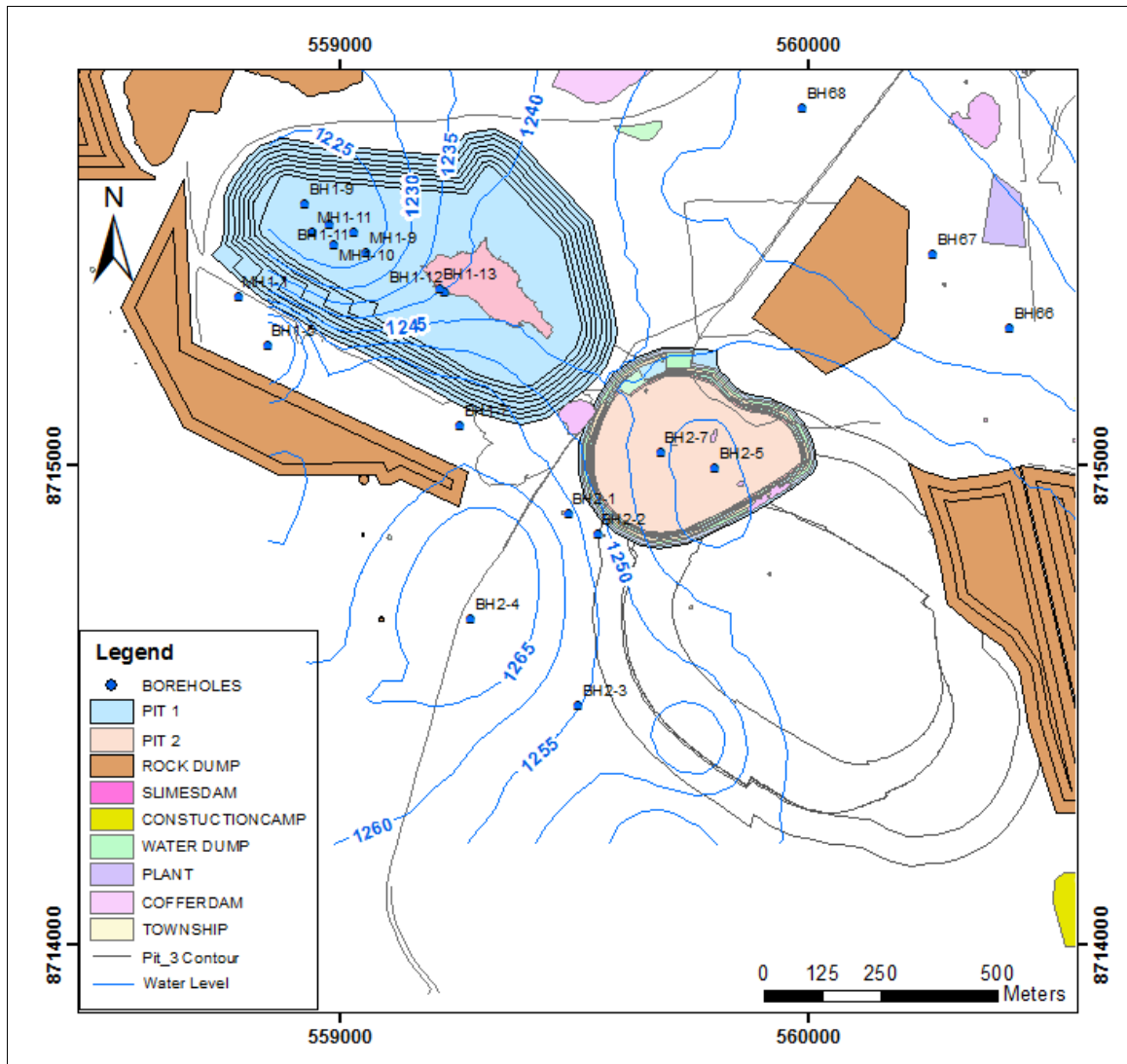


Figure 4-1: Ruashi piezometric map

Boreholes BH2-5 and BH2-7 were being pumped for plant and community water supply. Community supply borehole BH2-4 was not pumping at the time of the hydrocensus. The groundwater levels plotted in the piezometric map show high hydraulic heads (1 250 -1 272 meters above mean sea level (mamsl)) on the southern side of the pits. This was expected as the regional groundwater flow direction is from the south west. The deepest hydraulic head (1 222 mamsl) was recorded in Pit1 showing effects of continuous pumping at BH1-9 and BH1-10 and intermittent pumping at BH1-12 and BH1-13.

4.3 Drilling

The objective of the drilling phase was to initially characterise rock units in terms hydrogeological properties. The hydrogeological properties of the rock units would then be used to construct a conceptual hydrogeological model for the mine.

This researcher and fellow KLMCS employee, Mr Isadore Nyazorwe alternated (on monthly basis) in supervising the drilling work. West Australia (Pvt) Ltd DRC formerly Eastern Drilling (Pvt) Ltd SA ,were contracted by Metorex, owners of Ruashi Mine, to carry out large diameter (254 mm and larger) drilling of pumping boreholes. Ruashi Mine own a rig which was tasked with drilling of small diameter (203 mm) groundwater monitoring boreholes cased with 152 mm Ultraviolet treated Polyvinyl Chloride (UPVC). Air percussion drilling was considered the most suitable method in hard dolomitic formations. Mud rotary drilling method was used in clayey and loose unconsolidated formations like the malleable Roches Argillite Talceus (RAT) and Calcareous Mineral Noirs (CMN). At levels where huge rock fragments and cavity conditions with high yields were encountered, symmetrix (drilling and driving) method became handy.

4.3.1 Air percussion drilling method

Air percussion drilling method makes use of a pneumatic hammer crashing the formation driven by compressed air. The air is driven from an air compressor through the drill string towards the pneumatic hammer and drill bit. The compressed air also lifts out drill cuttings through the annulus between the drilled hole and the drill string. The blow yield at BH1-17 was measured using a V-notch as shown in Figure 4-2.



Figure 4-2: Air percussion drilling at dewatering borehole BH1-17 located in Pit 1. The foreground shows passage of groundwater through a V-notch.

4.3.2 Mud rotary drilling method

Mud rotary drilling utilises tri-cone roller, carbide embedded, fixed-cutter diamond-impregnated drill bits to wear away at the cutting face. Rotating hollow drill pipes carry down bentonite or other powders infused drilling muds to lubricate, clean the drilling bit, control downhole pressures and carry drill cuttings. The mud travels back to the surface through the space between the outside of the drill string and drilled borehole, called the annulus. The drilling fluid also serves to cool the drill bit and stabilise the borehole walls, to prevent the flow of fluids between the borehole and surrounding materials, hence reduce cross contamination between aquifers.

4.3.3 Initial drilling

The objective of drilling the first deep borehole (BH3-39) located on the eastern side of Pit 3 was to intersect and characterise all lithologies from ground surface down to a depth of 250 m. It was also planned to use the borehole for community and plant water supply. Drilling of the groundwater exploration borehole BH3-39 began in September 2010 and was successfully completed in October 2010. Drilling began with a 444 mm (17.4 inches) diameter drill bit from ground surface to 222 meters below ground level (mbgl). The

lithologies intersected are presented in Table 4-1 and Figure 4-3. The borehole was deepened by drilling and driving 8" (8 inches) drop set of slotted steel casing string from 224 mbgl to 247 mbgl. The borehole was cased with 10" (254 mm) diameter mild steel casing. The drill cuttings that filled the bottom part of the borehole prevented the extension of 10" steel casing string beyond 224 mbgl. Four pumping chambers were installed between 142 m to 148 m, 172 m to 178 m, 190 m to 196 m and 206 m to 212 m. The pumping chambers are lengths of the casing string that are plain (unscreened). The pump sump is aligned to these pumping chambers to prevent turbulent flow to the pump.

Blow yields were measured at 5 m intervals and the final blow yield measured at the end drilling was 432 m³/hr. Groundwater physicochemical parameters were also measured during drilling. Total dissolved solids (TDS) and pH were measured as 144 mg/L and 7.8 respectively. Water strikes were also noted during the drilling. The shallow water strikes identified at 22 m and 55-60 m were sealed off in order to measure the individual water strike yield in the SDS Formation.

After installation of casing string, the borehole was developed by jetting out water until free of suspended matter. The borehole development exercise was run for 6 hours. A cement and bentonite plug was constructed between 80 mbgl and 112 mbgl. The upper annulus space between 80 and 5 mbgl was backfilled with clay. Sanitary seal construction and well head (capping) construction completed borehole. Table 4-1 is a compilation of hydrogeological results for BH3-39.

Table 4-1 : Hydrogeological summary log for groundwater exploration borehole BH3-39

Drilling Depth(m)		Lithology	Water Strike (mbgl)	Yield (m ³ /hr)	Rest Water Level (mbgl)	TDS (mg/L)
From	To					
0	2	Topsoil, orange, yellowish, loose, dry				
2	10	Laterite, silty, semi-consolidated, reddish orange, moist				
10	21	Laterite, deep red, minor orange shades				
21	33	Laterite, pale red, fine, muddy	22	0.1	17.8	
33	39	Laterite, reddish orange, very fine, with dark grey-black iron ferricrete	39	1.6	16.5	180
39	51	Laterite, black, dark red, muddy ferricrete				
51	56	Siltstone, red and white, laminated	55	20.2		
56	75	RAT breccia- quartz gravel, fine matrix to very large clasts >3cm. Clear, milky, black and vuggy	60 70	22.5		180
75	77	Highly talcose very thinly laminated red and yellow shale		seepage		
77	94	Highly talcose, white shale				
94	108	RAT Breccia, white, with black and clear quartz	95	8	14.7	68
108	122	RAT, highly talcose shale, moderately weathered				
122	164	SDS, dolomitic shale, weathered, grey	122	121.2		142
164	197	SDS, dolomitic shale, slightly weathered	164	248.4	19.9	
197	250	SDS, dolomitic shale, fractured, malachite mineralised	197	432.6	19.9	144

The drilling information was used to plot a borehole construction log presented in Figure 4-3.

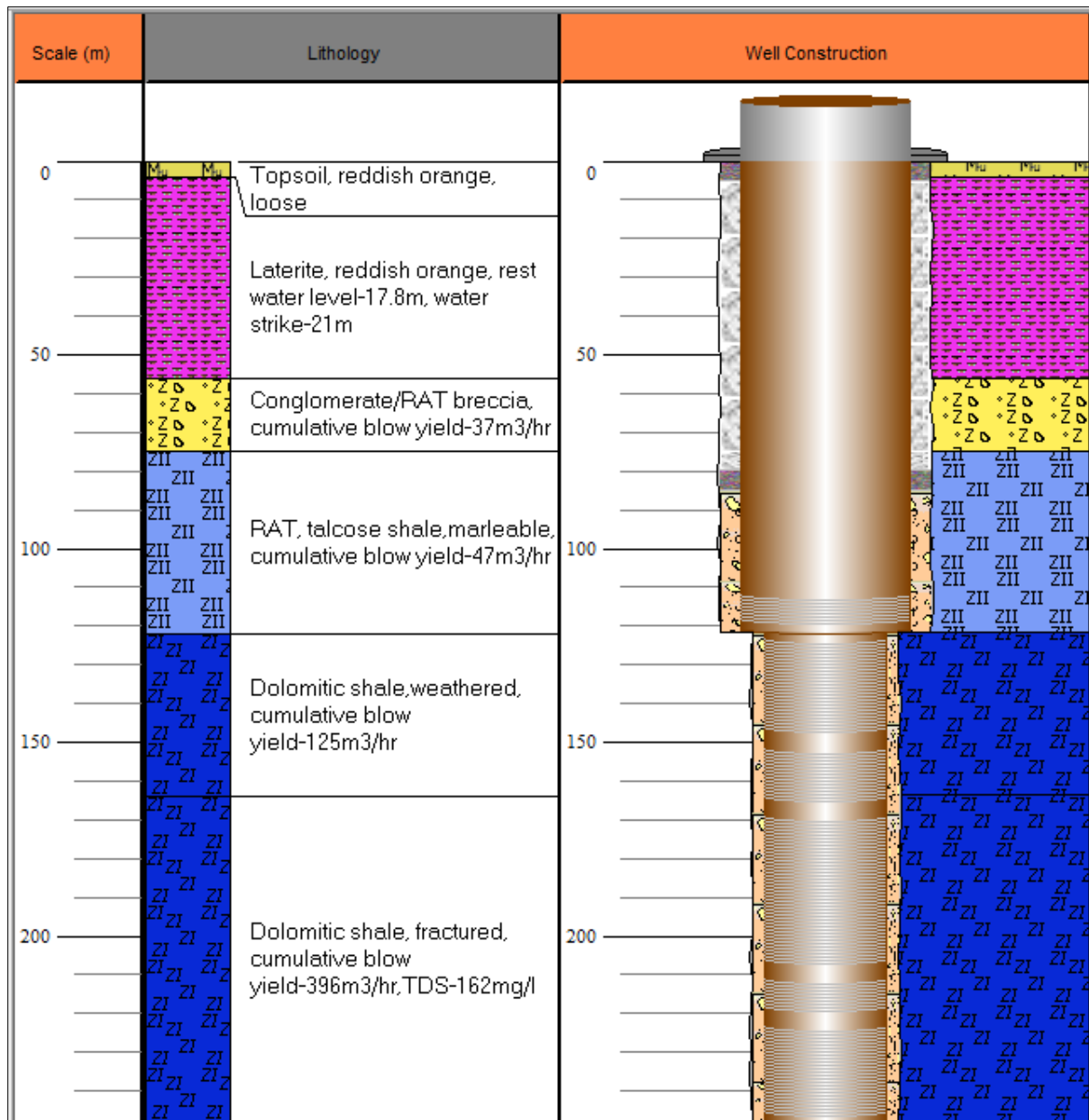


Figure 4-3: Borehole BH3-39 lithological and construction log

It was planned to carry out test pumping at borehole BH3-39 and observe the cone of depression created by pumping. As such it was necessary to install piezometers at various distances away from the pumping well. Eight groundwater monitoring boreholes of various depths were constructed at distances of 40 m and 80 m away from borehole BH3-39. Four of these monitoring boreholes were located perpendicular to the strike of the SDS Formation and the other four along the strike of the SDS. Table 4-2 summarises the eight groundwater monitoring boreholes. For ease of distinction pumping wells and groundwater monitoring wells are prefixed “BH” and “MH” respectively. Borehole construction logs for the groundwater monitoring boreholes are included in Appendix A.

Table 4-2: Pumping and groundwater monitoring borehole information

Borehole	X	Y	Depth (mbgl)	Location	Target	Objective	
BH3-39	560330	8714427	247	East of Pit 3	SDS/Lower Roan Aquifer	Determine aquifer hydraulic parameters. Understand flow directions and initial hydrogeological conceptualisation.	
MH3-1	560297	8714450	250	40m NW of BH3-39	Along strike. SDS/Lower Roan aquifer	Determine extent of cone of depression and groundwater flow direction.	
MH3-2	560352	8714461	250	40m NE of BH3-39	Across strike. SDS/Lower Roan aquifer		
MH3-3	560362	8714406	250	40m SE of BH3-39	Along strike. SDS/Lower Roan aquifer		
MH3-4	560308	8714392	250	40m SW of BH3-39	Across strike. SDS/Lower Roan aquifer		
MH3-5	560415	8714382	250	80m SE of BH3-39	Along strike. SDS/Lower Roan aquifer		
MH3-6	560287	8714356	250	80m SW of BH3-39	Across strike. SDS/Lower Roan aquifer		
MH3-7	560373	8714406	100	40m SE of BH3-39	Along strike. RAT breccia aquifer.		Evaluate hydraulic continuity between RAT breccia and Lower Roan aquifers.
MH3-8	560319	8714392	80	40m SE of BH3-39	Across strike. RAT Breccia aquifer.		

4.3.4 Main drilling phase

The main phase borehole drilling began in September 2010 with Pit 3 perimeter groundwater monitoring boreholes, followed by in-pit groundwater monitoring boreholes and large diameter emergency dewatering boreholes. Six boreholes (MH3-1, MH3-2, MH3-3, MH3-4,

MH3-6 and MH3-5) were completed in five months, indicating a slow progress primarily due to drilling challenges encountered in collapsing lithologies and poor site coordination by drilling contractor. All monitoring boreholes were completed between February and April 2011. By the end of July 2011, eight of the nine large diameter dewatering boreholes had been completed. Additional borehole drilling (BH2-28 and BH2-29) to dewater Pit 2 was completed but drilling of dewatering borehole in Pit 3 was abandoned by the mine for financial reasons. The shallow groundwater monitoring boreholes (less than 80 m deep) were intended to penetrate only the shallow aquifers (Kundelungu sandstone, Laterite and RAT). In the deep boreholes (greater than 80 m), the annular space in the shallow lithologies was filled with bentonite to minimise mixing with deep aquifer water.

Upon completion of drilling, each borehole was cased and developed according to the approved design. A well head concrete block of standard dimensions (1 m length x 1 m width x 0.5 m height) was constructed at each borehole. A marker post was placed at each completed borehole.

Emergency dewatering boreholes were designed to accommodate big capacity pumps to enable extraction of high water volumes from the Roan dolomitic aquifers. These boreholes were drilled using drill bit diameter sizes between 16 and 18 inches (18") and cased with 14" steel. The major water strikes were encountered within the Roan aquifer at various depths between 35 and 120 mbgl. High yields ranging between 200 and 300 cubic metres per hour (m^3/hr) were recorded, mostly in the lower sections of the brecciated siliceous and vuggy dolomite (SDS). Details of lithologies intersected, water strikes, blow yield estimates, rest water level measurements, borehole coordinates and borehole construction details are included in Table 4-3, Table 4-4 and Table 4-5. Water strike and water level units are given in metres below ground level (mbgl), elevation in metres above mean sea level (mamsl) and blow yield in cubic metres per hour (m^3/hr). Borehole log plots are presented in Appendix A.

Table 4-3: Dewatering boreholes

BH No.	BH Depth (m)	Casing diameter (mm) and Material	Date Completed	Location (Y)	Location (X)	Collar Elevation (mamsl)	Water strike (mbgl)	Blow Yield (m ³ /hr)	RWL (mbgl)	Main Aquifer Formation	Main Aquifer lithology
BHAP1	120	254 UPVC	28-07-2011	8716535.3	560546.8	1266.70	15	20	4.13	Laterite	Siltstone
BH1-15	100	305 steel	31-05-2011	8715540.0	558940.3	1242.86	15, 65	312	14.30	RSC	Siliceous vuggy Dolomite, massive
BH1-16	100	305 steel	15-06-2011	8715470.5	559046.0	1243.00	16 ,63	320	15.33	RSF	Dolomitic, siliceous , grey Shale
BH1-17A	90	305 steel	05-07-2011	8715235.0	559442.0	1237.82	11.5	250	10.50	RSF	Siliceous dolomitic Shale, weathered
BH1-18A	98	305 steel	31-08-2011	8715234.2	559260.8	1237.70	16, 35, 69, 74	17, 550	15.76	RSF	Siliceous dolomitic Shale, weathered
BH2-7	80	254 UPVC	23-04-2011	8714978.0	559742.7	1240.0	15	70	2.00	Saprolite	Earthy, talcose, clayey gravels
BH3-12	125	254 UPVC	14-05-2011	8714877.9	560258.4	1272.00	112	0.2, 5.5	21.30	SDS	Dolomitic Shale
BH3-11	114	254 UPVC	13-04-2011	8714691.6	560423.5	1272.86	35	80	22.70	Siltstone	Siltstone, brown, grey, lime chalk
BH3-39	247	254 steel	23-10-2010	8714427.6	560330.0	1270.57	21;56;12 3	396	17.80	Dolomite	Dolomite,sandy,grey,weathered
BH3-10	100	305 steel	27-04-2011	8714670.9	559980.3	1252.9	30	100	8.46	Sandstone	Sandstone, coarse, white, grey.
BH3-13	106	305	20-05-2011	8714495.8	560204.1	1252.0	9, 37	7, 78	7.80	Shale	Siliceous, dolomitic Shale
BH2-29	112	305 steel	05-10-2011	8714924.9	559809.1	1233.31	23	476	4.82	SDS	Dolomitic shale, graphitic, manganeseous
BH2-28	86	305 steel	27-09-2011	8715048.1	559747.6	1240.60	22	96	3.00	SDS	Dolomitic Siltstone
BH69B	140	228 UPVC	20-10-2011	8715236.3	560601.7	1274.13	52	62	28.30	Kundelungu Shale	Kundelungu dolomitic Shale, brown

Table 4-4: Groundwater monitoring boreholes

BH No.	BH Depth (m)	Final Casing diameter (mm) and Material	Date Completed	Location (Y)	Location (X)	Elevation (mamsl)	Water Strike (mbgl)	Water Strike (mamsl)	Blow Yield (m ³ /hr)	Rest water level (mbgl)	Main Aquifer Formation	Main Aquifer lithology
MH1-1	70	114 steel	22-02-2011	8715578.0	559525.1	1279.78	61	1218.7	<0.5	30.30	Shale	Shale, grey and yellow, talcose,
MH1-2	60	114 steel	26-02-2011	8715538.0	558686.7	1286.493	42	1244.4	<0.5	16.60	Shale	Shale, grey and yellow, talcose,
MH1-3	58	114 steel	08-03-2011	8715154.0	559088.5	1290.046	42	1248.0	3	21.00	Shale	Shale, grey and yellow, talcose
MH1-13	70	152 UPVC	10-06-2011	8715503.6	559326.4	1245.145	7; 55	1238.1	126	2.86	RSC	Siliceous vuggy dolomite
MH1-14	60	152 UPVC	13-06-2011	8715325.6	559274.2	1237.72	8;33; 38-60	1229.7	113	9.52	RSC	Siliceous vuggy dolomite
MH1-15	70	152 UPVC	15-06-2011	8715224.0	559461.9	1238.02	17, 42	1221.0	94	10.55	RSC	Siliceous vuggy dolomite
MH1-16	70	152 UPVC	17-06-2011	8715300.9	559496.3	1243.55	18,52	1225.5	72	0.00	RSC	Siliceous, vuggy dolomite
MH2-1	80	114 UPVC	18-02-2011	8715089.0	560054.6	1275.34	38	1237.3	3	27.30	Siltstone	Siltstone , Breccia, quartz pebble
MH2-2	70	152 UPVC	15-03-2011	8714814.4	559302.9	1287.04	35	1252.0	6	19.12	Shale	Shale, grey, black, laminated
MH2-3	74	114 UPVC	15-05-2011	8715070.6	559652.9	1240.00	18, 54	1222.0	68	13.40	Sandstone	Sandstone, coarse, white,sucrosic
MH2-4	70	152 UPVC	02-06-2011	8715046.9	559907.3	1245.17	15	1230.1	33	6.00	Sandstone	Quartzitic Sandstone
MH2-5	80	152 UPVC	01-07-2011	8714922.6	559822.9	1240.59	5	1235.5	15	3.00	RSC	Siliceous vuggy malachite, dolomite
MH2-6	30	152 UPVC	05-07-2011	8714905.0	559785.0	1240.18	45	1195.1	3.5	6.99	RSC,	Siliceous vuggy malachite, dolomite

BH No.	BH Depth (m)	Final Casing diameter (mm) and Material	Date Completed	Location (Y)	Location (X)	Elevation (mamsl)	Water Strike (mbgl)	Water Strike (mamsl)	Blow Yield (m ³ /hr)	Rest water level (mbgl)	Main Aquifer Formation	Main Aquifer lithology
MH2-7	70	203 UPVC	03-06-2011	8715026.3	559768.5	1240.05	16,26,43-70	1224.0	293	10.66	RSC	RSC, Siliceous vuggy dolomite
MH3-1	250	114 Steel	28-09-2010	8714450.0	560297.5	1270.27	22;210,237	1232.4	48.4	17.95	SDS	Dolomitic shale, grey, fractured
MH3-2	123	114 Steel	22-11-2010	8714461.5	560352.5	1270.67	28;53;108	1242.6	49	20.21	Breccia	Breccia, RAT, clear hard quartz
MH3-3	206	114 Steel	22-11-2010	8714406.2	560362.5	1270.56	26;32;165	1244.5	73	18.30	SDS	Dolomitic shale, grey, fractured
MH3-4	250	114 Steel	07-12-2010	8714392.5	560308.7	1271.16	76;104;116	1229.3	34.5	17.70	SDS	Dolomitic shale, grey, fractured
MH3-5	230	114 Steel	05-12-2010	8714211.3	559681.5	1269.89	24-26,61	1262.1	7, 47	5.42	SDS	Dolomitic shale, grey, fractured
MH3-6	149	114 Steel	03-11-2010	8714356.2	560285.5	1272.01	39;76;98	1232.7	58.4	18.62	Sandstone	Sandstone, quartzitic
MH3-6b	150	114 Steel	20-03-2011	8714351.7	560281.7	1272.33	61	1211.3	5.5	21.00	Sandstone	Sandstone, quartzitic
MH3-7	69	114 Steel	11-02-2011	8714693.0	560390.1	1272.58	37	1235.5	10;16	16.97	Laterite	Laterite, brown clayey
MH3-7A	70	152 UPVC	29-07-2011	8714693.5	560389.7	1271.60	21	1250.6	5	15.20	Laterite	Laterite, brown clayey
MH3-8	65	152 UPVC	08-03-2011	8714526.0	560167.6	1250.71	6	1244.7	15	4.00	Siltstone	Manganeferous siltstone
MH3-9	73	152 UPVC	09-03-2011	8714753.0	560138.5	1253.77	30	1223.7	0.5	19.79	SDS	Siltstone/sandstone.
MH3-10	64	152 UPVC	12-03-2011	8714569.0	560034.7	1250.46	6	1244.4	5	2.40	SDS	Sandstone, conglomeritic
MH3-11	60	152 UPVC	22-03-2011	8714426.6	559751.5	1283.32	21	1262.3	0.05		Laterite	Laterite, yellowish orange, loose, dry

BH No.	BH Depth (m)	Final Casing diameter (mm) and Material	Date Completed	Location (Y)	Location (X)	Elevation (mamsl)	Water Strike (mbgl)	Water Strike (mamsl)	Blow Yield (m ³ /hr)	Rest water level (mbgl)	Main Aquifer Formation	Main Aquifer lithology
MH3-14	100	152 UPVC	03-09-2011	8714443.3	560165.9	1253.12	25	1228.1	0.05	13.2	RAT	Breccia, clear, black, hard
MH3-15	100	152 UPVC	20-08-2011	8714477.7	560227.6	1253.32	11; 15	1242.3	5	11.04	SDS	Dolomitic, Shale, grey, weathered and fractured
MH3-16	100	152 UPVC	22-08-2011	8714583.5	560213.7	1250.87	39	1211.8	14	8.27	Breccia	RAT Breccia, with very hard creamy indurated shale and dolomitic clasts

Table 4-5: Environmental monitoring boreholes

BH No.	BH Depth (m)	Final Casing diameter(mm) and Material	Date Completed	Location (Y)	Location (X)	Elevation (mamsl)	Water strike (mbgl)	Water strike (mamsl)	Blow Yield (m ³ /hr)	Rest water level (mbgl)	Main Aquifer Formation	Main Aquifer lithology
GWD-5	53	152 UPVC	21-02-2011	8715424.0	561249.1	1267.5	5	1262.5	3	2.90	Laterite	Laterite, gravelly, clayey
GWD-6	50	152 UPVC	23-02-2011	8715585.0	559975.9	1274.6	30	1244.6	2.5	19.35	Silt	Siltstone, red brown, clayey
GWD-7	75	152 UPVC	25-02-2011	8715579.0	559749.5	1275.0	67, 75	1208.0	<0.5, 5	20.54	Siltstone	Siltstone, brown
GWD-8	50	152 UPVC	03-03-2011	8715381.0	560234.5	1274.4	42	1232.4	<0.5	19.00	Shale	Shale, brown, silty and gritty

4.3.5 Borehole drilling summary

A total of 14 pumping and 34 groundwater monitoring boreholes were drilled during this research. The rock units intersected are represented by pictures of core recovered (see Table 4-6) during the geotechnical drilling conducted a month prior the start of this research.

Based on the rock units intersected and the distribution of water strikes encountered, five major aquifer units underlie the Ruashi Mine, namely Laterite, Kundelungu Sandstone, RAT, CMN and SDS. The hydrogeological characteristics of these rock units are discussed in the conceptual hydrogeological model presented in Chapter 5 of this dissertation. Perched zones are present mainly in the RAT. The highest blow yield (396 m³/hr) was recorded in the SDS. Most of the boreholes in Pit 2 intersected Black Ore Mineralised Zone (BOMZ) compartments in the SDS at shallow depths between 24 and 45 mbgl. SDS and Laterite lithologies were intersected in all boreholes with RAT being common as well. Thin localized layers of RAT breccia were intersected in boreholes located along the boundary between Pit 1 and Pit 2. Weathering and fracturing extend to depths up to 80 mbgl. Fracturing and minor weathering at depth is associated with lithological contact zones.

Table 4-6: Pictures of core recovered from geotechnical drilling

<p style="text-align: center;">Laterite</p> 	<p style="text-align: center;">BOMZ</p> 
<p style="text-align: center;">SDS</p> 	<p style="text-align: center;">RAT</p> 
<p style="text-align: center;">CMN</p> 	<p style="text-align: center;">Sandstone</p> 

4.4 Aquifer hydraulic testing

4.4.1 Introduction

Aquifer hydraulic testing was conducted to determine the transmissivity and storativity characteristics of the aquifers. The first aquifer hydraulic testing work commenced on 7 June 2011 and was completed on 12 June 2011. The second test began on 12 July 2011 and was completed on 26 July 2011. During the second test, there were several power failures hence the data could not be interpreted accurately. The pump testing was conducted on a single pumping well BH3-39 located at about 50 m east of Pit 3 perimeter. Drawdown and recovery was monitored in nine cluster groundwater monitoring boreholes located along and across the lithology strike. The positions of the pumping well and observation boreholes are presented in Figure 4-4. Groundwater monitoring boreholes MH3-1, MH3-2, MH3-3 and MH3-4 are located at 40 m away from the pumping borehole BH3-39. The other groundwater monitoring boreholes MH3-5, MH3-6B, MH3-8, MH3-10 and MH2-3 are located at 80 m, 80 m, 160 m, 260 m and 840 m respectively away from the pumping borehole.

4.4.2 Objectives

The specific objective of the testing was to characterise the prevailing hydrogeological conditions in and around Pit 3 site including:

- hydraulic properties of the aquifers
- rate of spread of cone of depression
- aquifer yields

4.4.3 Methodology

The aquifer hydraulic testing procedure involved:

- three drawdown step tests each lasting a maximum period of 1 hour
- Constant rate discharge test lasting for a maximum period of 72 hours
- 48 hour recovery monitoring or 95% recovery or whichever was earlier

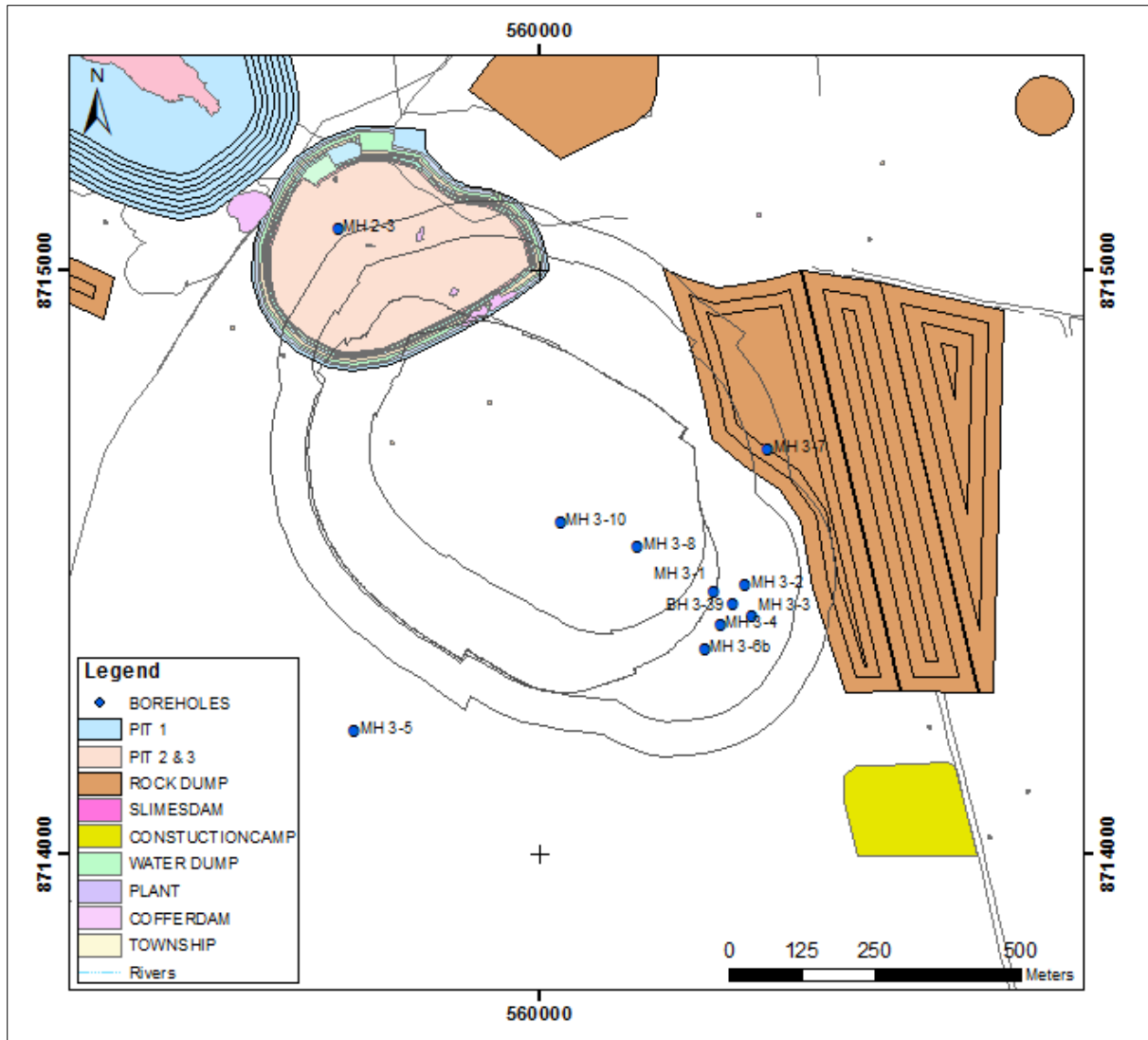


Figure 4-4: Ruashi map showing positions of pumping borehole BH3-39 and monitoring boreholes

4.4.3.1 Step drawdown test

Step drawdown test with discharge rates ranging from 36 m³/hr to 144 m³/hr was conducted on the pumping borehole BH3-39. Three step drawdown tests with pumping rates of 36 m³/hr, 72 m³/hr and 133 m³/hr were completed. A further step could not be conducted as the pump had reached its maximum pumping capacity. Figure 4-5 is a plot of step drawdown test results obtained from the first test at pumping borehole BH3-39. Drawdown in the pumping borehole was 6 m at the end of the last step.

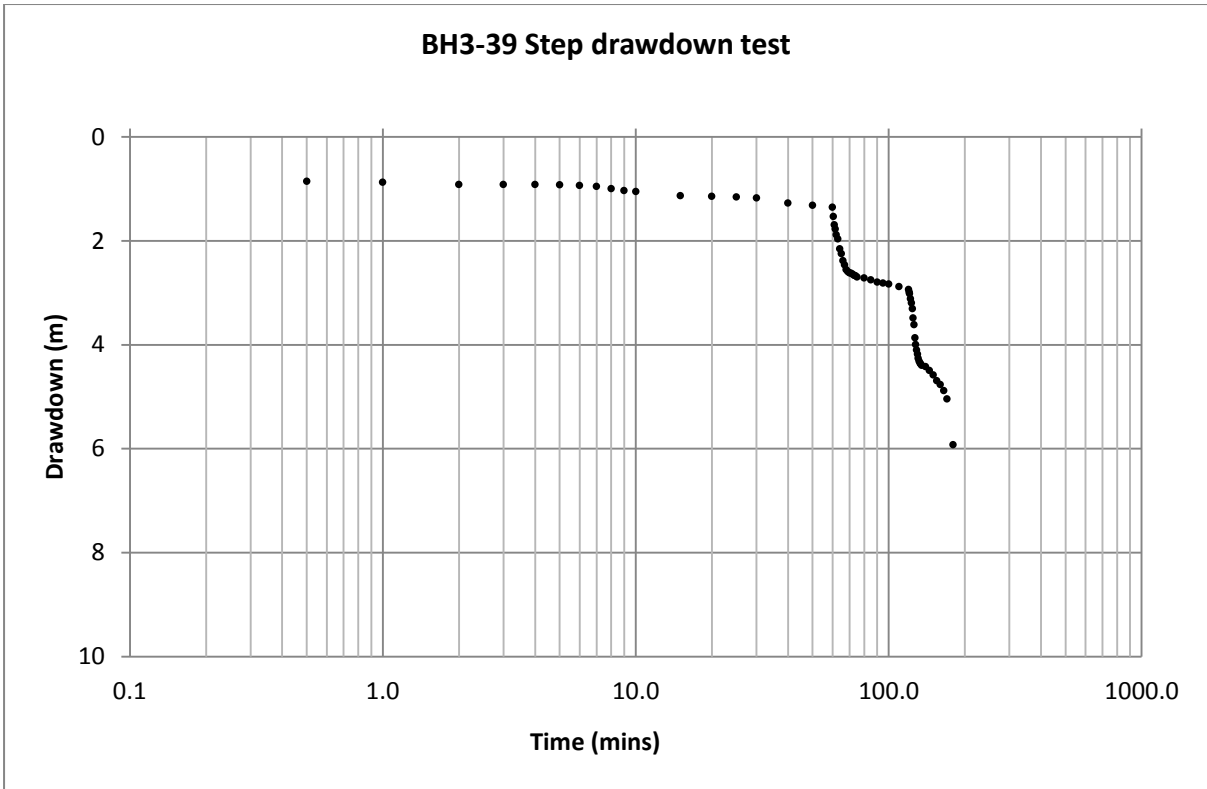


Figure 4-5: Step drawdown test plot of data recorded at borehole BH3-39

4.4.4 Constant rate test and recovery

After completion of step drawdown test, the pumping borehole was allowed to achieve at least 95% recovery. Following the 95% recovery, borehole BH3-39 was pumped at a constant rate of 144 m³/hr for a period of 72 hours. With an available drawdown of 94.3 m, the pumping created drawdown of 10.5 m in the pumping borehole. The borehole recovered to within 1.38 m of the static water level (23.71 mbgl) after 48 hours. The constant rate test (CRT) pumping and recovery graphs are presented in Figure 4-6 and Figure 4-7 respectively.

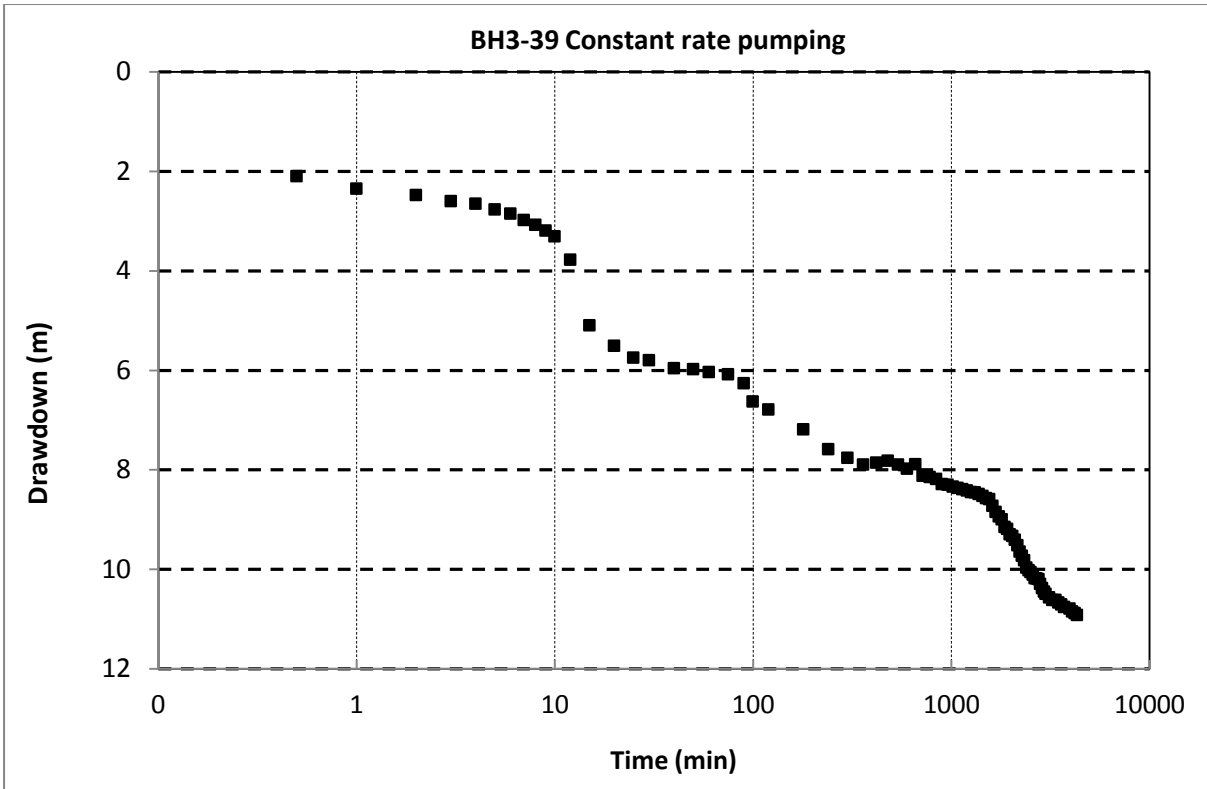


Figure 4-6: Constant rate test pumping drawdown at BH3-39

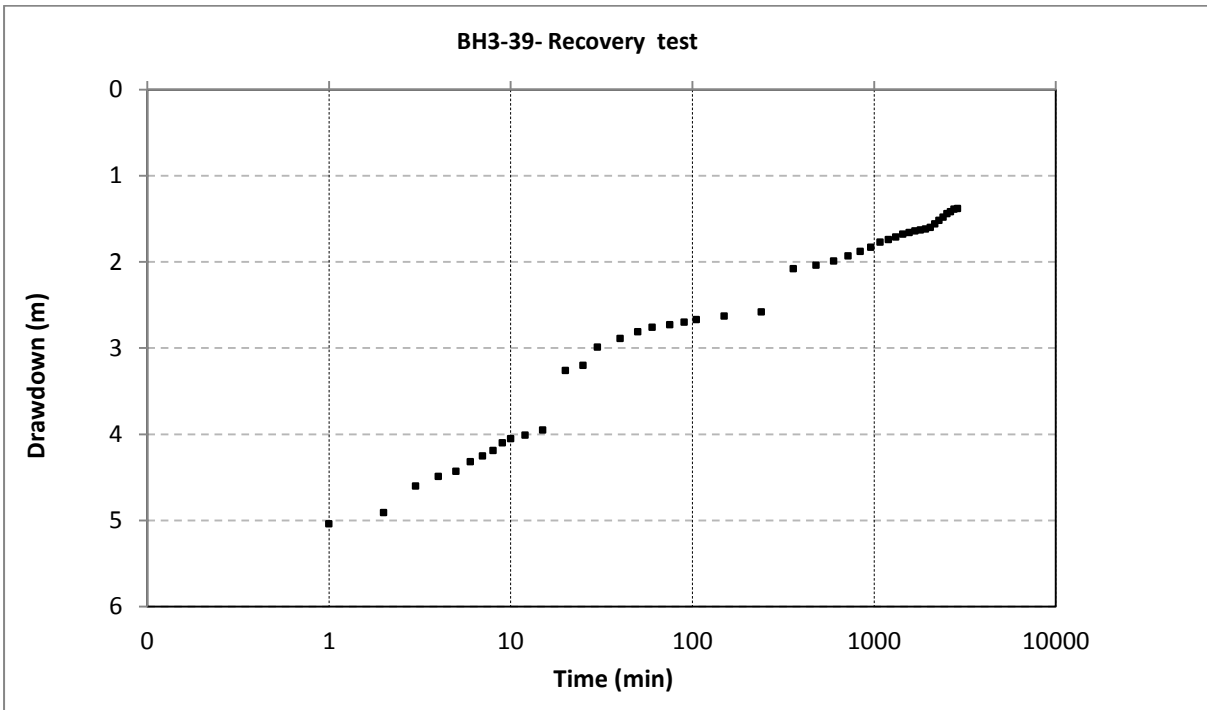


Figure 4-7: Recovery after constant rate pumping at BH3-39

4.4.4.1 Drawdown in observation boreholes

Significant drawdown in observation boreholes was noted after 8 hours of pumping. Figure 4-8 is a plot of drawdown observed in monitoring boreholes during constant rate pumping of borehole BH3-39. Observation boreholes located along lithology strike namely, MH3-1, MH3-3 and MH3-5 had quicker response to pumping than MH3-2, MH3-4, MH3-6B located across the lithology strike.

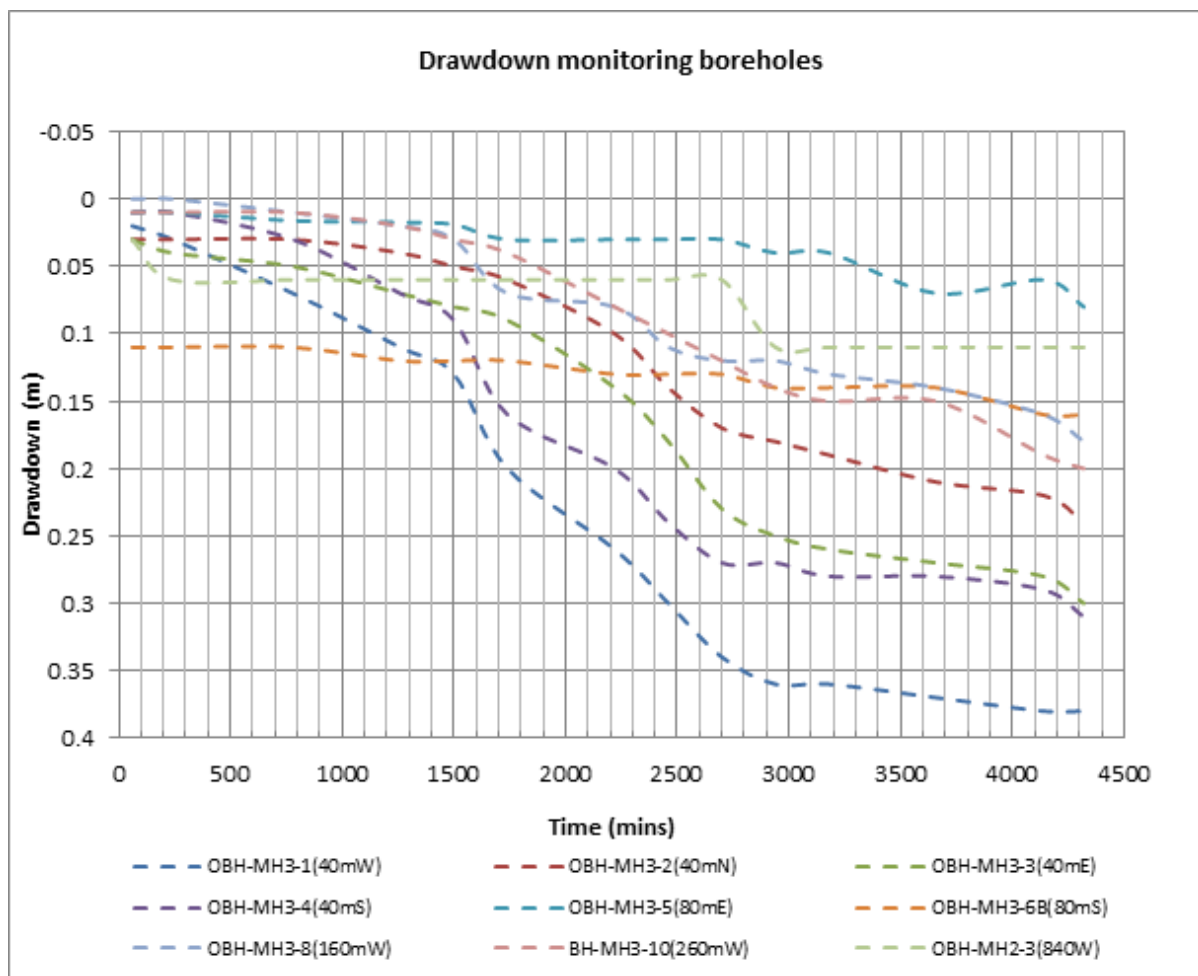


Figure 4-8: Drawdown observed in monitoring boreholes during constant rate pumping of borehole BH3-39

4.4.5 Aquifer hydraulic testing summary

Although the three day aquifer hydraulic testing at borehole BH3-39 provided initial estimates of aquifer hydraulic parameters for the Roan aquifer, the pumping rate of 144 m³/hr was insufficient to stress the aquifer in order to get more reliable aquifer response to pumping.

Nevertheless, the aquifer hydraulic testing results can be used to extrapolate required pumping rates to dewater the mine.

4.5 Hydrochemical sampling

4.5.1 Introduction

Dissolved constituents in the water provide clues on its geologic history, the soil and rock masses through which it has passed, and its mode of origin within the hydrologic cycle. Therefore the source and its flow path can be traced using water chemistry, provided the characters revealing this can be reliably discriminated (Freeze and Cherry 1979). Measurements of temperature, PH, total dissolved solids (TDS), electrical conductivity (EC), dissolved ions, dissolved oxygen, and careful use of isotopes, provides adequate data to carry out hydrochemical analysis (Fetter 1999). As such, in order to provide a geochemical snapshot of Ruashi Mine, all accessible groundwater points were sampled during the drilling and testing programme.

4.5.2 Field measurements

Handheld electrical conductivity (EC), temperature and pH meters were used to measure field physicochemical parameters. EC values range from 5.7 mS/m to 556 mS/m. Conductivity higher than 556 mS/m was recorded only at borehole GWS2, located close to the Return Water Dam. Values of pH values range from 5.32 to 8.17.

4.5.2.1 Groundwater sampling

A total of 24 boreholes were sampled and the water samples were couriered to Regen Laboratory in South Africa for analysis. Equipped boreholes were sampled through breather pipes installed on the discharge line. Unequipped boreholes were sampled using a submersible bladder pump. Monthly sampling of wells located on the perimeter of the Tailings Storage Facility (TSF) is done by Ruashi Mine Environment department. The groundwater and surface water samples are analysed at CRAA Laboratory in Lubumbashi. Daily pH monitoring is undertaken at the TSF, Storm Water Dam, Coffey Dam, Plant process water line and the Return Water Dam.

In order to assess the accuracy of hydrochemical analysis from Regen Laboratory, water quality analysis results were imported into WISH (Windows Interpretation System for Hydrogeologists) and PhreeqC Geochemical Modelling softwares. WISH and PhreeqC were used to determine electro-neutrality by calculating the charge balance for each sample. The Regen Laboratory analysis percentage error in electro-neutrality of 3.8% was deemed acceptable. Hydrochemical analysis results are presented in Table 4-7.

Table 4-7: Ruashi hydrochemistry (Value of -1.00 denotes parameter was not analysed by Laboratory)

Site Name	pH	EC mS/m	TDS mg/l	Ca mg/l	Mg mg/l	Na mg/l	K mg/l	Palk mg/l	Malk mg/l	Cl mg/l	SO4 mg/l	NO3-N mg/l	F mg/l	Fe mg/l	Mn mg/l	HCO3 mg/l	Cu mg/l	Co mg/l	Zn mg/l
BH3-39	8.08	17.30	-1.00	3.80	16.90	4.61	3.16	0.00	94.00	3.00	7.10	0.11	0.48	0.87	2.61	94.00	0.02	0.13	0.03
MH3-1	7.84	25.80	-1.00	11.40	21.00	9.80	2.00	0.00	122.00	4.00	23.10	1.10	0.73	0.49	5.31	122.00	0.06	0.19	0.03
MH3-2	8.17	28.20	-1.00	24.00	22.00	3.80	2.80	0.00	157.00	3.00	6.90	0.66	0.23	0.07	0.03	157.00	0.04	0.00	0.02
MH3-3	7.94	21.70	-1.00	21.50	31.00	2.50	1.20	0.00	193.00	2.00	1.00	0.29	0.28	0.00	0.00	193.00	0.00	0.00	0.04
MH3-4	7.76	25.80	-1.00	11.40	20.00	10.30	2.00	0.00	128.00	4.00	24.20	1.30	0.79	0.49	5.14	128.00	0.06	0.18	0.02
MH3-6	7.88	27.90	-1.00	18.00	26.00	3.90	2.40	0.00	151.00	4.00	6.20	0.60	0.40	0.00	0.05	151.00	0.01	0.00	0.07
MH3-6B	8.01	37.10	282.00	32.80	26.00	10.40	6.10	0.00	178.00	8.00	38.10	1.20	0.69	1.43	-1.00	178.00	-1.00	-1.00	-1.00
MH3-8	7.46	10.00	78.00	11.60	4.00	4.00	1.00	0.00	40.00	3.00	14.20	0.72	0.23	-1.00	-1.00	40.00	-1.00	-1.00	1.00
MH3-9	7.48	5.89	50.00	2.80	6.00	3.40	0.50	0.00	24.00	3.00	12.50	-1.00	-1.00	0.03	-1.00	24.00	-1.00	-1.00	1.00
MH3-10	7.89	27.40	178.00	21.20	25.00	3.60	2.10	0.00	159.00	3.00	8.10	-1.00	0.35	-1.00	-1.00	159.00	-1.00	-1.00	-1.00
MH1-3	7.86	23.60	174.00	15.90	17.00	13.90	2.40	0.00	116.00	4.00	28.60	0.68	0.46	0.20	-1.00	116.00	-1.00	-1.00	-1.00
MH2-1	7.42	13.50	88.00	11.80	8.00	5.30	1.20	0.00	57.00	4.00	15.50	0.60	0.31	0.03	-1.00	57.00	-1.00	-1.00	-1.00
MH2-2	7.29	43.30	282.00	42.30	18.00	7.60	4.20	0.00	85.00	5.00	114.00	1.20	0.89	-1.00	-1.00	85.00	-1.00	-1.00	-1.00
GWD5	6.66	31.60	216.00	5.10	5.00	61.10	0.50	0.00	116.00	19.00	40.30	-1.00	0.26	0.16	-1.00	116.00	-1.00	-1.00	-1.00
GWD6	7.20	14.60	94.00	16.10	7.00	3.20	1.60	0.00	49.00	4.00	23.10	0.80	0.38	0.03	-1.00	49.00	-1.00	-1.00	-1.00
GWD7	7.51	25.80	168.00	25.2	16.00	4.90	2.70	0.00	110.00	4.00	33.90	-1.00	0.26	0.03	-1.00	110.00	-1.00	-1.00	-1.00
GWD8	7.61	13.50	90.00	11.90	8.83	4.48	1.08	0.00	60.00	4.00	15.30	0.46	0.24	-1.00	-1.00	60.00	-1.00	-1.00	-1.00
BH1-16	7.95	35.60	230.00	28.00	31.70	1.86	1.54	0.00	195.00	3.00	20.40	0.60	0.38	-1.00	0.05	195.00	-1.00	-1.00	0.02
BH1-17	8.00	36.50	232.00	30.50	30.20	2.82	1.66	0.00	192.00	4.00	12.70	1.50	0.23	0.02	0.02	192.00	-1.00	0.11	0.04
MH2-5	7.70	23.00	148.00	19.9	15.10	2.90	2.18	0.00	109.00	4.00	8.90	1.80	0.28	0.02	0.09	109.00	0.01	0.07	0.04
GWS1	5.70	5.70	38.00	2.06	0.78	7.47	0.31	0.00	10.00	4.00	10.80	-1.00	-1.00	0.01	0.05	10.00	0.03	0.01	0.04
GWS2	5.32	556.0	4844.00	57.40	32.30	1339.0	1.43	0.00	15.00	37.00	2750.00	-1.00	0.92	0.01	2.37	15.00	0.06	0.70	0.26
GWD3	5.84	6.40	40.00	1.51	0.54	9.42	0.10	0.00	11.00	3.00	11.10	0.50	0.22	0.02	0.03	11.00	-1.00	-1.00	0.03
GWD4	5.72	10.40	60.00	4.55	1.62	10.50	0.93	0.00	13.00	2.00	25.40	0.39	1.00	0.01	0.10	13.00	-1.00	0.03	0.07

4.5.3 Water quality summary

A summary of the hydrochemical analysis of the 24 samples collected is given below:

- Sulphate concentration is <40 mg/L for most boreholes, with a high value of 114 mg/L recorded in borehole MH2-2;
- Borehole GWS2 recorded elevated Sodium (Na), Chloride (Cl) and Sulphate (SO₄) concentrations compared to the rest of the boreholes;
- Chloride is generally low in most boreholes with concentration of approximately 4 mg/L. However, a relatively elevated concentration of 19 mg/L in GWD5 located at TSF perimeter was noted;
- The average Bicarbonate concentration for the 24 samples is 99 mg/L;
- The average Calcium and Magnesium concentration for the 24 samples is 45 mg/L and 35 mg/L respectively.

4.6 Groundwater levels

Groundwater monitoring at Ruashi Mine began in September 2009. All boreholes identified during the hydrocensus and recently drilled boreholes were included in the monitoring network. It was noted that groundwater levels continued to decline after the end of each rainy season. A general groundwater level decline trend for most of the non-pumping boreholes was noted during the months of May and June 2011. On 27 May and 28 May 2011, pumping began at BH1-15 and BH1-17A respectively and induced water level decline by about 10m in boreholes BH1-9 and BH1-10 located at about 15 m away from the pumping boreholes in Pit 1. The pumping at these two boreholes was stopped on 29 May 2011 resulting in water level recovery by about 9 m.

Water levels were not measured in pumping boreholes that were not equipped with piezometric tubes. Rainfall data, abstraction volumes and groundwater level monitoring data for Pit 1, Pit 2, Pit 3 and the TSF was used to plot graphs presented in Figure 4-9, Figure 4-10, Figure 4-11 and Figure 4-12. In general water levels follow topography closely. Water levels in the pits area were interpolated and a plot of water level with respect to pit floor elevation was produced (see Figure 4-13).

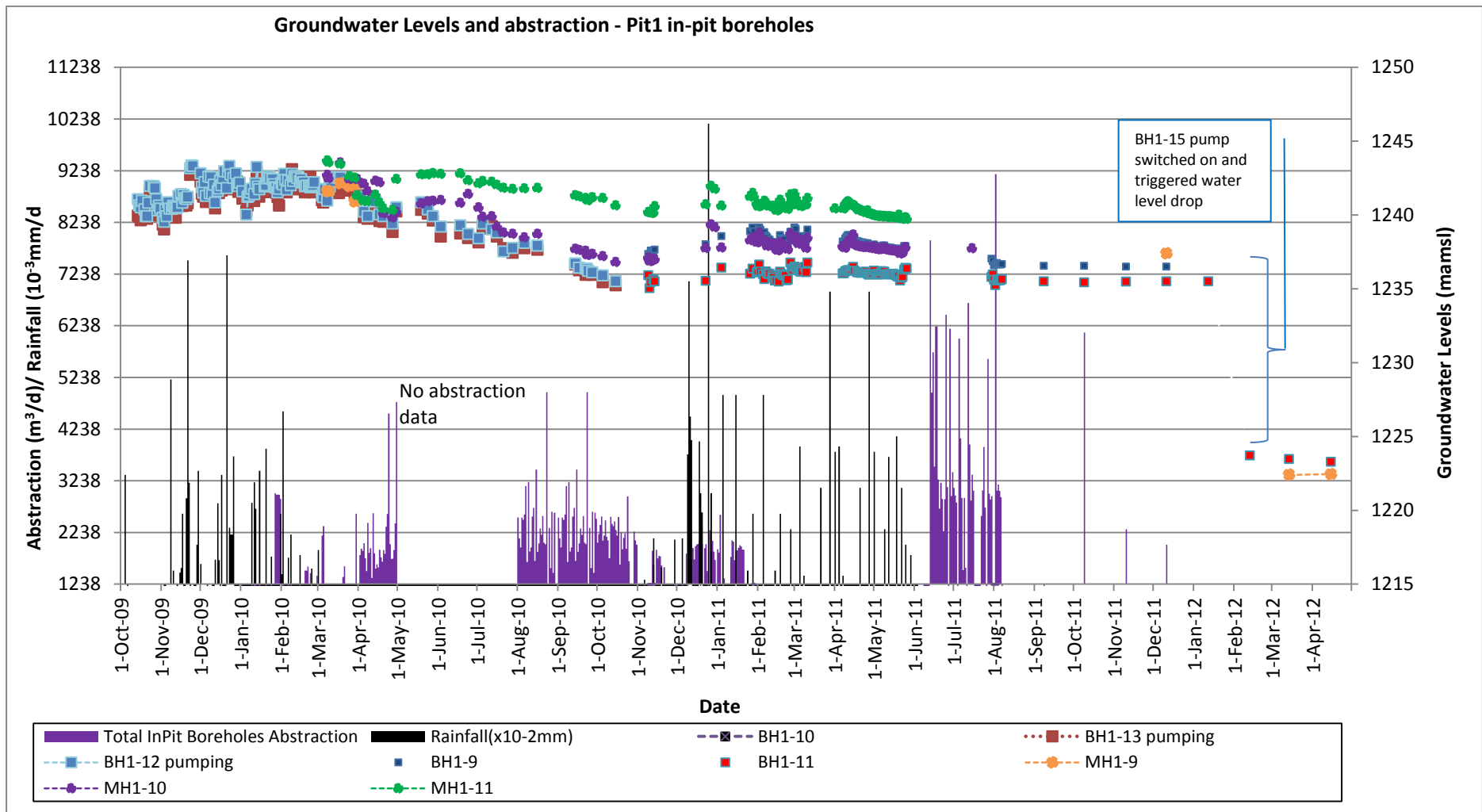


Figure 4-9: Declining water levels in Pit 1

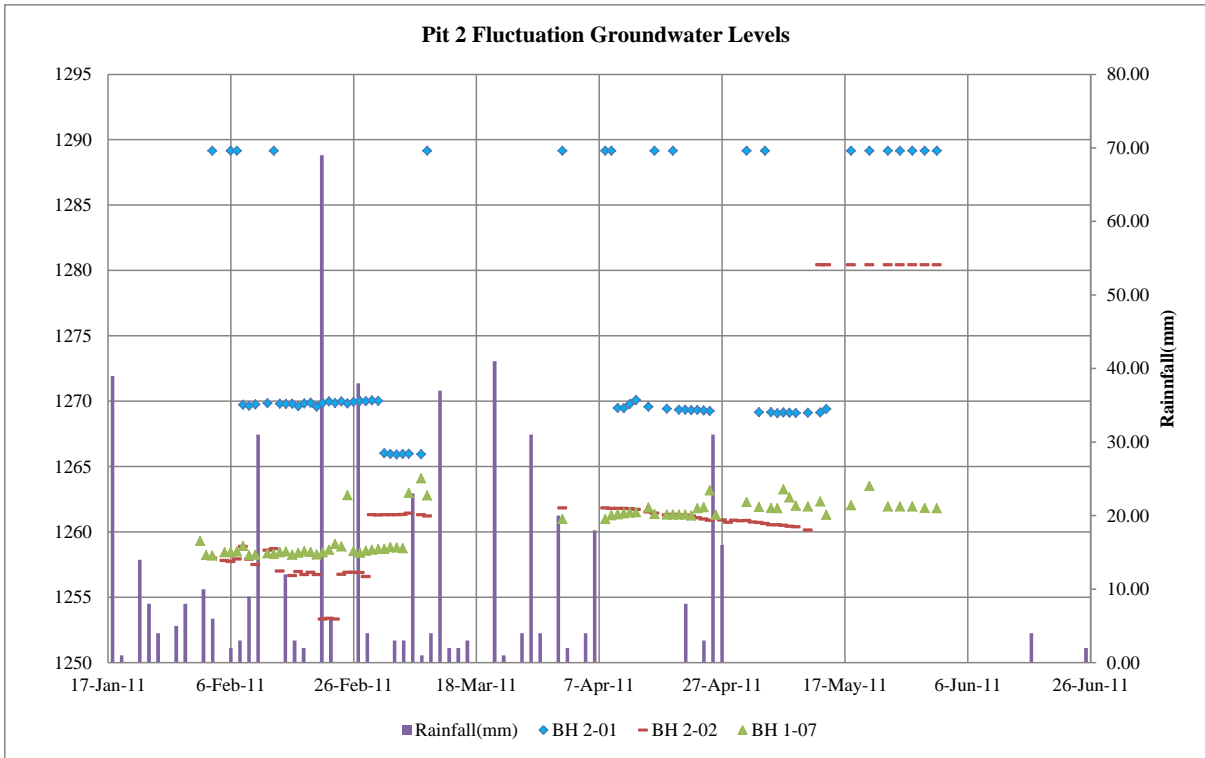


Figure 4-10 : Fluctuating groundwater levels in Pit 2

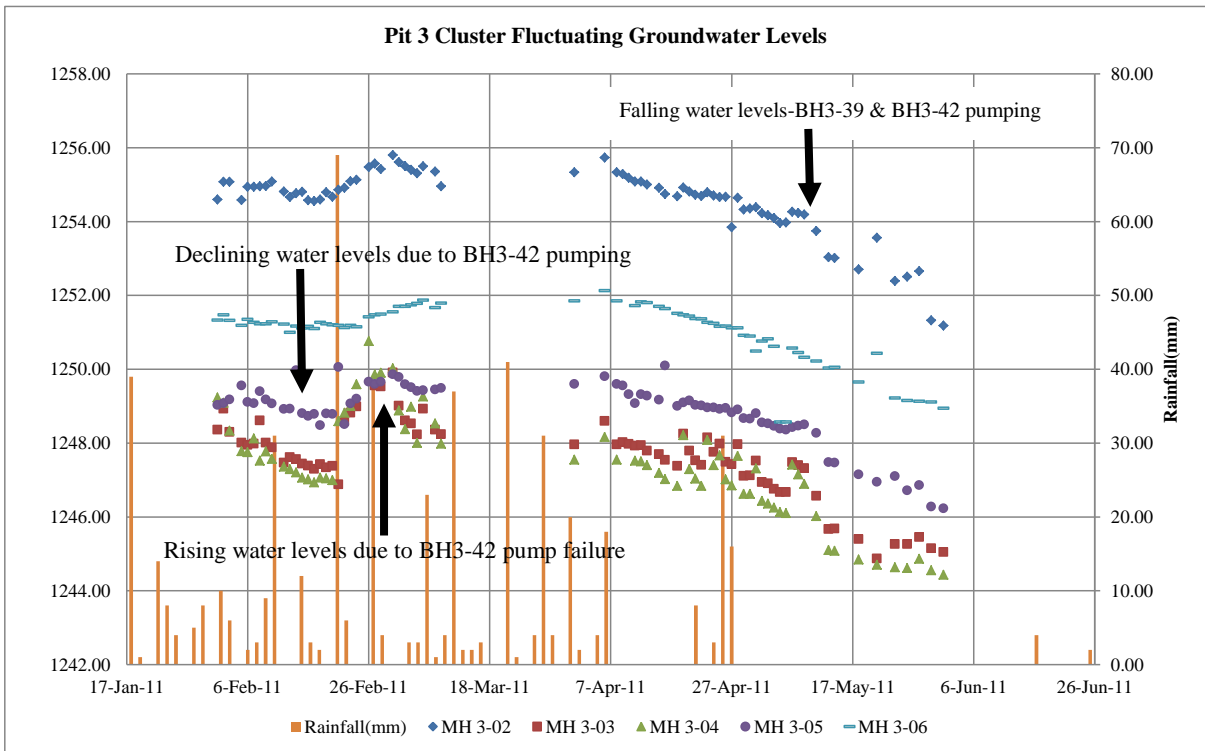


Figure 4-11 : Fluctuating groundwater levels in Pit 3

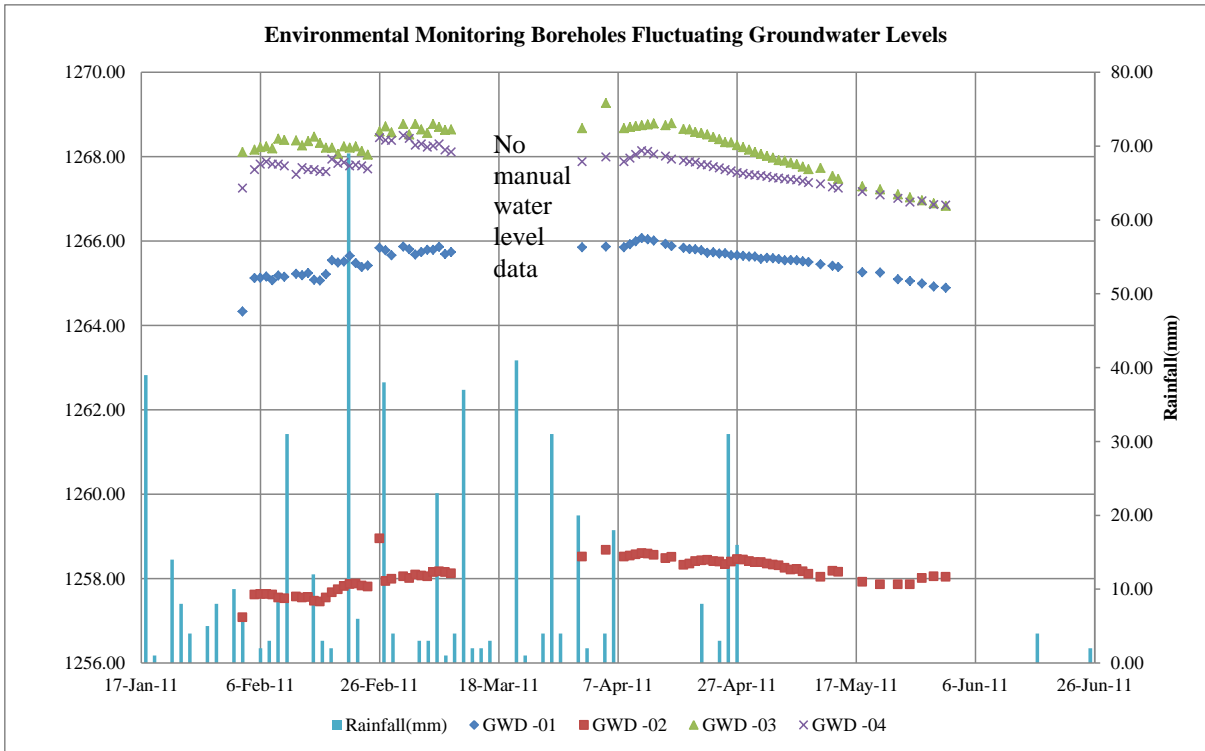


Figure 4-12: Fluctuating groundwater levels observed in boreholes located along TSF perimeter

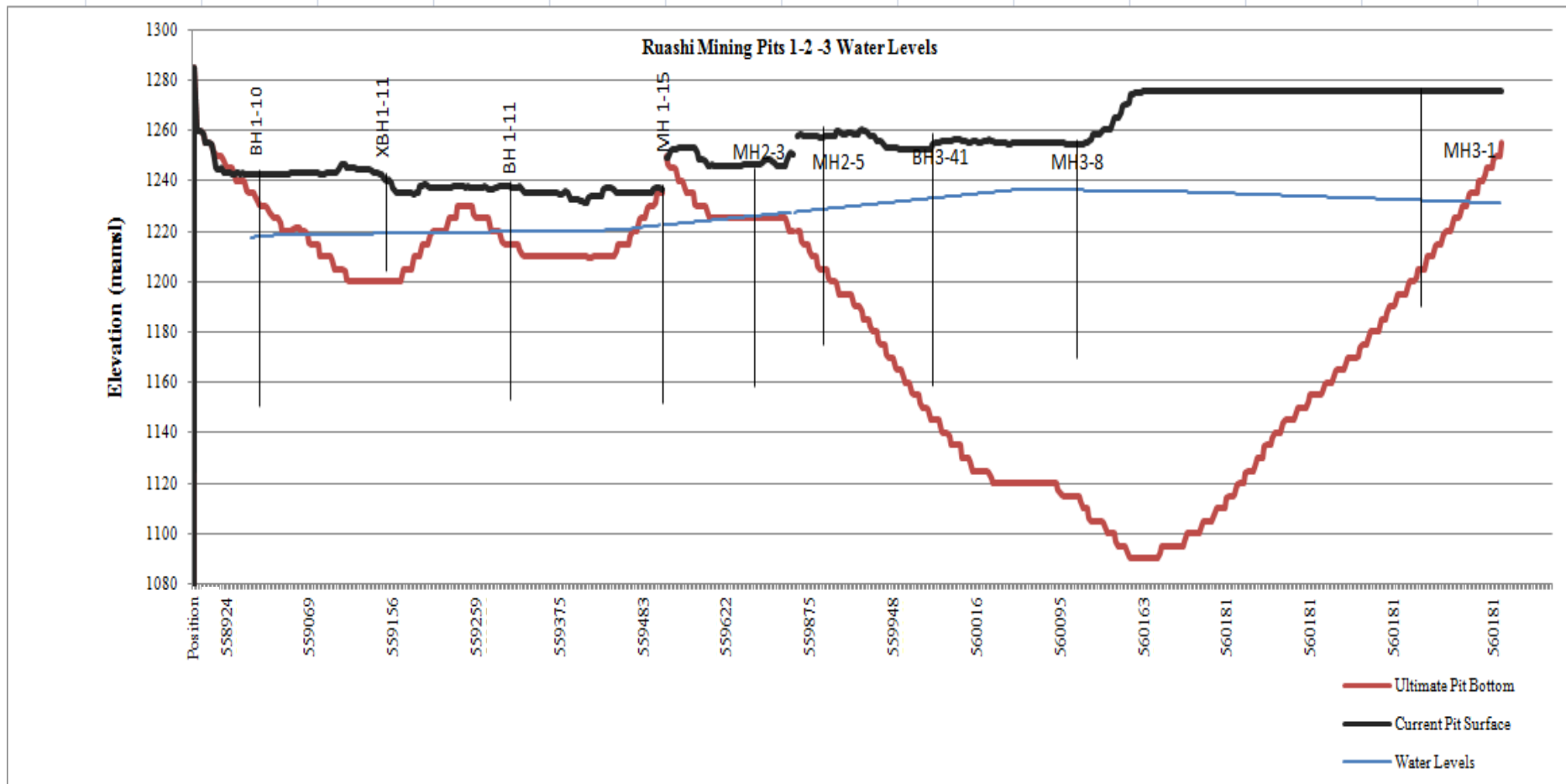


Figure 4-13: Ruashi water levels with respect to pit floor levels-February 2012

In general, the following trends were noted:

- Water levels showing continuous rise at the start of each rainfall season;
- Water levels showing a decline before the rainfall season, levelling off and showing water level rise from following heavy rains in mid-December to March of each year (2010-2012);
- Water levels showing fluctuations in boreholes located at the TSF perimeter. Shallow groundwater levels of less than 5 mbgl and sharp groundwater level rise in GWD3 during episodes of increased recharge from TSF;
- Water level decline in the pits due to pumping. The pumping induced the reversal of groundwater flow direction in the area between the TSF and the pits.

4.7 Groundwater abstraction

Groundwater abstraction volumes through the pumping boreholes were recorded. However, there is limited groundwater level data gathering from pumping boreholes because most of boreholes are not equipped with piezometric tubes through which a dipper can access the water levels. For much of the year 2011, the Regideso (Water Supply Authority) boreholes, BH2-7 and BH1-5 were pumping an average of 3 500 m³/d. These boreholes supplied the Regideso Tank for a period of 18-24 hours a day. During 2011, the discharge from the Regideso Tank to the community averaged 3 400 m³/d.

A summary plot of pumping and delivery volumes to Regideso Tank and Plant is presented in Figure 4-14.

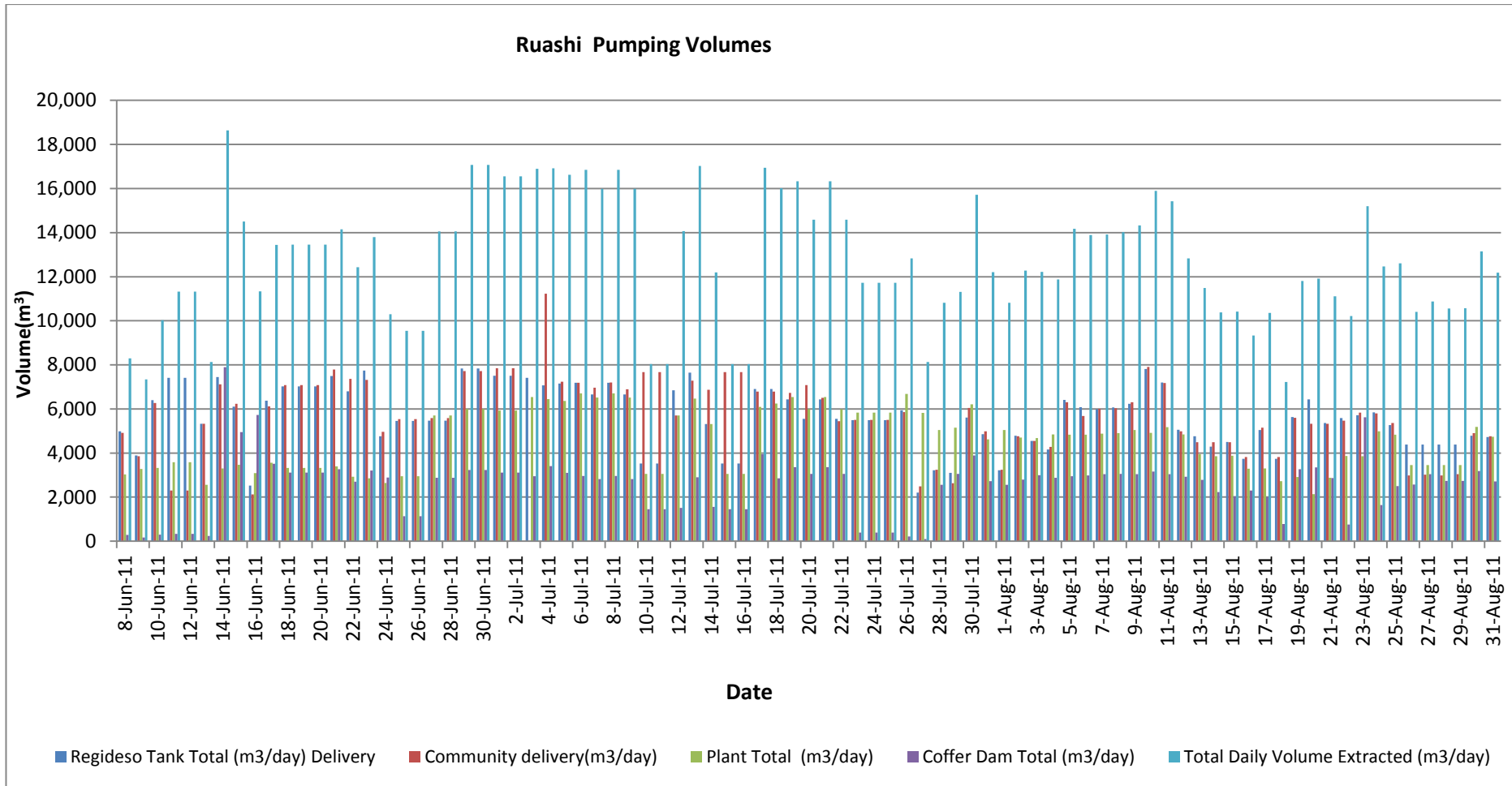


Figure 4-14: Daily pumping volumes for Regideso Tank, Plant and Coffer dam delivery boreholes

4.8 Field data collection summary

The field data collection exercise was important in providing key information to be used in the construction of conceptual hydrogeological model for the mine. The hydrocensus gave a framework on which planning for drilling and aquifer hydraulic testing was based. A total of 14 emergency dewatering and community supply boreholes were drilled in the pits area, whilst 34 boreholes were added to the existing groundwater monitoring network. Dolomitic shale (SDS) was the most common rock type intersected while BOMZ and RAT were noted in a few boreholes. Weathering is limited to approximately 120 mbgl. The deep Roan aquifer is anisotropic in character as proven by the variation in the depth of water strikes encountered. Water levels in the shallow aquifer vary from 1.02 to 17 mbgl. Water levels for the deep aquifer vary from 15.23 to 62.5 mbgl. Groundwater gradients vary from 0.005 close to the TSF and 0.03 towards the open cast pits.

Aquifer hydraulic testing was conducted at pumping borehole BH3-39 at a constant rate of 144 m³/hr. Drawdown was observed in nine groundwater monitoring wells located at various distances from the pumping borehole. Twenty-four (24) samples were collected from different boreholes for hydrochemical analysis.

The next chapter discusses the results of the field programme. It includes interpretation of borehole drilling data presented as lithology cross sections, interpretation of aquifer hydraulic testing data and estimation of aquifer hydraulic parameters.

5 CONCEPTUAL HYDROGEOLOGICAL MODEL

5.1 General

In order to establish why the problem of high volume water inflow into Ruashi Mine exists, it was essential that a clear understanding of the hydrogeological regime be obtained. Once the hydrogeological regime has been understood, a conceptual model of groundwater flow can be developed. Hydrogeological model conceptualisation is a process in which data describing field conditions are assembled in a systematic way to describe groundwater flow processes at a site.

The data gathered during the field investigation phase was used to develop a conceptual hydrogeological model for the mine. Piezometric maps drawn using mine records and current water level measurements gave an insight into the behaviour of groundwater flow regime with time and depth of mining. Groundwater chemistry gave the means through which groundwater flow paths and aquifer connectivity could be defined.

The conceptual model forms the basis for understanding groundwater occurrence and flow mechanisms and feed into numerical groundwater flow modelling which culminates in the simulation of mine pit inflows. The conceptual model aids in determining the modelling approach and choice of numerical modelling software. The conceptual model is discussed below.

5.2 Geology

5.2.1 Drilling findings

Siliceous Dolomitic Schist (SDS) is the predominant rock type intersected by the deep boreholes. The weathered and altered dolomite referred to as Black Ore Mineralised Zone (BOMZ) occurs as compartments predominantly within the SDS. Boreholes drilled in the Pit 3 area intersected Laterite underlain by Roches Argillaceous Talceus (RAT) breccia. Below the RAT breccia is 15-20 m thick RAT layer which in turn is underlain by 40-80 m thick SDS. Below the SDS underlies Sandstone, Siliceous Rock with Cavities (RSC) or Foliated Siliceous Rock (RSF). The actual thickness of the Sandstone, RSF and RSC could not be established as all boreholes are shallower than 500 m.

Boreholes in Pit 2 intersected CMN, siliceous dolomitic Siltstone and BOMZ. High blow yield in the BOMZ resulted in back-pressure and subsequent reduced penetration rates. The RAT breccia in Pit 2 is about 15 m thick. The RAT breccia is underlain by an about 29 m thick hard, quartzitic, vuggy, grey to cream talcose Shale. Below the talcose Shale is highly

weathered and fractured quartzitic Siltstone which extends to a depth of about 54 m. The Siltstone is iron stained along fractures, indicating probable groundwater flow channels. The Siltstone in Pit 2 is characterised by large cavities mostly encountered at 39-45 mbgl, with rock fragments of diameters of up to 5 cm blown out of boreholes during drilling. These cavities could be related to old mine workings (as per communication with Ruashi Mine Geologists). Coarse grained Sandstone was encountered from 54 to 64 mbgl, overlying fractured and occasionally quartzitic black Shale from 64 to 79 mbgl. The lithology bedding planes, fractured and weathered zones could probably be preferred groundwater flow channels. The degree of fracturing and weathering determine the size of groundwater bearing compartments as evidenced by abrupt yield changes and differences between adjacent rock formations.

Boreholes in Pit1 intersected mainly boudinaged SDS, RSC and RSF and compartments of BOMZ. Difficult drilling conditions were encountered in the collapsing zones of the loose BOMZ. The presence of boudins and fractures could indicate that periods of folding and associated faulting could have pushed the less permeable and older formations, like the RAT closer to ground surface. The older rocks like RAT were not intersected in Pit 1 as they could have been eroded.

5.2.2 Weathering and fracturing

Weathering and associated alteration was encountered from ground surface to depths of approximately 80 mbgl in most boreholes. Fracturing was encountered at various depths between ground surface and 200 mbgl. It was also noted that fracturing and weathering was associated with contact zones and bedding planes.

5.2.3 Stratigraphy

The rocks underlying Ruashi Mine belong to the Katangan system. The Katangan system is composed of sedimentary rocks of the late Proterozoic era, a succession of interbedded Quartzites, Sandstones, Conglomerates, Shales, Siltstones, Dolomites, Limestones, Argillites and dolomitic Shales. These rocks are subdivided into two broad groups namely the younger Kundelungu series and older Roan Series. According to Maarten and Muechez (2011) these sedimentary rocks were deposited (possibly around 820 million years (Ma)) in an intra-continental rift followed by a proto-oceanic rift system that finally evolved into a syn- to post-organic sequence. Locally the system consists of Kundelungu series overlain by Roan series. Table 5-1 presents Ruashi stratigraphy. The thickness of each lithology was estimated from results of the percussion drilling phase of this research, geotechnical drilling and previous reports on the Katangan System.

Table 5-1: Ruashi stratigraphy

Series	Formation Group	Lithology	Thickness (m)
Kundelungu	Upper Kundelungu	Diamictites overlying Shale, dolomitic Shale, sandstone and minor Limestone	15-80
	Laterite	Weathered ferruginous Laterite	2-50
ROAN	RGS	Massive to stratified Dolomite	60-130
	CMN	Talcose Dolomite with Shale	0-20
	BOMZ	Weathered and altered Dolomite	0 -20
	SDS	Dolomitic Shale with graphite bands	50 - 80
	SDB	Dolomitic Shale/Siltstones with minor carbonate bands	10 - 15
	RSC	Massive to vuggy silicified Dolomite	12 - 25
	RSF	Fissile Dolomite siliceous/dolomitic Shale	+5
	DSTRAT	Variably stratified Dolomite	+15
	RAT	Dolomitic, sandy argillaceous, talcose Dolomite	20-60

5.2.4 Structure

The major structure at Ruashi Mine is an overturned syncline. The fold and faulting structures in the Lufilian Arc, along which Ruashi Mine lies, were formed during the Lufilian orogeny (Maarten and Muchez, 2011). The Lufilian Arc defines a large arcuate orogenic belt containing sediments of the Katanga Supergroup. Maarten and Muchez (2011) noted that during the Lufilian orogeny (600-500 Ma) the Katanga Supergroup and Basement were deformed together. The Katanga sediments were pushed over the Basement and movement was predominantly in the ENE direction. This is evidenced by boudins present in the SDS with an approximately NE orientation and well preserved in the orientations of the discontinuities at the mine.

Faults are evident on the pit walls and are associated with small shear zones that could have brecciated the RAT, which is predominant along the Pit 1-Pit 2 boundary. The faults dip steeply to the south at approximately 70° to sub-vertical and created a heavily fractured zone

called a brecciated zone which forms the contact between the Roan and Kundelungu series.

The major joints trend approximately N135⁰ and are mainly open providing excellent channels for water transfer between formations (Maarten and Muchez 2011). Where closed they are in-filled with mainly carbonates, vein quartz, clay and secondary minerals. These joints represent typical tension joints.

Maarten and Muchez (2011) stated that preliminary analysis of structural geology suggests sinistral movement over a long period of time. Both ductile and brittle forms of deformation exist and can be seen clearly in the excavated mine pit walls, all having orientation in harmony with the patterns of strain occurring in the ground between faults. If the ductile deformation occurred at depth and the brittle deformation at higher levels in the crust it can be argued that the area has been progressively strained during a long period of uplift. This phenomenon is supported by the presence of small faulted folds.

5.3 Groundwater occurrence

5.3.1 General

The shallow Laterite aquifer was intersected in most boreholes drilled except for boreholes inside the pits where the pit excavation level was deeper than the base of the Laterite. Significant quantities of groundwater were noted at the base of the Laterite and at a shallower depth towards Luano and Kebumba Rivers and their associated flood plains (as noted in boreholes GWD2 and GWD3). The alluvial aquifer is widespread on the north-eastern side of Ruashi property except in the high lying ground.

The deep water bearing zones are controlled by the lateral and vertical distribution of the deeper fractures, weathering and lithology contact zones in Roan Formation. Mostly seepage and very low yields were noted in the Laterite and RAT while high yields were recorded in the lower lying SDS, RSC and RSF proving the presence of localized, poorly developed and well developed anisotropic aquifers. Based on the blow yields recorded during drilling, the most prolific aquifer in the area was identified to be the SDS.

5.3.2 Water strikes

The majority of boreholes intersected significant quantities of groundwater at depths between 20 and 30 mbgl. The shallowest water strikes (less than 5 mbgl) were encountered in boreholes (GWD1, GWD2, GWD3 and GWD4) located on the Tailings Storage Facility (TSF) perimeter. These shallow groundwater strikes could be related to continuous recharge

from the TSF. Water strikes in the deep boreholes were encountered at depths ranging from 22.5 mbgl to 235 mbgl. Multiple water strikes (but low yielding) were associated with the shallower Kundelungu Formation between 5 and 40 mbgl. High yielding water strikes were encountered mostly within the Roan Formation between 35 and 220 mbgl. A plot of water strike frequency with depth is presented in Figure 5-1.

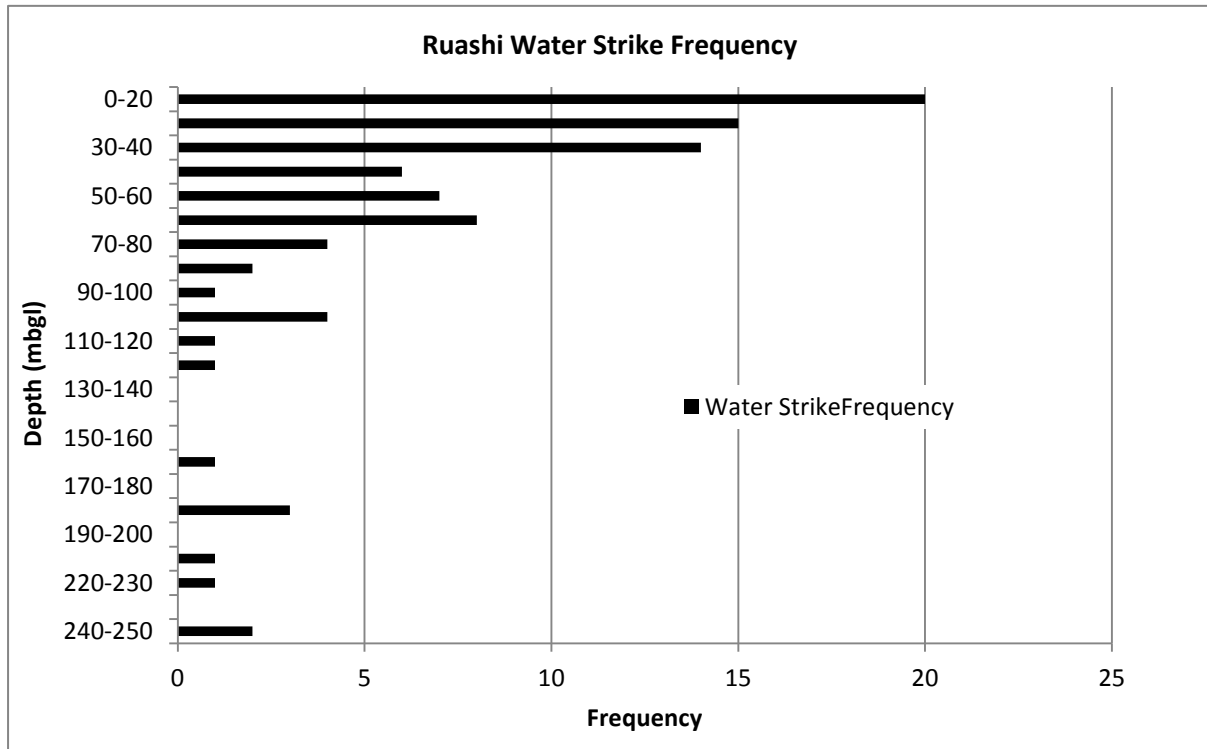


Figure 5-1: Water strike frequency recorded during drilling campaign

The total number of water strikes represents the total count of water strikes recorded in 48 boreholes during the drilling stage. This plot is necessary to clearly show the distribution of water strikes with depth. The frequency distribution of water strike with depth indicates the highest frequency at depths shallower than 20 mbgl. However the frequently occurring water strikes at depths shallower than 20 mbgl can be interpreted to be the water table. The deep aquifer shows water strike frequency spread throughout the depth range confirming the anisotropic character of the aquifer.

5.3.3 Blow yield

Low blow yields (less than 10 m³/hr) were associated with the shallow aquifer. In contrast, high blow yields ranging between 20 and 396 m³/hr were measured in the deep boreholes. The Laterite and Kundelungu aquifer average blow yield was 10 m³/hr. Blow yields for the Roan aquifer ranged between 15 and 396 m³/hr. The highest blow yield (396 m³/hr) was

recorded in the deepest pumping borehole (BH3-39). The final blow yield at BH3-39 indicated the presence of high yielding SDS aquifer. In general, blow yield increased with depth as presented in Figure 5-2, a plot of blow yield recorded during drilling at BH2-4. The bars in purple colour represent the yield contribution for a particular depth range. The sky blue colour bars combined with the purple bars combined represent the cumulative blow yield.

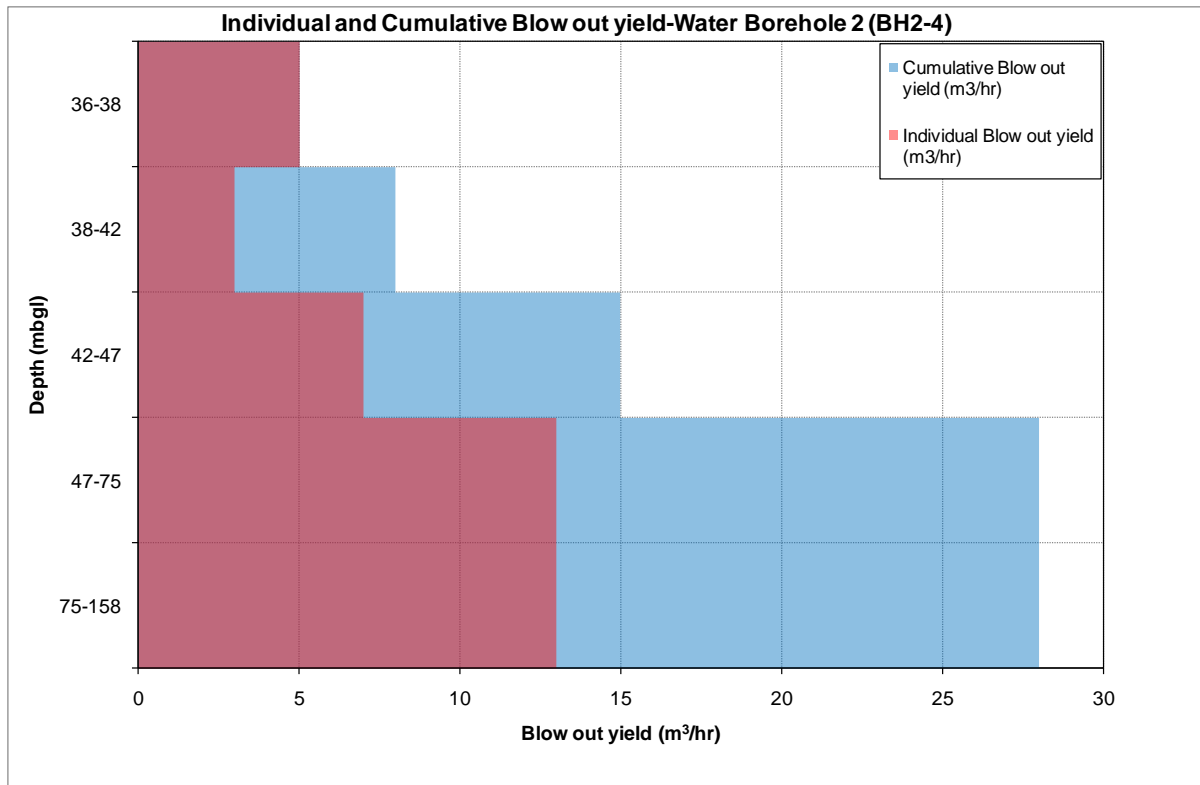


Figure 5-2: Blow yield increase with depth recorded at BH2-4

Drilling results from the deep boreholes indicated that much of the water was yielded from the extensively fractured SDS. Preliminary drilling results had suggested that the RAT was an aquiclude. Remarkably, groundwater albeit low quantities were recorded in the RAT encountered at borehole BH3-39. The distribution of “water strikes” and associated blow yield in the RAT is evidence of the presence of groundwater and can thus be used as a semi-quantitative assessment of whether the RAT unit is a potential aquifer or aquitard. The blow yield recorded in the RAT suggested that this unit is somewhat permeable and not necessarily an aquitard.

5.4 Aquifer hydraulic parameters

5.4.1 Estimating aquifer hydraulic parameters

Single well aquifer tests provide reliable aquifer transmissivity estimates. Storage coefficient estimates are made from observation of drawdown in monitoring boreholes placed at various distances from the pumping well. This is only true for observation wells fully penetrating the aquifer. Multi-borehole tests improve the level of confidence in the transmissivity and storage coefficient estimates. Single-borehole aquifer tests are frequently analysed with the Cooper-Jacob equation (1946) due to its simplicity. In applying the Cooper and Jacob straight equation (1946) method it was assumed that radial and horizontal flow existed (Van Tonder and Dzanga (2002)). The Cooper Jacob equations (Equation 5-2 and Equation 5-3) used for calculating aquifer transmissivity and storage coefficient are given by:

$$T = \frac{2.3Q}{4\pi\Delta s} \quad \text{(Equation 5-1)}$$

$$S = \frac{2.25Tt_0}{r^2} \quad \text{(Equation 5-2)}$$

Where:

Δs is the gradient of the straight line fit on the drawdown against time semi-log plot

r is the distance of the piezometer from the pumped well (m); t is the time since pumping has started (days);

Q is the constant well discharge (m^3/d);

T is aquifer transmissivity (m^2/d) and S is the aquifer storativity.

When a line is extended until it intercepts the time axis in where $s(r, t) = 0$ (the interception point will have the coordinates $s(r, t) = 0$ and $t = t_0$, t_0 is used in the equation to determine S).

The Cooper Jacob and Theis equations are incorporated in WISH software into which aquifer hydraulic testing results were imported. The analysis gave the values as follows:

- The Cooper Jacob method estimated transmissivity of the Roan to be $256 \text{ m}^2/\text{d}$
- The Theis method estimated transmissivity of Roan as $295 \text{ m}^2/\text{d}$ and storage coefficient of 2.2×10^{-3} .

When the observation borehole drawdown graphs are used, boreholes drilled into low permeable aquifer sections yield transmissivity estimates for the most prolific horizons. The spatial variance of aquifer hydraulic parameters gives the degree of heterogeneity of the aquifer system.

5.4.2 Groundwater flow phases deduced from aquifer hydraulic testing

Results of borehole BH3-39 constant rate pumping are plotted in Figure 5-3, a drawdown semi-log graph showing five distinct phases of groundwater flow. The constant rate test (CRT) graph plotted from drawdown results from the pumping borehole is typical of aquifers with double porosity response. The response is a result of an aquifer system consisting of high permeability and low storage in the fracture network. Conversely, the porous matrix is characterized by low permeability and high storativity. During early time, the fractures are dewatered as depicted by steep drawdown slopes. As pumping progresses, the matrix starts to contribute to the flow. The drawdown rate tends to decrease after this early time and the curve becomes flatter, representing increased flow from both fractures and matrix storage. As pumping progresses, fracture flow becomes depleted and only matrix flow would dominate, resulting in increased drawdown slope at late time.

Flow phase 1

During early pumping time, the plot shows typical Theis response when free water rapidly flows from fracture and well bore storage. The gradient of the graph dips sharply at the end of this phase as fractures are dewatered and all the well bore storage is pumped out.

Flow phase 2

The flow is slower at the beginning of the phase as dewatering of fractures continues. The graph flattens towards the end of the phase as radial groundwater flow from the Roan aquifer matrix becomes dominant. The bottom Roan aquifer material, namely the RSF and RSC have interconnected vugs which promote swift groundwater flow towards zones of lower hydraulic potential. Conversely the RAT and CMN lithologies retard groundwater flow as shown by delayed drawdown response in observation borehole MH3-2 which was constructed in the RAT. The flattening after the Theis response is reminiscent of unconfined or semi-confined conditions.

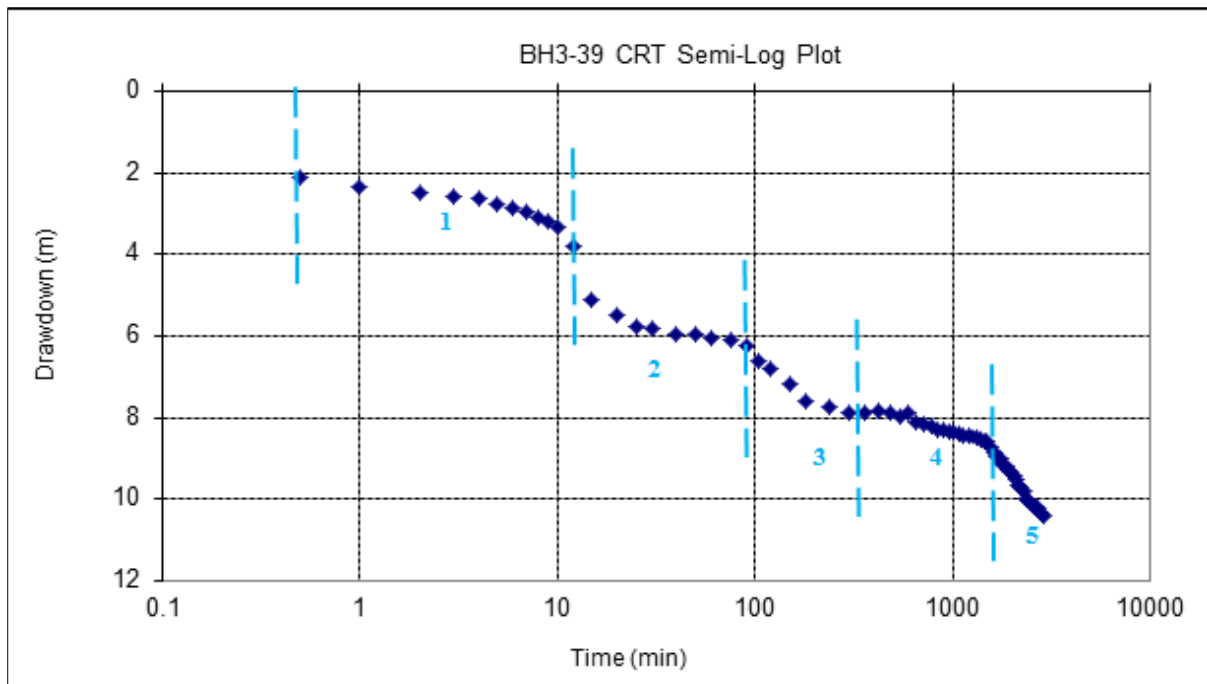


Figure 5-3: Semi-log plot of drawdown (linear scale) against time (log scale) showing groundwater flow phases 1 to 5 described in the paragraphs below this caption.

Flow phase 3

Phase 3 shows a steep drawdown response and could be due to dewatering of fracture at 29 mbgl and retarded flow from the RAT aquitard. The RAT has to some extent impermeable boundary effects which severely reduce groundwater flow towards the pumping borehole.

Flow phase 4

The curve shows radial acting flow indicating gradual increase of water flow from the SDS formation towards the pumping borehole.

Flow phase 5

Phase 5 shows steep dipping of the curve typical of low or no-flow boundary effects. The low flow effects could be due to low supply of groundwater from the highly hygroscopic RAT. These effects could have manifested in the plot if the aquifers were stressed by increasing the pumping yield to above 144 m³/hr. This was not possible as the pumping capacity could not exceed 144 m³/hr.

The aquifer testing results confirm the presence of near surface, slightly developed fracturing and weathering associated with the shallow Laterite and RAT breccia zones and the well-developed fracturing in deeper dolomitic aquifers of the Roan series. Zones of higher

transmissivity provide preferred groundwater flow paths and swift groundwater movement. Point dilution tests carried out by Groundwater Consulting Services (GCS) in 2005 estimated hydraulic conductivity values ranging from 0.31 to 1.22 m/d for the shallow aquifer. These low values confirm the limited aquifer development of the shallow aquifer. Hydraulic conductivity values ranging from 1.5 to 11 m/d, for the deep aquifer, confirm the presence of better developed fracturing.

5.4.3 Derivative flow characterisation

Derivative drawdown diagnostic plots are very sensitive to small changes in drawdown, thus can easily be used to identify the effects of hydrogeological boundaries and establishment of various groundwater flow regimes (Samani *et al.* 2006). Figure 5-4 is a derivative plot for BH3-39 constant rate pumping. The flow regimes that are clearly shown by the graph are positions of dewatered fractures. The derivative plot is a very effective tool in locating the positions of fractures, typically depicted by sinus wave forms. The derivative graph is decreasing at the position of fractures and increases after the fractures have been dewatered. The drawdown reached positions of fractures after 5, 85, 600 and 1 000 minutes of pumping. This means that the fractures identified by BH3-39 CRT are at 26.5, 29.7, 31.7 and 32 mbgl. The derivative plot also helps in understanding the rate of spread of the cone of depression.

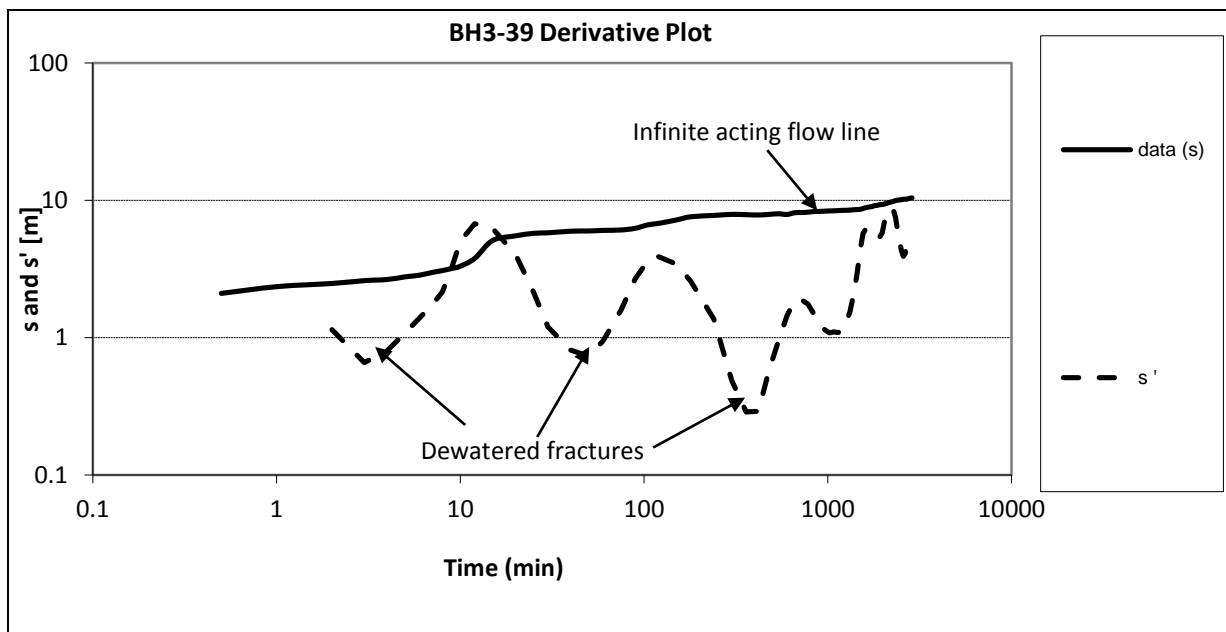


Figure 5-4: Derivative plot showing dewatered fractures

Well bore storage factors could not be clearly seen on the graphs and could be because the borehole had been pumping for at least 48 hours before the start of the aquifer hydraulic test.

In general, the dip in the derivative plot after well bore storage is often attributed to the double porosity behaviour or recharge boundary (Van Tonder 2001b). The transition period from the initial Theis response to the total system response is characterised by the dip in the drawdown derivative. The dip in the drawdown derivative after the initial typical Theis curve is due to the rapid release of water from the fractures. Radial acting flow is dominated by groundwater contribution from the matrix. The Cooper Jacob method for estimating aquifer hydraulic properties is accurately done by fitting a straight line on the radial acting flow period on a semi-log plot.

5.4.4 Aquifer diffusibility

The spread of the cone of depression in an aquifer system is governed by the equation $\frac{T}{S}$ (Equation 5-3), where T is the transmissivity and S is the storage coefficient of the aquifer. The extent of the cone of depression can also be defined by dividing the distance (r) of the observation borehole from the pumping borehole by the response time. The response time defines the time it takes for quantifiable drawdown to be measured in the observation borehole since the start of the pumping. Table 5-2, Table 5-3 and Figure 5-5 are aquifer diffusibility results from the pumping borehole and observation boreholes.

Table 5-2: Drawdown in boreholes along lithology strike

Pumping borehole	Observation borehole	r (m]	Response time (min)	Spread of cone of depression (m/min)
BH3-39	MH3-1	40	60	0.6
BH3-39	MH3-3	40	60	0.6
BH3-39	MH3-5	80	60	1.3
BH3-39	MH3-8	160	180	0.8
BH3-39	MH3-10	260	1890	0.13
BH3-39	MH2-3	840	2370	0.35

Table 5-3: Drawdown in boreholes across lithology strike

Pumping borehole	Observation borehole	r (m)	Response time (min)	Spread of cone of depression (m/min)
BH3-39	MH3-2	40	80	0.5
BH3-39	MH3-4	40	80	0.5
BH3-39	MH3-6B	80	100	0.3

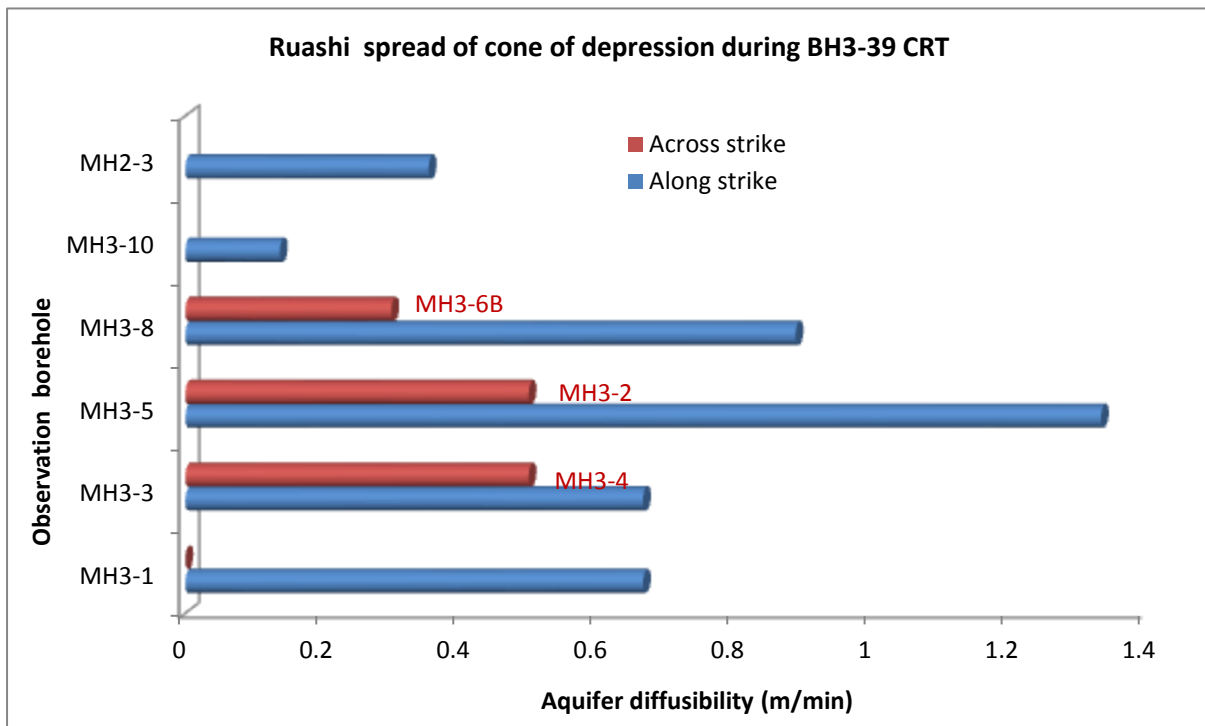


Figure 5-5: Spread of cone of depression during test pumping at BH3-39

It is clear in Figure 5-5 that the spread of the cone of depression was faster along the lithology than across strike.

5.5 Hydrostratigraphy

As discussed in Section 5.2.3 rocks of the younger Kundelungu formation overlain by older Roan series are found at Ruashi Mine. Blow yields observed during drilling, preliminary pumping response and aquifer hydraulic testing results indicate that the hydrogeological system consists of two groups of aquifers (shallow Kundelungu Sandstone and deep Roan dolomitic rocks) separated by unconformable brecciated contact. The north-eastern part of the mine is underlain by predominantly Kundelungu Formation. The southern part of the

mine where pits are located is composed of predominantly dolomitic schists of up to 250 m thick capped by a clayey Laterite layer.

5.5.1 Aquifers

i. Weathered regolith aquifer

The weathered regolith consists of weathered Laterite in the pits area south of the centre waste rock dump and weathered Kundelungu group in the tailings storage facility (TSF) area located north-east of the rock waste dump. Results from drilling show that weathering depths reach approximately 120 mbgl.

Such weathering depths have been identified to be the major root of air percussion drilling failures due to 'cave-ins' and collapse of loose weathering residue. The depth of weathering in the Laterite increases towards the south reaching 120 mbgl, where the topography is flat promoting infiltration during rainfall events. Groundwater Consulting Services (GCS 2006) estimated the hydraulic conductivity of the upper weathered zone to be 9.16 m/d.

ii. Weathered and Altered Dolomite (WAD)/BOMZ - Upper Roan aquifer

The unit consists of 40 m thick highly weathered and decomposed Dolomite and becomes moderately weathered to fresh with depth. Porosity for the unit was estimated to be 20-25%, with moderate to high permeability within the weathered zones. Based on aquifer hydraulic testing results from borehole BH3-39, the transmissivity of the unit was estimated as 256 m²/d. The storage coefficient was estimated to be 2.2 x 10⁻³. The weathered Dolomite is clayey in some places and the clayey material is expected to reduce the permeability of the Dolomite.

iii. Siltstone

This lithology underlies the Dolomite in some places and is slightly weathered to extremely weathered, with sub-horizontal fracturing and parting. The Siltstone is dark grey in colour and slightly fractured with some small scale folds indicating ductile failure. The Siltstone is moderately fractured at oblique angles to layering with some secondary dissolution cavities. Most of the joints observed in the Siltstone layer are closed and in-filled with mainly vein quartz and clay. Permeability is interpreted to be low; hence where it is not fractured, this lithology is likely to act as an aquitard.

iv. Sandstone

This unit consists of argillaceous, fine to medium grained feldspathic and arkosic Sandstone, inter-bedded with Siltstone, Mudstone and Shale that is occasionally dolomitic. The Sandstone is moderately weathered and vuggy in some places. The vugs could be a result of dissolution of weak minerals like feldspars. Porosity is moderate to high and is estimated to be 15%-20% where enhanced by connected vugs. Permeability is estimated as moderate to high.

v. Roches Argillaceous Talcose (RAT) breccia

This unit is interpreted to be a product of brittle failure when the Roan series was pushed over the Kundelungu series during the Katangan deformation. This postulation is supported by the presence of Roan series clasts in the RAT breccia.

The breccia consists of very hard, fractured RAT, with calcite, dolomite and quartz gravels and pebbles. The possibility of breccia being solution breccia rather than fault breccia cannot be ruled out. Due to the fractured characteristics, breccia forms the aquifer within the RAT aquitard. Yields within the RAT breccia range from 5 to 40 m³/hr. The highest blow yield (40 m³/hr) was recorded in the RAT breccia at groundwater monitoring borehole MH3-6B. Boreholes drilled on the south of Pit 2 show very quick drawdown response to pumping indicating that the RAT breccia is an aquifer.

vi. Siliceous Dolomitic Schist (SDS)

This unit consists of moderately weathered dolomitic Shale, although highly weathered and friable horizons have been observed within the moderately weathered upper zone. The lithology consists of vugs, thus enhancing the porosity and permeability. Sub-horizontal fracturing is dominant. The measured blow yields of up to 396 m³/hr proved that the SDS is the most profuse aquifer at the mine. Aquifer hydraulic testing (at BH3-39) analysis results estimated transmissivity of this unit to be 252 m²/d. Porosity is moderate to high, in the region of 20%-25%.

vii. Roches Siliceous Cellulaires (RSC)

The base of the Roan Formation consists of highly weathered Shale, Conglomerate and Sandstone. The lithology is highly friable and ferruginous, with vugs being dominant near the base of the unit. The vugs show some degree of interconnectivity, which would enhance groundwater flow. Sub-horizontal fracturing is dominant. Although indurated Sandstone and Conglomerate horizons are not highly weathered, they show moderate to high fracturing. The

base of the Roan series has Iron (Fe) stained fractures indicative of active groundwater flow. Blow yields recorded in the Roan series suggest that the SDS and RSC units could be the main groundwater storage and flow conduits at Ruashi Mine. Porosity was estimated to be 20%-30%, with moderate to very high permeability.

viii. Roches Siliceuses Feuilletées (RSF)

This unit consists of relatively thin impersistent layers of foliated siliceous Dolomite below the RSC. It is an assemblage of massive grey Dolomite that is coarsely recrystallized, with often large black crystals of dolomite. This unit is highly dolomitic and intensely silicified. Based on the results of aquifer hydraulic testing and in comparison with the SDS, porosity was estimated to be 15%-25% and permeability estimated in the range of 200 m²/d to 400 m²/d.

ix. Dolomitic Stratigraphy (DSTRAT)

This unit was not intersected during the drilling phase of this research. Maarten and Muechez (2011) described the unit as dolomitic rocks with fine grained texture. The Dolomites are rich of detrital Micas in a chaotic order. Diagenetic Quartz is abundant, but irregularly distributed.

x. Kundelungu Sandstone

The Kundelungu Sandstone lies in the north-eastern corner of the mine area in the vicinity of the TSF. It is a fine to medium grained Sandstone, occasionally indurated, moderate to highly weathered. Where it is indurated, weathering is weak. Porosity was estimated to be 5%-15% with low permeability. GCS (2006) Feasibility Study estimated the conductivity of the Sandstone to be approximately 0.1 m/d.

5.5.2 Aquiclude

Roches Argillaceous Talscose (RAT)

Drilling and aquifer hydraulic testing results indicate that the RAT is an impermeable to semi-permeable talcaceous and argillaceous Shale. Drilling results indicated that groundwater potential is very poor with yields only enhanced where faults/breccia is present. The RAT is only permeable where it is brecciated or fractured. Yields in the RAT breccia are very low, mostly less than 1 m³/hr. The estimated hydraulic conductivity is less than 0.01 m/d. The lithology outcrops in the south of the mine.

5.5.3 Aquitard

Calcareous Mineral Noirs (CMN)

This unit is calcareous malleable argillite. The CMN was intersected by most boreholes drilled in the north-west of Pit 1 and Pit 2. Water logging conditions were observed in the north eastern parts of Pit 2 where the CMN is dominant. Groundwater seepage horizons were identified in the overlying Laterite and pond on Pit 2 CMN dominated floor. At groundwater monitoring borehole MH1-16 located in Pit 1, artesian conditions exist and could be due to CMN confining the underlying SDS unit. Permeability is estimated to be low in orders of less than 0.001 m/d.

The results of borehole drilling and aquifer hydraulic testing were used to produce cross sections presented in Figure 5-6, Figure 5-7 and Figure 5-8.

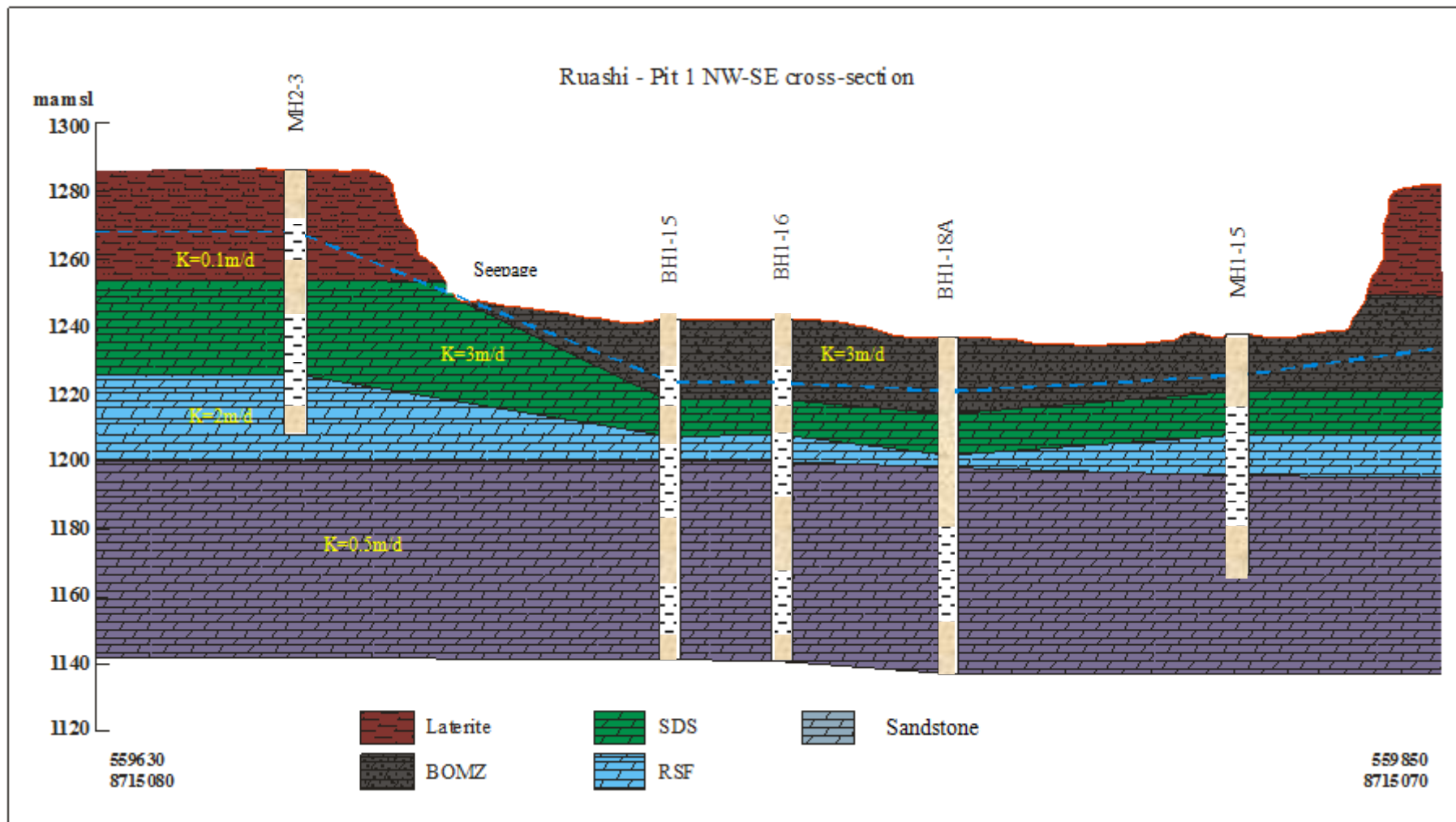


Figure 5-6: Pit 1 NE-SW cross section indicating the hydraulic conductivity zones

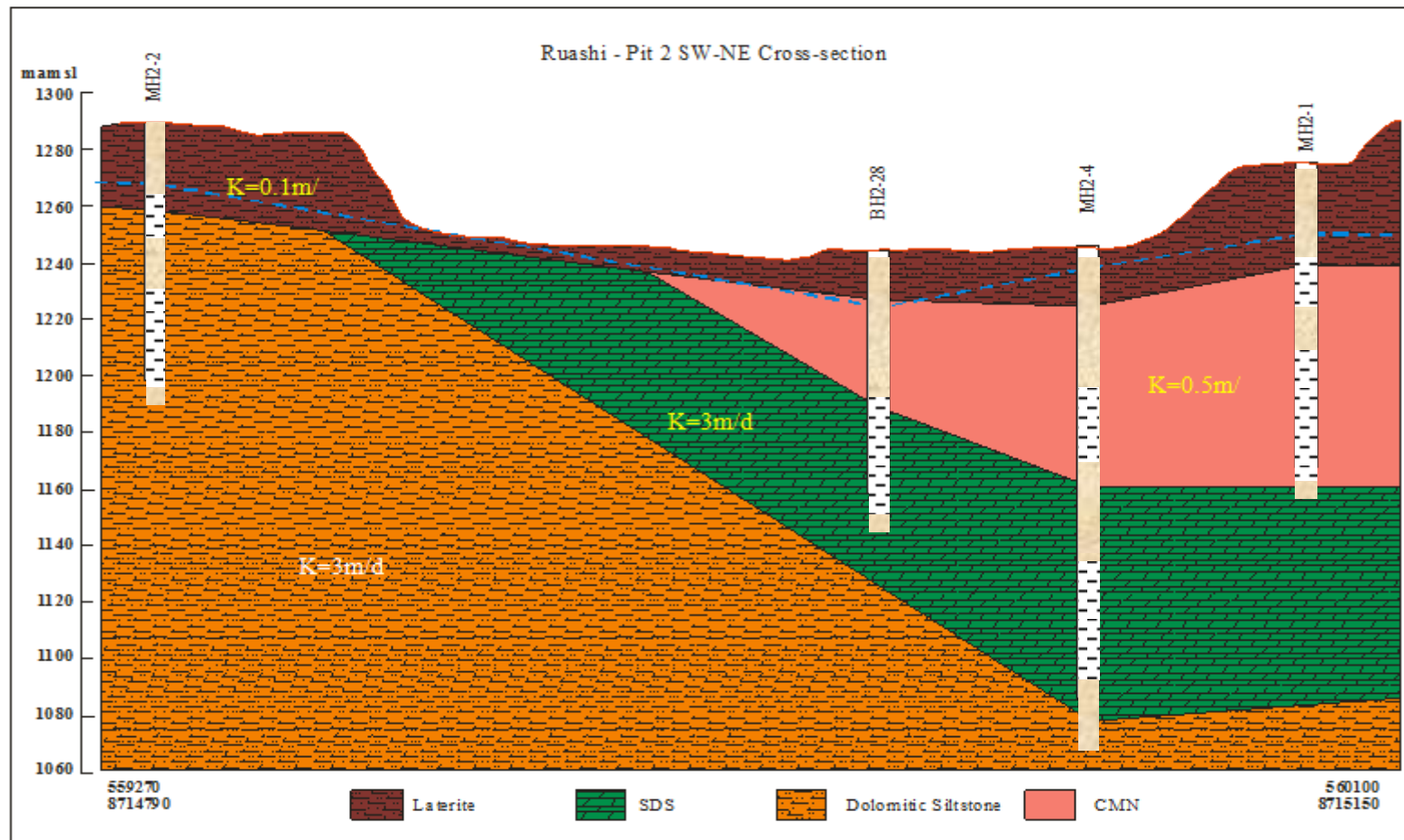


Figure 5-7: Pit 2 SW-NE cross section indicating the hydraulic conductivity zones

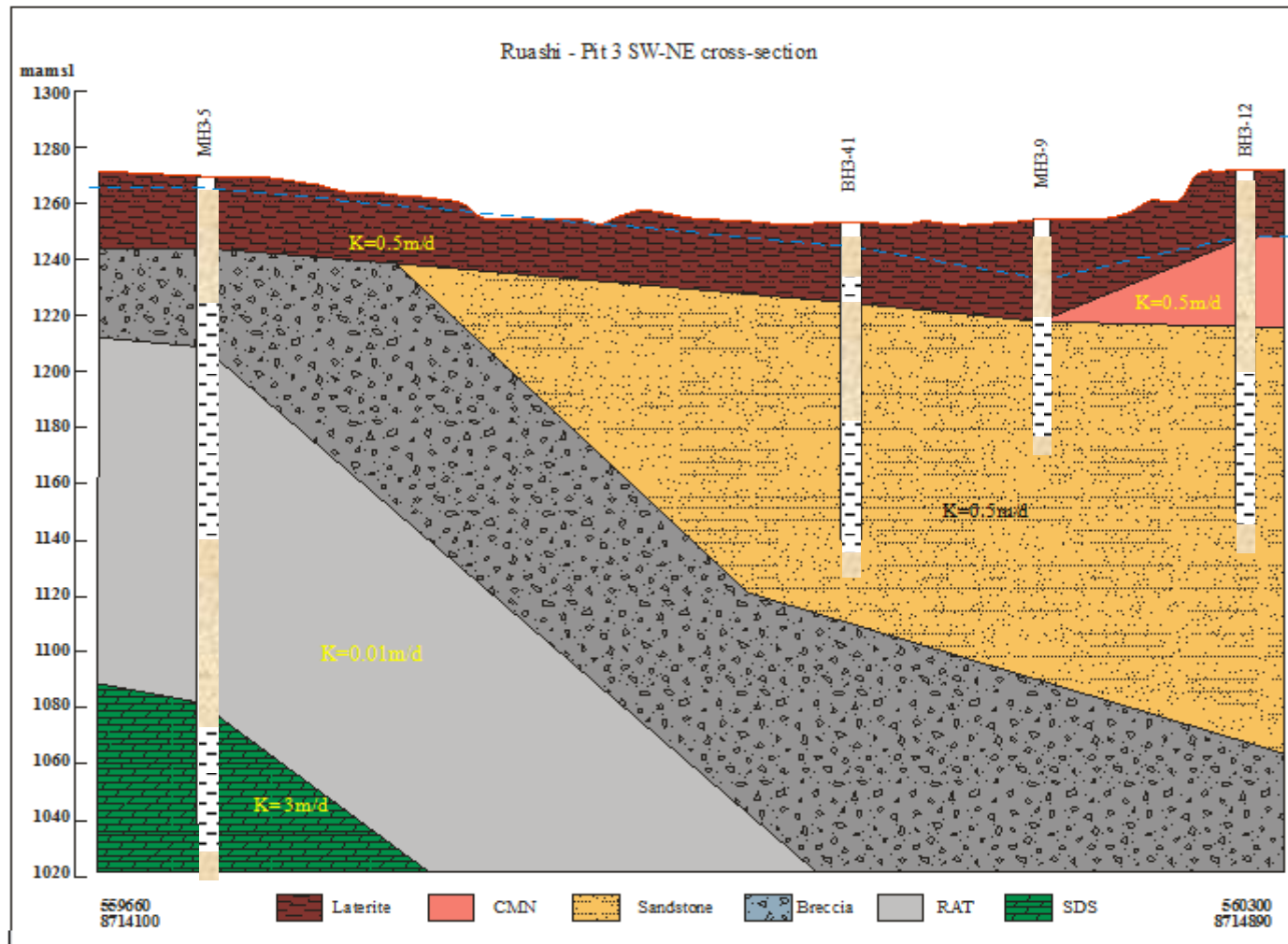


Figure 5-8: Pit 3 SW-NE cross section indicating the hydraulic conductivity zones

5.6 Water levels

5.6.1 Water levels and topography

Water levels were measured in all the drilled boreholes. The water levels follow topography to a large extent, as shown in Figure 5-9, indicating unconfined conditions. This could be an indication of a high degree of interconnectivity between shallow and deep aquifers and hence the system acts like a single aquifer.

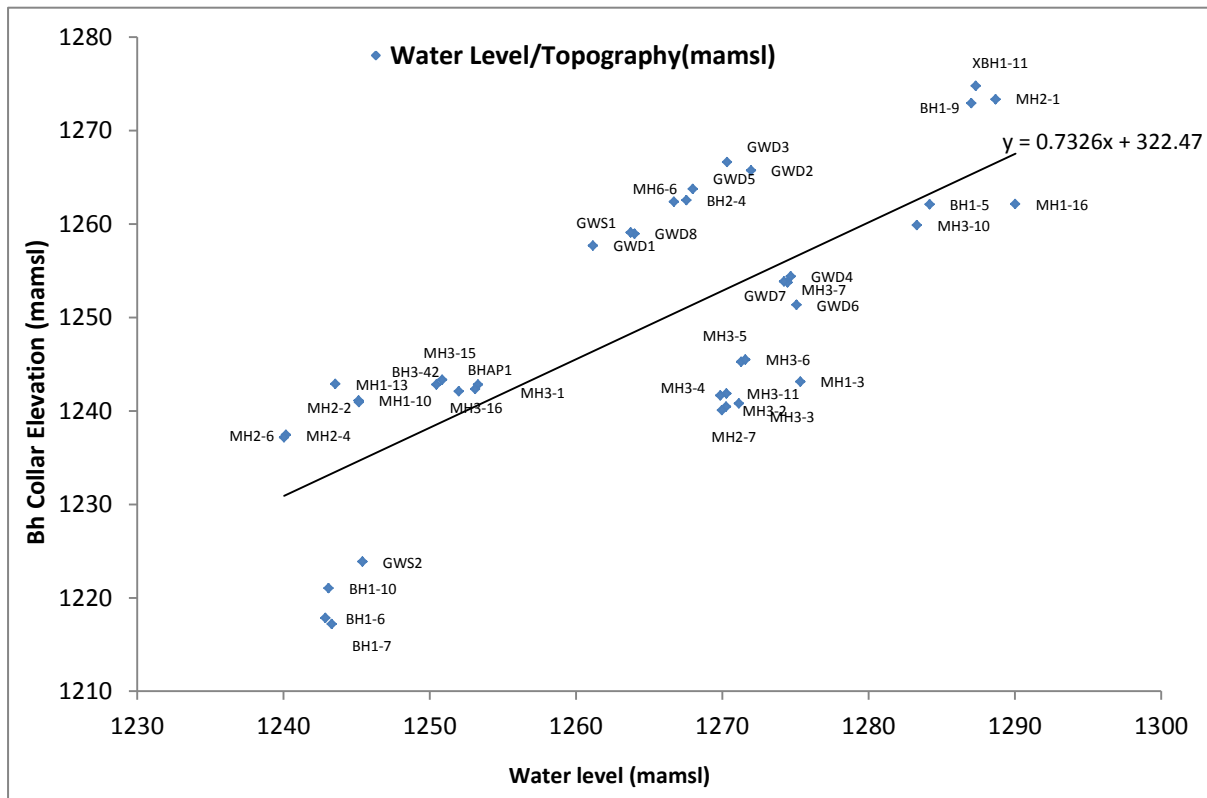


Figure 5-9: Ruashi water levels versus topography

Although Ruashi Mine aquifer system is largely unconfined, some local confining conditions were noted to be associated with areas where the CMN overlies the dolomitic aquifers. For example groundwater monitoring borehole BH1-16 located in the CMN is artesian.

5.6.2 Groundwater gradient

Groundwater gradients measured in the area indicate that groundwater in both the shallow (Kundelungu and Laterite) and deep aquifers (Roan) flows from the elevated areas towards the rivers. The general groundwater flow direction is from south west to north east towards the Luano and Kebumba River floodplains. The Kebumba and Luano River floodplains are relatively flat and groundwater gradients are gentle at 0.005 (1:200) as measured between

the TSF boreholes and the boreholes close to Ruashi community to the extreme south-west of Ruashi Mine area. The area around the three pits proved much steeper groundwater gradients at 0.03 (1:30) as measured between the rock dump located in the middle of the Tailings Dam and the three pits. The steep gradients could be attributed to pit dewatering and pumping for community and plant supply.

5.6.3 Hydraulic continuity

Blow yields and aquifer hydraulic testing results suggest that there is enhanced hydraulic continuity between the deep aquifer and the shallow aquifer. The aquifers are unconfined but local confining and artesian conditions were noted at MH1-16 located in Pit 1 where the CMN overlies BOMZ. Restricted hydraulic continuity occurs where unfractured RAT and CMN occur. Rest water levels for the deep and shallow aquifers are comparable in the pits area but significant water level difference occurs close to the TSF which is continuously recharged by tailings.

Ruashi Mine hydrogeology compiled from drilling and aquifer hydraulic testing results is presented in Table 5-4.

Table 5-4: Ruashi hydrostratigraphic units and hydraulic parameters

Unit No.	Hydro stratigraphic unit	Lithology	Lithology Thickness (m)	Model Layer	K (m/d)	Storativity	Comment
1	Laterite	Weathered ironstones and sandstone, clay.	50	1	0.01	0.001	Topmost lithology with blow yield of 20 m ³ /hr. Hydraulic parameters estimated from drilling and testing of BH3-39, MH3-1, MH3-2, MH3-3, MH3-5 and MH3-6
2	Kundelungu	Sandy Clay, Sandstones, Shales and Siltstones	100-200	2	0.1	0.03	Estimated from drilling. Yields of approximately 3 m ³ /hr recorded at BH69 and BH69B. Hydraulic conductivity adapted from GCS 2006 Point Dilution Test Report.
3	CMN	Deeply weathered and fractured siltstones and Limestones.	50	4	0.1-0.5	0.02	Estimated from drilling of BH2-28, BH2-29, BH3-36 and MH2-7. Blow yields range 5-20 m ³ /hr.
4	ROAN Supergroup	Highly weathered and fractured and altered Dolomites, dolomitic Shales, Sandstones and Siltstones of ROAN Supergroup.	200	5	2-7	0.02	The Supergroup is composed of BOMZ, SDS, SDB, DSTRAT, RSF and RSC. Sub-units identified from drilling at BH3-39, MH3-1, MH3-3, MH3-4, BH1-15, and BH1-16, The highest blow yield of 396 m ³ /hr for the Supergroup was recorded at BH3-39.
5	RAT	RAT, a malleable argillite, and RAT breccia which forms part of the zone of relaxation immediately south of the pit	120	3	<0.01	-	Impermeable to semi-permeable in the RAT. Yields enhanced in breccia. Blow yield of 17 m ³ /hr recorded at BH3-39 in RAT breccia.
6	RAT Breccia	Quartzitic RAT breccia, pebbly and fractured, conglomerate in some places	30	-	-	-	Significant blow out yields of approximately 10 m ³ /hr recorded at groundwater monitoring boreholes located south of Pit 2.

5.6.4 Groundwater flow pattern as deduced from water temperature

Groundwater temperatures were measured during drilling. Groundwater temperature cross section (Figure 5-10) shows that the shallow aquifer consisting of the Laterite, RAT and RAT breccia water is essentially downward flow from higher (cooler) levels near surface. The deep aquifer consisting of Roan Series water is upward flow from deeper (warmer) levels. Fault and fracture zones, weathered zones, cavities and bedding planes act as major conduits of water inflow to the mine. These structures act as both mixing and drainage zones.

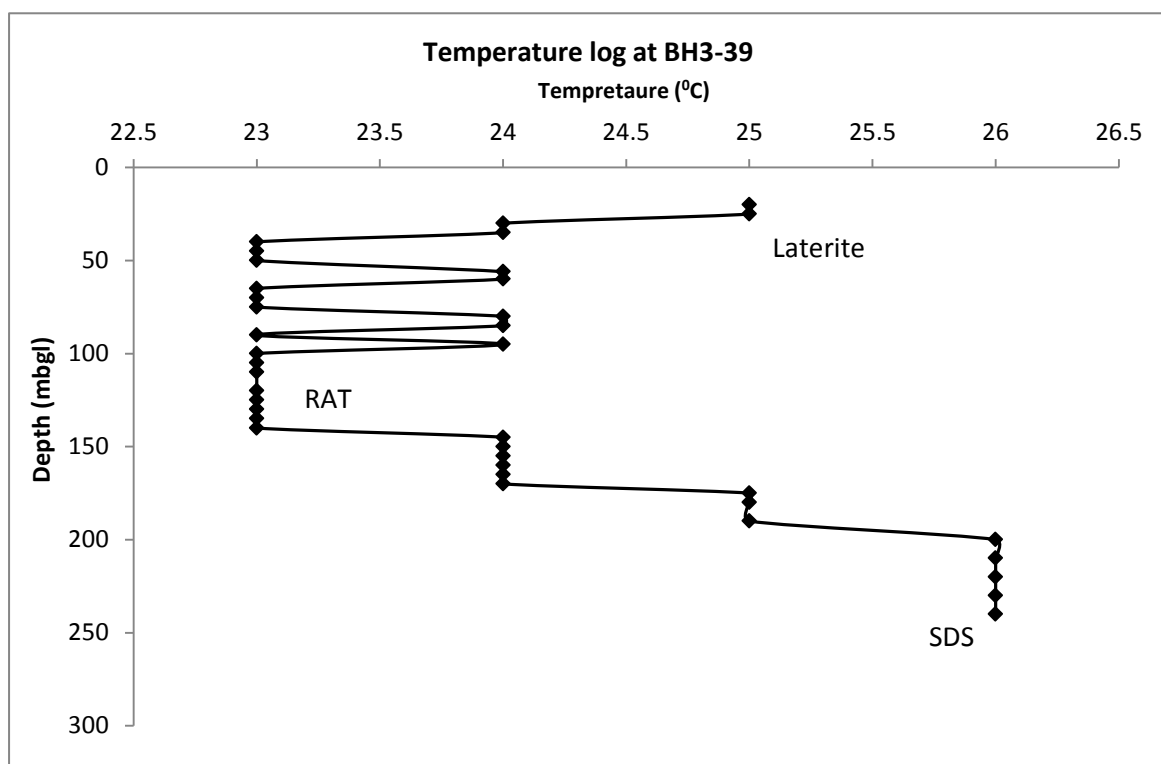


Figure 5-10: Borehole BH3-39 temperature log

Within the deep aquifers, notably, RAT breccia, BOMZ and SDS, there was very little significant temperature change. This could be an indication that groundwater from the top SDS aquifers moves so rapidly into the bottom units hence very limited mixing and temperature equilibration time. This phenomenon is suggestive of a drainage zone where shallow aquifer water upwells from deep levels and vice-versa depending on which zone is colder and warmer. The records of water level behaviour during drilling show that as we go down from ground level, we go through zones which allow water to be lost from the borehole and therefore fairly permeable. These zones are interspaced with others where groundwater

levels rise in a borehole, indicating that they are separated from the draining zones by relatively impermeable thickness of CMN and RAT strata and they themselves contain water under great pressure head than the overlying aquifer.

The dominant zones are those where no substantial changes of pressure heads occurs with depth, indicating either no flow of groundwater or equipotential surfaces which are essentially vertical, as would occur with horizontal flow. Outside the pits area of mining influence the strata is generally less disturbed and there is a distinct difference between the hydrostratigraphic and lithostratigraphic units respectively. However in the pits area, where the rock has been further fractured by blasting, there is no difference between hydrostratigraphic and lithostratigraphic units. Fractures and old mining cavities have created hydraulic connection within the Roan hydrostratigraphic units. The temperature relationship between the shallow and deep aquifers shows that there is upwelling of water.

5.7 Aquifer Recharge

Groundwater recharge can be defined in a general sense as the downward flow of water reaching the water table, forming an addition to the groundwater reservoir (Lerner *et al.*, 1990). According to Healy (2010), precipitation, the source of natural recharge, is the dominant component in the water budget for most watersheds. There is direct recharge from rainfall through infiltration straight into the ground and indirect recharge from concentration of surface runoff along watercourses. Recharge boundaries occur where the aquifer unit intercepts surface water systems or geologic units with significantly higher storage capacity and hydraulic conductivity than the aquifer in question. Recharge boundaries can occur due to a unit's contact with a river, stream, dam, lake, or a zone of very high conductivity. Groundwater recharge is one of the most important hydrogeological processes to be quantified in water supply studies in arid and semi-arid areas. Recharge is generally concentrated in topographic depressions and as preferential flow along fractures and faults. Recharge within Ruashi Mine is primarily from rainfall and the groundwater system discharges to the surface water system.

5.7.1 Chloride mass balance method

Estimating recharge

According to Van Wyk et al. (2011) semi-Arid terrain rainfall recharge to groundwater occurs in cycles. The chloride mass balance method of estimating groundwater recharge appears to be the simplest, cheap and universal method of estimating recharge from precipitation. If a steady state is attained between the chloride flux at the surface and the chloride flux beneath

the evapotranspiration and the mixing zone, the chloride mass balance can be used to estimate recharge.

Beekman *et al.* (2000) outlined a method to estimate the recharge to groundwater from rainfall using chloride measurements for rainwater and groundwater. Chloride is a conservative ion, when water is concentrated by evaporation chlorinity increases. Knowing the initial chloride of rain water and the measured chloride in groundwater, one can calculate the percentage of recharge out of rainfall using Equation 5-4.

$$\text{Recharge} = \frac{P \text{ (mm)} * C_{1r} \text{ (mg/1)}}{C_{1gw} \text{ (mg/L)}} * 100\% \quad \text{(Equation 5-4)}$$

Where P is annual precipitation; C_{1r} is the chloride in rainfall; C_{1gw} is the chloride in groundwater; dry chloride deposition is assumed to be negligible.

The same method can be applied to Ruashi Mine. The harmonic mean of the measured chloride concentration in rainfall at Ruashi Mine was analysed to be 0.53 mg/L. The chloride concentration in rainfall value 0.53 mg/L is taken as representative of the chloride concentration of the local rainfall. The calculated harmonic mean groundwater chloride content for 24 boreholes is 3.72 mg/L. Using the formula above, the recharge,

$$R = (0.53/3.72) \times 100\% = 14\%.$$

Recharge is estimated as 14% of mean annual precipitation, corresponding to 280 mm of rainfall per annum. The assumptions underlying the chloride mass balance method are that:

- There is no other source of chloride into the water recharging the groundwater other than that from meteoric water.
- Chloride is considered to be conservative.

Albeit these assumptions, the method can be considered to be an oversimplification of reality as it does not take into account other factors like:

- Contamination of boreholes
- the problems associated with rainfall sampling
- sample size
- other sources of chloride source besides rainfall
- dry boreholes

Regardless of the method being seemingly simple, estimation of groundwater recharge has never been straightforward or easy. The calculated recharge value of 14% seems high compared to universal values. This could be attributed to thick vegetation that reduces evaporation rates during rainfall events. The contribution of preferential groundwater flow along fracture networks resulting in groundwater and rainfall chloride concentrations of a similar magnitude cannot be ignored. Recharge through fractures and other structures that increase permeability of materials reduce the water residence time in the unsaturated zone. Limited residence time reduces dissolution of chloride bearing minerals and the concentration of the groundwater by evapotranspiration, at times giving large errors in the estimation of groundwater recharge. The other factor could be that the samples were collected during the same season in a small area hence could be biased. Longer term rainfall data can eliminate the bias and give a more representative value of chloride in rainfall.

5.7.2 Recharge from Tailings Dam

Ruashi recharge and evaporation from the tailings dam varies seasonally. During the dry season, evaporation is more than groundwater infiltration/recharge and the inflow from the plant discharge to the tailings dam is evaporated before it infiltrates. During the rainy season, the total volume of water from the plant as tailings discharge and recharge from rainfall exceeds evaporation, which is also low during the rainy season.

Evaporation rates have been estimated at 3 mm/d from evaporation rates obtained from Lubumbashi Airport. The average flow to the plant is 227 m³/hr and this consists of 70 m³/hr flow from the Coffey Dam and 157 m³/hr from plant supply boreholes. Total outflow from the plant to the tailings dam is 214 m³/hr; with an influx of 13 m³/hr from the milling pond to the return water dam (RWD). The outflow from the milling pond to the RWD is significantly reduced as the channel is not lined and a significant volume is lost through infiltration.

The discharge channel from the tailings dam to the return water dam indicates intermittent flow as shown by the dry canal (Figure 5-11). High volume flow is experienced during the rainy season. The estimated pumping rate from the return water dam back to the plant is 40 m³/hr, however the pumping is not regular, with pumping episodes of once in a week or two weeks. It can be concluded that water losses from the tailings dam to the return water dam are small, with the bulk of the water being either evaporated or infiltrating into the groundwater system.



Figure 5-11: Canal from Tailings dam to Return Water Dam

During the wet season, total inflow from plant discharge and rainfall is 11 073 m³/d. With an evaporation rate of 2 407 m³/d and assumed 10% of total inflow lost to RWD, 7 759 m³/d is assumed as the infiltration rate during the wet season. During the dry season, total inflow is estimated as 5 296 m³/d, with an evaporation rate of 6 949 m³/d, thus no infiltration during the dry season.

5.8 Water Quality

In an aquifer system, due to the different mobility of the chemical elements and the chemical processes that occur in the subsurface environment, anion evolution sequences occur as groundwater circulates through the aquifer. Groundwater quality may also change due to cation exchange reactions when two different types of groundwater mix, for example when saltwater intrudes freshwater or when freshwater mixes with saltwater. This sequence can be explained in terms of mineral availability and mineral solubility. The sequence can be summarized is as follows:

Bicarbonate → bicarbonate-chloride → chloride-bicarbonate → chloride-sulphate → chloride.

This means, the higher the residence time of groundwater in the aquifer, the more it dissolves chemical constituents and evolves from bicarbonate to chloride dominated water.

5.8.1 Groundwater classification

Tri-linear or Piper diagrams graphically depict the relative concentrations of the dominant ions. The main purpose of the piper diagram is to indicate samples that have similar compositions. This plot reveals useful properties and relationships for large sample groups. The relative concentrations of the major ions in percent meq/l are plotted on the cation and

anion triangles. The projected points on the middle diamond shape represent both cations and anions.

Ruashi hydrochemical analysis data was used to plot Piper diagram presented in Figure 5-12. Based on the Piper diagram two distinct types of groundwater can be described. The pits area is dominated by Calcium-Magnesium-Bicarbonate (Ca-Mg-HCO_3) type of water, which defines recently recharged water from precipitation. The origin of the recently recharged groundwater could be through fractures that connect the deep and shallow aquifers. Two of the groundwater samples can be described as predominantly Calcium-Magnesium-Sulphate (Ca-Mg-SO_4) type of water. The elevated Sulphate (SO_4) concentration in borehole GWS2 may be associated with chemical reactions such as the oxidation of sulphides or contamination.

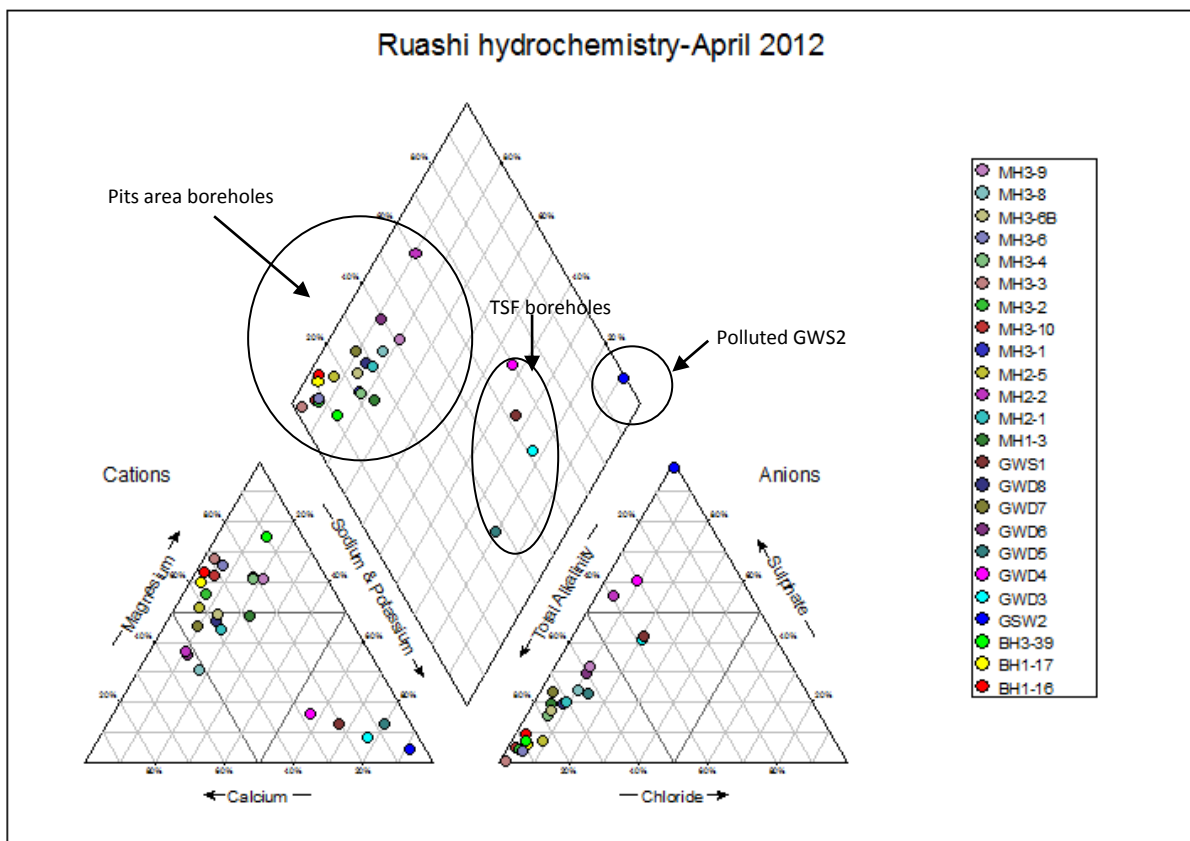


Figure 5-12: Piper plot showing hydrochemical groups of boreholes at the mine

Samples from TSF boreholes (indicated in Piper diagram) show an intermediate character ($\text{Na-SO}_4\text{-HCO}_3$) which suggests mixing of relatively fresh water and contaminated water. Evidence of groundwater pollution from the tailings dam as interpreted from the Piper diagram is further confirmed by high concentrations of Sodium (Na), Potassium (K) and Chloride (Cl), the high conductivity of the water (EC) and pH for borehole GWS2 located on the Storm Water Dam perimeter. These four parameters form major constituents of the

tailings composition and can be used to assess groundwater pollution and identify potential sources at the mine.

5.8.2 Distribution of groundwater types and facies

The flow of groundwater in the deeper aquifers at Ruashi is driven by recharge from rainfall and tailings storage facility (TSF). Three hydrochemical facies have been identified and these are:

- Mound water (Na+K-HCO₃-SO₄)-this facies underlies the majority of the tailings storage area and return water dam and is distinguishable based on its high electrical conductivity (EC approximately 550 mS/m).
- Recent recharged water (Ca-Mg-HCO₃)-this facies underlies the majority of the aquifers especially in the pits area. This water type was found to be of better quality because of its bicarbonate nature.
- Intermediate (Ca-Mg-HCO₃-SO₄) - this facies was identified in the boreholes between the TSF and the pits area. The groundwater mixing could have resulted from pumping in the pits which resulted in reversal of groundwater flow direction towards the pits.

5.8.3 Groundwater portability

In terms of the portability of the water, the water quality constituents were compared to the World Health Organisation (WHO) Standards for Potable Drinking Water (2011 fourth edition) and the South African Standard (SANS) Class 1 recommended levels for Potable Drinking Water. The DRC standard does not have explicit values on drinking water guidelines. The groundwater within Ruashi Mine is generally of good quality and suitable for drinking water, plant and general domestic use.

It was also noted that:

- The concentration of Iron (Fe) in boreholes BH3-9, MH3-1, MH3-4 and MH3-6B exceed WHO guideline value of 0.3 mg/L. In drinking water, Iron salts may precipitate as hard particles, that is, the insoluble iron (III) hydroxide. BH3-39 shall be used for community water supply hence the elevated concentration of Iron could be a concern.
- The concentration of Manganese in boreholes BH3-39, MH3-1 and MH3-4 exceed WHO guideline value of 0.4 mg/L. Several epidemiological studies associate adverse neurological effects with exposure to manganese in drinking water.

- Elevated concentration of Sodium in environmental monitoring borehole GWD5 could be attributed to leakage from the contaminated tailings dam water or groundwater mixing with contaminated surface water.

5.8.4 Aquifer vulnerability

The shallow Laterite and weathered Kundelungu Shales that constitute the shallow aquifers have no barrier from surface water infiltration and pollutant transportation; and therefore could be at risk of being polluted. Elevated levels of manganese at boreholes MH3-1 and MH3-4 and Sulphate near the Storm Water Dam and the TSF confirms small scale yet active pollution transport. Elevated levels of manganese were detected in water that was being pumped from BH2-7 located in Pit 2 and this borehole had been used for community water supply. The borehole was later removed from the Ruashi community water supply circuit as a health measure. The deep Roan aquifer is less vulnerable to possible pollutant plume intrusion where the RAT or CMN restricts hydraulic continuity between the shallow and deep aquifers. Zones of higher permeability associated with the faults, fractures and bedding planes confirm the presence of potential pathways for the movements of contaminants and provide a localised link between the shallow and deeper aquifers.

5.9 Summary

Analysis of pumping volumes, water levels and drawdown response to pumping demonstrated that the drawdowns achieved are far much less than required to dewater the mine. This was clearly evident in the low drawdown of less than a metre recorded in the monitoring boreholes during aquifer hydraulic testing. There is evidence to suggest that Ruashi Mine groundwater could come from a number of sources, notably, the regional aquifer system, surface waters of the Luano and Kebumba Rivers and Tailings Storage Facility (TSF). The inflow boundary is unlikely to be just ground level. This means sub-surface recharge to the mining area via aquifers connected to distant catchments should also be considered. If the mine TSF is leaking into the aquifers, the leachate is added to the groundwater system which is also possibly mixed with waters of the Luano and Kebumba Rivers, should this be also leaking into the mine. The groundwater chemistry could be further complicated if there is recharge from a different catchment with dissimilar chemistry.

The next chapter discusses the numerical groundwater flow model that was developed using data gathered during the field investigation programme. The numerical groundwater flow model simulates groundwater flow in the mine. Different model scenarios are used to estimate pit flow volumes and predict optimum pumping rates required to dewater the mine.

6 NUMERICAL GROUNDWATER FLOW MODEL

6.1 Introduction

This chapter demonstrates that the conceptual groundwater flow model constructed from the knowledge gained from field work can be developed into a numerical groundwater flow model. The numerical model can be used not only for predicting future mine groundwater discharge but even more significant, to simulate various dewatering scenarios and eventually select the most suitable dewatering plan. The numerical groundwater flow model can facilitate formulation of a much needed long-term cost-effective solution to the groundwater flow problem. Only then will the economic viability of the mine be enhanced and dry working conditions realised.

Although this researcher had significant experience in groundwater flow modelling using Modflow and about half year experience in building three dimensional (3D) Feflow models, this numerical model was completed due to contributions from Mr Blessing Mudzingwa, a Senior Groundwater Flow Modeller. He taught this researcher how to calibrate the model using the Feflow code.

The main aim of the numerical model is to simulate the physical processes occurring within the hydrogeological system, by means of a governing equation which defines these processes. According to Moreno and Spitz (1996), the general governing equation for such a flow regime is a two dimensional groundwater flow system defined by flows only in the X and Y direction in a single layer. The equation defining the system is given by Equation 6-1:

$$\frac{\partial}{\partial x} (T_x \frac{\partial h}{\partial x}) + \frac{\partial}{\partial y} (T_y \frac{\partial h}{\partial y}) + \frac{\partial}{\partial z} (T_z \frac{\partial h}{\partial z}) = S \frac{\partial h}{\partial t} - R \quad \text{(Equation 6-1)}$$

Where T_x , T_y and T_z are transmissivity in the x, y and z direction respectively, S is aquifer storativity and R is recharge to or abstraction from aquifer.

The potential flow which describes the change in flux in response to change in potential is given by the Laplace Equation, which for

(a) Steady state

$$\Delta Q = [K_x \delta^2 h / \delta x^2 + K_y \delta^2 h / \delta y^2 + K_z \delta^2 h / \delta z^2] dx \cdot dy \cdot dz \quad \text{(Equation 6-2)}$$

and for

(b) Transient state flow

$$\Delta Q = [K_x \delta^2 h / \delta x^2 + K_y \delta^2 h / \delta y^2 + K_z \delta^2 h / \delta z^2] dx \cdot dy \cdot dz = \gamma^2 h = \{S/Kb\} \delta h / \delta t \neq 0 \quad \text{(Equation 6-3)}$$

Where:

Q= change in discharge

K= hydraulic conductivity

S= coefficient of aquifer storage

b= saturated aquifer thickness

h= total head

t= time

dx.dy.dz= volume of ground

$\gamma h = \frac{\delta h}{\delta x}, \frac{\delta h}{\delta y}, \frac{\delta h}{\delta z}$ = hydraulic gradient

Although analytical models are available to simulate groundwater flow systems, these methods become inadequate when solving complex and heterogeneous flow systems, hence the need for numerical models.

The conceptual model illustrates that the hydrogeological system at Ruashi Mine is heterogeneous as supported by the presence of groundwater compartments associated with the BOMZ and local confining conditions associated with the CMN.

The main steps in building the numerical model are as follows.

- i. Choice of model and modelling approach
- ii. Representation of mine geology, hydrology and hydrogeology
- iii. Input parameters to be used
- iv. Calibration of the model
- v. Simulation of groundwater flow
- vi. Formulation of a bankable dewatering plan.

6.2 Numerical modelling objectives

The main objectives of the numerical groundwater flow modelling are to simulate and predict mining impacts during the operational phase on:

- The potential inflows into the three open cast pits as mining advances
- Depression of groundwater levels
- Determine the radius of influence from mine dewatering; and
- Set up dewatering plan for the mine.

6.3 Mine infrastructure

The mine groundwater regime could be dictated by the following mine facilities.

6.3.1 Open Cast Pits

Ruashi Mine was originally planned for 17 years of continuous mining beginning in the year 2006. The mine infrastructure includes three open cast pits being mined out. Pit 1 is detached from Pit 2 and the area between Pit 2 and Pit 3 is being mined out and the two pits will eventually be merged into one pit. The operational phase conceptual model is based on the initial mining plan for the three pits. Pit 1 is the deepest, located WNW of Pit 2, with an April 2012 depth of approximately 40 m (1 230 mamsl). The April 2012 depth of Pit 2 was 1 235 mamsl, that is, about 30 mbgl. The elevation of Pit 3 floor was 1 238 mamsl in April 2012. The maximum depth for Pit 2 and Pit 3 is based on the mine plan of 180 m.

The operational time schedule for the open cast pits as stated in the mine plan is summarised as follows:

- Operational phase of merged Pit 2 and Pit 3 (area of 517 303.282 m²) is for 12 years, ending in 2022, the model assumes pumping to maintain dry conditions until 2022.
- Operational phase of Pit 2 (area of 243 945.642 m²) is for 10 years, from 2010 to 2022.
- Operational phase of Pit 1 (area of 388 797.733 m²) is for 6 years, from 2006 to 2014.

6.3.2 Tailing Storage Facility (TSF)

The TSF height as of April 2012 was 5 m and its surface area is 802 312.74 m². This phase represents the current operational situation and footprint area of the TSF. The operational phase is for 15 years, which starts from year 2006 to year 2022.

6.3.3 Waste rock dump

Waste rock dumps are located to the north-east, east and west of the pits. The waste rock dumps are expected to increase infiltration from precipitation into the Roan and Kundelungu aquifers significantly.

6.3.4 Storm water dam (SWD)

The storm water dam to the north of the open cast pits is lined and therefore the material underlying the dam will control seepage flow into the aquifer. All overland flow from the mine plant area from rainfall is channelled to the Storm Water Dam (SWD). The SWD has sufficient capacity to contain all the water from the plant area. The depth of the SWD is 3 m as measured during the parallel geotechnical study. The operational and post-closure time schedule for the SWD (area of 440 m²) is for 15 years, from 2007 to 2022.

6.4 Numerical modelling approach

A conceptual hydrogeological model for the mine (described in Chapter 5 of this dissertation) was constructed using the site specific data collected during the field investigation phase. The conceptual hydrogeological model was developed into a three-dimensional (3D) finite element groundwater flow model. The groundwater flow model was calibrated for steady state conditions using observed groundwater levels. The numerical model was later calibrated for transient conditions using aquifer test information gathered during the field phase. The groundwater flow and impacts of groundwater abstraction depend on the hydrogeological settings of the site which are systematically integrated into the model. The hydrogeological settings include controlling factors such as the topography and relief, surface hydrology and rainfall, geology and the properties of the aquifer system itself as determined from the field investigation.

6.4.1 Software selection

The code selected for modelling Ruashi Mine groundwater flow is Feflow. Feflow is used worldwide as a high-end groundwater modelling tool for simulating groundwater flow and solute transport. According to Diersch (2005), Feflow is capable of performing numerical modelling of density-dependent fluid flow, mass and heat transport. Feflow can efficiently be used to describe the spatial and temporal distribution of groundwater flow, to plan and design remediation strategies and to assist in designing alternatives and effective monitoring schemes. The software can also be used to simulate mine pit inflows.

6.4.2 Model area

The modelling area was selected based on a combination of topographical, geological and structural control. Boundaries of the numerical model were chosen to reflect the geometry of the groundwater system. The Luano and Kebumba Rivers were chosen as north-western and eastern constant head boundaries respectively. A topographic high water divide was identified as the southern constant head flow line. The northern boundary is a low valley with a constant shallow water level. The modelled area is approximately 15.7 km².

6.4.3 Hydrogeological boundaries

Boundary conditions constitute barriers to groundwater flow and sources of recharge. Surface water basin divides usually can be determined from existing topographical and geological maps. Recharge boundaries can be estimated from the groundwater level profile, tracer results and aquifer hydraulic tests. However in a mining environment, an additional complexity exists. Apart from the subsurface groundwater boundaries not necessarily matching with the surface water boundaries, the groundwater boundaries change with time as a result of stress relief due to excavation. Criteria for selecting boundary conditions are primarily topography, hydrology, geology and structure. The topography, geology and structure may yield boundaries such as impermeable strata or potentiometric surface controlled by surface water, or recharge/discharge areas such as inflow boundaries.

Boundary conditions in a groundwater flow model can be specified either as Dirichlet Type (or constant head), Neumann Type (or specified flux) or a mixture of the two (Cauchy). These boundaries are represented numerically by what is referred to as “constant-head” boundary condition. The following hydrogeological boundaries have been observed in the Ruashi Mine area.

- Eastern and western boundaries as Luano and Kebumba Rivers with combined length of 4 km;
- Northern model boundary as a shallow water divide with length of 2.2 km;
- Southern model boundary as a water divide line with length of 3 km;
- Total model perimeter boundary length of 8.6 km;
- Internal model boundary -The regional groundwater flow direction is from South West to North East. Groundwater in both the shallow and deep aquifers flows from the elevated areas towards the rivers following topography closely. The groundwater flow direction was reversed towards the pits due to continuous pumping for plant and community

water supply. Constant head boundary conditions were therefore specified along the Luano and Kebumba Rivers.

6.4.4 Model layers

The study site is represented by a five-layered model based on field data as discussed in the conceptual model presented in Chapter 5. The model layers are included in Table 6-1.

Table 6-1: Ruashi model layers

UNIT NUMBER	UNIT	THICKNESS (M)
1	LATERITE	20
2	KUNDELUNGU	150
3	CMN	100
4	RAT	50
5	ROAN	200

The base of the model was assumed to be impermeable.

6.4.5 Model properties

6.4.5.1 Finite element mesh

A finite element mesh was designed to provide a high resolution of the numerical solution. The finite element mesh comprises of a triangular mesh consisting of 17 240 elements and 10 614 nodes. Figure 6-1 is a three-dimensional (3D) view of the finite element mesh.

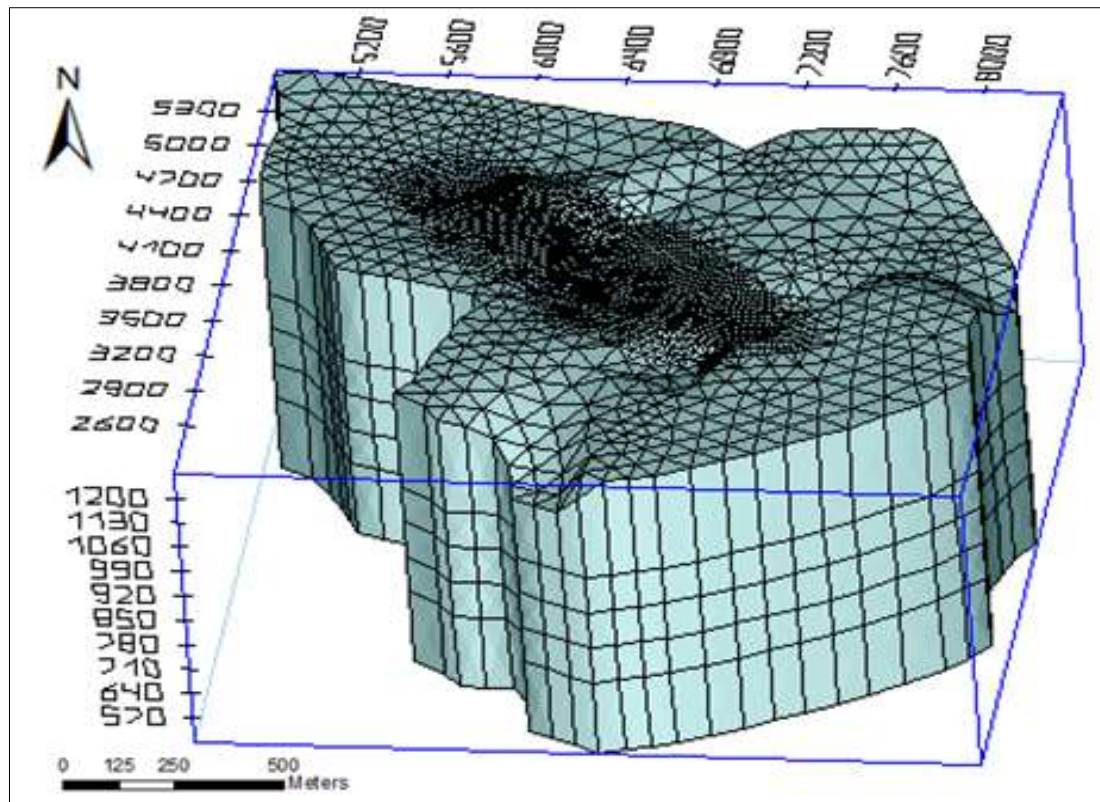


Figure 6-1: Ruashi finite element mesh showing refinement in the pits area

6.4.5.2 Water level

Initial hydraulic heads are presented in Figure 6-2 which shows depression in the pits area. Pristine shallow groundwater levels are associated with high elevated areas. This could indicate a strong correlation between groundwater levels and the surface topography. According to Bayesian extrapolation method, surface elevation plays an important role in the study and the assumption that groundwater flow directions conform to surface drainage.

6.4.5.3 Storativity

Determination of storativity is not required for the steady-state calibration. An estimate of the aquifer storativity was obtained from the calibration of the transient state groundwater flow model. A value of 0.02 is assigned for the transient simulations, according to "A Practical Guide to Groundwater and Solute Transport Modelling" by Moreno and Spitz (1996).

6.4.5.4 Recharge

The steady state calibration simulations were conducted using recharge value of approximately 280 mm per year, which corresponds to 14% of the estimated annual precipitation (MAP) of 2000 mm. Recharge to the tailings dam was estimated at 7 759 m³/d.

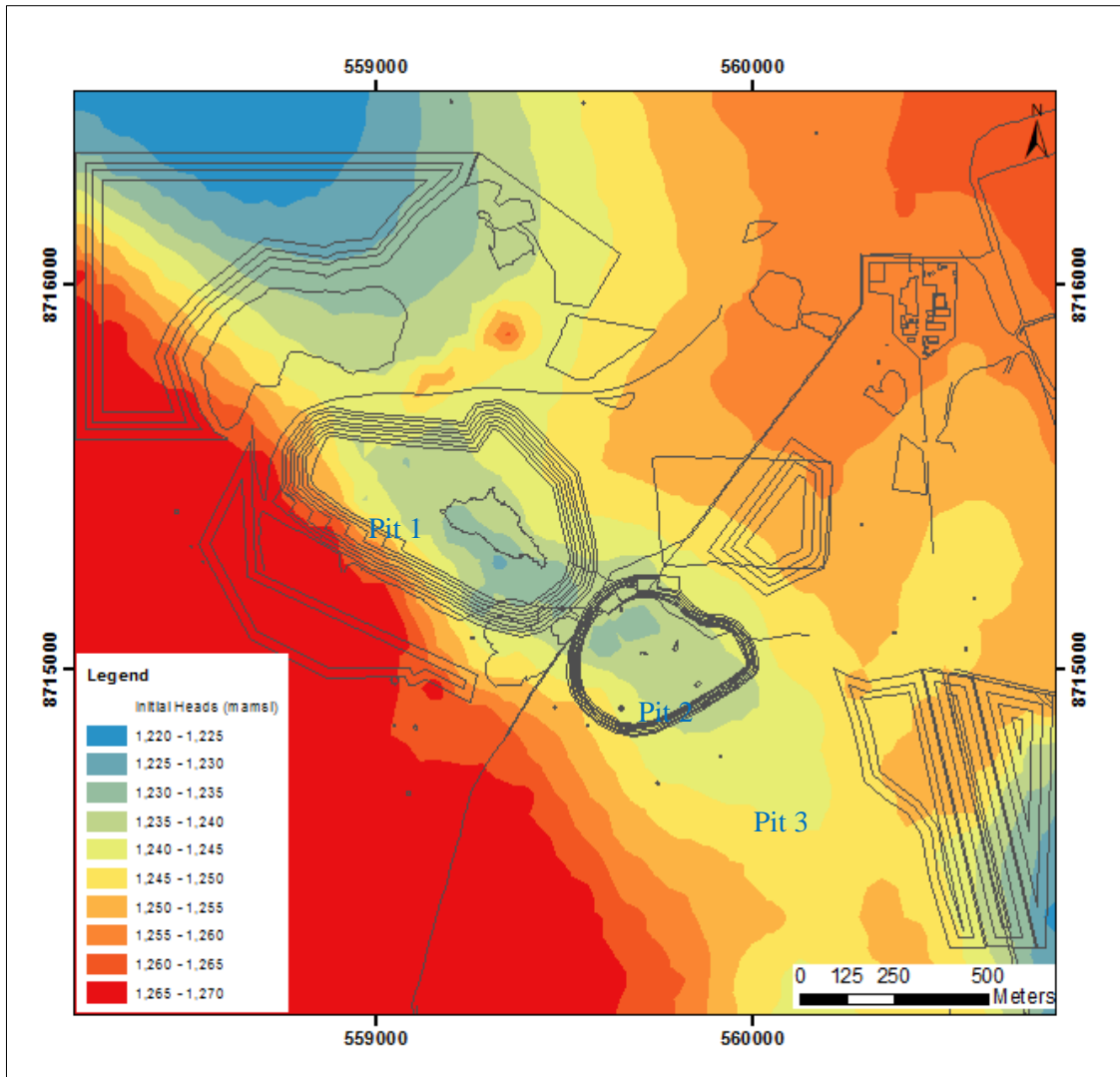


Figure 6-2: Ruashi initial heads map showing deep water level in the pits area due to pumping

6.4.5.5 Evapotranspiration

Evapotranspiration was estimated at 3 mm/d but was not specified in the model. It is assumed that the recharge specified in the model overcomes the effect of evapotranspiration losses from the system.

6.4.6 Aquifer transmissivity and hydraulic conductivity distribution

The study area transmissivity (T) value was calculated by assuming hydraulic conductivity values obtained from the aquifer hydraulic test carried out at borehole BH3-39 ($K=1.48$ m/d). Considering that the thickness of the Roan aquifer is about 200 m, the transmissivity equates to 292 m²/d.

6.5 Model calibration

The model was calibrated using water level heads which are a function of the product of the saturated aquifer thickness, the hydraulic conductivity and effective aquifer recharge. Should the average aquifer thickness be under/overestimated, this can be compensated for by adjusting hydraulic conductivity values during model calibration.

6.5.1 Steady state calibration

The reliability of a model can be evaluated by the accuracy with which it can reproduce observed results. Steady state calibration was done according to the American Society for Testing and Materials (ASTM) guidelines for calibration of the model (Anderson and Woessner 1992). In order to reproduce the observed groundwater behaviour, the model was calibrated using data from 2010 to 2011. The data comprised total volume of mine pumping, dewatering-borehole discharges and hydraulic conductivity values obtained from aquifer hydraulic test. Steady state calibration was accomplished by varying the hydraulic conductivity values within a realistic range based upon the field data and the recharge rate until a reasonable match between the measured groundwater elevations and the simulated groundwater elevations was obtained.

For the purpose of this modelling study, a constant recharge rate of 280 mm per year, estimated using field data and presented in Chapter 5, was considered reasonable and likely to result in similar regional predictions compared to spatially distributed recharge. The discharges from the mine were used as input data so as to obtain matching values of hydraulic conductivity for steady state conditions. In other words, the model was forced to produce the measured discharge in order to simulate the appropriate values of hydraulic conductivity, which would produce a groundwater level map similar to that produced from measured borehole water level data.

6.5.2 Steady state calibration results

Hydraulic conductivity values obtained during calibration ranged from 0.23 m/d in the shallow Laterite aquifer and 1.74 m/d in the deep Roan aquifer. The variation with depth was very little. In the shallow aquifer, the value changed from 0.23 m/d in the upper levels to 0.15 m/d. In the deeper aquifer, the hydraulic conductivity value changed from 1.74 m/d to 1.24 m/d. A correlation coefficient of 90% was obtained between observed and simulated water levels. The observed groundwater levels are plotted against the simulated water levels as shown in Figure 6-3. Deviations from the straight line indicating a perfect match between the observed and simulated values should be randomly distributed indicating that there is no bias towards over or under predicting the groundwater levels (Anderson and Woessner 1992).

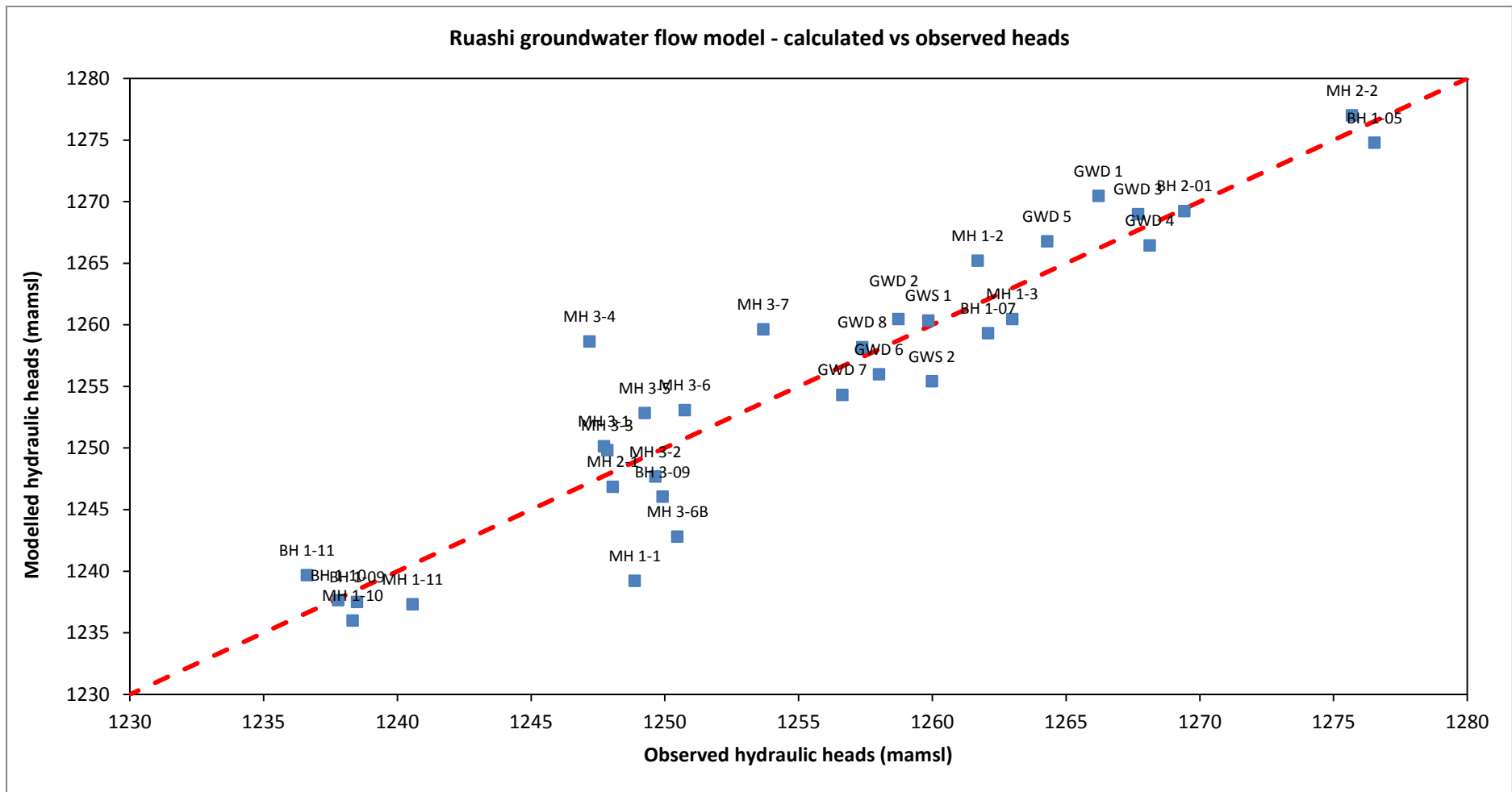


Figure 6-3: Ruashi observed versus simulated hydraulic head

Figure 6-4 is a water level map produced after steady state calibration. The calibrated model water level is similar to what would be expected, the water level closely conforms to local topographic features and shows depressions in areas that are affected by pumping.

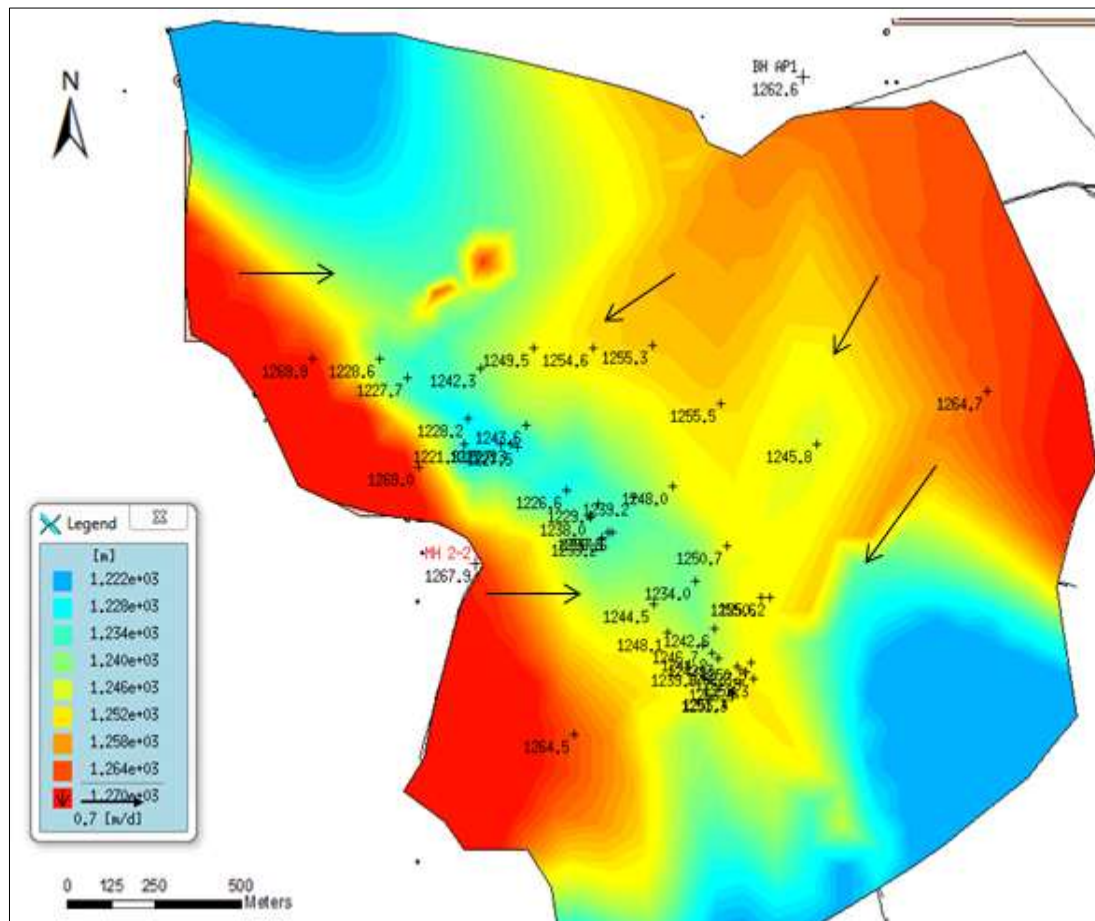


Figure 6-4: Groundwater flow in steady state showing water level flow from south western catchment and north eastern catchment towards the pits area

The difference between the simulated and the observed hydraulic head was calculated for each borehole. The error in the calibration was expressed by the mean error (ME) method as outlined by Anderson and Woessner (1992). Figure 6-5 shows a plot of the modelled versus observed errors.

The ME is the mean difference between measured and simulated water levels. The ME was evaluated as a ratio to the total water level change across the model domain. According to Anderson and Woessner (1992), if the ratio is small, the errors are only a small part of the overall model response.

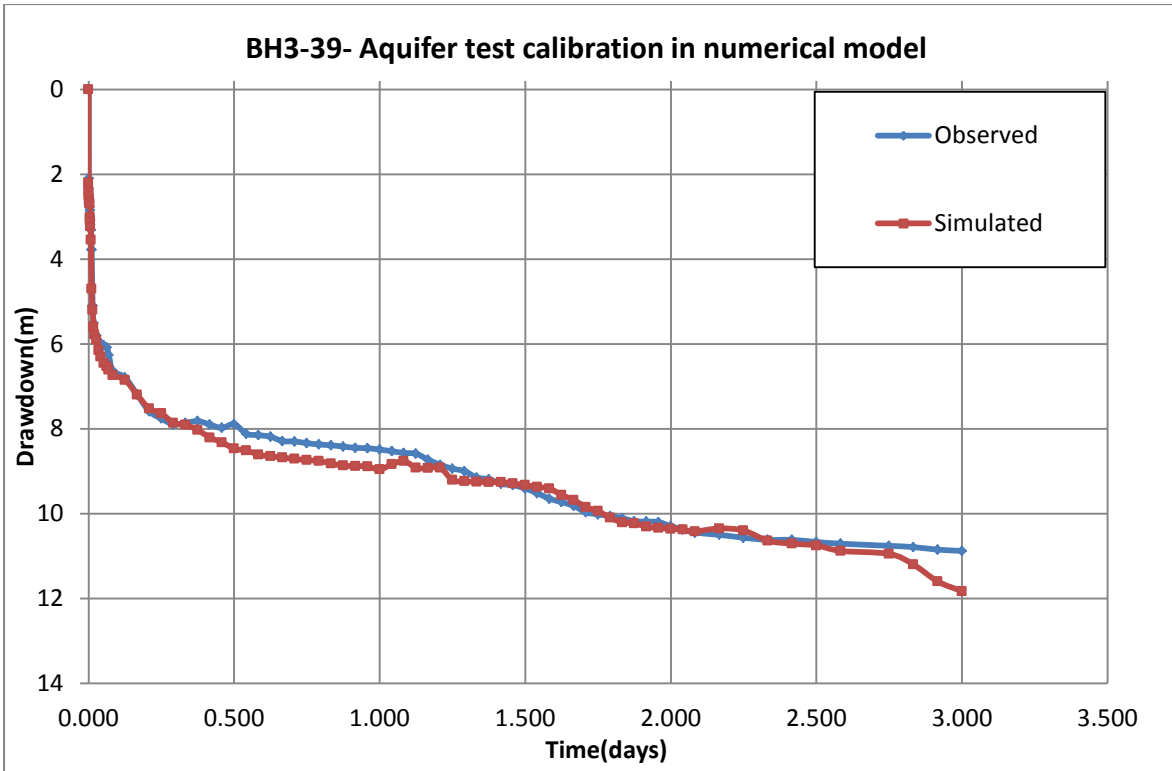


Figure 6-6: Observed vs. Simulated water level drawdown response at pumping well BH3-39

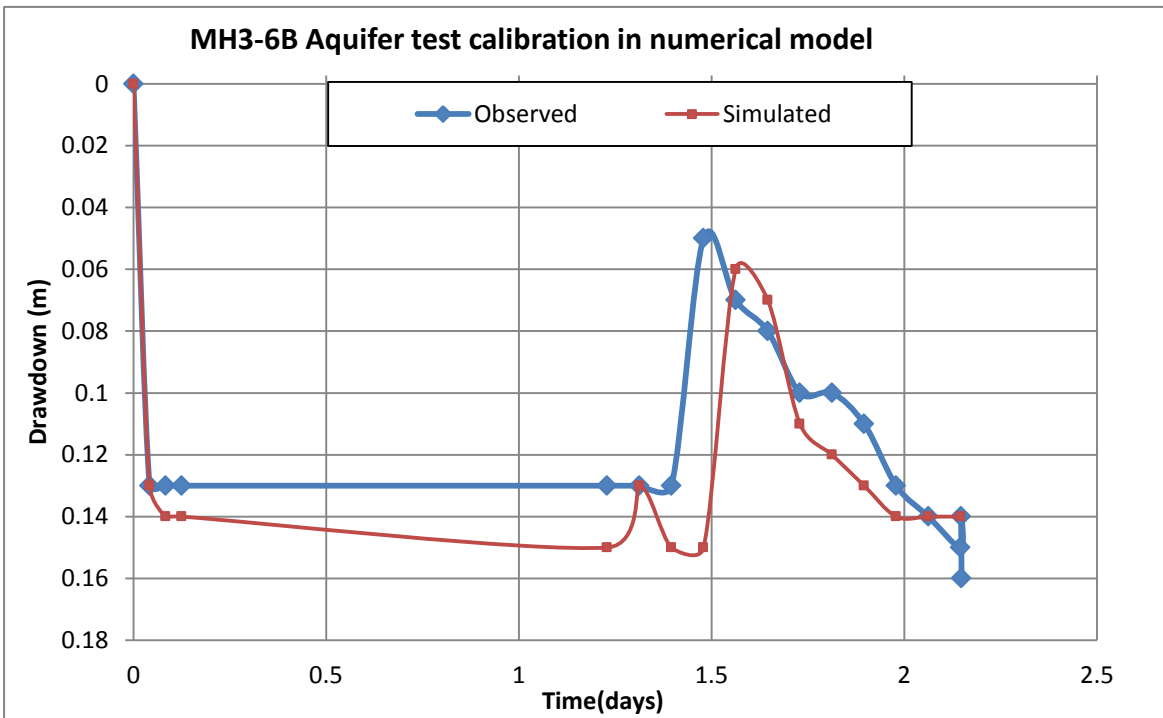


Figure 6-7: Observed vs. Simulated water level drawdown response at observation well MH3-6B located at 80 m south of pumping well BH3-39

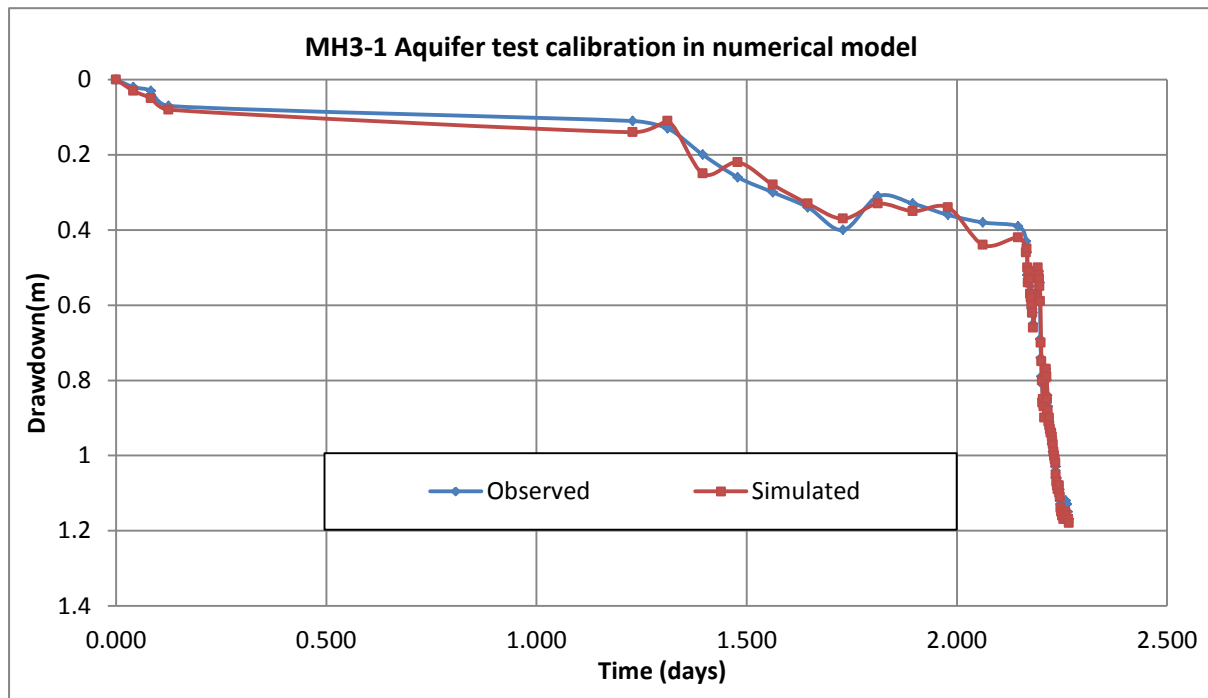


Figure 6-8: Observed vs. Simulated water level drawdown response at observation well MH3-1 located at 40 m west of pumping well BH3-39

6.6 Numerical groundwater flow scenarios

Scenario 1 to Scenario 3 were run to demonstrate the sensitivity of the numerical groundwater flow model to changes in pumping rates. This is necessary in determining the pumping rates that will be required to dewater the mine.

6.6.1 Scenario 1- Sixteen (16) boreholes each pumping 500 m³/d plus existing boreholes

In order to estimate the pumping volume required to lower the groundwater level to below final pit bottom level, that is, 180 mbgl (approximately 1 090 mams), the observed drawdown (10.5 m) during constant rate (3 400 m³/d) testing at BH3-39 was projected to 180 m. It was estimated that a pumping rate of approximately 42 000 m³/day would be required to lower the groundwater levels to 180 mbgl. Given that the existing pumping boreholes BH3-39, BH2-7, BH2-28 and BH1-15 are pumping at approximately 3 400 m³/day, 2 200 m³/day, 1 800 m³/day and 1 900 m³/day respectively, an additional 16 boreholes pumping approximately 2 000 m³/day will be required to achieve a total of 42 000 m³/d. The existing pumping boreholes plus an additional sixteen boreholes each pumping 500 m³/d were used in Scenario 1 to simulate drawdown changes over 16 years of mining. The simulated water levels are presented in Figure 6-9.

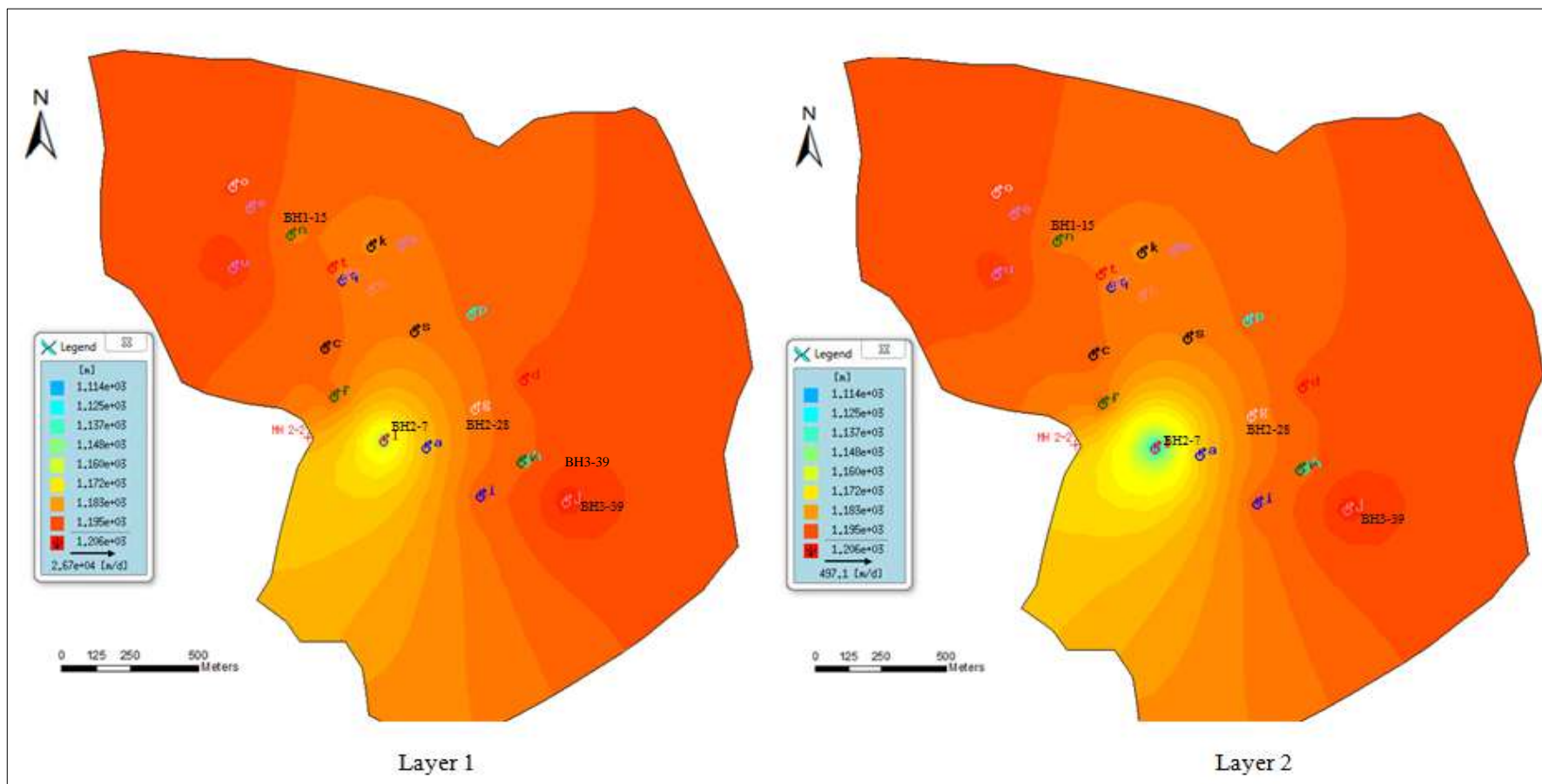


Figure 6-9: Simulated water level for Layers1 and 2 in Scenario 1 over operational time of 16 years

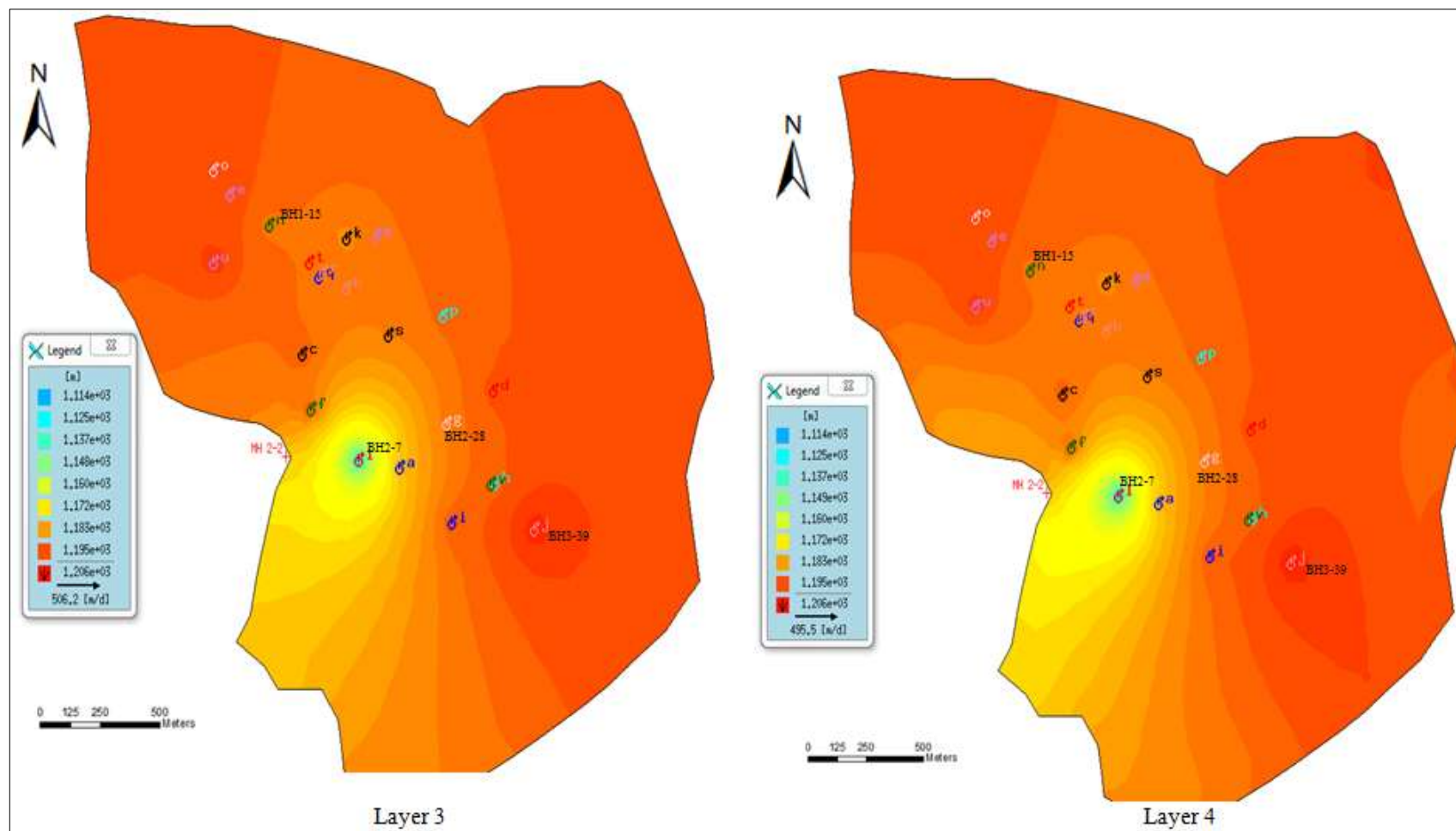


Figure 6-9: Simulated water level for Layers 3 and 4 in Scenario 1 over operational time of 16 years

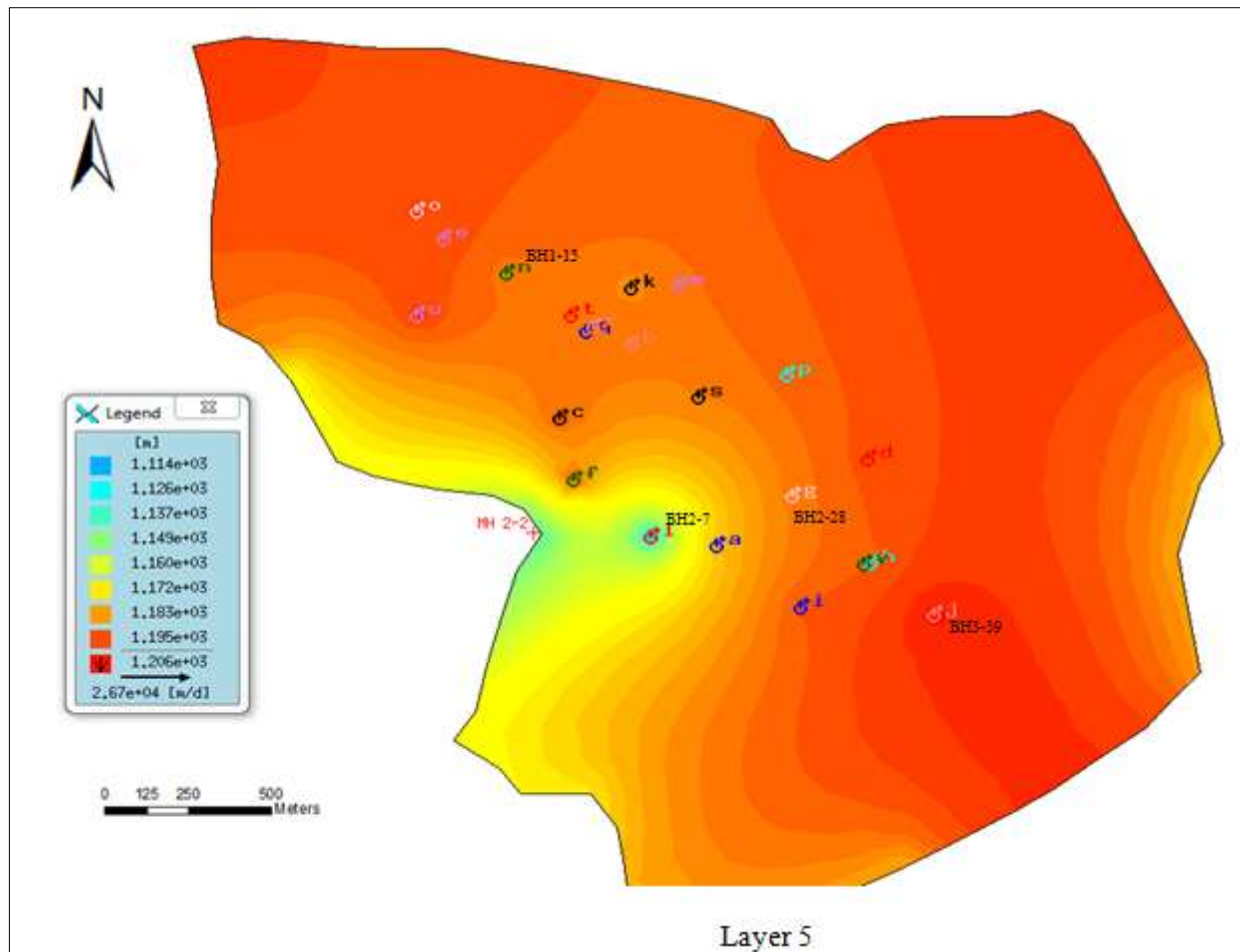


Figure 6-9: Simulated water level for Layer 5 in Scenario 1 over operational time of 16 years

6.6.2 Scenario 2 - Sixteen (16) boreholes each pumping 1 000 m³/d plus existing boreholes

Sixteen boreholes each pumping 1 000 m³/d were used in Scenario 2 to simulate drawdown changes over 16 years of mining. The pumping rates for the existing four pumping boreholes stated in Scenario 1 were maintained. The simulated water levels are presented in Figure 6-10. It is clear in the water level maps for all five layers that the simulated water level reached about 1 110 mamsl after 16 years of continuous pumping. However the water levels in layers 3, 4 and 5 observed at pumping borehole BH2-7 reached approximately 1 084 mamsl. This could be attributed to BH2-7 high pumping rate of about 2 200 m³/d.

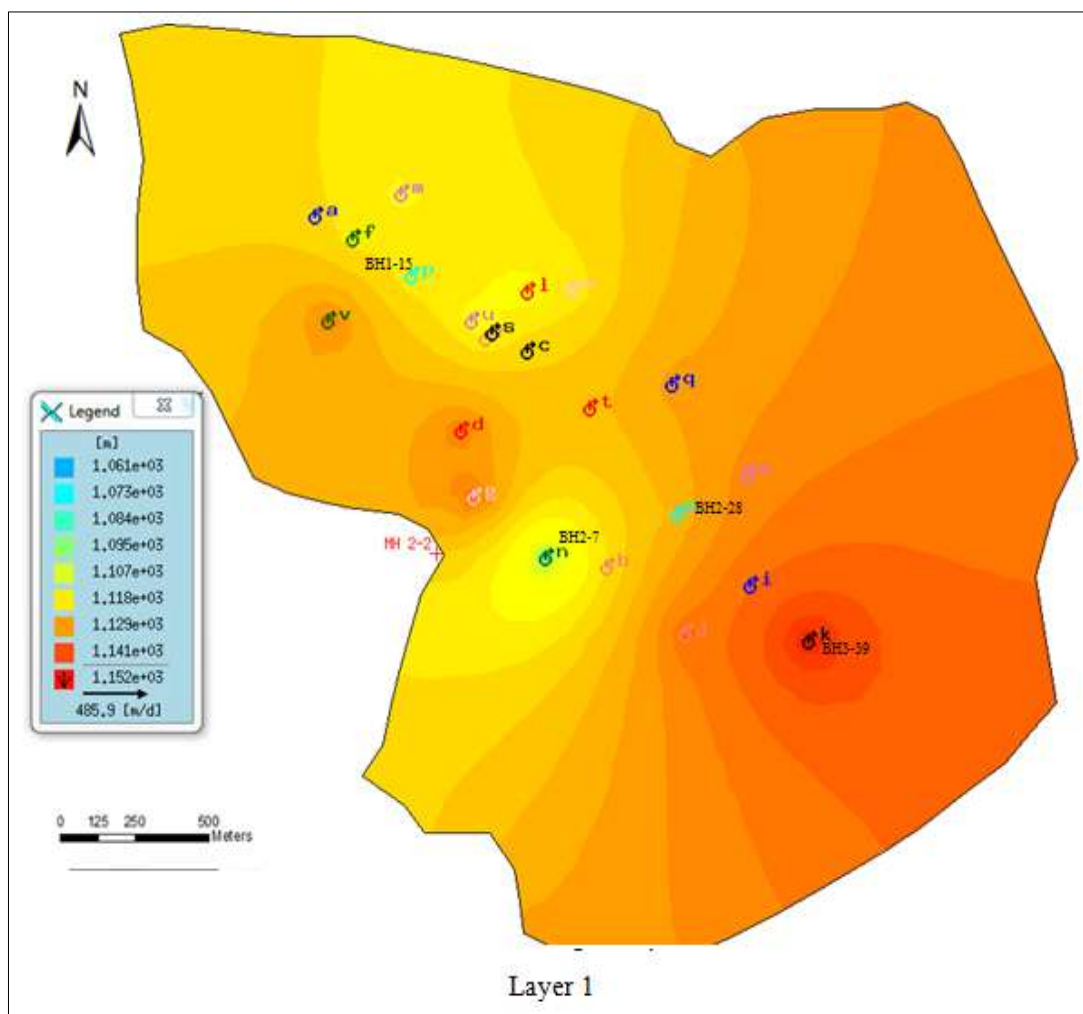


Figure 6-10: Simulated water level for Layer 1 in Scenario 2 over operational time of 16 years

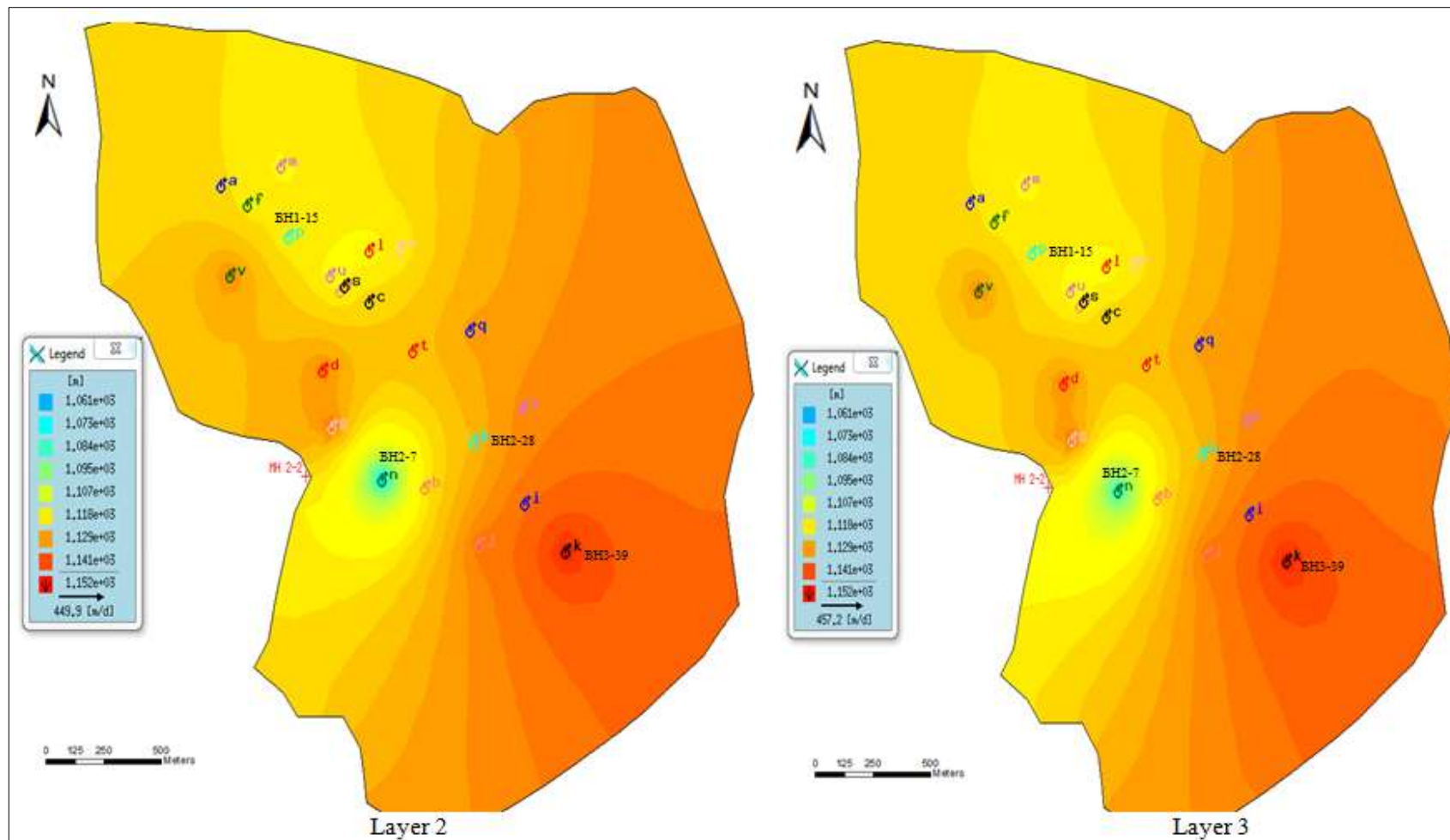


Figure 6-10: Simulated water level for Layers 2 and 3 in Scenario 2 over operational time of 16 years

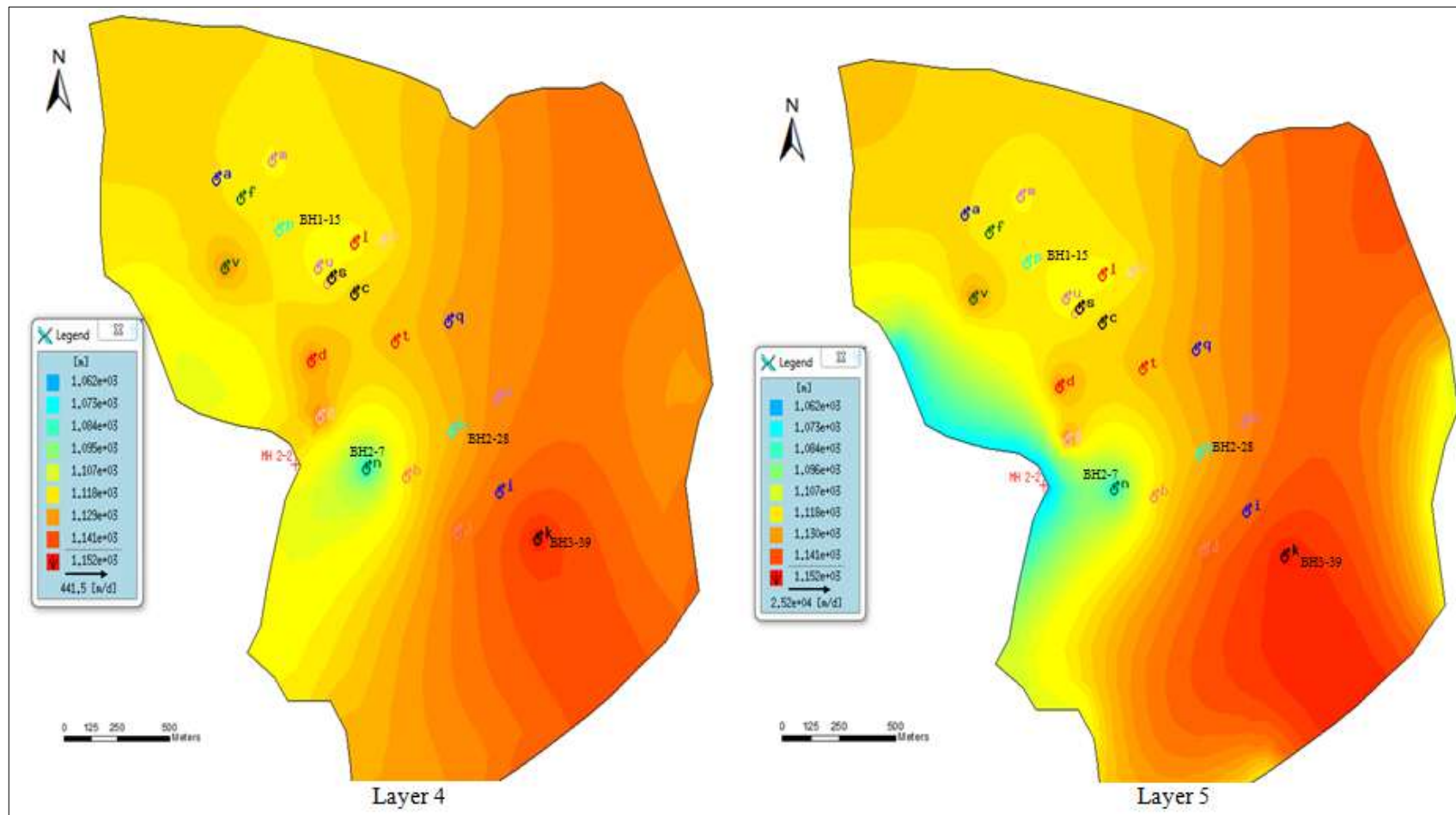


Figure 6-10: Simulated water level for Layers 4 and 5 in Scenario 2 over operational time of 16 years

6.6.3 Scenario 3- Sixteen (16) boreholes each pumping 2 000 m³/d plus existing boreholes

Using the same number of boreholes as in Scenarios 1 and 2, the pumping rate for the sixteen boreholes was increased to 2 000 m³/d per borehole. The pumping rates for the existing boreholes were maintained. The simulated water levels are presented in Figure 6-11. It is clear in the simulated water levels for layers 2 to 5 that the water levels reached about 1 088 mamsl after 16 years of continuous pumping. A deeper water level of approximately 1 079 mamsl is observed in the south west of Layer 5.

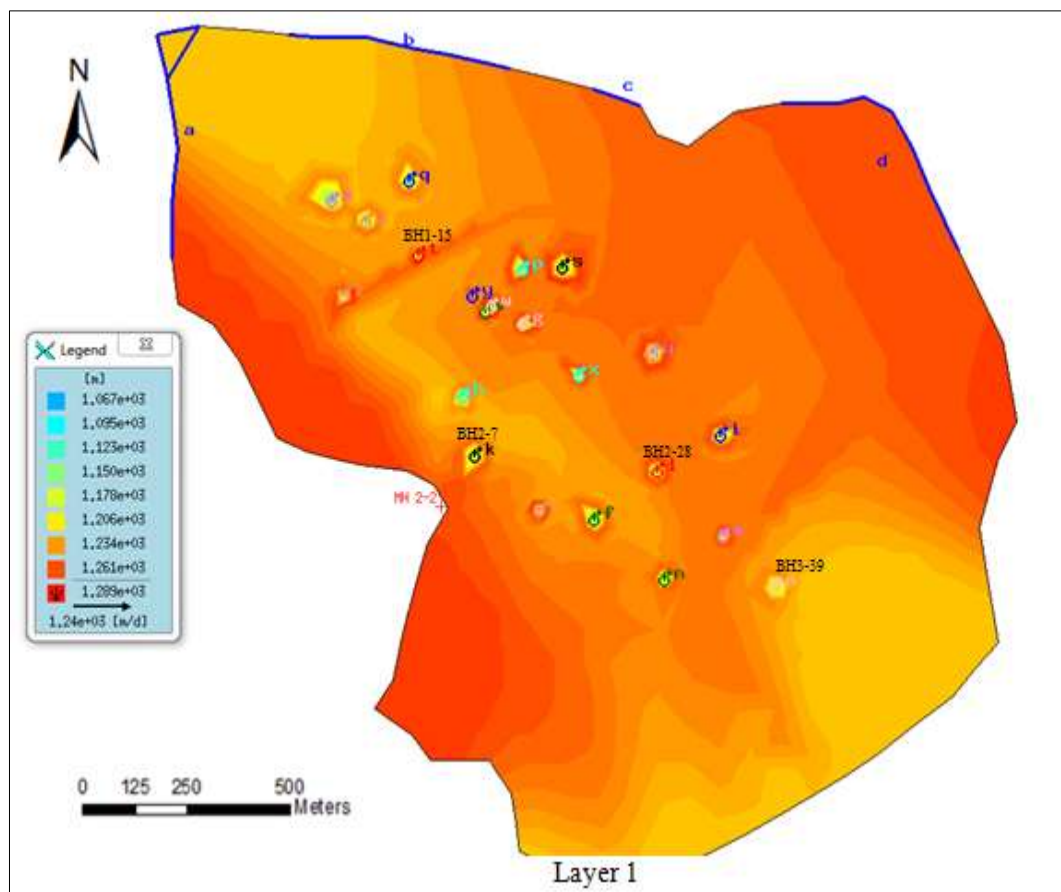


Figure 6-11: Simulated water level for Layer1 in Scenario 3 over operational time of 16 years

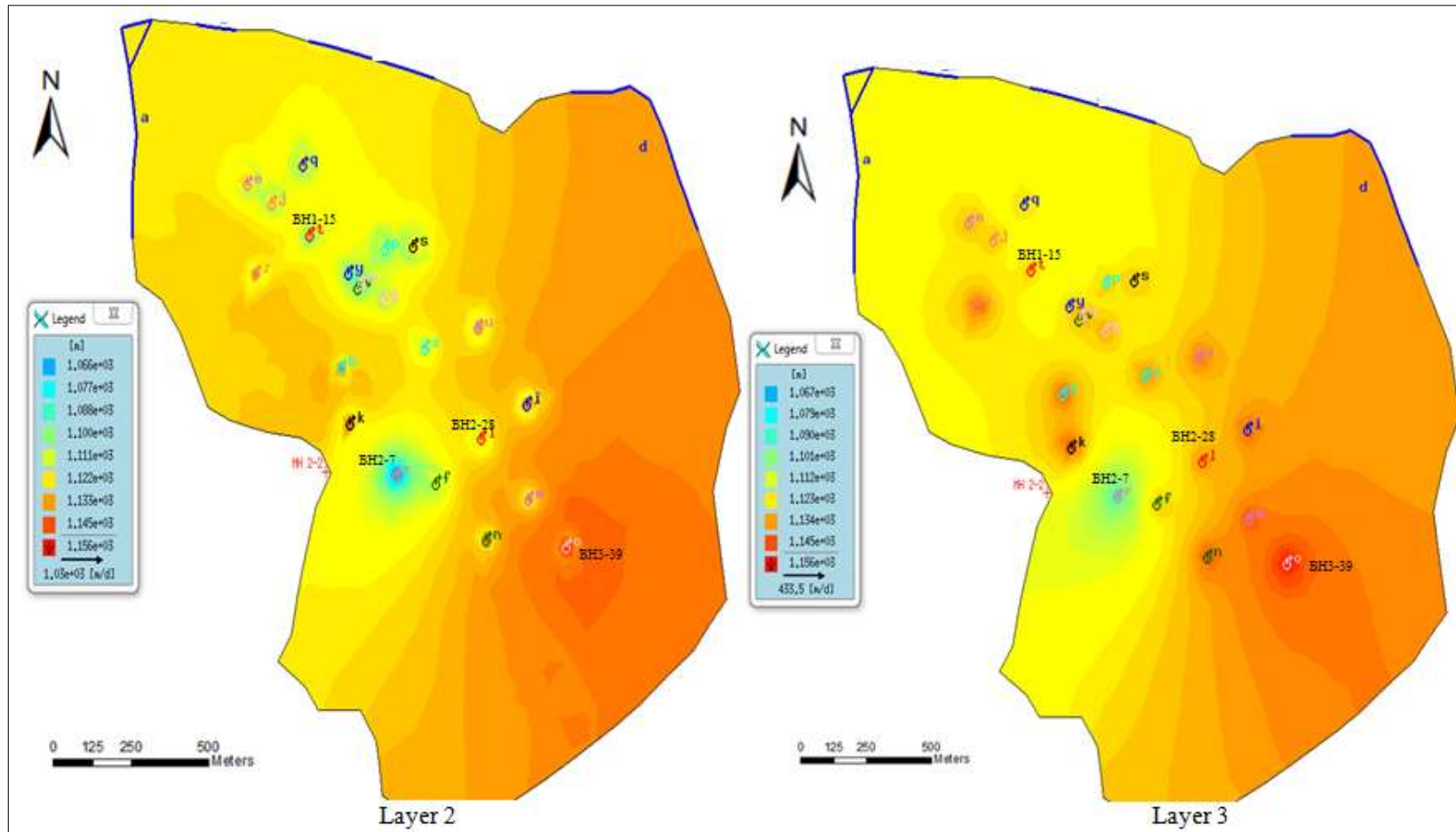


Figure 6-11: Simulated water level for Layers 2 and 3 in scenarios 3 over operational time of 16 years

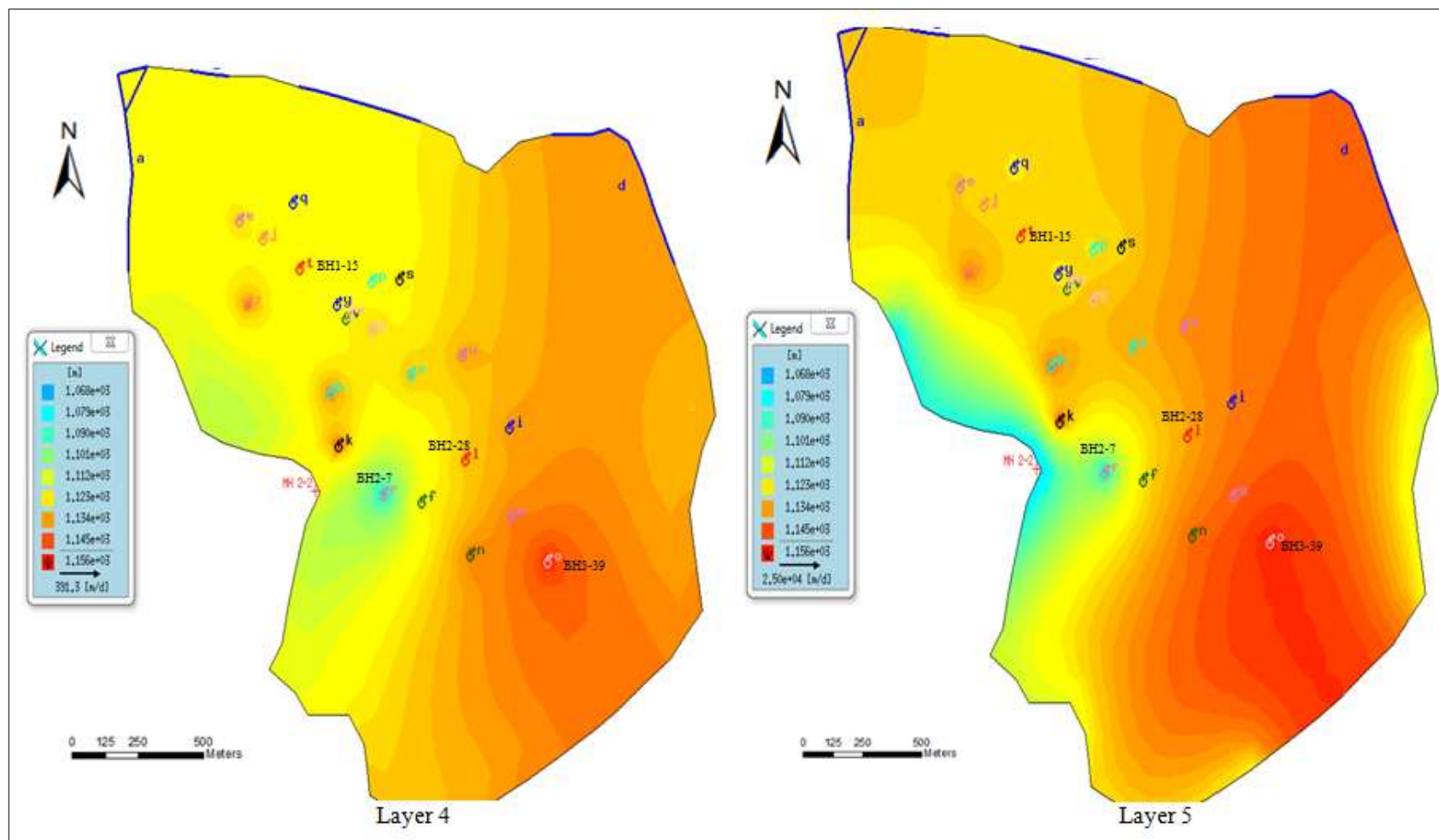


Figure 6-11: Simulated water level for Layers 4 and 5 in Scenario 3 over operational time of 16 years

6.7 Simulated flow through the inner and outer model boundary

The Budget Analyser, a computing tool included in Feflow was used to simulate groundwater entering and exiting the simulated area. Areal fluxes are due to infiltration and recharge from various sources. The imbalance represents the difference between the groundwater flowing into and flowing out of the system. Imbalance-In represents a gain in storage and Imbalance-Out indicate a loss in the system. Table 6-2 and Table 6-3 present simulated groundwater flow into and out of the modelled area and groundwater flow through the three boundary types.

Table 6-2: Simulated groundwater flow through inner and outer model boundaries

Year	Flux Through In (m ³ /yr)	Flux Through Out (m ³ /yr)	Areal Fluxes In (m ³ /yr)	Areal Fluxes Out (m ³ /yr)	Imbalance-In (m ³ /yr)	Imbalance-Out (m ³ /yr)
2012	53 518	891 554	1 220 787	65 732	317 020	-
2013	53 491	814 063	1 155 867	341 133	54 159	-
2014	55 385	849 457	1 261 108	332 705	134 327	-
2015	55 114	1 066 265	1 498 041	50 928	435 961	-
2016	54 042	943 426	1 423 613	3 242 945	209 933	-
2017	114 986	1 019 336	1 536 584	322 102	310 133	-
2018	55 201	1 350 397	1 781 888	48 043	438 650	-
2019	54 378	1 797 424	1 703 608	319 448	358 883	-
2020	55 491	1 275 982	1 805 608	318 408	266 052	-
2021	70 832	1 663 413	2 033 196	46 826	393 788	-
2022	54 936	1 976 771	1 954 506	317 043	284 364	-

Table 6-3: Simulated groundwater flow through model boundary conditions

Year	Flux In (m ³ /yr) Dirichlet 1st kind	Flux Out (m ³ /yr) Dirichlet 1st kind	Flux In (m ³ /yr) Neuman 2nd kind	Flux Out (m ³ /yr) Neuman 2nd kind	Flux In (m ³ /yr) Cauchy 3rd kind	Flux Out (m ³ /yr) Cauchy 3rd kind
2012	127 385	81 326 380	5 228 260	-	4 015	20 075
2013	129 210	81 385 875	5 215 850	-	3 650	20 075
2014	151 475	84 894 620	5 192 855	-	193 815	51 100
2015	168 995	92 547 210	5 231 910	-	1 460	31 025
2016	171 550	94 309 795	5 230 815	-	1 460	32 850
2017	181 770	101 878 435	5 215 120	-	6 101 340	54 750

Year	Flux In (m ³ /yr) Dirichlet 1st kind	Flux Out (m ³ /yr) Dirichlet 1st kind	Flux In (m ³ /yr) Neuman 2nd kind	Flux Out (m ³ /yr) Neuman 2nd kind	Flux In (m ³ /yr) Cauchy 3rd kind	Flux Out (m ³ /yr) Cauchy 3rd kind
2018	204 400	111 722 485	5 231 545	-	114 610	1 427 880
2019	205 495	113 638 005	5 227 165	-	4 745	66 104 055
2020	214 255	120 564 975	5 221 325	-	47 450	7 032 820
2021	226 300	129 539 960	5 235 560	-	1 415 835	33 777 465
2022	228 125	131 350 725	5 233 735	-	31 390	66 325 975

6.8 Simulated pit inflows

6.8.1 Modelling methodology and simulation of pit inflows

The open cast pit plans have been incorporated into the flow model by specifying constant head cells in the model at the elevation of the floor of the pit excavation where mining is taking place. The elevations of the constant head cells in the model were therefore specified exactly according to the depth of mining with time. The June 2012 pit floor elevations were set at 1230 mamsl for Pit 1, 1235 mamsl for Pit 2 and 1238 mamsl for Pit 3. Flow constraints were imposed on the constant heads such that water can only be removed from the system.

Groundwater flow into the open cast pits varied with depth. Table 6-4 and Figure 6-4 show simulated total flows into the open cast pits. The maximum total inflow of approximately 42 000 m³/d was predicted to occur after 11 years of mining in the year 2022. The inflows predicted by the model may be somewhat higher than currently experienced, this is due to the high recharge value of 280 mm per annum, combined with the absence of a more detailed mine plan.

The simulated maximum inflow into Pit 3 was simulated to be 21 650 m³/d after 11 years of mining. The simulated maximum flow into Pit 2 is 8 510 m³/d and will occur in the year 2022. Pit 1 was predicted to experience inflow of about 11 237 m³/d by the end of Pit 1 mining in the year 2021. The mine plan indicates that there will be no mining in Pit 1 after the year 2021.

Table 6-4: Predicted inflow into Ruashi open cast pits

Year	Pit 1 inflow (m³/d)	Pit 2 inflow (m³/d)	Pit 3 inflow (m³/d)	Total (m³/d)
2012	9 465	3 473	1 378	14 316
2013	10 631	3 868	1 195	15 694
2014	9 898	4 044	4 736	18 678
2015	10 682	4 848	8 747	24 277
2016	10 046	4 814	11 462	26 323
2017	10 227	4 964	14 481	29 673
2018	10 090	5 250	16 798	32 139
2019	11 219	5 841	18 187	35 248
2020	11 213	6 229	19 444	36 888
2021	11 237	7 201	20 379	38 817
2022	No mining	8 509	21 649	41 383

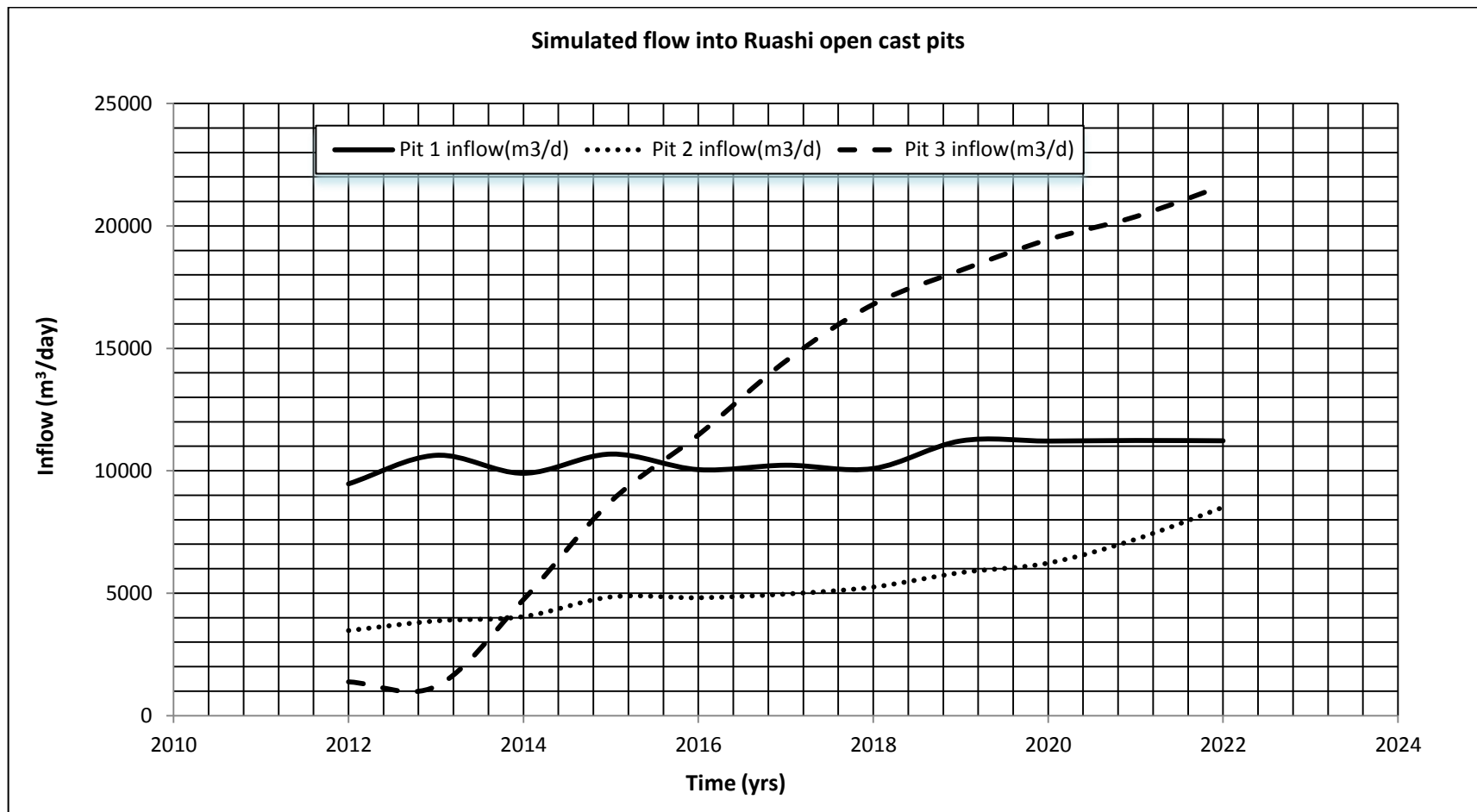


Figure 6-12: Simulated flow into Ruashi open cast pit

6.8.2 Drawdown changes over 11 years of mining

Figure 6-13 shows the simulated versus observed drawdown caused by mine dewatering activities at the current pumping rates of about 15 000 m³/d. The maximum water level drawdown in the area of mining is in the order of 55 m. The shape and size of the drawdown cone will depend upon the mining activity, the aquifer geometry and aquifer hydraulic parameters and will depend on the installed dewatering system. The dewatering cone propagates as depth of mining progresses. The simulation gave the following water level impacts during mining:

- After 1 year, drawdown of 10 m will be observed at a distance of 1.6 km from the pit perimeter;
- The drawdown cone will continue to increase as the pit floors deepen and water levels decline. After 4 years, the drawdown will be 37 m in the central part of Pit 1;
- After 10 years, drawdown of 43 m will have expanded to 3.5 km from the pit perimeter;
- At the time mining completion in 2022, the drawdown cone will have expanded such that 55 m of drawdown is experienced at a distance of approximately 8 km. This drawdown induced by current pumping rates is insufficient as mining is expected reach 180 mbgl.

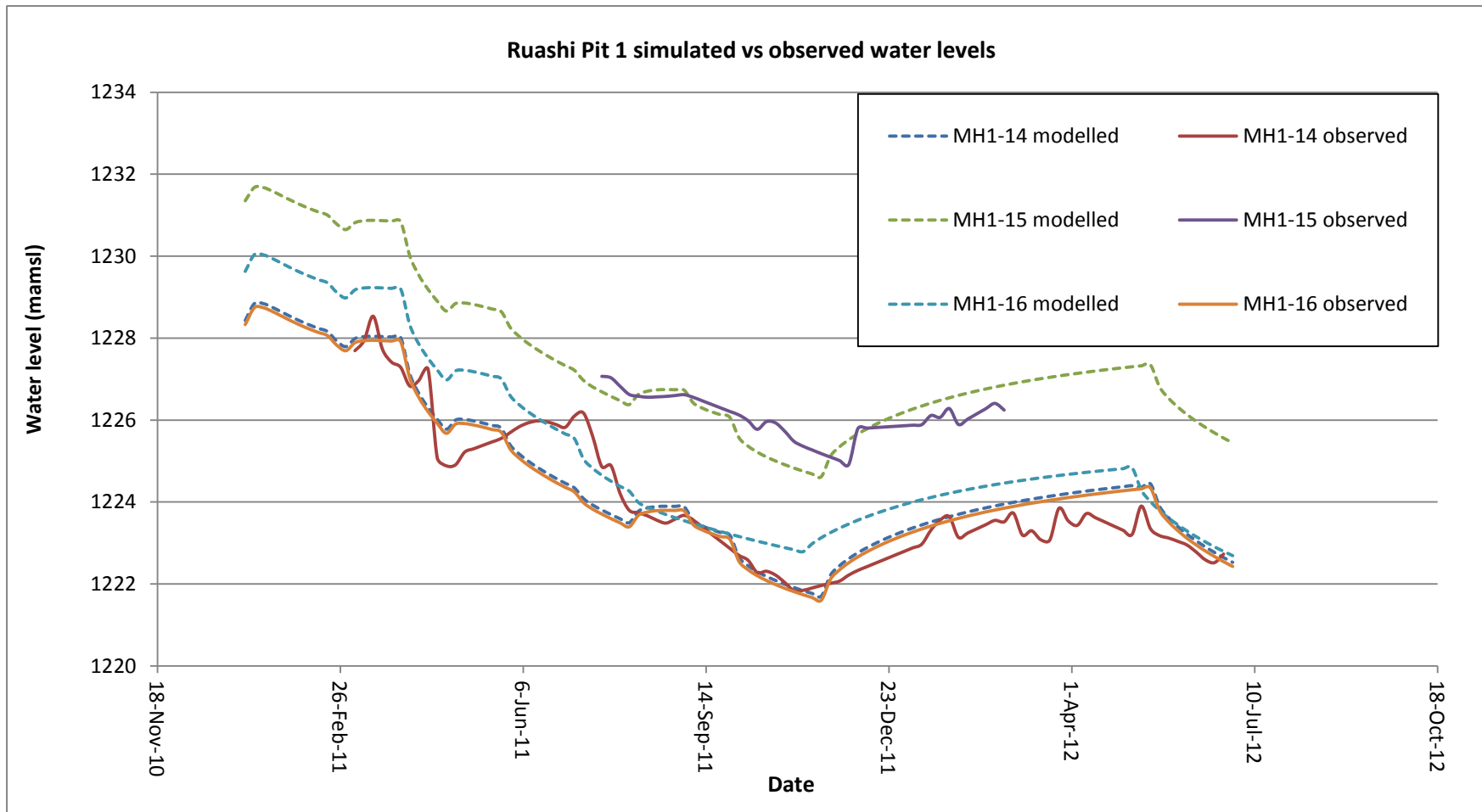


Figure 6-13: Ruashi simulated versus observed water levels

6.9 Summary

This chapter presents the five-layered 3D groundwater flow model that was performed to simulate groundwater flow through Ruashi Mine and predict inflows to the three open cast pits. The model is a Finite Element (FE) triangular mesh consisting of 17 240 elements and 10 614 nodes.

Defining the model boundaries is a critical task: The extent of the shallow aquifer system covers the whole mine. The aquifer system drains towards the Luano and Kebumba Rivers hence these rivers were chosen as constant head boundaries. The other boundaries followed high and low topographic and groundwater divides to the south and north of the mine.

Transmissivity value of $292 \text{ m}^2/\text{d}$ estimated from aquifer hydraulic testing was assigned to the deep Roan aquifer whilst lower values estimated from drilling results were assigned to the shallower Kundelungu aquifer units. Recharge value of 280 mm per year, estimated from field data using the Chloride Mass Balance method was assigned to the model. Storage coefficient values were varied during model calibration.

Model calibration runs that link hydraulic gradients to mine discharge provide an indication of the values for hydraulic conductivity. Steady state calibration was achieved by varying the hydraulic conductivity values until a 90% correlation between the measured and simulated water levels was achieved. Transient calibration was run such that the model was able to simulate the observed drawdown during aquifer hydraulic testing.

Based on the current pumping capacity of $15\,000 \text{ m}^3/\text{d}$, the model predicted a maximum drawdown of 55 m. However with an additional set of 16 boreholes pumping $2\,000 \text{ m}^3/\text{d}$ each, the predicted maximum drawdown is slightly over 180 m. The simulated total inflow to the three pits is $42\,000 \text{ m}^3/\text{d}$ after 11 years of continuous mining.

The model serves to complement field studies and therefore should not replace field investigation and monitoring. Time dependent values for hydraulic conductivity, storage coefficient, discharge and boundary conditions may change as the mine evolves therefore the numerical model for the mine should be supported by a parallel field study programme during the life of the mine.

The next chapter discusses the application of preliminary pumping data and numerical model results in designing a strategy for dewatering the mine.

7 DEWATERING STRATEGY

7.1 Introduction

Uncontrolled inflow of groundwater poses several problems to open cast mining, foremost of which is its catastrophic effect on slope stability. Ruashi Mine experiences two major problems notably (a) slope failure and (b) flooding of pit floors (refer to Section 1-2). These problems have made the installation of an effective dewatering system inevitable. The success of dewatering the open pits at Ruashi Mine will depend on how well the hydrogeological system is understood. Due to the complexity of the hydrogeological environment at the mine, the current dewatering system is not effective. At the current stage the magnitude of collapse of pit walls and flooding at Ruashi Mine depends primarily on the groundwater levels, the hydraulic conductivity of the rock units in the high walls and the local recharge to the groundwater system (refer to Chapter 5). The most effective dewatering method for the mine depends on the site-specific hydrogeological conditions as set out in Section 5.2.1 and Table 5-4. The majority of modern mines use a combination of sump pumping, grouting, and strategically designed active pumping and water interception systems. In general, dewatering a mine in advance of mining will have the following benefits:

- Slope stability and safety
 - reduced risk of flooding and pit floor ponding
 - dry work environment
- Production
 - higher production rates due to increased excavation volumes
- Environmental
 - reduced pollution plume development risk from mining oil/fuel residues
 - clean water harvest from the pits area

7.2 Possible dewatering methods

It is important to consider the various options for dewatering and relate to the existing hydrogeological system at Ruashi Mine. The hydrogeological system and mining method guide in the choice of the most effective dewatering method. The following section discusses the advantages and disadvantages of common dewatering methods and their applicability to Ruashi Mine.

7.2.1 Grouting

The aquifers at Ruashi Mine are characterised by double porosity (matrix and fracture). According to *Bowell et al.* (2002), grouting is difficult in double porosity aquifers because one can never seal all the fractures/fissures and interconnected pore networks which means that sudden inflows can still occur. Furthermore, Ruashi Mine practices blasting hence disturbance of rock mass due to such mining practices will open up fissures previously sealed by grouting.

7.2.2 Storm water control

Ruashi Mine is located between the equatorial and tropical rainforests with rainfall exceeding 1 200 mm per annum. The storm drain at Ruashi Mine does not completely surround the pits. Some sections of the storm drain are located within the stress relief relaxed zone resulting from open pit excavation. The stress relief relax zones have been observed to collapse during rainfall events. Overland flow from rainfall episodes, interflow and baseflow are contributors to open pit flooding. It is good practice to strategically construct water diversion infrastructure like drainage canals that are connected to functioning storm water systems.

7.2.3 Vertical pit perimeter boreholes

A logistically simple method for dewatering pits at Ruashi Mine could be the installation of vertical pumping boreholes along the pit perimeter. According to Hague and Germishuys (1999), the major advantage of perimeter boreholes is that once installed in the correct site they can last the entire life of the mine. The boreholes are sited along the pit perimeter hence will not interfere with pit excavation activities. There is large space for drilling along the pit perimeter compared to pit floors where drilling sites can be constrained by mining activities like ore extraction and haulage. Pit perimeter boreholes can be installed prior to mining and can intercept lateral flow. Their best application is where flow to the pit is lateral and where hydraulic conductivity is primarily horizontal (Hague and Germishuys, 1999). In aquifers where permeability is low and where the aquifers are anisotropic, the impact of dewatering using pit perimeter boreholes might not be effective on the centre of the pit. In the case of some localised perched zones in Ruashi Pit 1 and Pit 2, the perimeter boreholes can be augmented by in-pit boreholes. In order to effectively dewater the aquifers, pit perimeter boreholes usually have to be deeper than the ore body.

7.2.4 In-pit vertical boreholes

Vertical boreholes can be installed in the pits temporarily or permanently. In-pit boreholes are best applied in compartmentalised rock mass. Pit 2 at Ruashi Mine is a classic example

where perched zones created by CMN exist in the north and compartments of BOMZ or RAT in the west. Since in-pit boreholes can be installed in the ore zones, they create most drawdown below the pit floors. They can be installed to the bottom of the ore zone or alternatively can be shallow as they can be deepened as mining progresses. Vertical inflow through the bottom of the pit can be intercepted by vertical in-pit boreholes. The major disadvantage of installing vertical boreholes in the centre of the pit is that it may be difficult to mine around them. The casing has to be cut short each time the pit floor is lowered. Drilling activities may interfere with ore extraction and haulage logistics. Regardless of the disadvantages, Ruashi Mine installed pilot dewatering boreholes in the pits and these boreholes were installed as an emergency measure to lower the local groundwater table.

7.2.5 Horizontal drain holes

One technique which may be utilised to improve the stability of the pit walls is to install horizontal drains. According to Hague and Germishuys (1999), in-pit horizontal drain holes increase slope stability and can drain and/or depressurise through zones of high permeability. This dewatering method is passive and no special location is needed. In-pit horizontal drain holes are generally inexpensive as they are drilled at small diameters. Holes of say 5 to 10 cm in diameter are drilled horizontally near the toe of the slope and extend to the targeted dewatering zone. The holes can be lined with perforated casing to allow smooth inflow of groundwater. Drilling logistics can be made easier by nesting a number of holes in one location. Once the horizontal drain holes have been installed, groundwater flows into the drain holes towards sumps and eventually pumped out of the pit. In this way the groundwater level can be lowered and improve slope stability and dry working conditions.

7.2.6 Pit sumps

Pit sumps are small holes excavated at the bottom of the pits for the purpose of passively collecting groundwater. They usually augment other dewatering methods like the in-pit wells. Pit sumps have been used in Pit 1 at Ruashi Mine since mining commenced in 2006. Pit sumps can be dug to a depth (say 3 metres below the pit floor) and pumps are installed to actively pump the groundwater out of the pit. In order to aid passive flow of groundwater towards the sumps, the pit floors have to dip towards the sumps. Pit sumps are a relatively cheap method of capturing passive flow of groundwater (Hague and Germishuys 1999). The major disadvantage of the pit sump method is that the method may not be effective where groundwater flow rates exceed pumping capacity as the pit floors can be flooded. Pit sumps have to be replaced or deepened each time the pit floor is lowered as mining progresses.

7.3 Pit 1 Dewatering

When mining in Pit 1 commenced in 2006, seepage on the pit walls was noted at about 17 mbgl. Two 50 m deep pumping boreholes, namely BH1-12 and BH1-13, located 20 m apart, were installed in the centre of Pit 1 (refer to hydrocensus map shown in Figure 4-1). These boreholes were installed to actively dewater and lower the groundwater level in Pit 1 in advance of mining. In order to monitor the effect of dewatering, groundwater monitoring boreholes MH1-9, MH1-10 and BH1-11 were installed in PIT 1 at 20 m, 15 m and 25 m away from BH1-12. Groundwater monitoring borehole MH1-11 was installed at about 55 m west of BH1-12 on Pit 1 perimeter.

7.3.1 Flow response to preliminary pumping

During the period beginning October 2009 ending February 2010, boreholes BH1-12 and BH1-13 were pumping an average of 69 m³/hr and 72 m³/hr respectively. The response to pumping is depicted by hydrographs presented in Figure 7-1. The hydrographs show that BH1-12 and BH1-13 pumping rates were not sufficient to lower the groundwater levels to below pit floor. In February 2010, the submersible pumps in the pumping boreholes BH1-12 and BH1-13 were replaced with bigger capacity pumps and the pumping rates were increased to 233 m³/hr and 217 m³/hr respectively. As a result of increased pumping rates, the drawdown increased. Borehole BH1-11 hydrograph confirms the water level lowering impact of the adjacent pumping borehole BH1-12. All boreholes in Pit 1 recovered quickly when the pumps were shut off due to power loss. An additional dewatering borehole, BH1-15, was installed in the central eastern side of Pit 1 and was commissioned at the end of December 2010. The borehole (BH1-15) was pumping at average rate of 150 m³/hr. Data from the eastern section of the pit shown in BH1-11 hydrograph confirm that BH1-15 pumping began cutting off recharge to the pit, with an accompanying fall in hydraulic heads.

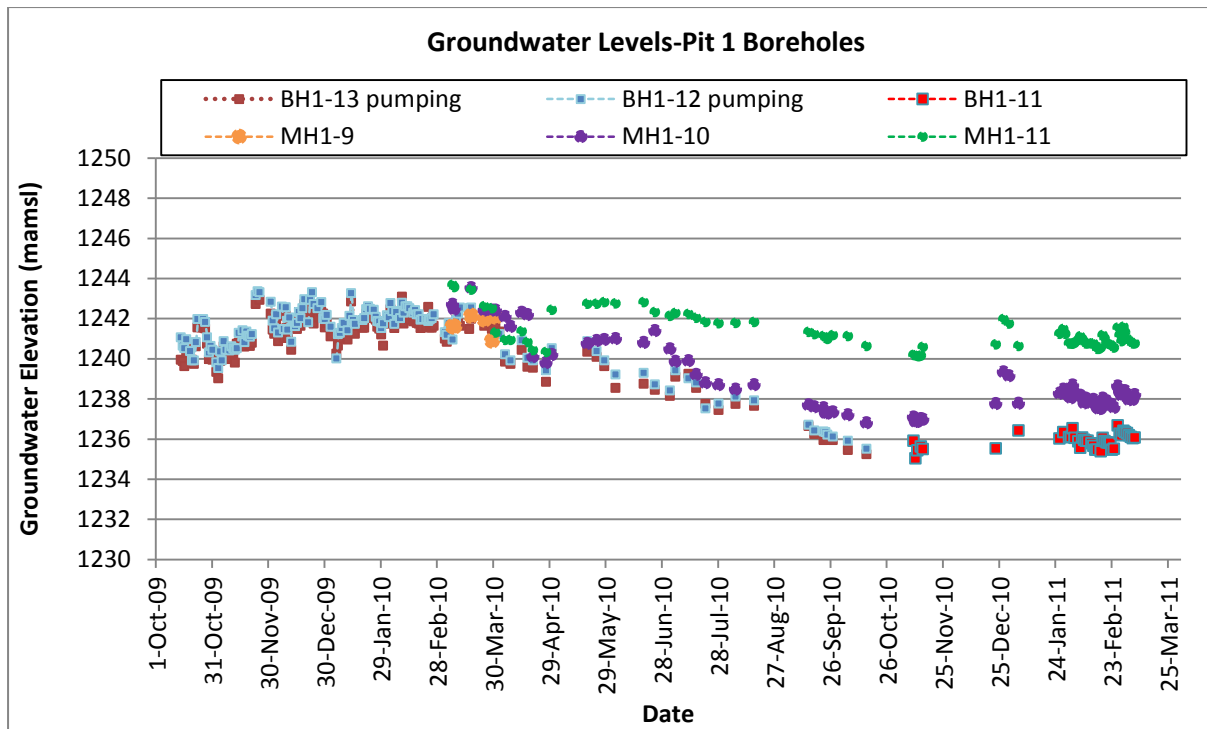


Figure 7-1: Pit 1 declining groundwater levels

In general, over most of the pit and pit slope, there was groundwater level lowering rate of about 0.4 m/month. Boreholes on the central and western sections of the pit show that there was a steady reduction in heads caused by the existing active dewatering and associated passive seepage.

However the hydrograph for groundwater monitoring borehole MH1-1 located at about 55 m away from the pumping boreholes shows delayed response to pumping indicating that the cone of depression dips away from the centre of the pit. The delay in initial response to pumping indicates that the aquifers are unconfined and are therefore hydraulically connected. This was supported by the evidence of the pumping test carried out at BH3-39 discussed in the conceptual hydrogeological model (Chapter 5). However, there are some confined compartments in the north-eastern corner of Pit 1 as evidenced by artesian conditions at borehole MH1-16.

7.3.2 Pit 1 Dewatering strategy

The conceptual hydrogeological (Chapter 5) model and numerical groundwater flow model (Chapter 6) for Ruashi Mine demonstrate that an effective dewatering system for Pit 1 should consist of a combination of elements, as follows:

7.3.2.1 Recharge interception

The modelling assumes that there is significant recharge flow from surface water drainage. The constant head along Luano River forming the northern boundary of the model contributes approximately 432 000 m³/d to the model domain. The dewatering system is cut off recharge from the Sandstones and Luano River. Seepage mapping in Pit 1 identified a spring like type of flow with a flow rate of approximately 1 m³/hr. This represents significant recharge flow through fractures/conductive zones from the south of the pit. It is necessary to install a dewatering borehole along this fracture on the perimeter of the pit and intercept flow along the fracture/conductive zone.

7.3.2.2 Pit Perimeter Boreholes

Vertical pit perimeter boreholes will be required for active dewatering. Based on the planned mining terminal depth of 180 mbgl, the dewatering boreholes should preferably be at least 200 m deep so as to pump from below the pit bottom. The boreholes will lower the phreatic surface below the pit floor, and will have significant local effects on hydraulic heads at the toe of the walls. As discussed in Chapter 5, the most prolific aquifer, the SDS, dips towards the NE and plunges to the east. Groundwater is expected to flow along the bedding planes. As such, flow from the SDS is expected to increase towards the plunge direction, the east, to where it gets deeper. Seepage mapping identified heavy seepage from the south-west of the pit. Under these conditions, the pumping boreholes located around the periphery of the pit may prove practical and economical. The boreholes should be installed in excess of 200 m deep and the diameter has to be larger than 10 inches to accommodate bigger capacity pumps.

One pit perimeter borehole will be required on the north side of Pit 1. This pumping borehole will intercept any recharge from Luano River and its basin. The other pit perimeter borehole should be installed on the southern side of the pit preferably close to the high seepage zone and cut off flow to the pit. The third perimeter borehole should be installed on the BOMZ-RAT Breccia contact zone and intercept flow along this zone. All the pit perimeter boreholes should be screened in the high yielding SDS, BOMZ and Sandstone. Despite the fact that blow yields exceeding 250 m³/hr were recorded in boreholes drilled in Pit 1, the sustainable pumping yields of such boreholes are expected to be in the order of a third of the blow yield. Pumping volumes can be planned according to simulated pit inflows (Table 6-4) and can be adjusted with future model calibration results. The numerical model predicted a maximum inflow of slightly over 11 200 m³/day during the final year of mining in Pit 1. A total of six wells pumping on average of 100 m³/hr, as discussed in Scenario 3 in Section 6.6.3, will have a

combined pumping volume of slightly over 14 000 m³/day and this pumping capacity will effectively lower the phreatic surface.

As of 2011 and early 2012 the water level had been maintained at approximately 5 m below the pit bottom, whilst pumping at an average rate of 9 000 m³/day. However previous experience in mines with similar hydrogeological settings has shown that pit inflows gradually increase with increase in mining depths. Given the fact that groundwater monitoring boreholes (BH1-9, BH1-10 and MH1-10) located at about 25 m away from the pumping borehole showed quick response to pumping at BH1-12 and BH1-13, borehole spacing of 25-30 m between pumping boreholes will be sufficient to create a compound cone of depression below the pit floor.

7.3.2.3 In-Pit Boreholes

Based on the conceptual model and Scenario 3 in Section 6.6.3 of the numerical groundwater flow model, three in-pit boreholes should be installed, one in the centre of the pit and the other two boreholes at about 30 m west and east of the central borehole (see Figure 7-2). The western and central in-pit boreholes should be screened in the SDS, RSF and Sandstone to allow drainage from these units. The eastern in-pit borehole should be screened in the BOMZ which deepens towards the east. These in-pit boreholes are expected to lower the groundwater levels and consequently lower the chances of pit walls collapse and blow up of the pit floor. The probability of high pore water pressure development in the base of the pit increases with pit depth. If the pore water pressures become sufficiently large they can cause blow up of the base of the pit. In general, this probability increases where the lithology layering is horizontal or if significant horizontal tectonic stress exists in the rock. However, the probability of blow up at Ruashi Mine is low as the rock units are not horizontal and dip to the north-east.

The in-pit and pit perimeter boreholes should preferably be deeper than 200 m. If the boreholes are shallower than 180 m, then they can be deepened with the advance of mining. It was practically proven at BH3-39 that the size of casing in a borehole may limit pump size hence it is recommended to install casing larger than 10 inches (254 mm) in diameter. Much of the pit wall collapse was witnessed on the south and south-west. This could be attributed to the south-west regional groundwater flow direction. Groundwater flow is expected to be large from the south-west and will influence pore water pressures. Due to this effect, the pumping system should be designed with reasonable over capacity so that if one pumping unit becomes inoperative there is sufficient excess of pumping capacity to prevent the development of local areas of high water pressure which might cause instability.

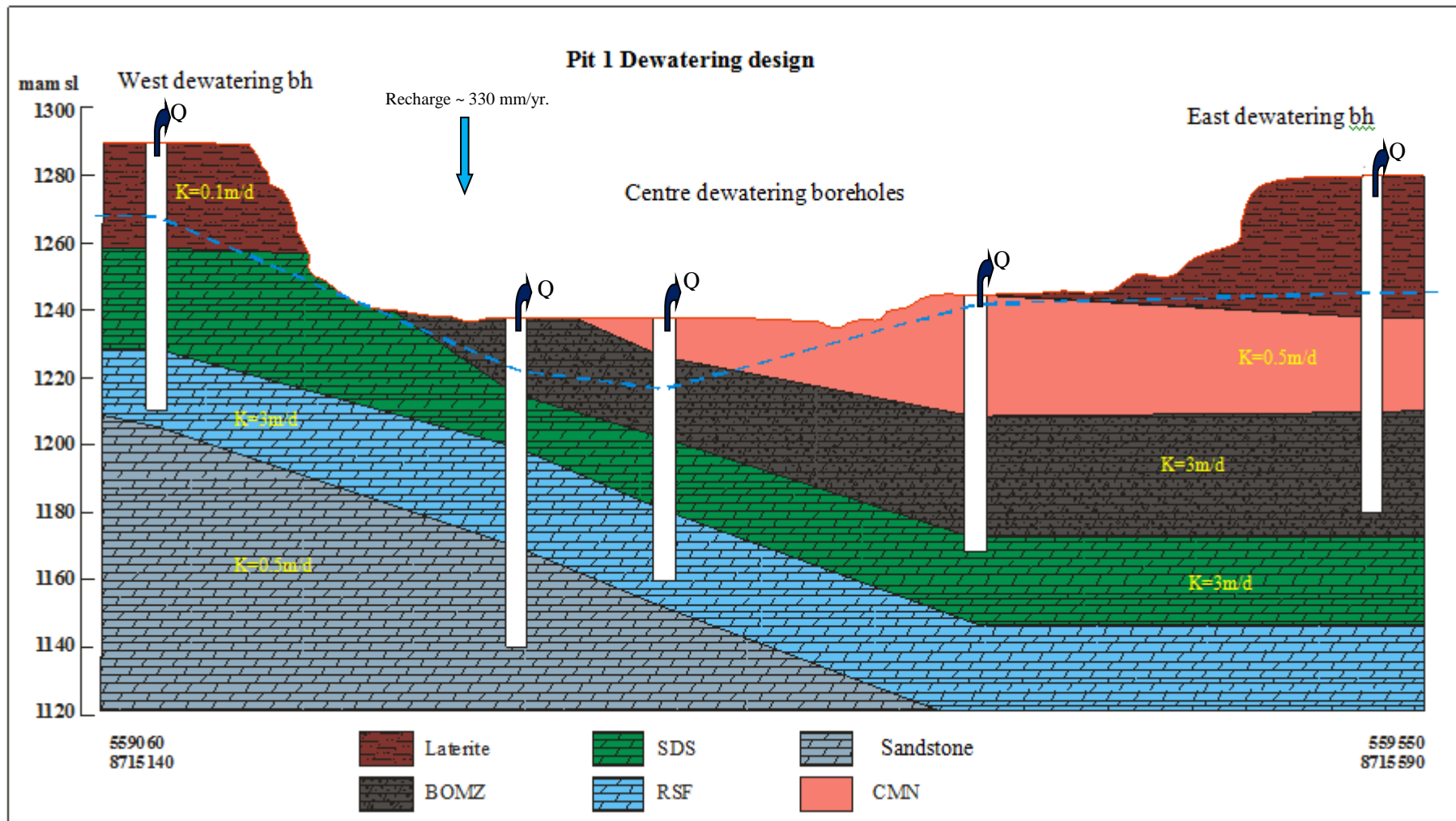


Figure 7-2: Positions of Pit 1 vertical boreholes

One standby pumping borehole should be installed at about 20-30 m west of the southern pit perimeter borehole. In order to evaluate the effectiveness of dewatering it is necessary to install groundwater monitoring boreholes/piezometers at key points in and around the pit to measure water levels. Pit 1 has six in-pit boreholes as listed in Table 4-3 and Table 4-4 (MH1-9, MH1-11, BH1-11, MH1-4, MH1-15 and MH1-16) and four pit perimeter boreholes (MH1-1, MH1-11, MH1-2 and MH1-13). All these monitoring boreholes are 40-80 m deep. They should be deepened to below pit terminal depth of 180 mbgl. These monitoring boreholes are monitored manually and automatic water level measurements can make the groundwater monitoring exercise more accurate and less labour intensive. Each piezometer should be equipped with an automatic water level and or temperature/conductivity logger. Normally it will be adequate to download water level/temperature/conductivity data on a monthly basis, with more frequent readings during the spring runoff period and following heavy rains.

7.3.2.4 Drainage Canal and Pit Sumps

In addition to drainage control within the pit itself, the control of surface drainage outside pit boundaries is necessary to ensure that surface water does not flow into the pit. The existing storm water drains and canals should be extended to the perimeter of the pit just outside the zone of stress relief (relaxation). Besides the extra pumping capacity required, water flowing into the pit percolates into surface fractures and openings, many of which have been created by blasting, develops cleft water pressures and may enhance rock breakup by freezing and thawing action. This aggravates pit wall collapse and the occurrence of local slides between benches. Reducing pore pressures will usually allow an increase in slope angle. An evaluation can be made of the cost of drainage versus the economic benefit to be gained by the increase of the slope angle that the drainage will allow.

The north east part of Pit 1 is dominated by the confining CMN (refer to cross sections presented in Figure 5-6 and Figure 5-8) and the resultant perched zones. These perched zones are not affected by the active dewatering with pumping boreholes. As such, seepage and significant flow from the perched zones is expected. Pit floor sumps should be constructed and harvest passive flow from the saturated perched zones. The sumps should be deep enough (say 1.5 m) so as to submerge pumps. Pipelines from the sumps should preferably be connected to the pipelines from dewatering boreholes and discharge water to storage facilities like the Coffey Dam.

7.3.2.5 *Blasting*

There are some zones in the eastern wall of Pit 1 that consist of alternating weak and strong bands in the BOMZ. The thin weak layers (see Figure 7-3) oriented to dip out of the slope frequently contribute to block failures. These zones remain saturated when the local groundwater level is lowered. In order to minimise the build-up of pore-water pressures in the Pit 1 eastern slopes, blasting the entire lower bench 5 to 10 metres wide around the toe of the slope may be required. *Bowell et al.* (2002) reported that the method of blasting was successfully used on Syncrude Tar Sand Project in Canada. Blasting was used to improve stability for draglines to operate on highwall benches.



Figure 7-3: Black Ore Mineralised Zone showing weak and strong bands in Pit 1. The foreground shows ponding of groundwater adjacent to pit wall

This area will have high permeability and will act as a large drain in allowing water to seep from the slope. Water from this area should be collected in one or more sump areas and pumped from the pit. Alternatively, selective controlled blasting may be used to reduce the pore pressures due to the volume increase caused by the blast.

7.4 Pit 2 and Pit 3 Dewatering

At the time of this research the ground between Pit 2 and Pit 3 was being mined out and the two pits will eventually be merged into one. Accordingly the discussion on the dewatering of the two pits was combined. Mining in Pit 2 and Pit 3 commenced in 2009 and 2011 respectively. Pit 2 has a smaller surface area compared to the original plans for Pit 1 and Pit 3. In general, Pit 2 experienced more widespread pit wall collapse compared to Pit 1 and Pit 3. Besides pore water pressure, the steep pit walls angles (about 60°) could have contributed to collapse of Pit 2 walls. As of April 2012, the average groundwater levels in groundwater monitoring boreholes in Pit 2 and Pit 3 was 35 mbgl and 15 mbgl respectively.

7.4.1 Flow response to preliminary pumping

At the beginning of 2010, there was only one pumping borehole (BH2-7) in the southern side of Pit 2. In April 2011 the borehole was deepened from 50 m to 80 m below the pit floor level (1283 mamsl). The borehole pumped an average of 290 m³/d for community supply. By the beginning of September 2011, the pit had been deepened from 1283 mamsl to 1240 mamsl. Consequently, flooding of Pit 2 began to inconvenience mining activities hence the need to actively dewater the pit. At the beginning of October 2011, two dewatering boreholes, BH2-28 and BH2-29, 25 m apart, were installed in the central part of Pit 2. Borehole BH2-28 began pumping an average of 150 m³/d soon after pump installation. The pump for BH2-29 had not been delivered to site. Pit 2 had four in-pit groundwater monitoring boreholes namely BH2-5, BH2-6, MH2-4 and MH2-6. The groundwater level on the periphery of Pit 2 was monitored through three pit perimeter boreholes notably BH2-4, MH2-1 and MH2-2.

In October 2011, a dewatering and test pumping borehole BH3-39 (as discussed in Section 4-4) was installed at about 50 m east of Pit 3 perimeter. The borehole was associated with eight cluster monitoring boreholes located at about 40 m and 80 m away from the pumping borehole. Six groundwater monitoring boreholes were installed in Pit 3. These are MH3-9, MH3-10, MH3-11, MH3-14, MH3-15 and MH3-16. The drawdown response to pumping observed in Pit 2 and Pit 3 is presented in Figure 7-4 and Figure 7-5 respectively.

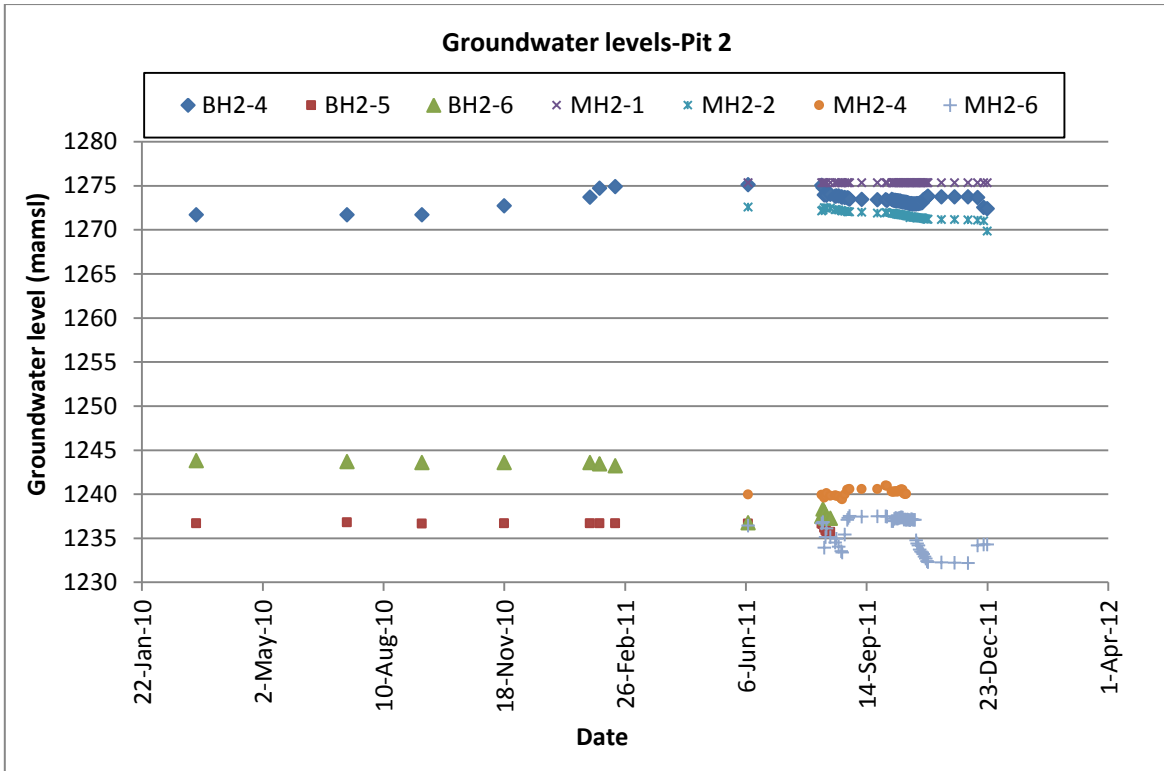


Figure 7-4: Fluctuating groundwater levels in Pit 2

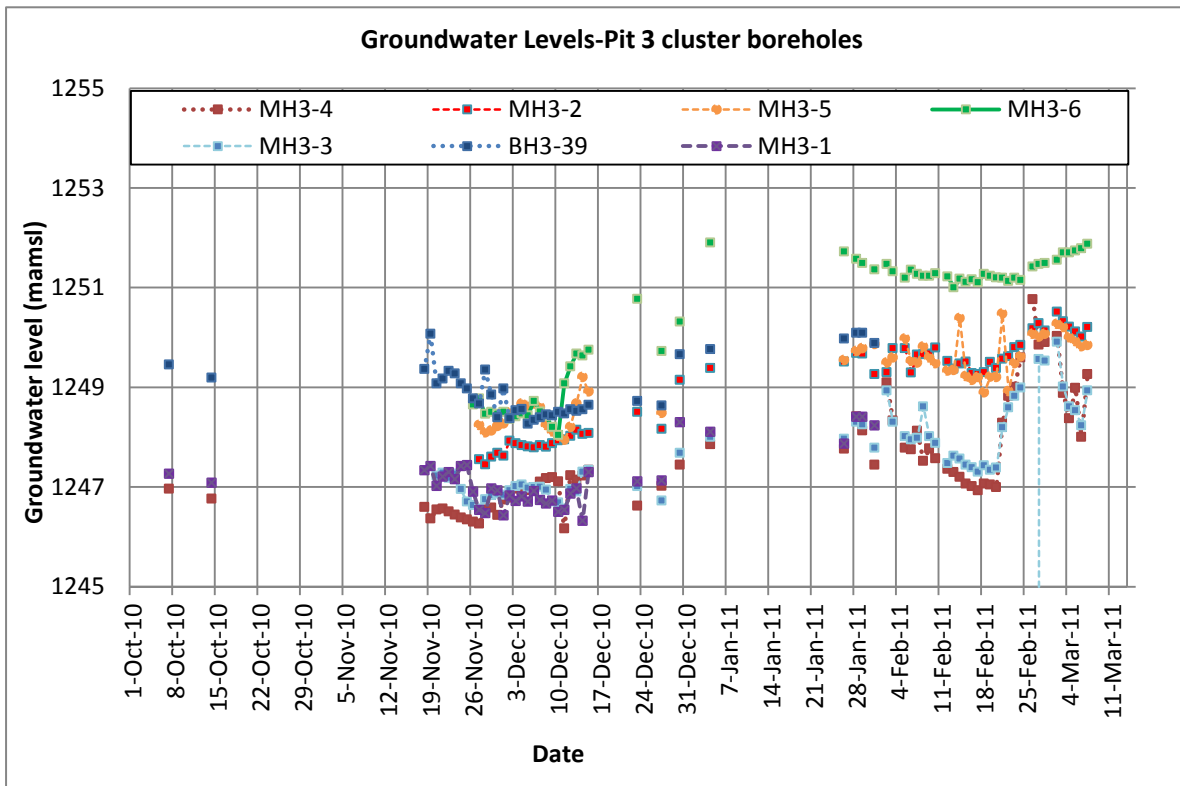


Figure 7-5: Fluctuating groundwater levels in Pit 3 cluster boreholes

The hydrographs for Pit 2 boreholes show that BH2-7 pumping rate at was not sufficient to lower the groundwater levels. In fact pit perimeter boreholes (BH2-4, MH2-1 and MH2-2) show steady water levels between June and December 2011. Regardless of continued pumping at BH2-7, the water level in pit perimeter borehole BH2-4 rose by about 0.6 m and stabilised until September 2011. However, by December 2011, the water levels in Pit 2 perimeter boreholes had declined by about 3 m. These fluctuations could be related to increased recharge during the rainfall season and evapotranspiration during the winter. This hypothesis is supported by the water level non-response to intermittent pump shut downs at BH2-7.

A similar pattern is displayed in hydrographs for in-pit boreholes which only began showing water level decline following the start of pumping at BH2-28 in October 2011. Groundwater monitoring borehole MH2-6 located at about 27 m east of BH2-28 indicated water level decline of 2 m between the first week of October 2011 and the first week of December 2011. This represents water level decline of about 1 m per month. However, no water level decline was observed in groundwater monitoring borehole MH2-4 located at about 20 m north-west of BH2-28. This non-response to pumping could be attributed to the occurrence of CMN aquitard in the north-west of Pit 2 (as discussed in Chapter 5). The CMN aquitard extends into the north-east part of Pit 1 where confining conditions are witnessed at artesian well MH1-16. The water level at BH2-6 located in the BOMZ at about 20 m south of BH2-28 declined by 6 m between February 2011 and August 2011. The decline could be attributed to general groundwater level decline in winter and response to pumping at BH2-7.

There was no active dewatering in Pit 3 but aquifer hydraulic testing was conducted at BH3-39 located at about 50 m east of Pit 3 perimeter. As discussed in Chapter 5, drawdown was monitored during aquifer hydraulic testing. Despite a sustained constant pumping rate of 144 m³/hr for a period of 72 hours, a maximum drawdown of only 10.5 m was recorded in the pumping borehole. Water level decline of between 0.1 to 0.4 m was observed in the cluster monitoring boreholes during the 72 hour constant rate test. None of the in-pit boreholes showed any response to pumping. After the aquifer hydraulic testing, BH3-39 continued to pump at 144 m³/hr for community and plant water supply. The hydrographs for cluster monitoring boreholes presented in Figure 7-5 show insignificant response to pumping. The temporal rise and decline in the water levels could be related to the effects of dry winter and summer rains. Despite intermittent power shut downs at BH3-39, the water levels in the cluster boreholes did not show any significant response.

7.4.2 Pit 2 and Pit 3 Dewatering strategy

The low drawdown observed during preliminary pumping and the presence of highly transmissive SDS and BOMZ in Pit 2 and Pit 3 guide to the requirement of a robust dewatering system consisting of a combination of elements, as follows:

7.4.2.1 Vertical Boreholes

Vertical in-pit and pit perimeter boreholes will be required for active dewatering of Pit 2 and Pit 3. The most prolific aquifer at the mine, the SDS, plunges to the east and is deeper in Pit 3 compared to Pit 2 (see Figure 7-6 and Figure 7-7). This lithology has bedding planes that could enhance swift groundwater flow. Consequently, flow from the SDS is expected to increase towards the plunge direction, the east. As the two pits will be terminated at a depth of 180 mbgl, the dewatering boreholes should preferably be at least 200 m deep and intersect the SDS. If the boreholes are drilled deeper than 180 mbgl, then dewatering can be effected from below pit bottom ahead of mining. As demonstrated in Scenarios 2 and 3 in Section 6.6, the boreholes should effectively lower the phreatic surface below the pit floor.

Seepage mapping identified heavy seepage on the south and north-west of Pit 2. Seepage on the south walls of Pit 2 is associated with groundwater flowing from the sandstones whilst the north-west is associated with perched zones in the CMN. In order to intercept flow from the sandstones on the south of Pit 2, pumping boreholes located along the periphery of the pit should be installed. The depth of these boreholes should be in excess of 180 m and their diameter should preferably be larger than 10 inches to accommodate bigger capacity pumps. Pumping volumes can be planned according to blow yields and simulated pit inflows (see Table 6-4) although these have to be adjusted with future model calibration results. The numerical model was used to predict a maximum flow into Pit 2 and Pit 3 to be slightly over 9 461 m³/d and 22 326 m³/d respectively during the final year of mining. Based on these results, Pit 2 will require four boreholes (see Figure 7-6) each pumping an average of 100 m³/hr. Based on Scenario 3 presented in Section 6.6, Pit 3 will require ten boreholes each pumping an of 100 m³/hr. As demonstrated in Scenarios 2 and 3, this pumping capacity is expected to effectively lower the phreatic surface and maintain dry working conditions in the pits.

Dewatering borehole BH2-29 located in the centre of Pit 2 should be equipped and augment pumping at BH2-28. One dewatering borehole should be installed in the north-west of Pit 2 and target to dewater the CMN. This borehole should be screened in both the BOMZ and the overlying CMN.

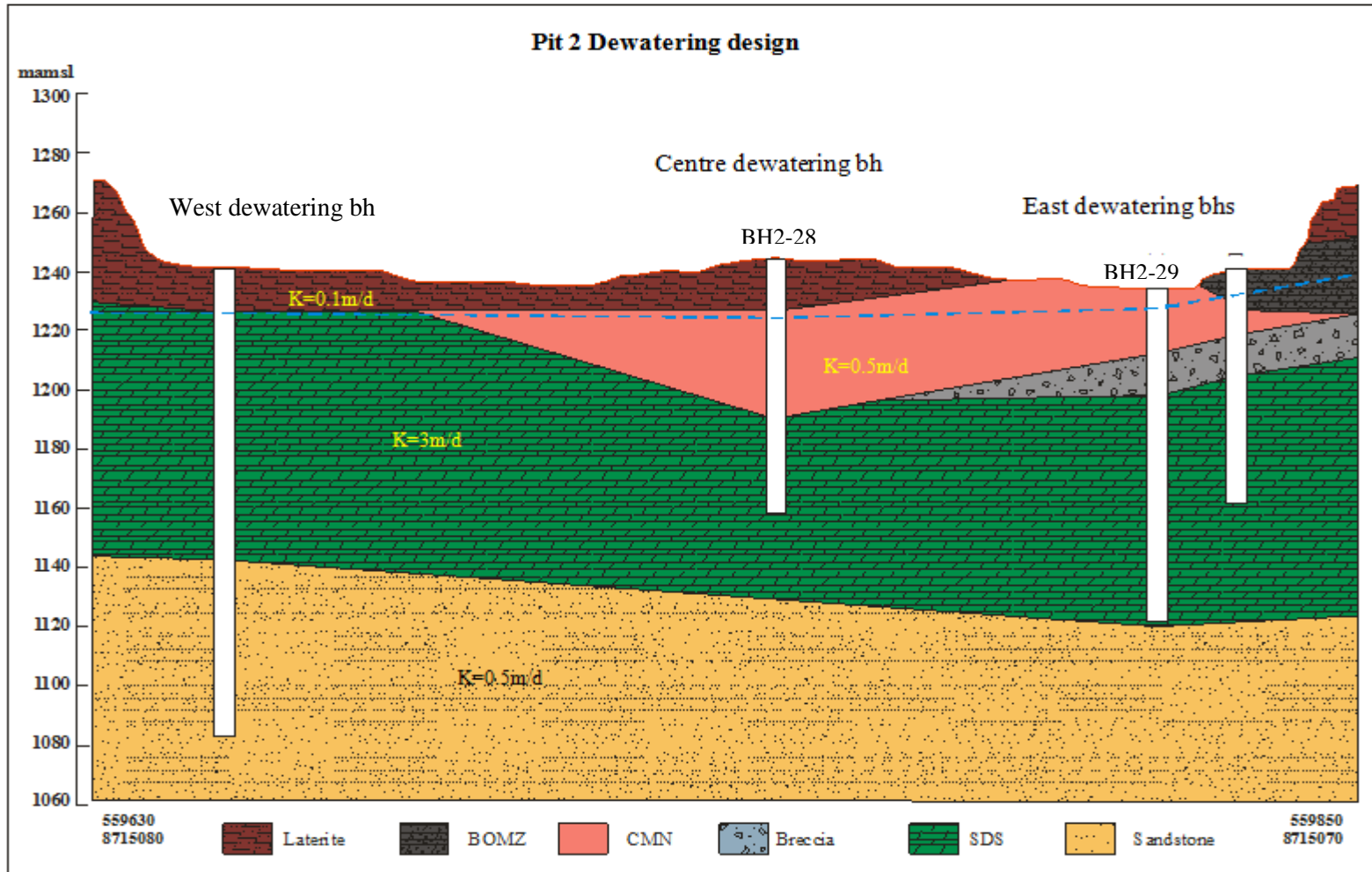


Figure 7-6: Vertical boreholes plan for Pit 2

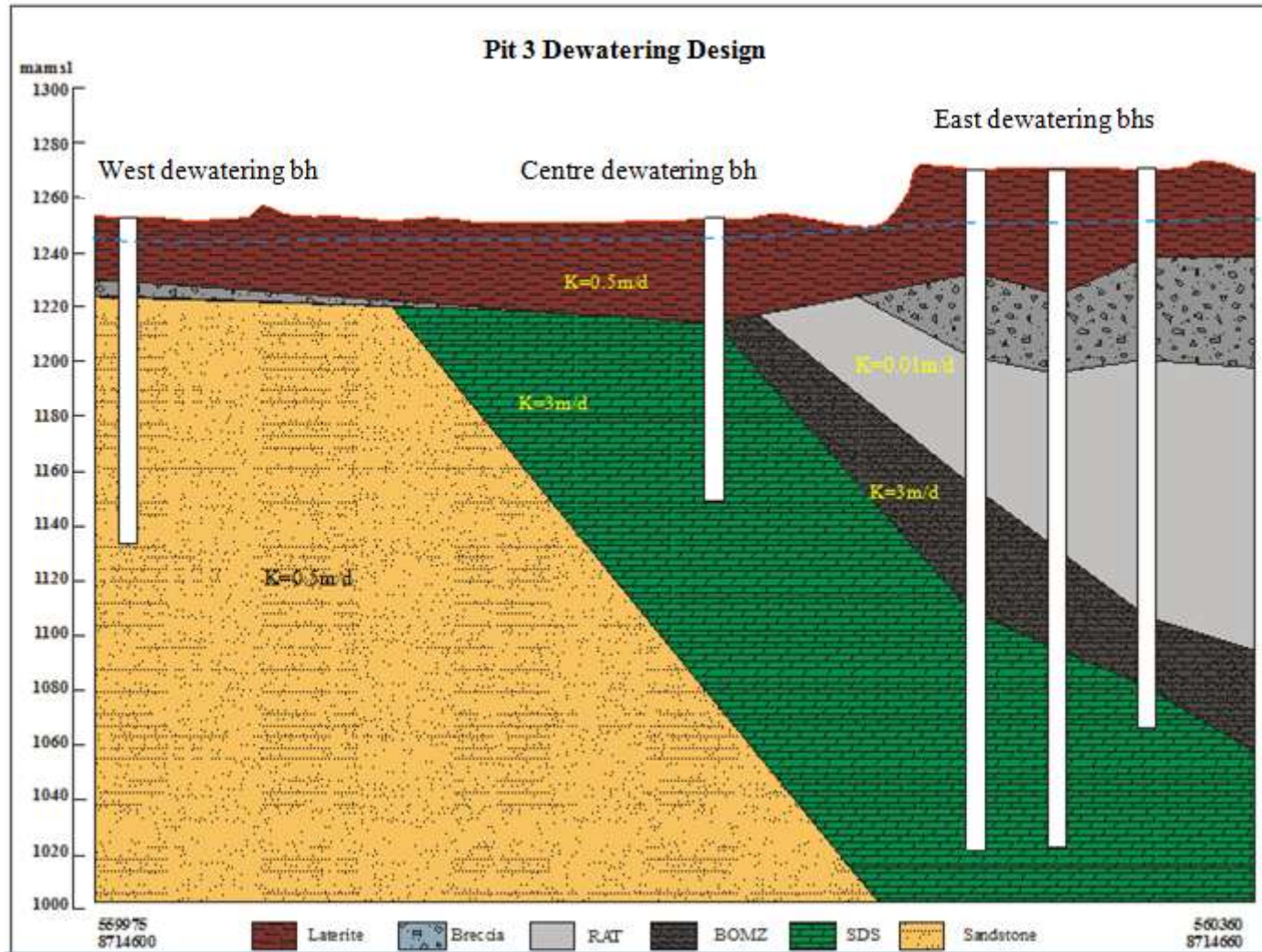


Figure 7-7: Vertical boreholes plan for Pit 3

As for the Pit 2 perimeter, one borehole should be installed on the northern side and should intercept any recharge from Luano River and Rock dump in the north should any occur. The other pit perimeter borehole should be installed on the southern side of Pit 2 and should be screened in the SDS and Sandstones. In this way the pumping will drain the sandstones and SDS and cut off flow to the pit. The third perimeter borehole should be installed on the BOMZ-RAT breccia contact zone between Pit 2 and Pit 1. This borehole should be screened in the BOMZ /RAT breccia zone and the SDS. The eastern side of Pit 2 will be dewatered by an in-pit borehole installed in the Pit 2-Pit 3 merged zone. Pit 3 has a wider diameter compared to Pit 1 and Pit 2 hence will require a dewatering ring comprising of boreholes inside the Pit (see Figure 7-8). These in-pit boreholes will be augmented by pit perimeter boreholes.

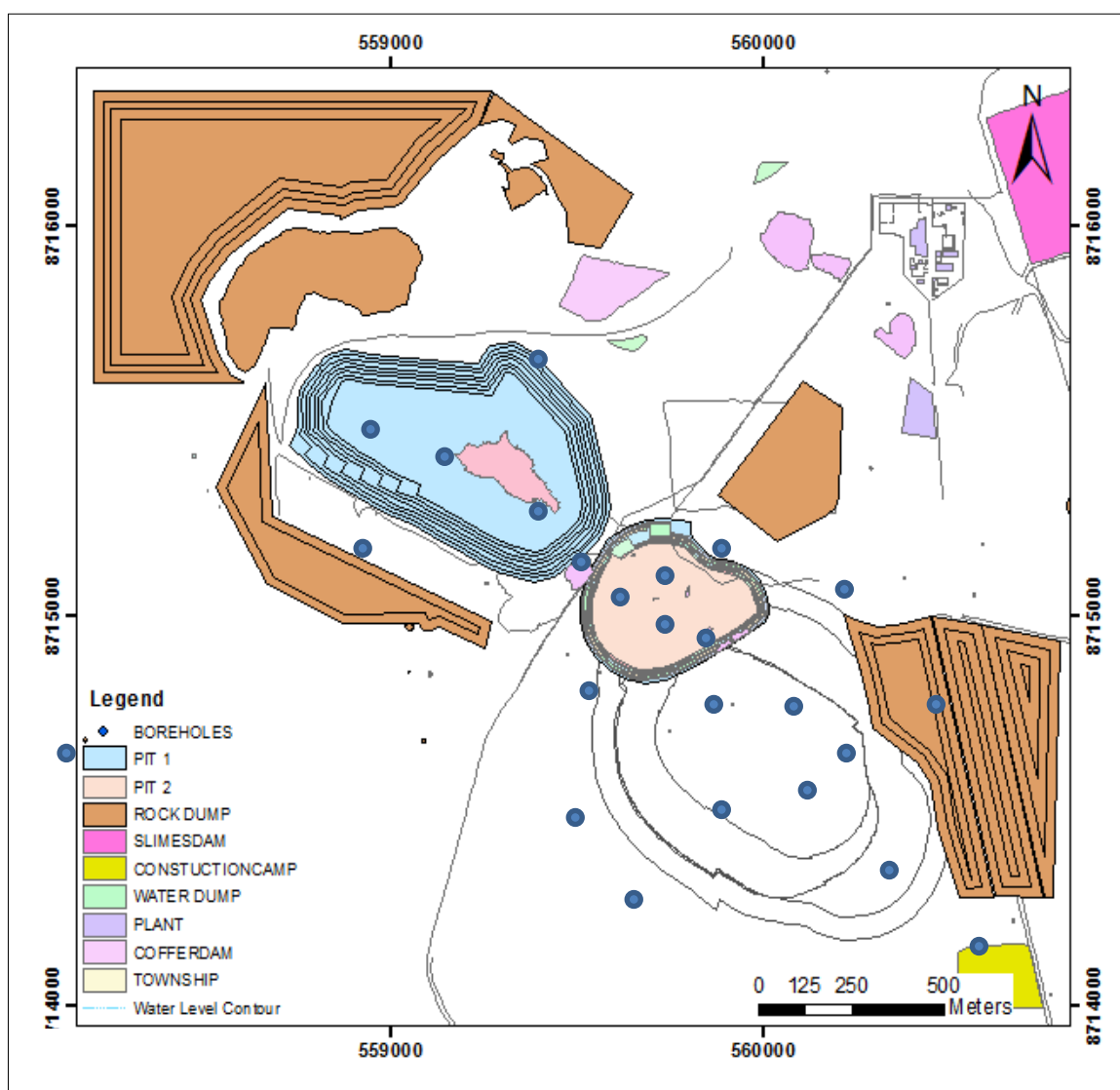


Figure 7-8: Ruashi map showing positions of proposed dewatering boreholes

A total of six in-pit boreholes should be installed, one in the centre of the pit and the other four on the east, south-west, north-east and north west forming a ring of radius of approximately 20 m away from the centre borehole. The sixth in-pit borehole should be installed on the Pit 2-Pit 3 boundary zone. The four perimeter boreholes should be installed in the south-east, north, south and north-north-west along a ring just outside the zone of relaxation. The eastern periphery of Pit 3 will be dewatered by the already in place BH3-39. The central borehole in Pit 3 should be screened in the Laterite, BOMZ and SDS. The boreholes on the south-west, west and north-west of the pit should be screened in the Laterite, RAT breccia and Sandstone. All the other boreholes (see Figure 7-7) in Pit 3 and its perimeter should be screened in the Laterite, Rat breccia, BOMZ and SDS. The RAT did not yield any water during drilling of Pit 3 cluster boreholes hence it is not necessary to screen the boreholes in this lithology. However, a transmissive zone through which drainage can occur can be created by blasting the RAT lithology. The SDS in Pit 3 is high yielding hence it would necessary to pump the boreholes simultaneously and alternate the pumping if the necessity arises.

In order to evaluate the effectiveness of dewatering continuous groundwater monitoring will be required. Pit 2 has two in-pit ground water monitoring boreholes. However these monitoring boreholes are shallower than 100 mbgl hence they should preferably be deepened to about 200 mbgl. The southern side of Pit 2 perimeter will require a groundwater monitoring borehole installed to a depth of 200 mbgl. Pit 3 has six cluster boreholes (MH3-1, MH3-2, MH3-3, MH3-4, MH3-5 and MH3-6) and two in-pit boreholes (MH3-8 and MH3-10) and these are used as monitoring points. These monitoring points should suffice as installing more monitoring points in Pit 3 might crowd the pit and become obstacles to mining. In order to get reliable data, each monitoring point should be equipped with an automatic water level and or temperature/conductivity logger. Normally it will be adequate to download water level/temperature/conductivity data on a monthly basis, with more frequent readings during the spring runoff period and following heavy rains.

7.4.3 Pit sumps and drainage canal

The control of surface drainage outside the boundaries of Pit 2 and Pit 3 is necessary to ensure that surface water does not flow into the pits. The existing storm water ditches and drainage canals in the mine plant and camps should be extended to the perimeter of the pits.

The north-west of Pit 2 is underlain by CMN which exhibits aquitard characteristics and the area is dominated by perched zones. These perched zones are not affected by the active dewatering at BH2-28. As such, pit floor sumps should be constructed and harvest passive flow from the saturated perched zones.

7.5 Summary

This chapter gives an account of the application of results from drilling, aquifer hydraulic testing, hydrochemistry, groundwater flow model and preliminary pumping in setting up a dewatering strategy for Ruashi Mine. The groundwater model, aquifer hydraulic testing results, plus practical field experience in groundwater level response to preliminary pumping, has shown that the most effective dewatering methods are vertical boreholes and pit sumps. By removing large amounts of water over a large area, the pumping boreholes and associated drains will bring the phreatic surface below the specified targets and will optimise the stability of the pit walls. Groundwater flow into a mine is traditionally controlled through methods of groundwater exclusion, abstraction, or a combination of exclusion and abstraction. Ruashi Mine dewatering can be accomplished through the use of a combination of pit perimeter and in-pit abstraction boreholes. In case of pit floor ponding then pit floor sumps will augment abstraction boreholes.

The drop in groundwater level during preliminary pumping means that a dewatering system consisting of vertical boreholes can effectively dewater the mine. As predicted by the numerical model, it is expected that approximately 11 000 m³/d, 9 000 m³/d and 22 000 m³/d will flow into Pit 1, Pit 2 and Pit 3 respectively. Surges of flow can be expected which are due to intersections of different sub compartments within the aquifer. These will usually be in hydraulic continuity with the main dewatering aquifer and will therefore not be sustained hence standby pumping boreholes can be used to augment pumping boreholes in operation. It will be important to minimise the amount of recharge that can infiltrate from Luano River and the adjacent rock dumps. Surface water should be diverted by canals and any overland flow should be drained out if possible.

The success of dewatering at Ruashi Mine will depend on:

- Installation of large diameter boreholes to below pit terminal depth of 180 mbgl.
- Subsequent equipping and continuous pumping of completed boreholes.
- Contingency boreholes equipped and ready to pump in the event one of the pumping boreholes breaks down and continuous groundwater monitoring programme and passive inflow extraction.

The next chapter discusses conclusions and recommendations deduced from field investigations at Ruashi Mine. Hydrogeological results from drilling, aquifer hydraulic testing results, hydrochemical analysis results, preliminary pumping response and numerical model simulations guide in formulating conclusions and recommendations.

8 CONCLUSIONS AND RECOMMENDATIONS

Conclusions and recommendations were derived for each chapter from the field programme, conceptual hydrogeological model, numerical groundwater flow model and the dewatering strategy for the mine.

8.1 Conclusions

8.1.1 Field programme

- Desk study and hydrocensus were successfully carried out at the Ruashi Mine. All existing borehole details at the mine were identified.
- A total of 48 shallow and deep groundwater monitoring, plant supply, community water supply and dewatering boreholes were drilled at the mine. The shallow boreholes were drilled to depths between 8 mbgl and 20 mbgl and the deep boreholes to depths of between 30 mbgl and 250 mbgl. Water strikes and blow yields recorded in shallow boreholes confirmed the presence of lowly transmissive Kundelungu and Laterite aquifers on the north-eastern corner of the mine. The deep boreholes confirmed the presence of a well-developed fracture system in the highly transmissive Roan Formation.
- Results of aquifer hydraulic testing indicated a higher rate of spread of cone of depression along the strike of lithologies compared to across the strike of the lithologies.

8.1.2 Conceptual hydrogeological model

- Ruashi Mine is located along dolomitic aquifers of the Roan series and Kundelungu series Sandstones and Shales that were deformed to form an overturned syncline. The mine is bounded to the west and east by Luano and Kebumba Rivers respectively. Two southern and northern topographic divides and flow lines form the northern and southern boundaries of the Ruashi Mine model area.
- Recharge in the area was estimated as 14% (280 mm) of mean annual precipitation.
- Groundwater in the Roan aquifer is controlled by the occurrence of bedding planes, vugs and fractures. The Roan aquifer is localized and anisotropic.
- Water levels in the shallow Kundelungu aquifer vary from 1.32 to 11 mbgl. The water levels for the deep aquifer vary from 17 to 64 mbgl.

- Groundwater gradients vary from 0.005 close to the tailings storage facility (TSF) area and 0.03 in the area between the central rock dump and the pits.
- The dominant groundwater type at the mine is Ca-Mg-HCO₃ and is potable in areas that are not contaminated by seepage from the TSF.
- Based on aquifer hydraulic test flow diagnosis, the groundwater system is defined as semi-confined to unconfined. Semi-confined conditions occur at local scales in compartments of the aquifer where CMN and RAT overlie the Roan dolomitic rocks and Kundelungu Sandstone layers.
- The drawdown derivative diagnostic analysis shows that the aquifer system displayed a typical Theis response.
- Hydraulic conductivity for the shallow aquifer was estimated to be 0.59 m/d and is high where the aquifer is coincident with weathered Laterite. The hydraulic conductivity of the deep Roan series aquifer was estimated to be 1.28 m/d and is enhanced by the well-developed fracture network and interconnected vugs.
- Restricted hydraulic continuity exists between the deep aquifer and the shallow aquifer. The CMN and RAT were noted to be aquitards which enhance local confining conditions and localised perched zones.

8.1.3 Numerical groundwater flow model

8.1.3.1 Modelling code

The numerical modelling was undertaken using Feflow 3D finite element modelling code. The flexibility in this code enabled great detail to be built into the model mesh around individual boreholes, open cast pits, with a broader model mesh away from the mining area.

8.1.3.2 Model area

The modelling area was selected based on a combination of topographical, geological and water divide and the area is approximately 15.7 km².

The model comprises 5 layers, 17240 elements and 10614 nodes. Total depth of the model is variable due to topography but below mining the model is 250 m deep. The base of the model was assumed to be impermeable. The 5 layers build into the model are:

- Layer 1 representing the shallow Laterite

- Layer 2 representing the shallow Kundelungu series
- Layer 3 representing the RAT
- Layer 4 representing the CMN
- Layer 5 representing the Roan series

8.1.3.3 Model calibration

- Steady state calibration was accomplished by varying the hydraulic conductivity values within a realistic range and a reasonable match between the measured groundwater elevations and the simulated groundwater elevations was obtained.
- A correlation coefficient of 91% was obtained between observed and simulated water levels. This correlation coefficient is considered acceptable.
- Transient calibration was achieved by simulating the response of the model to the aquifer hydraulic testing results. The numerical model was able to simulate the observed water level drawdown at the test yield for the test duration.

8.1.3.4 Modelling results

The planned mine life is until the year 2022. The maximum pit depth is 180 mbgl. The following key results were obtained from the numerical model:

- Groundwater flow to the 3 pits is unlikely to exceed 42 000 m³/d.
- The model demonstrated that the water level can be lowered to below pit terminal depth (180 mbgl). This drawdown can be achieved by installing 16 additional boreholes each pumping approximately 2 000 m³/d.

8.1.4 Dewatering strategy

- Based on model sensitivity discussed in the model scenarios section, a dewatering strategy comprising of a combination of vertical pit perimeter and in-pit boreholes complimented by pit sumps should suffice.
- Pumping boreholes should be installed guided by numerical model scenarios and will be complemented by sump pumping of passive pit inflows. The pumping volumes will be increased with updated values from future model calibration.
- Any water interceptions should be encouraged to drain wherever possible.

- The water should be piped out of the pits if at all possible, to avoid contamination.

8.1.5 Gap analysis

The following information gaps exist within the information analysed at Ruashi Mine:

- Water quality analysis carried by Lubumbashi University is incomplete. All water quality analysis should include all the major cations and anions (Ca, Mg, Na, K, SO_4^{2-} , HCO_3^- , and Total Alkalinity).
- Water levels were not monitored consistently throughout the period of study. Groundwater levels need to be monitored so that the data will be used to calibrate the numerical model.
- There are few rain gauges at the mine. High spatial variability of rainfall and rainfall chloride concentrations around Ruashi Mine was noted. More rain gauges are required within Ruashi mining area to measure the amount of rain falling around the pit area within one season.

8.2 Recommendations

The analysis of aquifer response to preliminary pumping, aquifer hydraulic testing results and pumping scenarios in the numerical model proved to be complementary in designing a dewatering strategy for the mine. It is expected these methods can be combined into one, comprehensive hydrogeological investigation method that yields bankable results.

Certainly, this research opens up possibilities for the application of three-dimensional simulation of groundwater flow in mines, in which flow volumes have been traditionally been estimated pumping tests. In this regard, the findings of this dissertation can be used as the starting point to find the value of integrated hydrogeological investigation.

Regarding the method for improving numerical models, it is necessary to conduct unit specific aquifer hydraulic tests and get better aquifer hydraulic parameters generate a more comprehensive library of patterns as described in Section 6.4.6. Additionally, the numerical should be continuously be calibrated with future monitoring data.

Based on the research findings and knowledge acquired on the Ruashi Mine hydrogeological system, the following aspects are recommended:

- The monitoring programme should be expanded and groundwater monitoring boreholes deepened to pit terminal depth as discussed in the dewatering strategy. The monitoring data can then be used to calibrate the numerical model.
- Packer tests should be carried out in the shallow Kundelungu and deep Roan aquifers. The tests enable improved estimates of hydraulic parameters for each lithology.
- Automated rain gauges should be installed to gather precipitation. The data will be useful in estimating recharge rates to the aquifer system.
- Water quality analysis should be carried out frequently. Water quality analysis gives an idea of the probable sources of groundwater.
- It is recommended that that deep (200 m) pumping boreholes should be drilled inside the pits and along the pit perimeter. These pumping boreholes should be used to dewater the pits in advance of mining. The numerical groundwater flow should be updated annually with the monitoring data to confirm the findings of the modelling and to provide early warning of any deviation from the modelling predictions.

8.3 Main contribution of the dissertation

This dissertation made a significant contribution to understanding the hydrogeological properties of aquifers at the mine. An integrated study of historical dewatering and mining records, structural geology, surface hydrology, groundwater chemistry was necessary. The results enabled the development of a conceptual hydrogeological model and numerical groundwater flow model to be used to predict future groundwater flow into the mine and future water level drawdown.

Specific important outputs from the research dissertation are as follows:

- Drilling of deep boreholes especially BH3-39 to a depth of 247 mbgl enabled hydrogeological characterisation of the deep Roan aquifer units. This hydrogeological data was not available at the mine at the start of this research.
- Proposal to carry out aquifer hydraulic testing and packer tests in individual lithologies and get more reliable aquifer hydraulic parameters.
- Aquifer hydrochemical sampling in drilled boreholes (24) enabled the hydrochemical characterisation of the aquifers at Ruashi Mine. It was noted that the hydrochemistry did not vary greatly hence it is highly likely that the aquifers at Ruashi Mine are hydraulically connected.

- Improved understanding of hydrogeological system of the mine.
- Improved understanding of groundwater flow and aquifer response during pumping of the aquifers.
- The numerical model demonstrated the typical aquifer response to different pumping scenarios. This helps in determining the optimum dewatering rates.
- The low drawdown observed during aquifer hydraulic testing and the simulated response to pumping under different scenarios with various pumping rates indicated that it is necessary to pump boreholes simultaneously. This will create a compound cone of depression and effectively dewater the mine.

Figure 8-1 is a flow diagram illustrating important steps that were and can be followed in order to understand the hydrogeological system in a mine and subsequently formulate a bankable dewatering strategy for the mine.

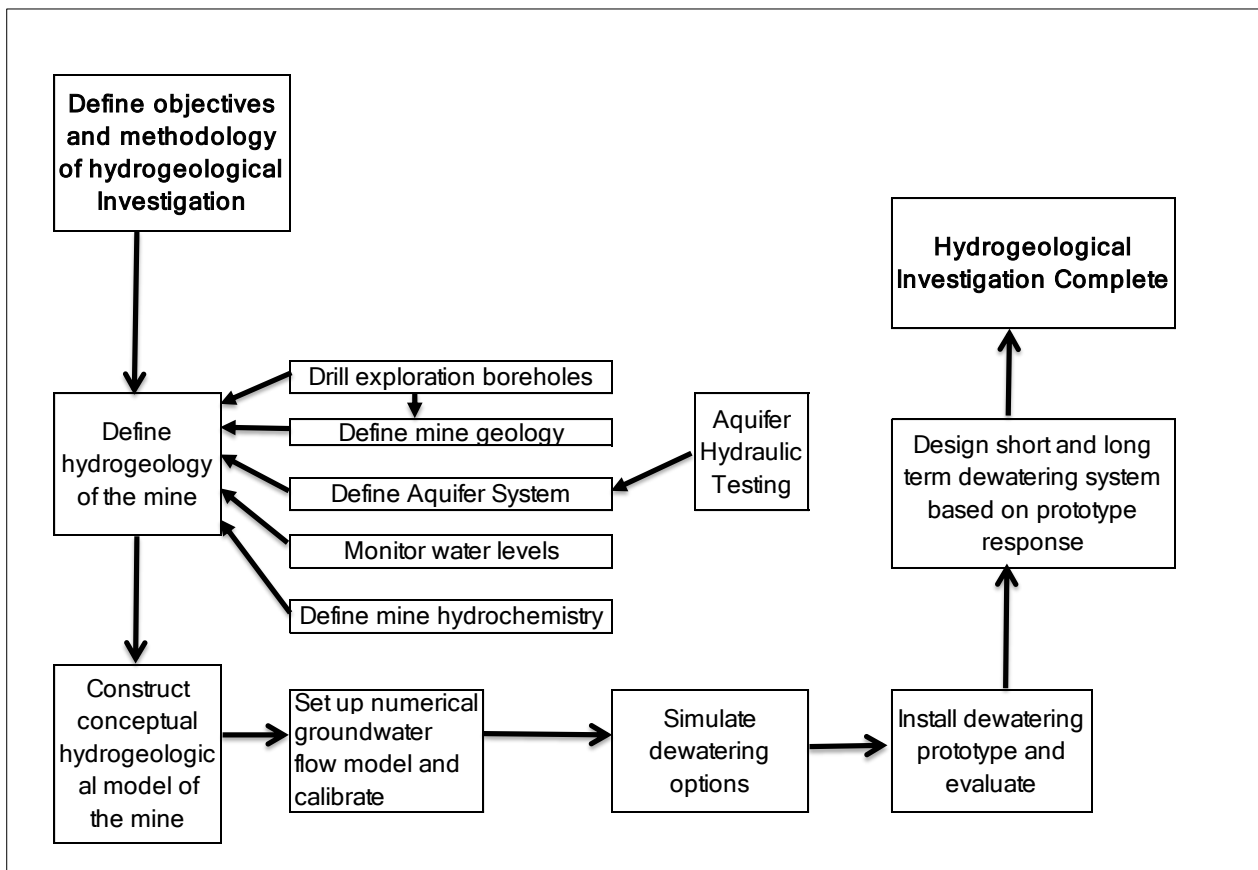


Figure 8-1: Flow chart illustrating important steps that can be followed in a mine hydrogeological investigation for dewatering

It is important to understand the hydrogeological properties of aquifers. Aquifer geometry helps in determining the channels through which the groundwater flows. The amount of water stored in an aquifer system can be estimated through calculation of aquifer storage coefficient from results of aquifer hydraulic testing. Aquifer hydraulic conductivity indicates the rate at which groundwater flow through the aquifer system and therefore the rate at which groundwater flows into the mine.

Groundwater chemistry results reveal that groundwater can be divided into that which originates from regional aquifers, surface water storages and recent recharge from precipitation. It was essentially established that groundwater flow to the mine is dominated by recent recharge from precipitation and flow from the regional aquifer system.

REFERENCES

- Acworth, R.I., Greenbaum, D. and Wyns, R. 2001.** The development of crystalline basement aquifers in a tropical environment, *Quarterly Journal of Engineering Geology*, 20, pp. 265-272.
- Alliquander, E. 2012.** Experience and Ideas of Development on the Control of Mining Under Karstic Water Hazard. IMWA Proceedings 1982B, International Mine Water Association 2012, pp. 8-10.
- Anderson, M. P. and Woessner, W. W. 1992.** Applied Groundwater Modelling: Simulation of Flow and Advective Transport. Academic Press, San Diego, California, USA, pp. 76-127.
- Beekman, H. E., Selaolo, E. and De Vries, J. J. 2000.** Groundwater recharge in the Kalahari, with reference to palaeo-hydrologic conditions. *J Hydrol* 238. pp. 76-120.
- Bird, P., Ben-Avraham, Z., Schubert, G., Andreoli, M. and Viola, G. 2006.** Patterns of stress and strain rate in Southern Africa, *J. Geophys. Res.*, 111, B08402, pp. 7-14.
- Brady, B.H.T. and Brown, E.T. 2002.** Rock Mechanics for Underground Mining, Dodrecht, Netherlands, Klower Academic publisher. pp. 33-82.
- Brawner, C. O. 2006.** Control of Groundwater in Surface Mining. Mining Department, University of B.C., Vancouver, Canada. *International Journal of Mine Water* 2006. pp. 1-16.
- Bowell, R. J., Connelly, R.J. and Saddler, P. K. J. 2002.** The hydrogeochemical dynamics of mine pit lakes. pp. 355-384.
- Davis, A. 2009.** Post-closure flooding of the Homestake Mine at Lead, South Dakota. *Mining Engineering*, March, Vol. 61, No.3, pp. 20-47.
- Daw, G.P. and Pollard, C.A. 2006.** Grouting for Groundwater Control in Underground Mining. *International Journal of Mine Water*, vol 5(4), 1986 pp. 1-40.
- Diersch, H.J. 2005.** FEFLOW Interactive, Graphics-based Finite-element Simulation System for Modelling Groundwater Flow, Contaminant Mass and Heat Transport Processes, WASY institute for Water Resources Planning and Systems Research Ltd, Berlin. pp. 80-147.
- Driscoll, F.G. 1995.** Groundwater and wells. St Paul Publishers, Minnesota, United States of America. pp. 61-133.

Fetter, C.W. 1999. Contaminant Hydrogeology, Prentice Hall, Upper Saddle River. pp. 56-72.

Freeze, R.A. and Cherry, J.A. 1979. Groundwater. Prentice Hall Inc., New Jersey USA. pp. 120-167.

Googlemaps. 2013. Map of Democratic Republic of Congo, 2013.
https://maps.google.com.qa/maps?q=map+of+democratic+republic+of+congo&ie=UTF-8&hq=&hnear=0x1979facf9a7546bd:0x4c63e5eac93f141,Democratic+Republic+of+the+Congo&gl=qa&ei= bA6UpLXKJW24APP_oGYCQ&ved=0CDUQ8gEwAA . Website accessed via online library on 10 September 2013.

Groundwater Counselling Services (GCS). 2006. GCS Report: 05.06-245/BFS/Final. Ruashi Copper and Cobalt Mine-Lubumbashi. Bankable Feasibility Study Hydrogeological Investigation. pp. 20-33.

Hague, I. and Germishuys, L. 1999. Practical Aspects of Water sealing at Konkola Copper Mine, Zambia. pp. 13-47.

Hargrave, P. and Metesh, J. 2003. Investigative Methods for Controlling Groundwater Flow to Underground Mine Workings. Montana Bureau of Mines and Geology. pp.1-26.

Hall, S.H. 2005. From Workshop Notebook, Tenth national outdoor Action Conference and Exposition, May 13-15, 2005, Las Vegas, Nevada. National Groundwater association, Colobus, Ohio, USA. Title of conference paper is "Practical Single-Well Tracer Methods for Aquifer Testing. pp. 9-17.

Healy, R.W. 2010. Estimating Groundwater Recharge. Cambridge University Press, The Edinburgh Building, Cambridge CB2 8RU, United Kingdom, pp.10-56.

Kellgren, N. and Sander, P. 2000. Benefits of incorporating remote sensing techniques as a methodological approach for improved borehole siting in fractured rock aquifers. In: Sililo O. (ed) *Groundwater: past achievements and future challenges*. Proc. 30th IAH Congress, Cape Town, South Africa, 26 Nov-1 Dec 2000. Balkema, Rotterdam, pp 175-180.

Kruseman, G.P. and De Ridder, N.A. 1994. Analysis and evaluation of pumping test data. Second Edition, pp.193-233.

Lerner, D.N., Issar, A. and Simers, I. 1990. A Guide to understanding and estimating natural recharge, Int. contribution to hydrogeology, I.A.H. Publ., Vol.8, Verlag Heinz Heisse, pp. 345.

Lydall, M.I. and Auchterlonie, D. A. 2011. The Democratic republic of Congo and Zambia: A Growing Global “Hotspot” for Copper-Cobalt mineral Investment and Exploitation. pp. 25-33.

Lloyd, J.W. and Edwards, M.G. 2000. Modelling of Groundwater flow in fractured rock aquifers, Quart Colorado School of mines, Vol 80, no.1 pp123-167.

Maarten, H. and Mucchez, P. 2011. Stratiform and vein-type deposits in the Pan-African Orogeny in Central and Southern Africa: Evidence for Multiphase Mineralisation. pp. 24-57.

Mandzic, E.H. 1992. Mine Water Risk in Open Pit Slope Stability. Mine Water and the Environment. 11(4): pp 35-42.

MINESAFE, Vol 10, No. 4. 1999. The Mining Operations Division. Department of Minerals and Energy, Western Australia. Accessed on 22 January 2013 via http://www.dmp.wa.gov.au/documents/Magazine/007_MineSafe.pdf .pp 6-7.

Moreno, J. and Spitz, K. 1996. A Practical Guide to Groundwater and Solute Transport Modelling. pp. 74-126.

Rubio, R.F. and Lorca, D.F. 1993. Mine Water Drainage. International Mine Water Association 2006. Mine Water and The Environment, Vol 12, Annual Issue, 1993. pp. 107-130.
Samani, N., Pasandi, M. and Barry, D.A. 2006. Characterizing a heterogeneous aquifer by derivative analysis of pumping and recovery test data. Journal of Geological Society of Iran 1:29-41 Available via www.gsoi.ir , accessed on 11 November 2012. Pp. 22-37.

Singh, R.N. and Vutukuri, V.S. 2006. Mine Inundation-Case Histories. Mine Water and the Environment, Vol 14, Annual Issue, Paper 9, 1995 pp. 114-130.

Spivey, A.M. 1991. Universal Distinct Element Code (UDEC) Modelling of the Hanging Wall Response to Zero Anticline Mining at Central Shaft, Nkana Division. Zambia Consolidated Copper Mines Limited, Technical Division, Kalulushi Zambia, pp. 23-87.

SRK. 2007. Ruashi Phase 2 Project: Environmental and Social Impact Assessment. Volume III. Environmental and Social Management Plan. Report No. 367509/ESMP pp.12-17.

Straskraba, V. 1991. Future Mine Dewatering Strategy for the Nkana Mine Area, Unpublished report for Zambia Consolidated Copper Mines, Ltd. pp. 23-32.

University of Karlsruhe. 2008. World Stress Map Rel. 2008. <http://dc-app3-14.gfz-potsdam.de/pub/maps/africa.gif>. Heidelberg Academy of Sciences and Humanities,

Geophysical Institute, University of Karlsruhe. Website accessed via online library on 17 March 2013.

Van Tonder, J.G. and Dzanga, P. 2002. Interpretation of single-well tracer tests using fractional-flow dimensions Part 2: A case study. *Hydrogeology Journal* 1-29.

Van Tonder, G.J., Kunstmann, H. and Xu, Y. 2001b. FC program, software developed for DWAF by the Institute of Groundwater Studies. Institute of Groundwater Studies, University of the Free State, South Africa.

Van Tonder, G. J., Bardenhagen, I., Riemann, K., Van Bosch, J., Dzanga, P. and Xu, Y. 2001. Manual on Pumping Test, Analysis in fractured - Rock Aquifers. Institute of Groundwater Studies, University of the Free State. Bloemfontein, South Africa. pp.10 -28.

Van Wyk, E., Van Tonder, G.J. and Vermeulen, D. 2011. Characteristics of local groundwater recharge cycles in South African semi-arid hard rock terrains-rainwater input Water. *SA* 37:2:133-152. Available via www.wrc.org.za, accessed on 15 October 2012.

WHO Guidelines for Drinking-water Quality. 2011. World health organisation (WHO) 4TH EDITION. pp. 219-251.

Williams, R.E. 1986. Mine Hydrogeology, Society of Mining Engineers Inc, Littleton, Colorado, USA. pp. 136-172.

Appendix A

Borehole details and borehole logs

a) Dewatering boreholes

BH No.	BH Depth (m)	Final Casing diameter (mm)	Date Completed	Location (Y)	Location (X)	Collar Elevation (mamsl)	Water Strike (mbgl)	Blow Yield (m ³ /hr.)	Rest Water Level (mbgl)	From	To	Lithology
BHAP1	120	254mm uPVC	28/07/2011	8716535.3	560546.8	1266.703	15	20	4.13	1266.7	1246.7	Laterite, brown, silty, clayey
										1246.7	1236.7	Silt, grey
										1236.7	1146.7	Siltstone, grey, hard, calcite veined at 114m
BH 1-15	100	305mm steel	31-05-2011	8715540.0	558940.3	1242.865	15, 65	312	14.30	1242.9	1211.9	WAD and BOMZ, black, loose
										1211.9	1203.9	Dolomitic, siliceous shale, grey
										1203.9	1142.9	Siliceous vuggy dolomite, massive
BH 1-16	100	305mm steel	15/06/2011	8715470.5	559046.0	1243.000	16, 63	320	15.33	1243.0	1210.0	WAD and BOMZ, black, loose
										1210.0	1201.0	Dolomitic, siliceous shale, grey
										1201.0	1143.0	Siliceous vuggy dolomite, massive
										1204.9	1183.9	Dolomitic, siliceous shale, grey
BH 1-17A	90	305mm steel	05/07/2011	8715235.0	559442.0	1237.828	11.5	250	10.50	1237.8	1204.8	WAD and BOMZ, black, loose
										1204.8	1168.8	Dolomitic, siliceous shale, grey
										1168.8	1147.8	Siliceous vuggy dolomite, massive
BH 1-18A	98	305mm steel	31/08/2011	871534.2	559260.8	1237.700	16, 35, 69, 74	17, 550	15.76	1237.7	1208.7	Siliceous Dolomitic shale, weathered
										1208.7	1204.7	WAD, weathered loose, dry
										1204.7	1168.7	Siliceous Dolomitic shale, highly fractured
										1168.7	1139.7	black, manganeseiferous, graphitic
BH 2-27										1231.0	1228.0	Dolomitic brown shale weathered
										1228.0	1218.0	Dolomite, ferruginous /silicic/vuggy
										1218.0	1178.0	Silicic quartzitic light grey dolomite
										1178.0	1163.0	Silty manganeseiferous dolomite
										1163.0	1158.0	Shale, laminated, micaceous, dolomitic
BH 3-12	125	254mm uPVC	14-05-2011	8714877.90 0	560258.4	1272.000	112	0.2, 5.5	21.30	1272.0	1265.0	Laterite, clayey gravels, RGS

BH No.	BH Depth (m)	Final Casing diameter (mm)	Date Completed	Location (Y)	Location (X)	Collar Elevation (mamsl)	Water Strike (mbgl)	Blow Yield (m ³ /hr.)	Rest Water Level (mbgl)	From	To	Lithology
BH 3-36										1265.0	1215.0	Saprolite, cream white CMN
										1215.0	1147.0	Shale light grey dolomitic, silty, talcose RGS
BH 3-11	114	254mm uPVC	13-04-2011	8714691.69 9	560423.5	1272.869	35	80	22.70	1250.2	1235.2	Laterite, gravely, red, brown, talcose
BH 3-37										1235.2	1215.2	Dolomite, light brown, talcose
										1215.2	1160.2	Sandstone, grey, brown talcose
										1160.2	1135.2	Siltstone, brown, grey, lime chalk
BH 3-9	247	254mm steel	23-10-2010	8714427.66 0	560330.	1270.570	21;56;123	396	17.80	1253.8	1249.8	Topsoil, yellowish orange, loose
BH 3-39										1251.8	1237.8	Laterite, red, slightly silty, weathered
										1237.8	1205.8	Laterite, weathered, greyish brown
										1205.8	1175.8	Dolomite, sandy, grey, weathered
BH 3-10	100	305mm s	27-04-2011	8714670.93 2	559980.3	1252.9	30	100	8.46	1244.5	1228.5	Laterite, brown, gravely talcose
BH 3-41										1228.5	1224.5	Silt, deep brown
										1224.5	1152.5	Sandstone, coarse, white, grey.
										1152.5	1124.5	Sandstone & siltstone grey
BH 3-13	106	305mm	20-05-2011	8714495.80 0	560204.1	1252.0	9, 37	7, 78	7.80	1252.0	1214.0	Ferruginous gravels, clayey, brown
										1195.0	1177.0	Siliceous, dolomitic shale
										1177.0	1149.0	Dolomitic siltstones
BH2-29	112	305mm steel	05/10/2011	8714924.94	559809.11 2	1233.317	23	476	4.82	1233.31	1211.3	Topsoil
										1211.31	1196.3	Brecciated CMN & dolomitic siltstone
										1196.31	1169.3	Dolomitic siltstone, moderately fractured
										1169.31	1121.3	Dolomitic shale, graphitic, manganeseous
BH2-28	86	305mm steel	27/09/2011	8715048.11	559747.66 3	1240.609	22	96	3.00	1240.60	1186.6	CMN, Talcose

BH No.	BH Depth (m)	Final Casing diameter (mm)	Date Completed	Location (Y)	Location (X)	Collar Elevation (mamsl)	Water Strike (mbgl)	Blow Yield (m ³ /hr.)	Rest Water Level (mbgl)	From	To	Lithology
										1186.6	1173.6	Dolomitic siltstone
										1173.6	1154.6	black, manganeseiferous, graphitic
BH69B	140	228mm uPVC	20/10/2011	8715236.35	560601.794	1274.138	52	62	28.30	1274.13	1250.1	Calcareous terrigenous sediments
										1250.1	1227.1	Dolomitic siltstone, saprock
										1227.1	1114.1	Kundelungu dolomitic shale, brown

b) Groundwater monitoring boreholes

BH No.	BH Depth	Casing diameter (mm)	Date Completed	Location (Y)	Location (X)	Elev. (mamsl)	Water Strike (mbgl)	Blow Yield (m ³ /hr)	Rest Water Level (mbgl)	From	To	Lithology
MH 1-1	70	114 steel	22-02-2011	8715578.00	559525.100	1279.786	61	<0.5	30.30	1249.5	1237.5	Saprolite, brown, clayey
										1237.5	1210.5	Shale, grey and yellow, talcose,
										1210.5	1203.5	Silt, dark brown, talcose,
										1203.5	1179.5	Siltstone, brown
MH 1-2	60	114 steel	26-02-2011	8715538.00	558686.700	1286.493	42	<0.5	16.60	1269.9	1254.9	Laterite, brown, clayey
										1254.9	1226.9	Shale, grey and yellow, talcose,
										1226.9	1209.9	Silt, dark brown, talcose
MH 1-3	58	114mm steel	08-03-2011	8715154.00	559088.500	1290.046	42	3	21.00	1269.0	1258.0	Laterite, brown, clayey
										1258.0	1229.0	Shale, grey and yellow, talcose
										1229.0	1227.0	Silt, red brown, clayey
										1227.0	1211.0	Sandstone, vuggy white, conglomeritic

BH No.	BH Depth	Casing diameter (mm)	Date Completed	Location (Y)	Location (X)	Elev. (mamsl)	Water Strike (mbgl)	Blow Yield (m ³ /hr)	Rest Water Level (mbgl)	From	To	Lithology
MH 1-13	70	152 uPVC	10-06-2011	8715503.66 5	559326.446	1245.145	7; 55	24;126	2.86	1245.1	1223.1	WAD and BOMZ, loose
										1223.1	1209.1	Siliceous dolomitic shale
										1209.1	1175.1	Siliceous vuggy dolomite
MH 1-14	60	152mm	13-06-2011	8715325.6	559274.2	1237.72	8;33; 38-60	113	9.52	1229.7	1205.7	WAD and BOMZ, loose
										1205.7	1191.7	Siliceous dolomitic shale
										1191.7	1159.7	Siliceous vuggy dolomite
MH 1-15	70	152mm	15-06-2011	8715224.0	559461.9	1238.02	17, 42	94	10.55	1238.0	1210.0	Wad, BOMZ, loose, grey black
										1210.0	1196.0	Siliceous dolomitic shale
										1196.0	1168.0	Siliceous vuggy dolomite
MH 1-16	70	152mm	17-06-2011	8715300.9	559496.3	1243.55	18,52	72	0.00	1243.6	1221.6	Wad, BOMZ, loose, grey black
										1221.6	1199.6	Siliceous, dolomitic shale, grey
										1199.6	1173.6	Siliceous, vuggy dolomite
MH 2-1	80	114mm	18-02-2011	8715089.	560054.6	1275.34	38	0.5;3	27.30	1248.0	1239.0	Saprolite, brown, clayey
										1239.0	1199.0	Shale, grey and yellow, talcose,
										1199.0	1193.0	Cavity
										1193.0	1168.0	Siltstone , Breccia, quartz pebble
MH 2-2	70	152mm	15-03-2011	8714814.4	559302.9	1287.04	35	6	19.12	1267.9	1257.9	Laterite, grey, talcose
										1257.9	1247.9	Silt, deep brown
										1247.9	1217.9	Siltstone ,sandstone, brown
										1217.9	1197.9	Shale, grey, black, laminated
MH 2-3	74	114mm	15-05-2011	8715070.6	559652.9	1240.00	18, 54	5, 68	13.40	1251.3	1226.3	Laterite, gravely, red, brown
										1226.3	1224.3	Shale, light brown, talcose
										1224.3	1141.3	Siltstone, grey, brown talcose
										1141.3	1081.3	Sandstone, coarse, white,sucrosic
MH 2-4	70	152mm	02-06-2011	8715046.9	559907.3	1245.17	15	33	6.00	1245.2	1197.2	Laterite, gravely, red, brown
										1197.2	1087.2	Quartzite Sandstone

BH No.	BH Depth	Casing diameter (mm)	Date Completed	Location (Y)	Location (X)	Elev. (mamsl)	Water Strike (mbgl)	Blow Yield (m ³ /hr)	Rest Water Level (mbgl)	From	To	Lithology
MH 2-5	80	152mm	01-07-2011	8714922.6	559822.9	1240.59	5	5;15	3.00	1240.6	1234.6	brown, grey talcose
										1234.6	1226.6	WAD, earthy, grey talcose, clayey
										1226.6	1160.6	Siliceous vuggy malachite, dolomite
MH 2-6	30	152mm	05-07-2011	8714905.0	559785.0	1240.18	45	3.5	6.99	1240.2	1220.2	Saprolite, brown, grey talcose
										1220.2	1157.2	WAD, earthy, grey talcose, clayey
										1157.2	1155.2	Siliceous vuggy malachite, dolomite
MH 2-7	70	203mm	03-06-2011	8715026.3	559768.5	1240.05	16,26,43-70	293	10.66	1240.1	1233.1	Weathered CMN, clayey, moist
										1233.1	1222.1	Silicified talcose shale, weathered
										1222.1	1215.1	RSC, Siliceous vuggy dolomite
										1215.1	1197.1	Breccia , huge fragments >4cm
										1197.1	1170.1	WAD, BOMZ, deeply weathered
MH 3-1	250	114mm	28-09-2010	8714450.0	560297.5	1270.27	22;210,237	48.4	17.95	1270.3	1232.3	Laterite, ferricrete, orange
										1232.3	1202.3	Breccia, RAT
										1202.3	1155.3	Highly talcose
										1155.3	1082.3	Wad, loose
										1082.3	1020.3	Dolomitic shale, grey, fractured
MH 3-2	123	114mm	22-11-2010	8714461.5	560352.5	1270.67	28;53;108	49	20.21	1270.7	1216.7	Laterite, minor orange shades
										1216.7	1208.7	Breccia, RAT, clear hard quartz
										1208.7	1147.7	Rat. Highly talcose
MH 3-3	206	114mm	22-11-2010	8714406.2	560362.5	1270.56	26;32;165	73	18.30	1270.6	1238.6	Laterite, minor orange shades
										1238.6	1213.6	Breccia, RAT, clear hard quartz
										1213.6	1105.6	Rat. Highly talcose
										1105.6	1082.6	Wad, black loose
										1082.6	1066.6	Dolomitic shale, grey, fractured
MH 3-4	250	114mm	07-12-2010	8714392.5	560308.7	1271.16	76;104;116	34.5	17.70	1271.2	1167.2	Laterite, minor orange shades

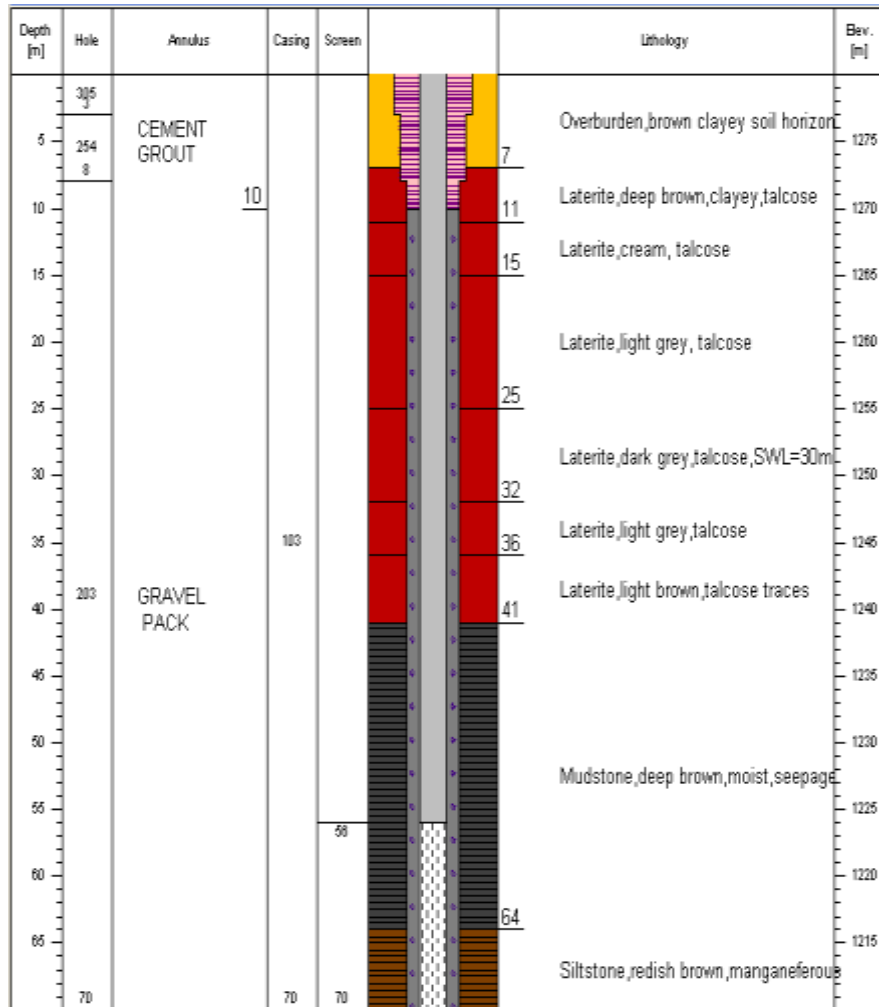
BH No.	BH Depth	Casing diameter (mm)	Date Completed	Location (Y)	Location (X)	Elev. (mamsl)	Water Strike (mbgl)	Blow Yield (m ³ /hr)	Rest Water Level (mbgl)	From	To	Lithology
										1167.2	1155.2	Breccia, RAT, quartz, clasts >2cm
										1155.2	1129.2	Rat. Highly talcose
										1129.2	1056.2	Dolomitic shale, grey, fractured
										1056.2	1021.2	Wad, black loose
MH 3-5	230	114mm steel	05-12-2010	8714211.320	559681.510	1269.890	24-26,61	7, 47	5.42	1269.9	1243.9	Laterite, minor orange shades
										1243.9	1208.9	Breccia, RAT, quartz, clasts >2cm
										1208.9	1081.9	RAT. Highly talcose
										1081.9	1041.9	Dolomitic shale, grey, fractured
MH 3-6	149	114mm steel	03-11-2010	8714356.250	560285.500	1272.015	39;76;98	58.4	18.62	1272.0	1230.0	Laterite, minor orange shades
										1230.0	1196.0	Breccia, RAT, quartz, clasts >2cm
										1196.0	1174.0	Rat. Highly talcose
										1174.0	1123.0	Sandstone, quartzitic
MH 3-6b	150	114mm steel	20-03-2011	8714351.755	560281.720	1272.337	61	5.5	21.00	1272.3	1212.3	Laterite, minor orange shades
										1212.3	1122.3	Sandstone, quartzitic
MH 3-7	69	114mm steel	11-02-2011	8714693.000	560390.100	1272.586	37	10;16	16.97	1272.6	1266.6	laterite, brown clayey
XMH 3-7										1266.6	1243.6	Clay, grey and yellow, talcose
										1243.6	1236.6	Silt, dark brown, talcose
										1236.6	1203.6	Siltstones and shale, quartz cobbles
MH 3-7A	70	152mm uPVC	29/07/2011	8714693.5	560389.7	1271.600	21	5	15.20	0.0	30.0	laterite, brown clayey
										30.0	70.0	Silt, dark brown, talcose
MH 3-8	65	152mm uPVC	08-03-2011	8714526.000	560167.600	1250.717	6	15	4.00	1250.71	1210.7	Laterite, reddish
										1210.7	1196.7	Breccia
										1196.7	1186.3	Manganiferous siltstone
MH 3-9	72.8	152mm uPVC	09-03-2011	8714753.000	560138.500	1253.776	30	0.5	19.79	1253.8	1248.8	Grey laterite.talcosic
										1248.8	1198.8	Sandstone coarse, white grey

BH No.	BH Depth	Casing diameter (mm)	Date Completed	Location (Y)	Location (X)	Elev. (mamsl)	Water Strike (mbgl)	Blow Yield (m ³ /hr)	Rest Water Level (mbgl)	From	To	Lithology
										1198.8	1180.8	Siltstone/sandstone.
MH 3-10	64.4	152 uPVC	12-03-2011	8714569.000	560034.700	1250.462	6	5	2.40	1250.5	1240.5	Gravel .laterite, red
										1240.5	1200.5	Sandstone, conglomeritic
										1200.5	1185.5	RAT, mineralized, sandstone, malachite
MH 3-11	60	152 PVC	22/3/2011	871426.639	559751.578	1283.321	21	0.05		1283.3	1279.3	yellowish orange, loose, dry
										1279.3	1273.3	Laterite, red, silty, weathered
										1273.3	1261.3	Laterite, weathered, reddish orange
										1261.3	1223.3	RAT, highly talcose, loose, dry
MH 3-14	100	152mm uPVC	03/09/2011	8714443.3	560165.991	1253.123	25	0.05	13.2	1253.12	1244.1	Breccia, clear, black, hard
										1244.12	1184.12	Highly talcose, white, shale
MH 3-15	100	152 uPVC	20/08/2011	8714477.7	560227.674	1253.324	11; 15	5	11.04	1253.32	1237.32	Reddish orange, very fine, with dark grey-black ferricrete
										1237.324	1222.32	RAT Breccia, clear and black very hard quartz, with very hard creamy indurated shale and dolomitic clasts
										1222.32	1181.3	dolomitic shale, grey, malachite, weathered and fractured
										1181.32	1153.32	Dolomitic wad, black, weathered
MH 3-16	100	152mm uPVC	22/08/2011	8714583.51	560213.761	1250.871	39	14	8.27	1250.871	1245.87	deep red, minor orange shades
										1245.87	1232.8	RAT Breccia, with very hard creamy indurated shale and dolomitic clasts
										1232.87	1213.87	Highly white talcose, shale
										1213.8	1150.8	Dolomitic wad, black, weathered

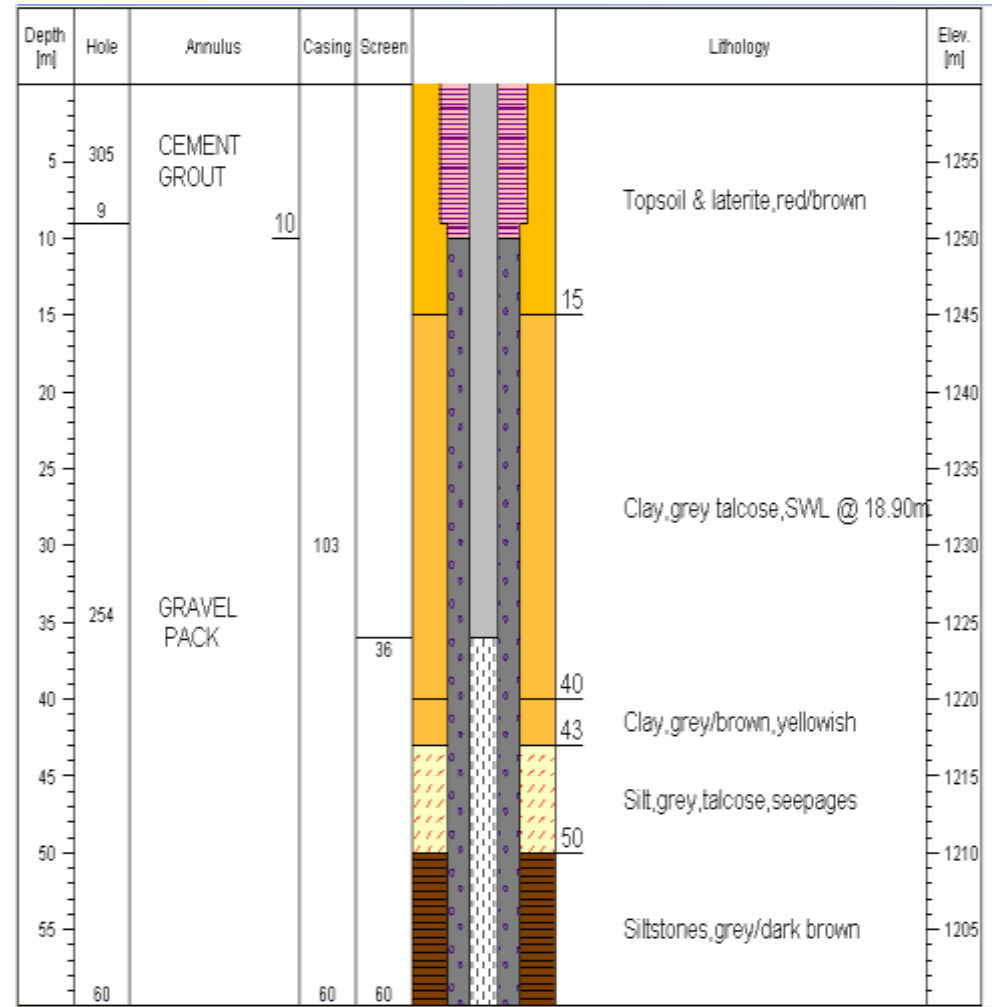
c) Environmental monitoring boreholes

BH No.	BH Depth (m)	Casing diameter (mm)	Date Completed	Location (Y)	Location (X)	Elevation (mamsl)	Water Strike (mbgl)	Blow Yield (m ³ /hr)	Rest Water Level (mbgl)	From	To	Lithology
GWD-5	53	152	21-02-2011	8715424.0	561249.1	1267.55	5	3	2.90	1264.7	1259.7	Saprolite, brown, clayey
										1259.7	1254.7	Laterite, gravely, red/brown
										1254.7	1211.7	Laterite, gravely, clayey
GWD-6	50	152	23-02-2011	8715585.0	559975.9	1274.69	30	2.5	19.35	1255.3	1237.3	Saprolite, brown, clayey
										1237.3	1225.3	Laterite, red, brown, silty
										1225.3	1205.3	Silt, red brown, clayey
GWD-7	75	152	25-02-2011	8715579.0	559749.5	1275.09	67, 75	<0.5, 5	20.54	1254.6	1224.6	Laterite, brown, clayey
										1224.6	1194.6	Red/brown, gravely
										1194.6	1179.6	Siltstone, brown
GWD-8	50	152	03-03-2011	8715381.0	560234.5	1274.48	42	<0.5	19.00	1255.5	1235.5	Red /brown, gravely
										1235.5	1205.5	Shale, grey, silty and gritty
										1235.5	1205.5	Shale, brown, silty and gritty

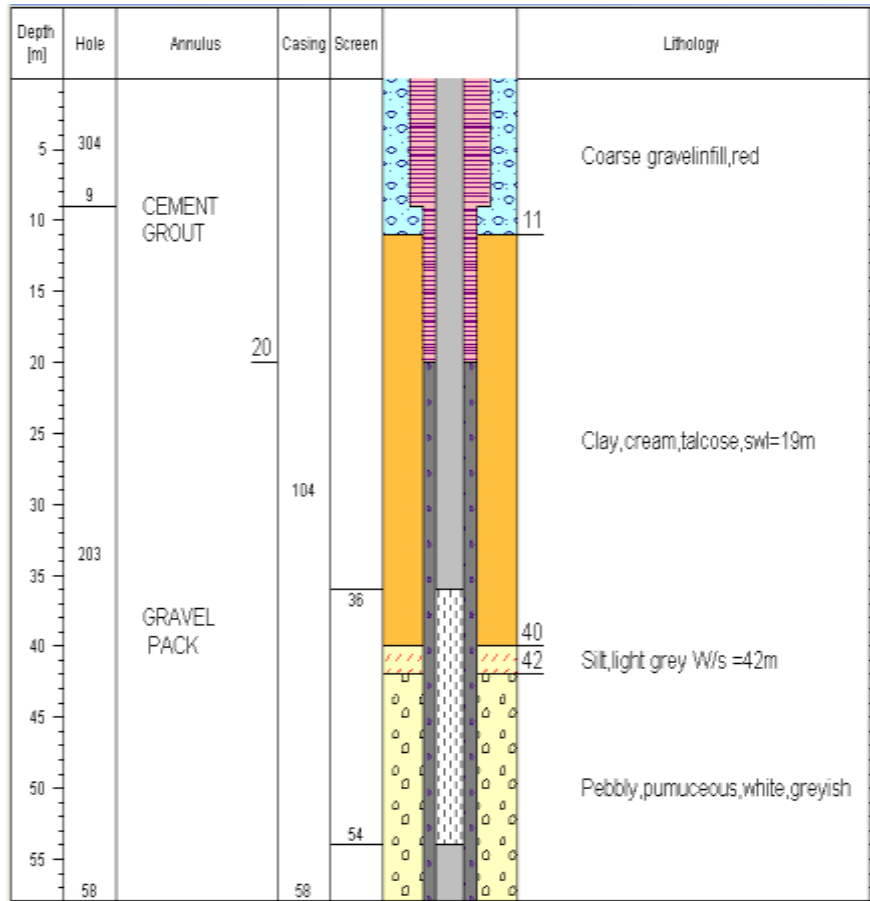
MH1-1



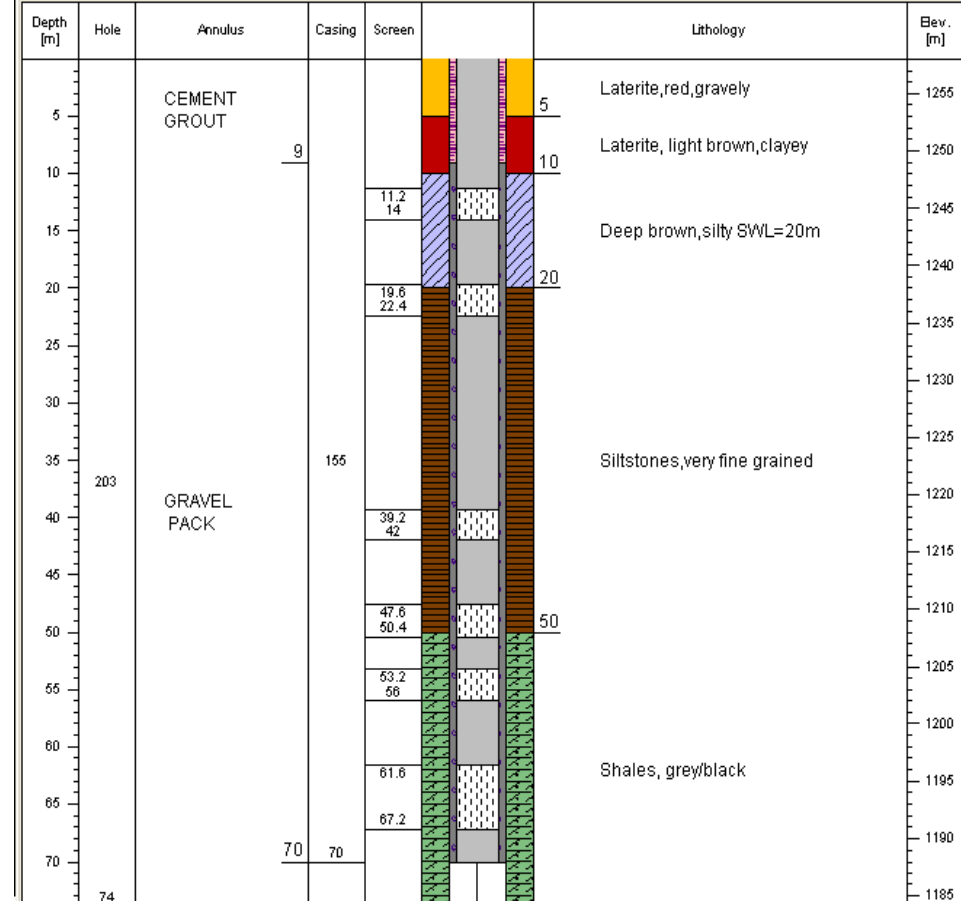
MH1-2



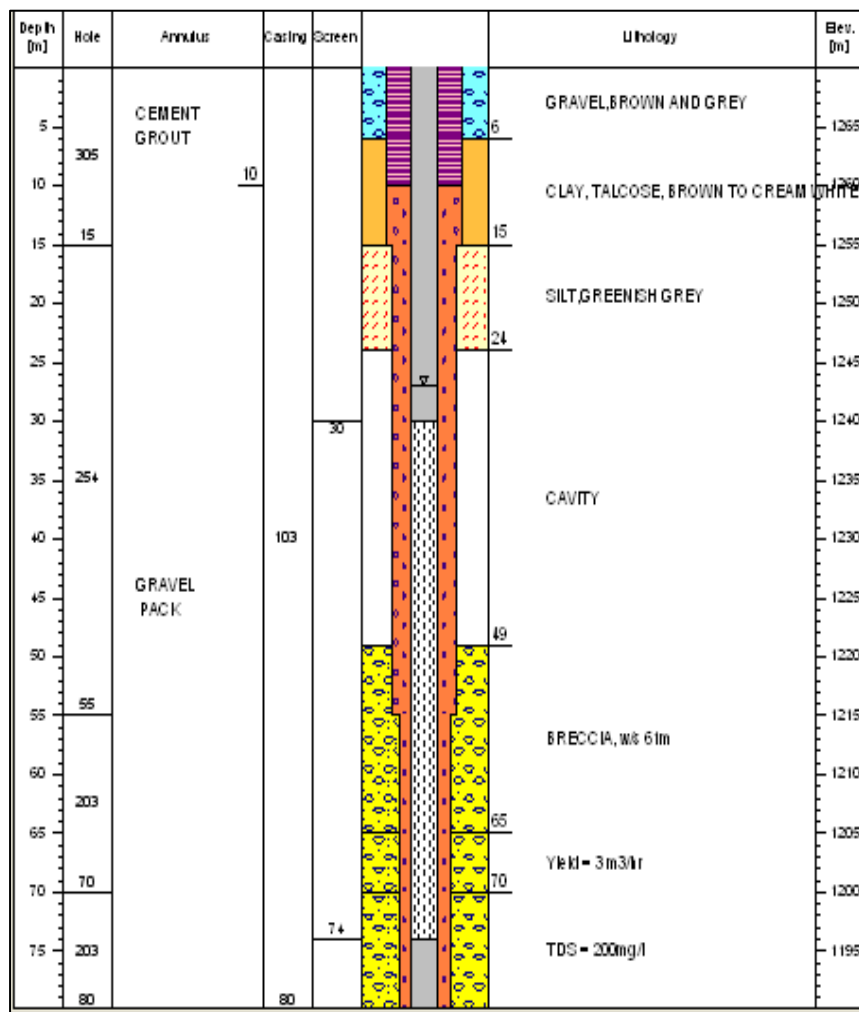
MH1-3



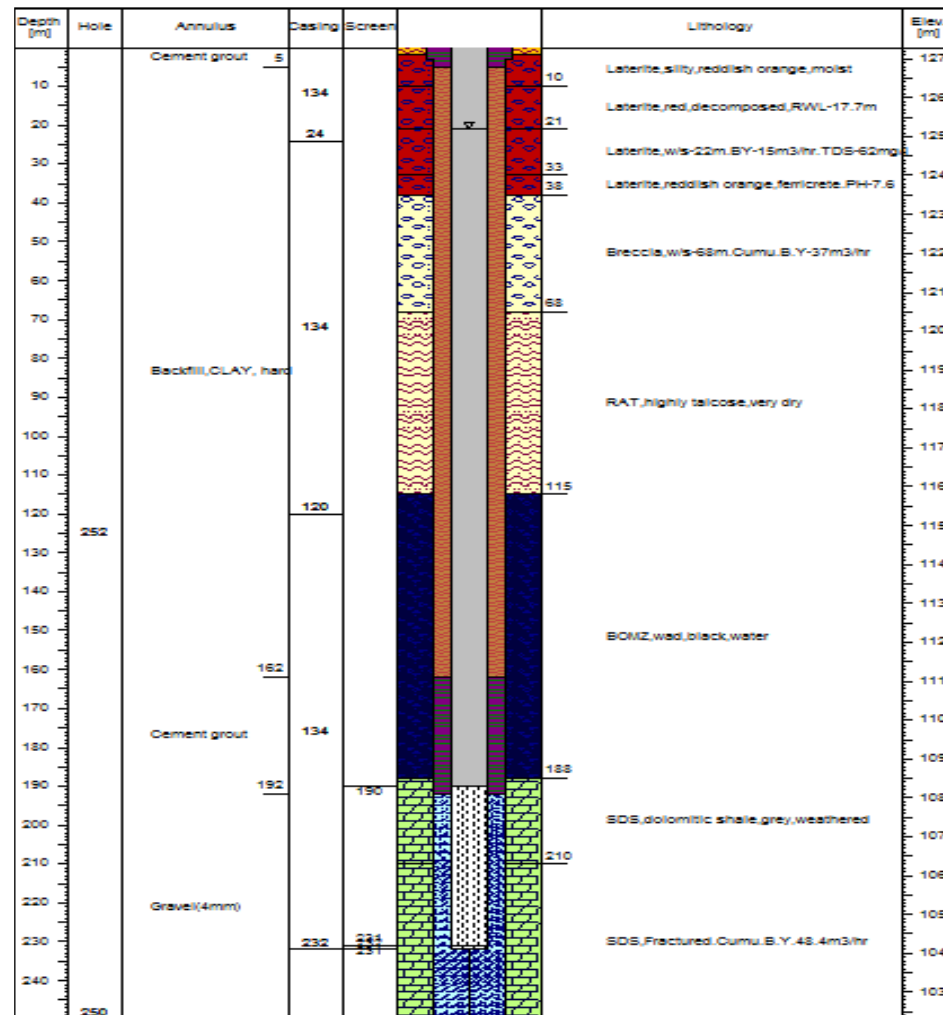
MH2-2



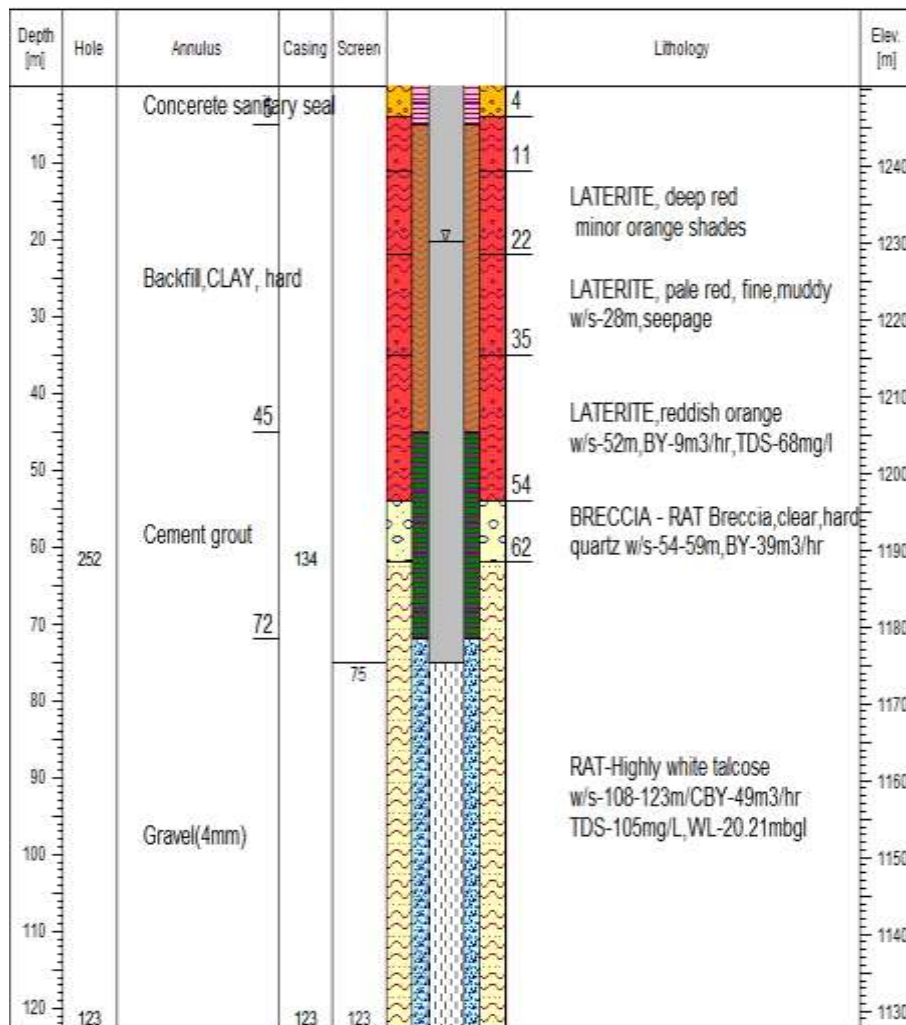
MH2-1



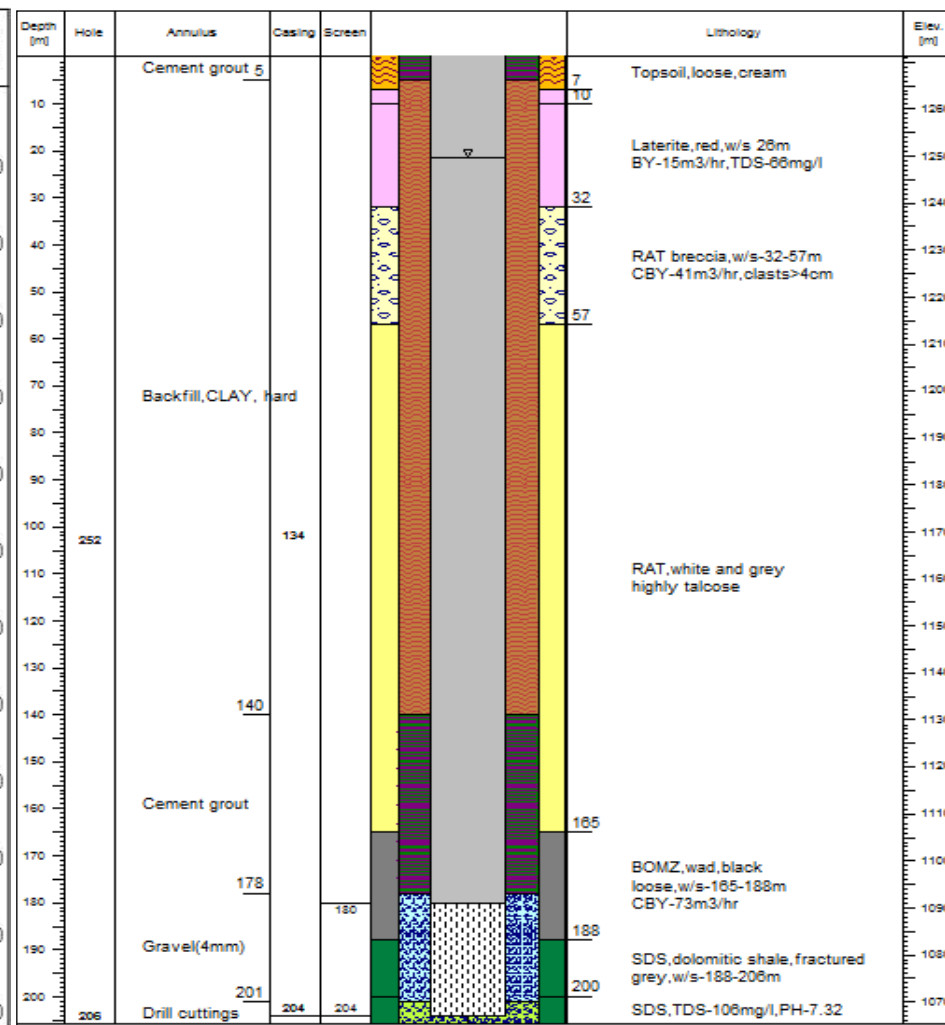
MH3-1



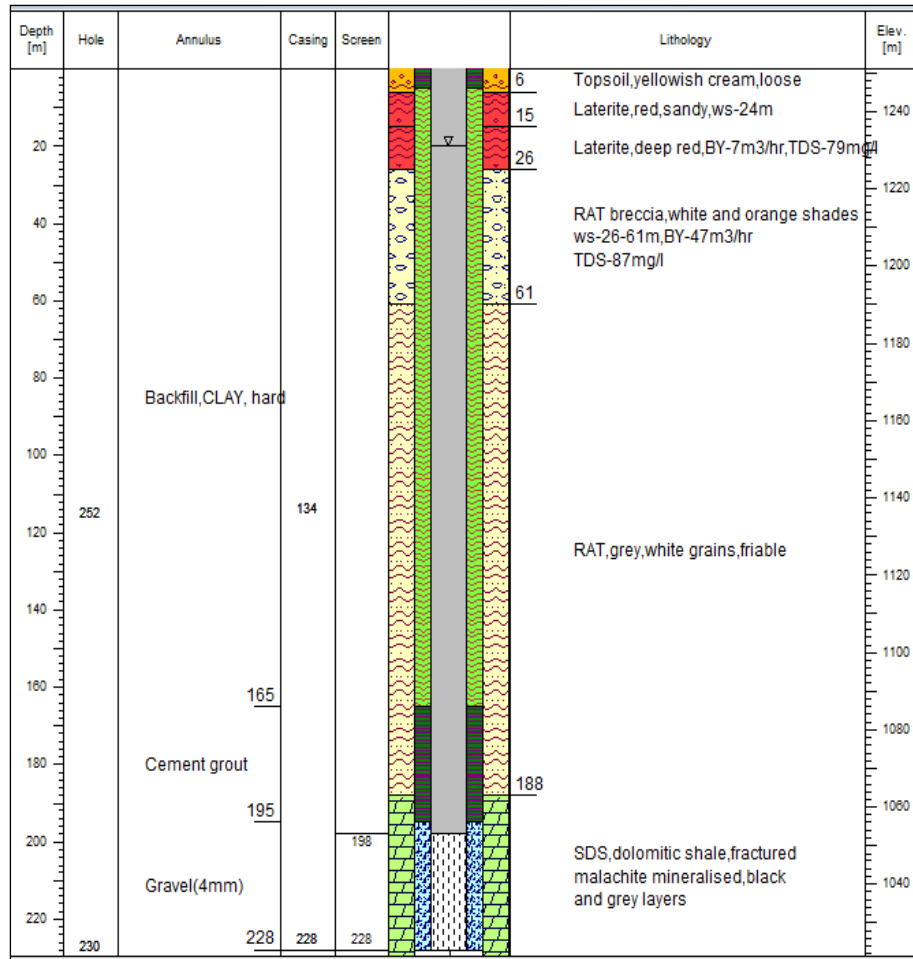
MH3-2



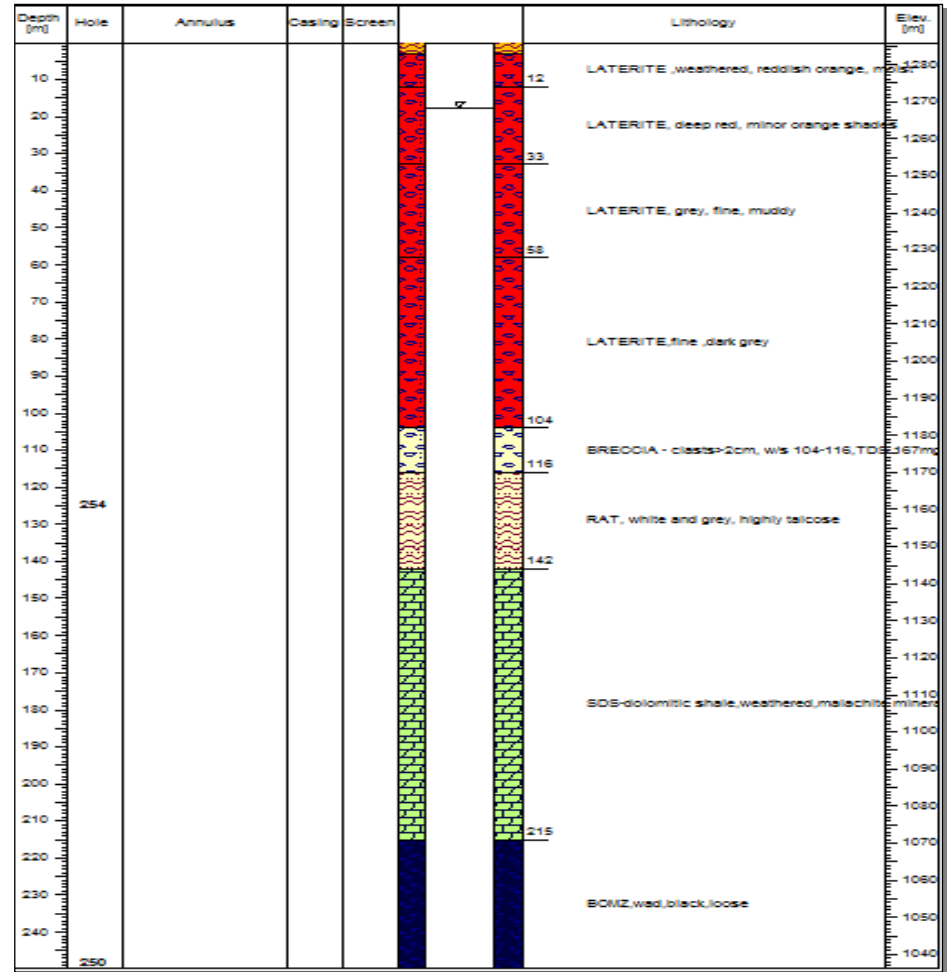
MH3-3



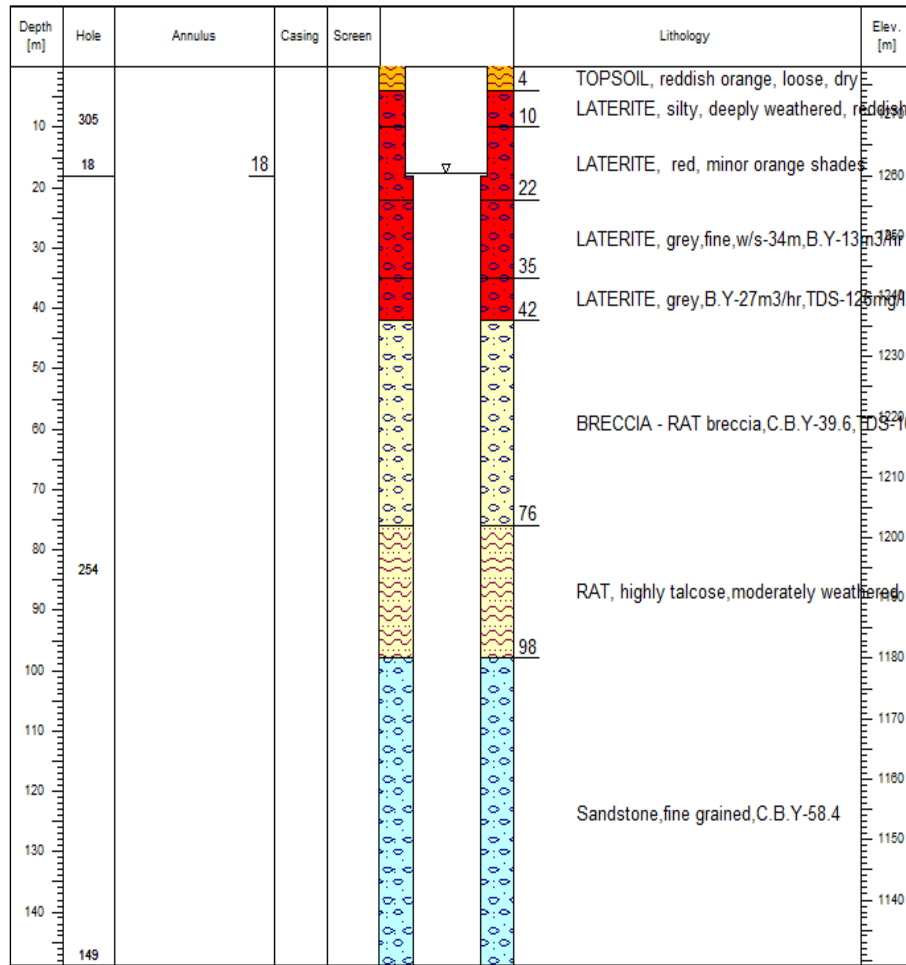
MH3-4



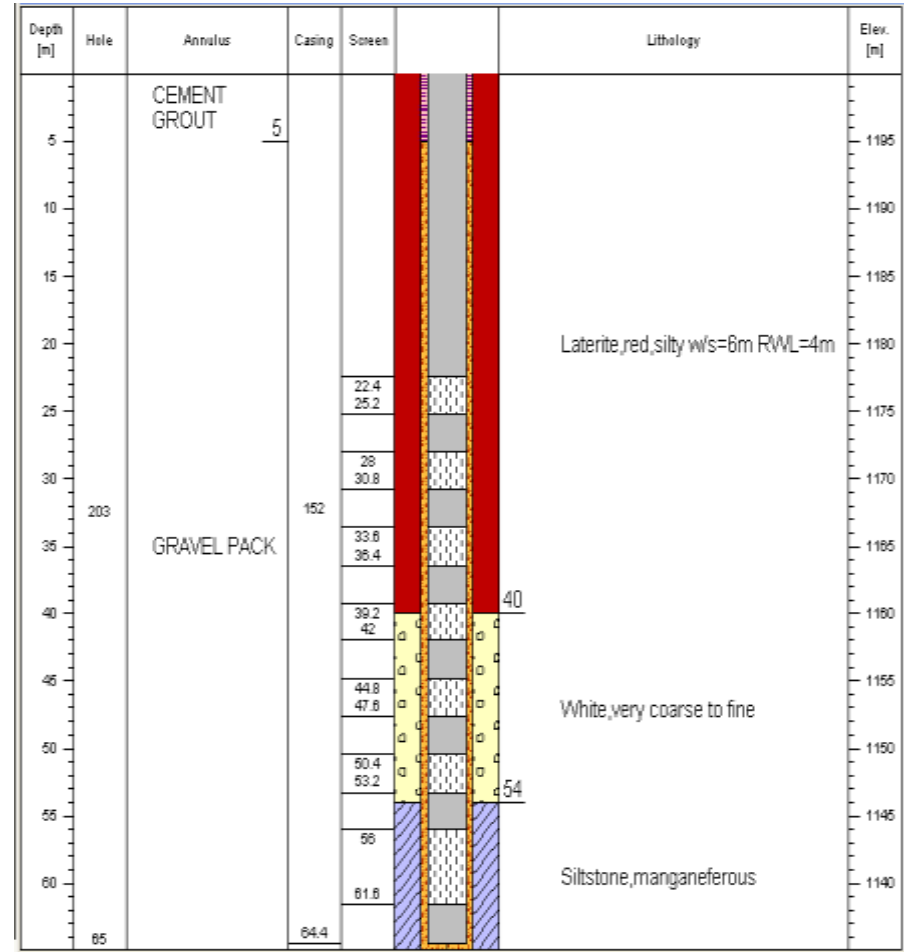
MH3-5



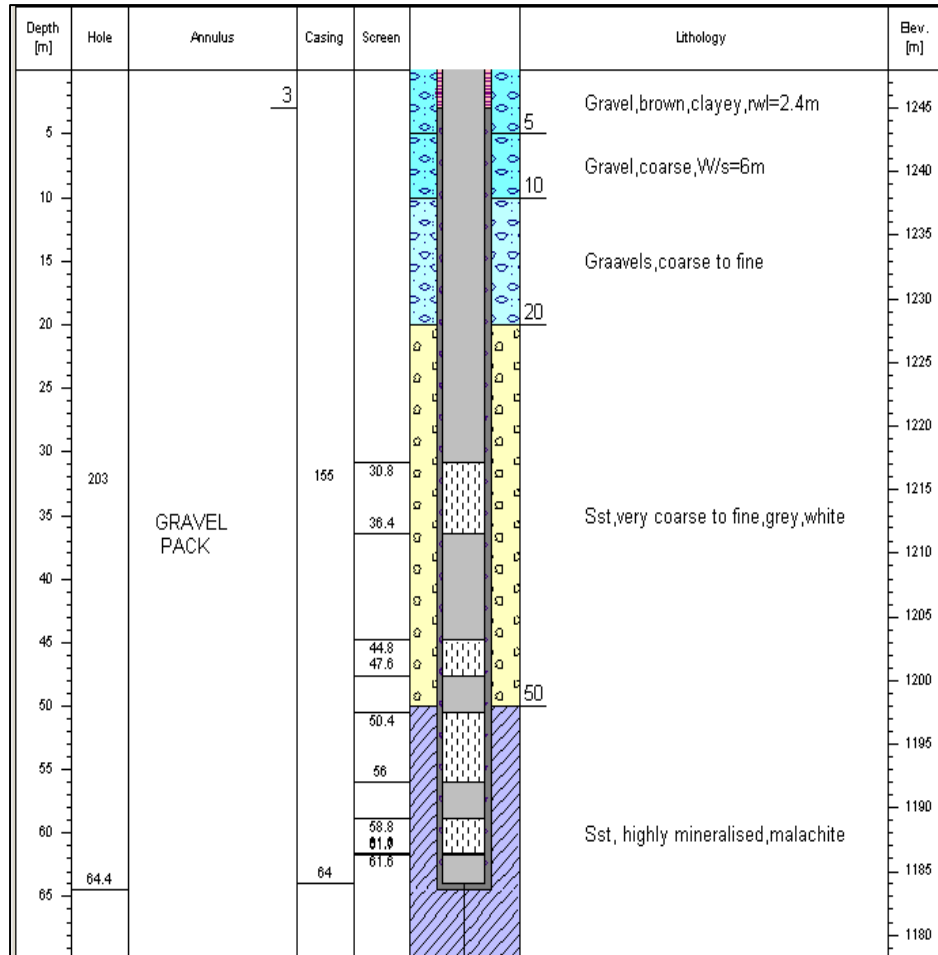
MH3-6B



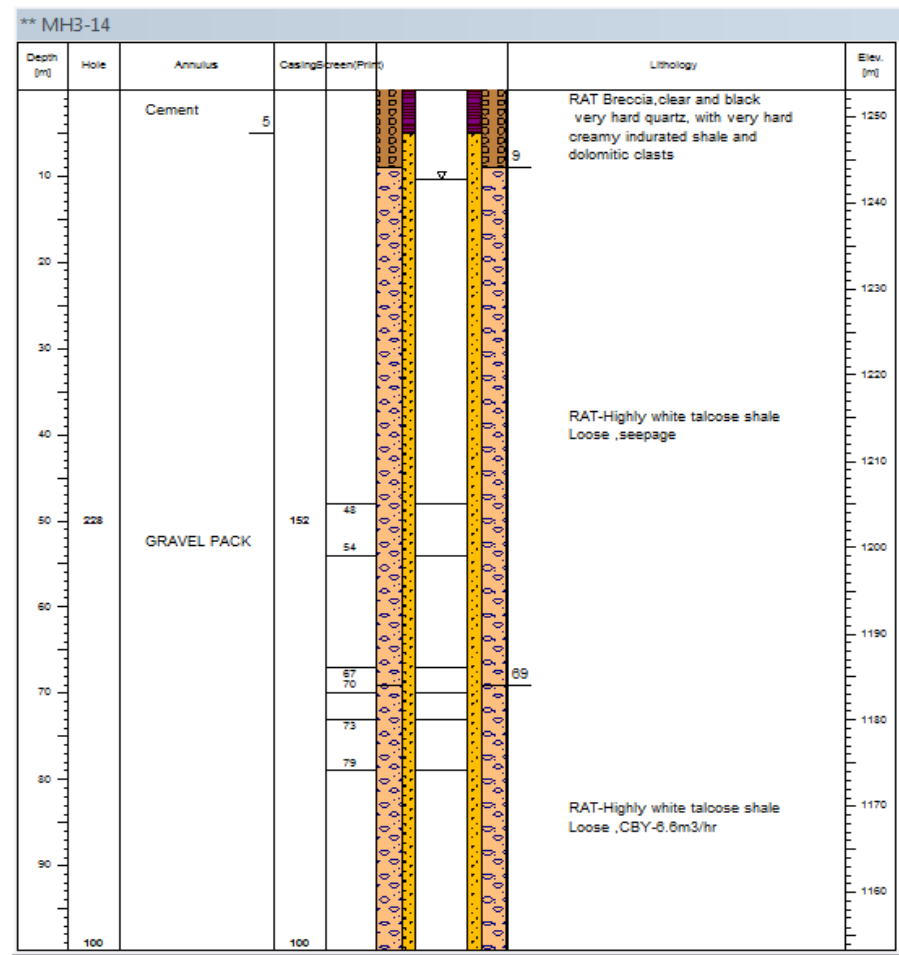
MH3-8



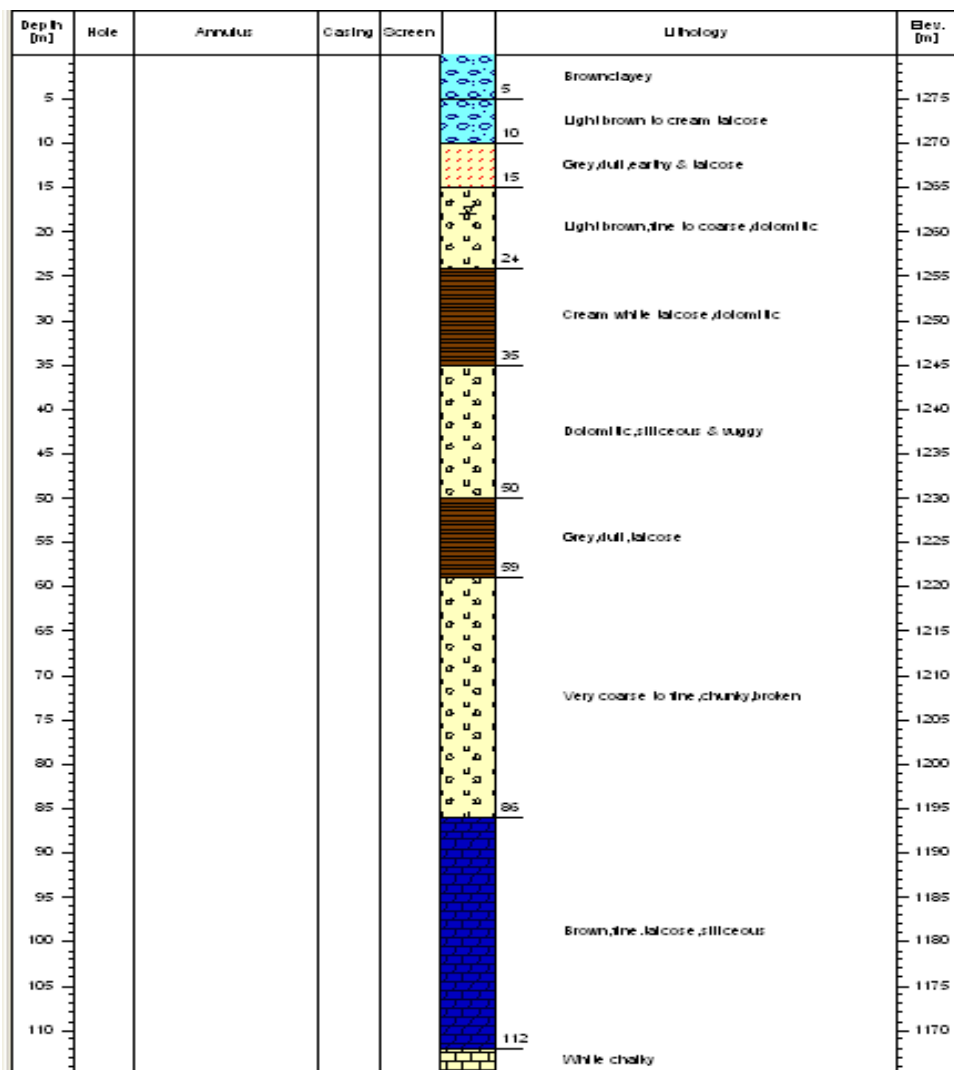
MH3-10



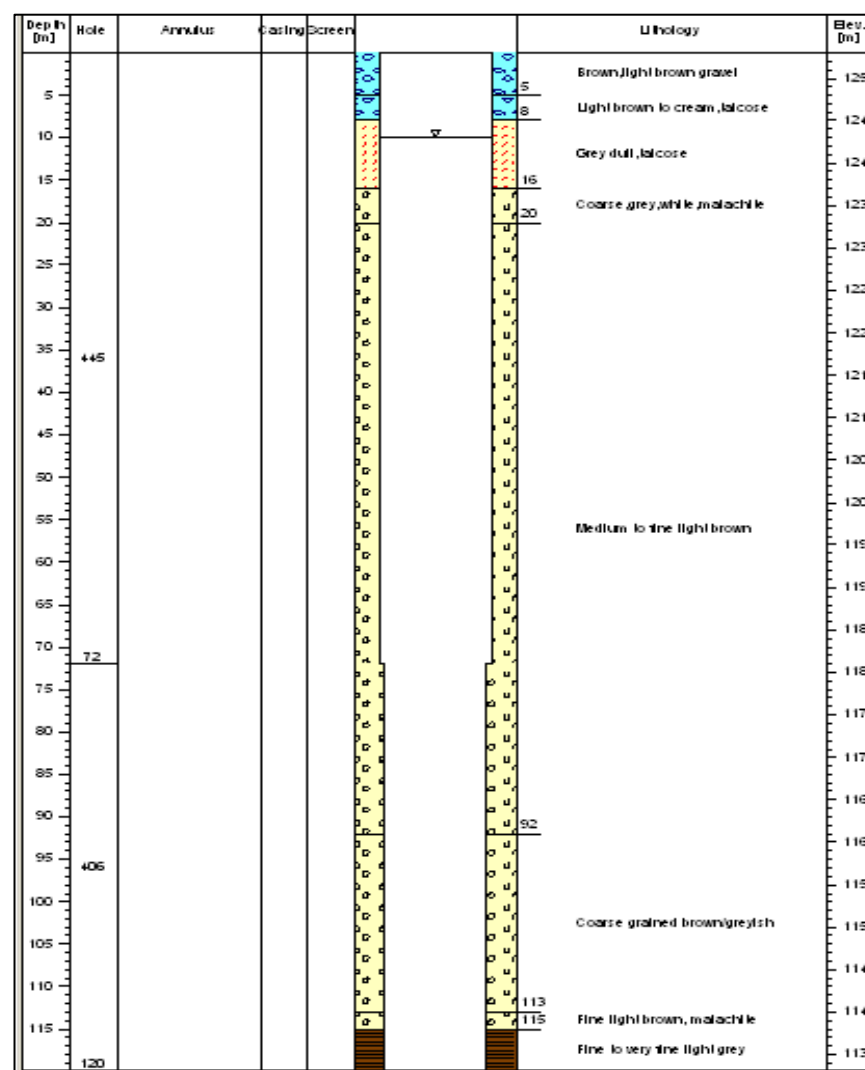
MH3-14



BH3-37

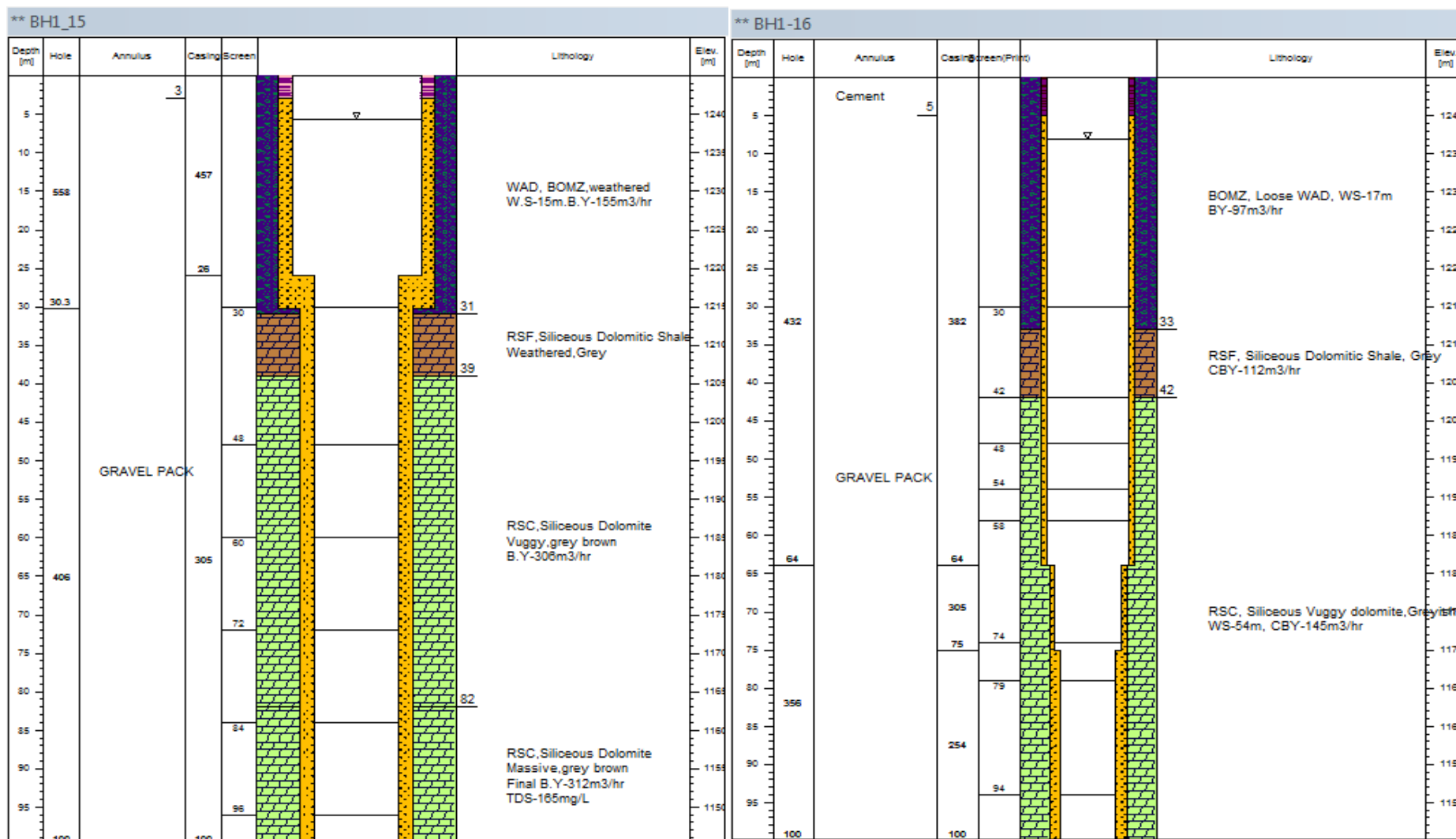


BH3-10

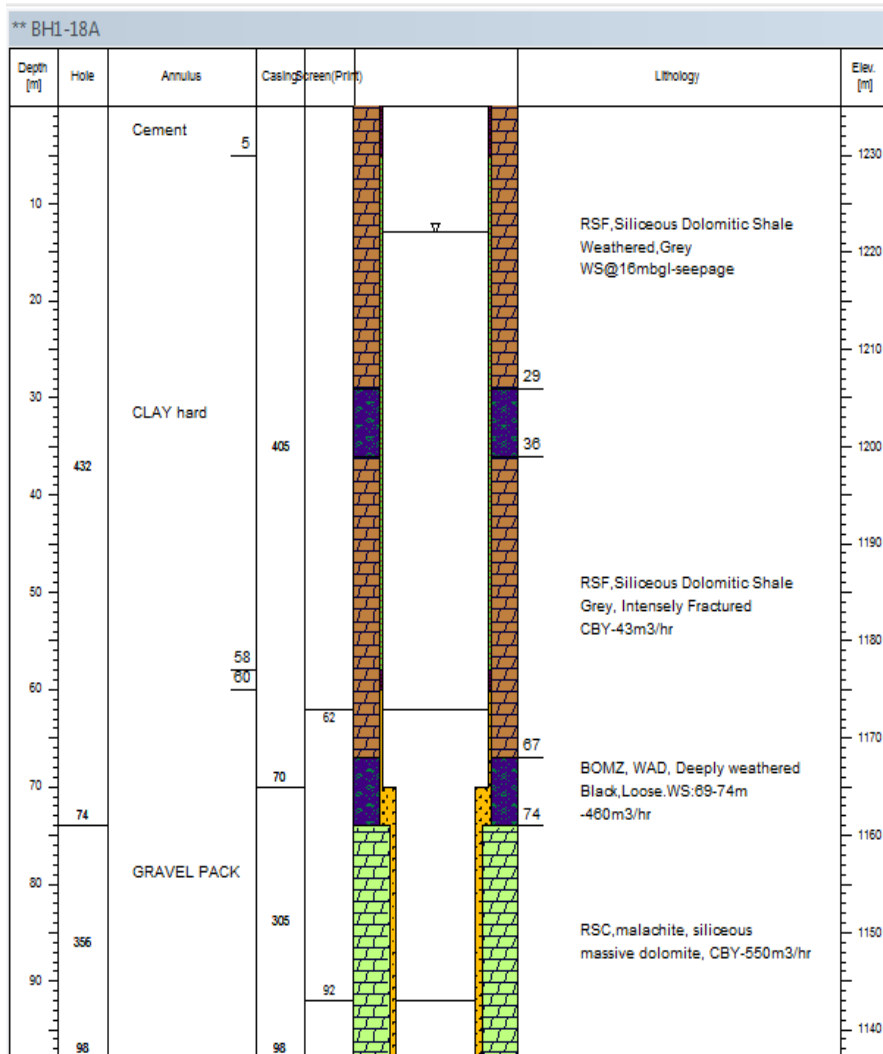


BH1-15

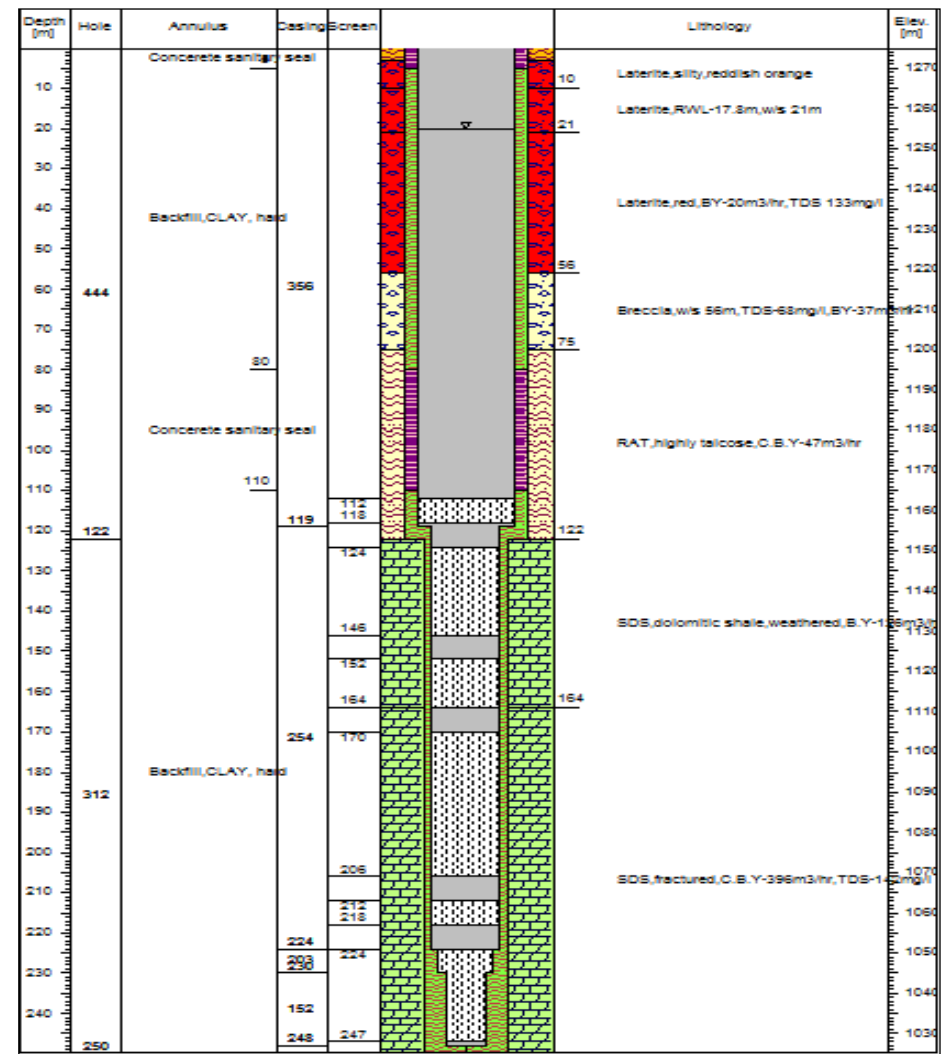
BH1-16



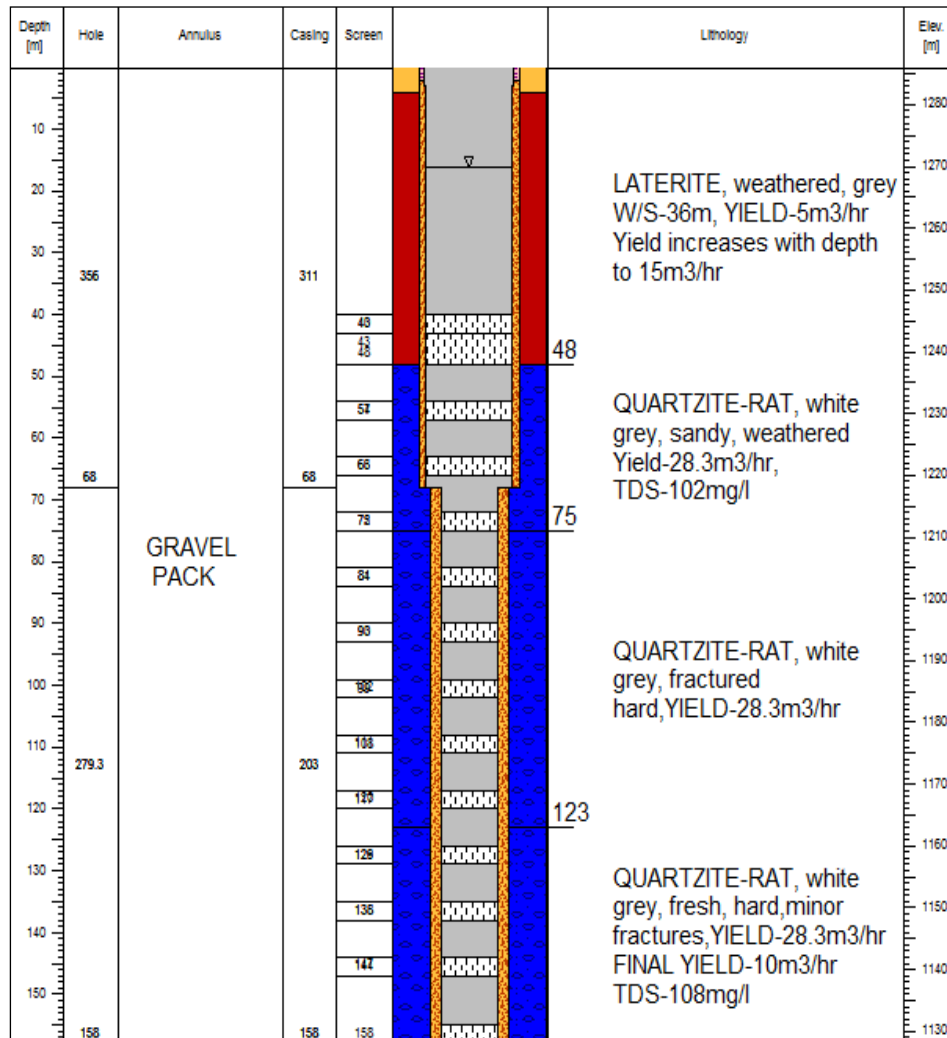
BH1-18A



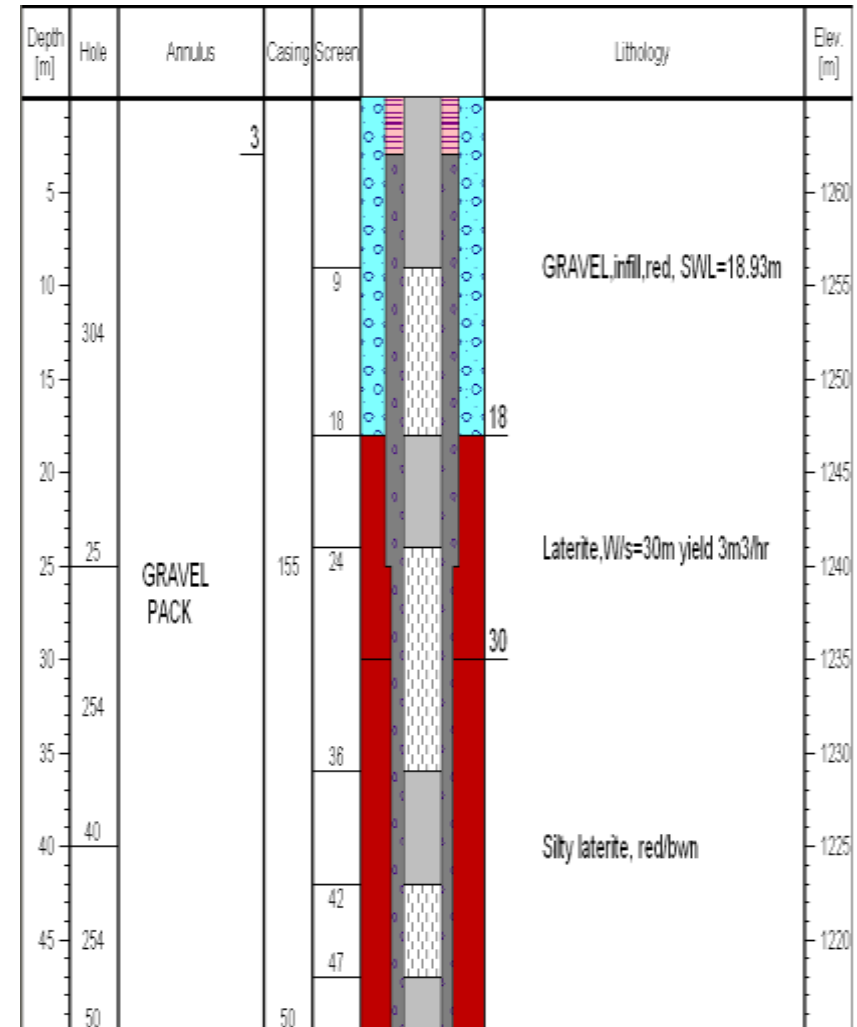
BH3-3



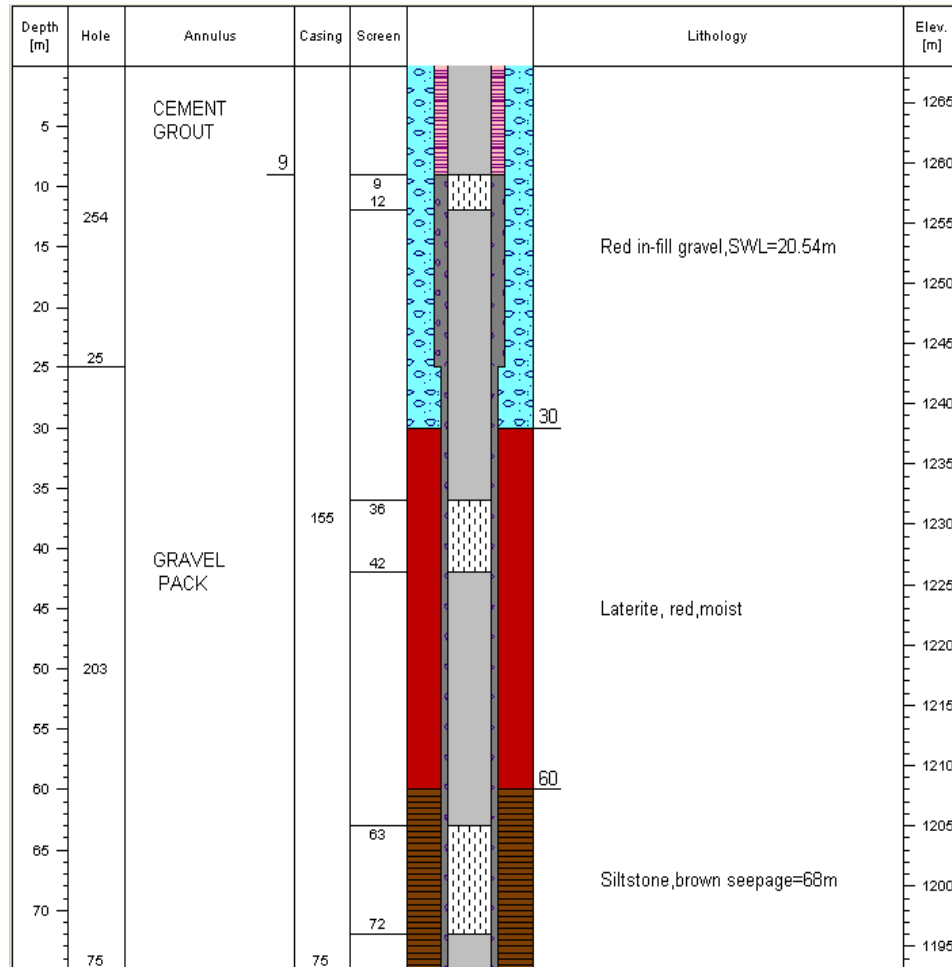
BH2-4



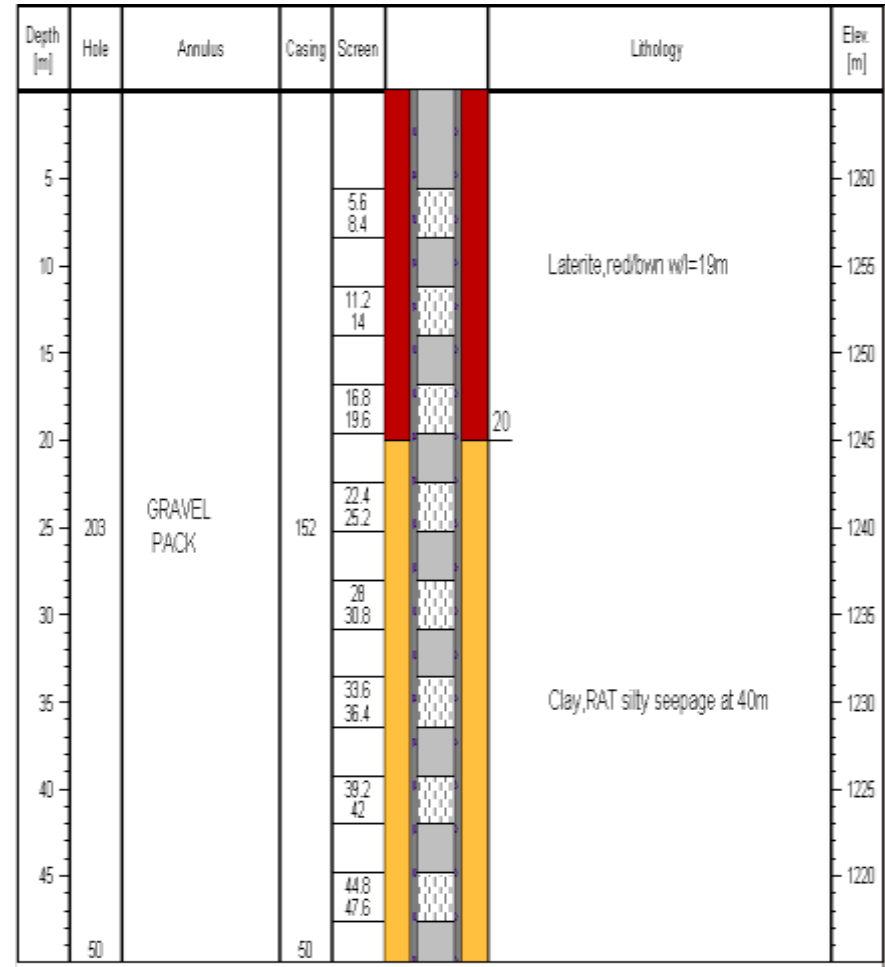
MH3-11



GWD-5



GWD-6



Appendix B

Aquifer hydraulic test data

BH3-39 Test 1-7-12th June 2011

Time :	Elapsed time (min)	Hrs.	Drawdown BH3-39		Time to fill (sec.)	Q	Remarks
			Water Level			m ³ /hr	<i>Cloudy water etc.</i>
	0.5		25.81	2.1		144	
	1.0		26.06	2.35			
	2.0		26.19	2.48			
	3.0		26.31	2.6			
	4.0		26.36	2.65			
	5.0		26.48	2.77			
	6.0		26.56	2.85			
	7.0		26.69	2.98			
	8.0		26.79	3.08			
	9.0		26.9	3.19			
	10.0		27.02	3.31			
	12.0		27.49	3.78			
	15.0		28.81	5.1			
	20.0		29.22	5.51			
	25.0		29.46	5.75			
	30.0	0.5	29.51	5.8			
	40.0		29.67	5.96			
	50.0		29.69	5.98			
	60.0	1.00	29.75	6.04			
	75.0		29.79	6.08			
	90.0	1.50	29.97	6.26			
	100.0		30.34	6.63			
	120.0	2.00	30.5	6.79			
	180.0	3.00	30.9	7.19			
	240.0	4.00	31.3	7.59			
	300.0	5.00	31.47	7.76			
	360.0	6.00	31.61	7.9			
	420.0	7.00	31.57	7.86			
	480.0	8.00	31.53	7.82			
	540.0	9.00	31.61	7.9			
	600.0	10.00	31.69	7.98			
	660.0	11.00	31.6	7.89			
	720.0	12.00	31.83	8.12			
	780.0	13.00	31.86	8.15			
	840.0	14.00	31.9	8.19			
	900.0	15.00	32	8.29			
	960.0	16.00	32.01	8.3			
	1020.0	17.00	32.05	8.34			
	1080.0	18.00	32.08	8.37			
	1140.0	19.00	32.1	8.39			
	1200.0	20.00	32.13	8.42			
	1260.0	21.00	32.16	8.45			
	1320.0	22.00	32.17	8.46			
	1380.0	23.00	32.2	8.49			
	1440.0	24.00	32.24	8.53			1 day
	1500.0	25.00	32.28	8.57			
	1680.0	28.00	32.56	8.85			
	1740.0	29.00	32.65	8.94			

	1800.0	30.00	32.71	9			
	1860.0	31.00	32.86	9.15			
	1920.0	32.00	32.9	9.19			
	1980.0	33.00	33.01	9.3			
	2040.0	34.00	33.04	9.33			
	2100.0	35.00	33.12	9.41			
	2160.0	36.00	33.23	9.52			
	2220.0	37.00	33.36	9.65			
	2280.0	38.00	33.44	9.73			
	2340.0	39.00	33.53	9.82			
	2400.0	40.00	33.68	9.97			
	2460.0	41.00	33.73	10.02			
	2520.0	42.00	33.77	10.06			
	2580.0	43.00	33.82	10.11			
	2640.0	44.00	33.89	10.18			
	2700.0	45.00	33.9	10.19			
	2760.0	46.00	33.91	10.2			
	2820.0	47.00	34.01	10.3			
	2880.0	48.00	34.09	10.38		2 days	
	2940.0	49.00	34.16	10.45			
	3000.0	50.00	34.21	10.5			
	3120.0	52.00	34.28				
	3240.0	54.00	34.33				
	3360.0	56.00	34.33				
	3480.0	58.00	34.38				
	3600.0	60.00	34.42				
	3720.0	62.00	34.47				
	3960.0	66.00	34.5				
	4080.0	68.00	34.56				
	4200.0	70.00	34.59				
	4320.0	72.00	34.63			3 days	
	4380.0	73.00					

RECOVERY TEST 1

PUMPING BOREHOLE		BH3-39		Commencement of test:			08:00
Supervisor:		Saki-WA		Completion of test:			
Location:		East of Pit3		S.W.L.:			m 23.71
Pump:				Pump Intake Depth			m 120
Constant Rate (Q):		144 m ³ /hr		Duration of test:			hrs 72
Consultant:		Lordrif KLMCS		Measure point above ground (m):			0
Time :	Elapsed time (min)	Hrs.	Water Level	Drawdown	Time to fill (sec.)	Q m ³ /hr	Flow meter
10:00:05	0.1		28.83	5.12		144	
10:01:00	1.0		28.75	5.04			
10:02:00	2.0		28.62	4.91			
10:03:00	3.0		28.31	4.6			
10:04:00	4.0		28.2	4.49			
10:05:00	5.0		28.14	4.43			
10:06:00	6.0		28.03	4.32			
10:07:00	7.0		27.96	4.25			
10:08:00	8.0		27.9	4.19			
10:09:00	9.0		27.81	4.1			
10:10:00	10.0		27.76	4.05			
10:12:00	12.0		27.72	4.01			
10:15:00	15.0		27.66	3.95			
10:20:00	20.0		26.97	3.26			
10:25:00	25.0		26.91	3.2			
10:30:00	30.0	0.5	26.7	2.99			
10:40:00	40.0		26.6	2.89			
10:50:00	50.0		26.52	2.81			
11:00:00	60.0	1.00	26.47	2.76			
11:05:00	75.0		26.44	2.73			
11:30:00	90.0	1.50	26.41	2.7			
11:55:00	105.0		26.38	2.67			
12:30:00	150.0		26.34	2.63			
14:00:00	240.0	4.00	26.29	2.58			
16:00:00	360.0	6.00	25.79	2.08			
18:00:00	480.0	8.00	25.75	2.04			
20:00:00	600.0	10.00	25.7	1.99			
22:00:00	720.0	12.00	25.64	1.93			
00:00:00	840.0	14.00	25.59	1.88			
02:00:00	960.0	16.00	25.54	1.83			
04:00:00	1080.0	18.0	25.48	1.77			
06:00:00	1200.0	20.00	25.45	1.74			
08:00:00	1320.0	22.00	25.42	1.71			
10:00:00	1440.0	24.00	25.39	1.68			
12:00:00	1560.0	26.00	25.37	1.66			
14:00:00	1680.0	28.00	25.35	1.64			
16:00:00	1800.0	30.00	25.34	1.63			
18:00:00	1920.0	32.00	25.33	1.62			
20:00:00	2040.0	34.00	25.31	1.6			
22:00:00	2160.0	36.00	25.27	1.56			
00:00:00	2280.0	38.00	25.23	1.52			
02:00:00	2400.0	40.00	25.19	1.48			
04:00:00	2520.0	42.00	25.15	1.44			
06:00:00	2640.0	44.00	25.13	1.42			
08:00:00	2760.0	46.00	25.1	1.39			
10:00:00	2880.0	48.00	25.09	1.38			

Test 2	Pumping BH3-39	CRT		RWL=28.55m			OBH-MH3-1	OBH-MH3-2	OBH-MH3-3	OBH-MH3-4	OBH-MH3-5	OBH-MH3-6B	OBH-MH3-8	BH-MH3-10	OBH-MH2-3
Real Time		Elapsed time (hr)	Drawdown BH3-9	W/ Level BH3-9			40 m W	40 m N	40 m E	40 m S	80 m E	80 m S	160 m W	260 m W	840 m W
11:00	0	0.0	0.00	28.55		0.0	29.95	27.68	29.99	30.92	27.78	28.25	8.16	13.85	14.11
11:40	40	0.7	2.84	31.39		60	29.93	27.57	29.99	30.91	27.76	28.23	8.16	13.81	14.14
11:50	50	0.8	4.35	32.9		120	29.66	27.66	29.85	30.93	27.76	28.2	8.16	13.82	14.17
12:00	60	1.0	4.41	32.96		180	30.02	27.67	29.9	30.95	27.74	28.21	8.17	13.83	13.94
12:10	70	1.2	4.46	33.01		1770	30.06	27.71	29.93	30.99	27.75	28.23	8.18	13.86	13.95
12:20	80	1.3	4.51	33.06		1890	30.08	27.73	29.95	31.01	27.75	28.24	8.19	13.88	13.95
12:30	90	1.5	4.58	33.13		2010	30.15	27.74	30.06	31.08	27.84	28.38	8.23	13.99	13.96
12:40	100	1.7	4.64	33.19		2130	30.21	27.78	30.13	31.12	27.76	28.3	8.24	13.93	13.97
12:50	110	1.8	4.66	33.21		2250	30.25	27.82	30.17	31.16	27.79	28.32	8.27	13.95	13.73
13:00	120	2.0	4.68	33.23		2370	30.29	27.85	30.22	31.2	27.81	28.33	8.29	13.97	13.69
13:10	130	2.2	4.71	33.26		2490	30.33	27.87	30.24	31.23	27.82	28.35	8.3	13.99	13.91
13:20	140	2.3	4.73	33.28		2610	30.26	27.86	30.2	31.19	27.82	28.35	8.28	14	13.98
13:30	150	2.5	4.74	33.29		2730	30.28	27.89	30.22	31.2	27.85	28.36	8.29	14	13.99
13:40	160	2.7	4.75	33.3		2850	30.31	27.9	30.21	31.2	27.84	28.38	8.32	14.04	13.96
13:50	170	2.8	4.77	33.32		2970	30.33	27.92	30.29	31.21	27.86	28.39	8.34	14.05	
14:00	180	3.0	4.79	33.34		3090	30.36	27.93	30.31	31.21	27.86	28.4	8.36	14.05	14.01
14:30	210	3.5	4.82	33.37		3092	30.33	27.93	30.25	31.23	27.87	28.39	8.34	14.06	
15:00	240	4.0	4.84	33.39		3094	30.34	27.92	30.26	31.24	27.88	28.41	8.35	14.07	14.03
15:30	270	4.5	4.86	33.41		3096	30.35	27.94	30.29	31.24	27.89	28.43	8.36	14.09	14.06
16:00	330	5.5	4.89	33.44		3098	29.85	27.51	29.9	30.94	27.42	28.29	8.24	13.88	10.78
17:00	390	6.5	4.92	33.47		3100									
18:00	450	7.5	4.95	33.5		3102	29.83	27.54	29.66	30.71	27.82	28.18	8.22	13.77	12.36
19:00	510	8.5	4.99	33.54		3104		27.64	29.8	30.85	27.83	28.22	8.25	13.84	12.95
20:00	570	9.5	5.03	33.58		3106	29.93	27.79	29.93	31.04	27.83	28.25	8.35	13.93	13.28

Test 2	Pumping BH3-39	CRT		RWL=28.55m			OBH-MH3-1	OBH-MH3-2	OBH-MH3-3	OBH-MH3-4	OBH-MH3-5	OBH-MH3-6B	OBH-MH3-8	BH-MH3-10	OBH-MH2-3
Real Time		Elapsed time (hr)	Drawdown BH3-9	W/ Level BH3-9			40 m W	40 m N	40 m E	40 m S	80 m E	80 m S	160 m W	260 m W	840 m W
21:00	630	10.5	5.03	33.58		3108	30.04	27.81	30.04	31.07	27.83	28.27	8.39	13.96	13.33
22:00	690	11.5	5.03	33.58		3110	30.1		30.15	31.14	27.81	28.3	8.37	14.04	13.49
24:00:00	810	13.5	5.04	33.59		3112	30.17	27.9	30.23	31.19	27.85	28.29	8.39	14.08	13.63
02:00	930	15.5	5.04	33.59		3114	30.26	27.96	30.25	31.24	27.87	28.41	8.41	14.11	13.68
04:00	1050	17.5	5.06	33.61		3116	30.31	27.96	30.28	31.26	27.91	28.41	8.59	14.1	13.81
06:00	1170	19.5	5.05	33.6		3118	30.38	27.98	30.31	31.3	27.93	28.43	8.59	14.13	13.84
08:00	1290	21.5	5.07	33.62		3120	30.41	28	30.34	31.33	27.97	28.47	8.46	14.15	13.87
10:00	1410	23.5	5.10	33.65		3122	30.47	28.04	30.41	31.35	28	28.48	8.46	14.18	13.97
12:00	1530	25.5	5.10	33.65		3124	30.49	28.05	30.44	31.4	28.01	28.5	8.48	14.21	13.86
14:00	1650	27.5	5.12	33.67		3126	30.47	28.05	30.41	41.39	28.03	28.5	8.48	14.7	13.89
16:00	1770	29.5	5.12	33.67		3128	30.47	28.05	30.41	41.37	28.05	28.49	8.49	14.2	13.89
18:00	1890	31.5	5.13	33.68		3130	30.48	28.05	30.43	31.38	28.06	28.51	8.49	14.21	14.03
20:00	2010	33.5	0.15	28.7		3132	30.5	28.08	30.43	31.41	28.08	28.52	8.51	14.23	14.09
22:00	2130	35.5	-0.24	28.31		3134	30.53	28.1	30.46	31.43	28.08	28.55	8.53	14.24	14.16
00:00	2250	37.5	4.60	33.15		3136	30.55	28.12	30.49	31.45	28.11	28.57	8.54	14.25	14.2
02:00	2370	39.5	4.76	33.31		3138	30.56	28.13	30.5	31.46	28.11	28.59	8.57	14.27	14.23
04:00	2490	41.5	4.77	33.32		3140	30.57	28.14	30.51	31.45	28.12	28.6	8.57	14.28	14.24
06:00	2610	43.5	4.94	33.49		3142	30.6	28.14	30.5	31.46	28.12	28.6	8.58	14.29	14.25
08:00	2730	45.5	4.99	33.54		3144	30.28	27.9	30.49	31.48	28.13	28.68	8.49	14.3	14.32
10:00	2850	47.5	5.04	33.59		3146	29.92	27.57	30.26	31.33	28.13	28.65	8.61	14.31	13.23
12:00	2970	49.5	5.07	33.62		3148	30.35	27.87	29.72	31	28.33	28.47	8.28	14.13	13.19
14:00	3090	51.5	5.12	33.67		3150	30.93	28.06	29.89	31.18	28.47	28.68	8.31	14.13	13.26
16:00	3210		5.12	33.67		3152	30.19	28.08	30.32	31.26	28.5	28.68	8.36	14.19	18.32
18:00	3330		5.13	33.68		3154	30.27	28.09	30.32	31.3	28.36	28.59	8.39	14.21	13.68

Test 2	Pumping BH3-39	CRT		RWL=28.55m			OBH-MH3-1	OBH-MH3-2	OBH-MH3-3	OBH-MH3-4	OBH-MH3-5	OBH-MH3-6B	OBH-MH3-8	BH-MH3-10	OBH-MH2-3
Real Time		Elapsed time (hr)	Drawdown BH3-9	W/ Level BH3-9			40 m W	40 m N	40 m E	40 m S	80 m E	80 m S	160 m W	260 m W	840 m W
20:00	3450		0.15	28.7		3156	30.35	28.11	30.31	31.33	28.04	28.6	8.43	14.23	14.11
22:00	3570		-0.24	28.31		3158	30.46	28.12	30.29	31.37	28.11	28.61	8.51	14.27	14.69
00:00	3690		4.60	33.15		3160	30.46	28.13	30.29	31.41	28.13	28.61	8.64	14.29	13.13
02:00	3810		4.76	33.31		3162	30.49	28.14	30.3	31.42	28.14	28.63	8.66	14.3	13.15
04:00	3930		4.77	33.32		3164	30.49	28.15	30.37	31.46	28.16	28.65	8.7	14.28	13.25
06:00	4050		4.94	33.49		3166	30.64	28.14	30.38	31.48	28.17	28.67	8.71	14.29	13.28
08:00	4170		4.99	33.54		3168	30.69	28.27	30.59	31.56	28.2	28.68	8.73	14.41	13.82
10:00	4290		5.04	33.59		3170	30.74	28.31	30.61	31.6	28.12	28.7	8.76	14.42	13.91
12:00	4410		5.12	33.67		3172	30.76	28.33	30.67	31.64	28.25	28.73	8.76	14.45	14.01
14:00	4530		5.12	33.67		3174	30.8	28.37	30.7	31.66	28.26	28.72	8.78	14.46	14.07
16:00	4650		5.14	33.69		3176	30.76	28.48	30.75	31.64	28.28	28.73	8.8	14.51	14.09
18:00	4770		5.14	33.69		3178	30.75	28.34	30.69	31.65	28.29	28.73	8.8	14.54	14.1
20:00	4890		5.14	33.69		3180	30.75	28.35	30.7	31.66	28.29	28.73	8.8	14.5	14.2
22:00	5010		5.16	33.71		3182	30.74	28.33	30.71	31.67	28.3	28.73	8.81	14.51	14.26
00:00	5130		5.18	33.73		3184	30.72	28.37	30.71	31.68	28.3	28.74	8.84	14.53	14.29
02:00	5250		5.19	33.74		3186	30.72	28.39	30.74	31.71	28.32	28.76	8.83	14.54	14.34
04:00	5370		5.20	33.75		3188	30.75	28.4	30.76	31.72	28.33	28.76	8.84	14.55	14.37
06:00	5490		5.23	33.78		3190	30.79	28.42	30.76	31.71	28.36	28.79	8.84	14.56	14.43
08:00	5610		5.27	33.82		3192	30.82	28.45	30.78	31.73	28.39	28.82	8.86	14.57	14.5
10:00	5730		5.28	33.83		3194	30.85	28.47	30.79	31.74	28.39	28.85	8.87	14.58	14.55
12:00	5850		5.31	33.86		3196	30.86	28.48	30.81	31.76	28.4	28.85	8.88	14.6	14.62
14:00	5970		5.32	33.87		3198	30.87	28.5	30.82	31.78	28.42	28.87	8.89	14.61	14.67
16:00	6090		5.32	33.87		3200	30.89	28.5	30.83	31.8	28.42	28.88	8.9	14.63	14.72
18:00	6210		5.32	33.87		3202	30.89	28.5	30.85	31.8	28.44	28.9	8.91	14.64	14.73

Test 2	Pumping BH3-39	CRT		RWL=28.55m			OBH-MH3-1	OBH-MH3-2	OBH-MH3-3	OBH-MH3-4	OBH-MH3-5	OBH-MH3-6B	OBH-MH3-8	BH-MH3-10	OBH-MH2-3
Real Time		Elapsed time (hr)	Drawdown BH3-9	W/ Level BH3-9			40 m W	40 m N	40 m E	40 m S	80 m E	80 m S	160 m W	260 m W	840 m W
20:00	6330		4.70	33.25		3204	30.89	28.48	30.83	31.79	28.45	28.89	8.92	14.64	14.74
22:00	6450		0.23	28.78		3206	30.92	28.53	30.86	31.83	28.47	28.9	8.92	14.67	14.81
00:00	6570		1.01	29.56		3208	30.92	28.49	30.86	31.85	28.48	28.9	8.93	14.69	14.88
02:00	6690		4.71	33.26		3210	30.94	28.53	30.87	31.83	28.47	28.92	8.9	14.69	14.88
04:00	6810		4.74	33.29		3212	30.95	28.49	30.89	31.85	28.48	28.93	8.92	14.7	15.1
06:00	6930		4.76	33.31		3214	30.96	28.53	30.89	31.87	28.5	28.93	8.93	14.7	15.18
08:00	7050		4.79	33.34		3216	30.96	28.55	30.9	31.89	28.52	28.93	8.96	14.72	15.21
10:00	7170		4.85	33.4		3218	30.98	28.56	30.93	31.9	28.53	28.94	8.98	14.73	14.83
12:00	7290		4.90	33.45		3220	31.01	28.56	30.94	31.9	28.53	28.95	8.98	14.75	14.85
14:00	7410		4.93	33.48		3222	31.01	28.57	30.95	31.9	28.54	28.95	9	14.76	14.85
16:00	7530		4.95	33.5		3224	31.02	28.55	30.96	31.91	28.54	28.96	9.01	14.77	14.86
18:00	7650		4.97	33.52		3226	31.03	28.58	30.97	31.92	28.56	28.97	9.02	14.77	14.87
20:00	7770		4.99	33.54		3228	31.03	28.6	30.97	31.93	28.57	28.97	9.03	14.78	14.88
22:00	7890		5.02	33.57		3230	31.04	28.61	30.98	31.92	28.58	28.98	9.04	14.79	14.86
00:00	8010		5.04	33.59		3232	31.04	28.62	30.98	31.94	28.58	28.98	9.05	14.8	14.89
02:00	8130		5.05	33.6		3234	31.07	28.63	31	31.96	28.6	28.98	9.06	14.81	14.93
04:00	8250		5.07	33.62		3236	31.08	28.64	31.01	31.98	28.6	28.99	9.07	14.81	14.81
06:00	8370		5.08	33.63		3238	31.09	28.66	31.01	31.99	28.62	28.99	9.09	14.82	14.83
08:00	8490		5.09	33.64		3240	31.1	28.66	31.01	31.99	28.62	29	9.09	14.83	14.83
10:00	8610		5.11	33.66		3242	31.1	28.67	31.02	31.99	28.63	29.02	9.1	14.83	14.84
12:00	8730		5.12	33.67		3244	31.1	28.67	31.02	32	28.63	29.02	9.1	14.83	14.84
14:00	8850		5.14	33.69		3246	31.11	28.67	31.03	32	28.64	29.03	9.11	14.84	14.85
16:00	8970		5.14	33.69		3248	31.11	28.67	31.03	32	28.64	29.04	9.11	14.84	14.85
18:00	9090		5.14	33.69		3250	31.1	28.66	31.03	32.01	28.65	29.07	9.12	14.83	13.32

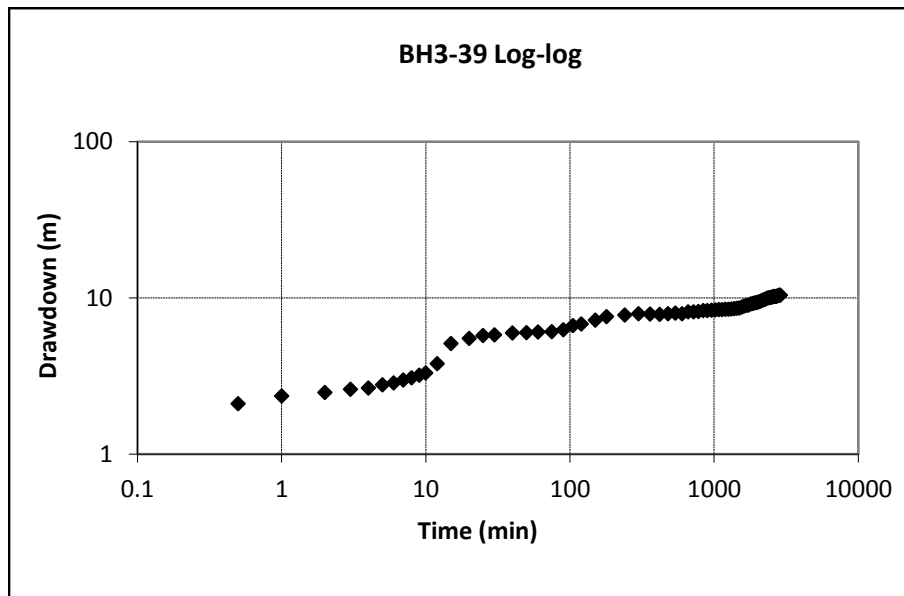
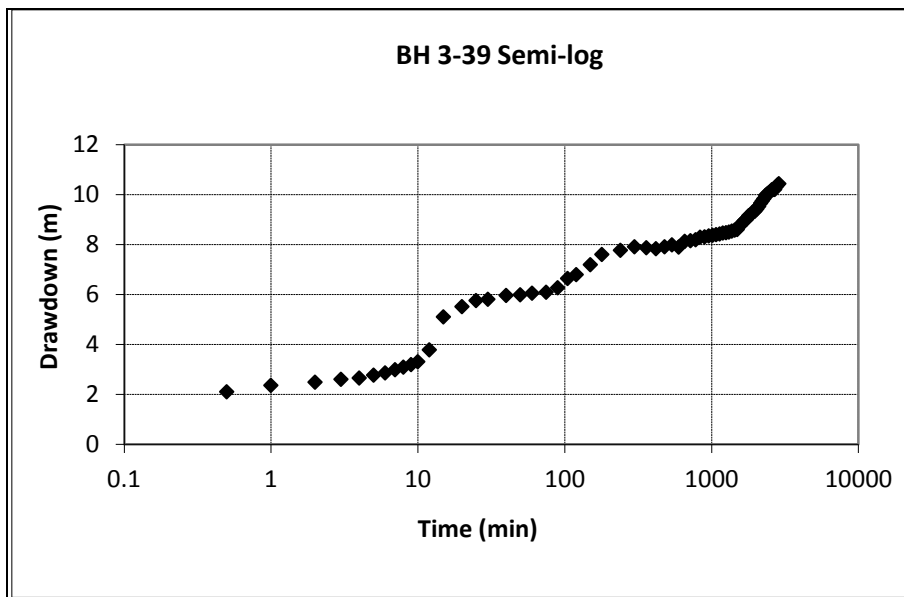
Test 2	Pumping BH3-39	CRT		RWL=28.55m			OBH-MH3-1	OBH-MH3-2	OBH-MH3-3	OBH-MH3-4	OBH-MH3-5	OBH-MH3-6B	OBH-MH3-8	BH-MH3-10	OBH-MH2-3
Real Time		Elapsed time (hr)	Drawdown BH3-9	W/ Level BH3-9			40 m W	40 m N	40 m E	40 m S	80 m E	80 m S	160 m W	260 m W	840 m W
20:00	9210		5.15	33.7		3252	31.1	28.67	31.02	31.98	28.66	29.11	9.12	14.83	13.7
22:00	9330		5.18	33.73		3254	31.07	28.68	31.02	31.97	28.67	29.11	9.13	14.84	13.79
00:00	9450		5.20	33.75		3256	31.08	28.69	30.03	31.97	28.67	29.12	9.14	14.85	13.84
02:00	9570		5.23	33.78		3258	31.08	28.7	30.03	31.98	28.66	29.14	9.15	14.83	14.25
04:00	9690		5.25	33.8		3260	31.1	28.71	31.05	32.01	28.66	29.16	9.13	14.83	14.29
06:00	9810		5.25	33.8		3262	31.12	28.71	31.06	32.02	28.69	29.21	9.13	14.83	14.29
08:00	9930		5.25	33.8		3264	31.12	28.69	31.06	32.02	28.69	29.23	9.13	14.82	14.28
10:00	10050		5.25	33.8		3266	30.96	28.62	30.98	31.92	28.68	29.23	9.09	14.22	14.31
12:00	10170		5.27	33.82		3268	30.85	28.62	30.88	31.56	28.68	29.23	8.96	14.1	14.37
14:00	10290		5.28	33.83		3270	30.7	28.63	30.85	31.5	28.69	29.24	8.93	14.02	14.48
16:00	10410		5.30	33.85		3272	30.69	28.63	30.81	31.47	28.69	29.24	8.88	13.91	14.62
18:00	10530		5.32	33.87		3274	30.66	28.63	30.79	31.3	28.7	29.23	8.86	13.82	14.61
20:00	10650		5.32	33.87		3276	30.6	28.62	30.71	31.27	28.69	29.22	8.87	13.74	14.63
22:00	10770		5.33	33.88		3278	30.55	26.62	30.68	31.2	28.69	29.22	8.81	13.74	14.66
00:00	10890		5.33	33.88		3280	30.51	28.6	30.62	31.13	28.69	29.21	8.82		
02:00	11010		5.34	33.89		3282									
04:00	11130		5.34	33.89		3284									
06:00	11250		5.34	33.89		3286									
08:00	11370		5.34	33.89		3288									
10:00	11490		5.34	33.89											
12:00	11610		5.35	33.9											
14:00	11730		5.35	33.9											
16:00	11850		5.36	33.91											
18:00	11970		5.39	33.94											

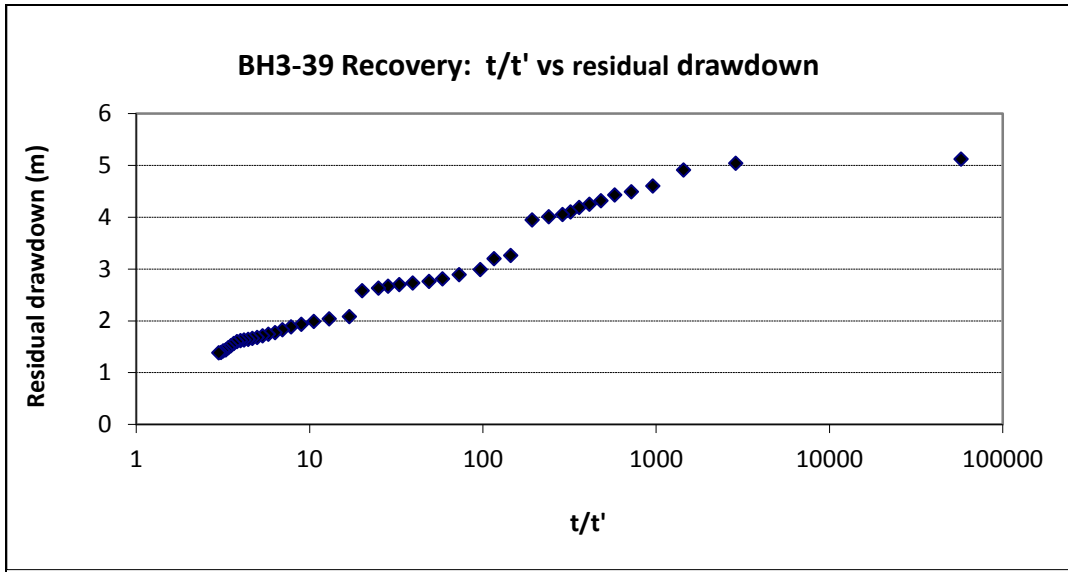
Test 2	Pumping BH3-39	CRT		RWL=28.55m			OBH-MH3-1	OBH-MH3-2	OBH-MH3-3	OBH-MH3-4	OBH-MH3-5	OBH-MH3-6B	OBH-MH3-8	BH-MH3-10	OBH-MH2-3
Real Time		Elapsed time (hr)	Drawdown BH3-9	W/ Level BH3-9			40 m W	40 m N	40 m E	40 m S	80 m E	80 m S	160 m W	260 m W	840 m W
20:00	12090		5.39	33.94											
22:00	12210		5.40	33.95											
00:00	12330		5.40	33.95											
02:00	12450		5.41	33.96											
04:00	12570		5.41	33.96											
06:00	12690		5.41	33.96											
08:00	12810		5.42	33.97											
10:00	12930		5.42	33.97											
12:00	13050		5.43	33.98											
14:00	13170		5.44	33.99											
16:00	13290		5.45	34											
18:00	13410		5.46	34.01											
20:00	13530		5.46	34.01											
22:00	13650		5.45	34											
00:00	13770		5.45	34											
02:00	13890		5.46	34.01											
04:00	14010		5.46	34.01											
06:00	14130		5.46	34.01											
08:00	14250		5.45	34											
10:00	14370		5.46	34.01											
12:00	14490		5.46	34.01											
14:00	14610		5.46	34.01											
16:00	14730		5.46	34.01											
18:00	14850		5.46	34.01											

Test 2	Pumping BH3-39	CRT		RWL=28.55m			OBH-MH3-1	OBH-MH3-2	OBH-MH3-3	OBH-MH3-4	OBH-MH3-5	OBH-MH3-6B	OBH-MH3-8	BH-MH3-10	OBH-MH2-3
Real Time		Elapsed time (hr)	Drawdown BH3-9	W/ Level BH3-9			40 m W	40 m N	40 m E	40 m S	80 m E	80 m S	160 m W	260 m W	840 m W
20:00	14970		5.45	34											
22:00	15090		5.45	34											
00:00	15210		5.46	34.01											
02:00	15330		5.46	34.01											
04:00	15450		5.46	34.01											
06:00	15570		5.46	34.01											
08:00	15690		5.46	34.01											
10:00	15810		5.46	34.01											
12:00	15930		5.46	34.01											
14:00	16050		0.10	28.65											
16:00	16170		3.91	32.46											
18:00	16290		3.75	32.3											
20:00	16410		4.90	33.45											
22:00	16530		4.97	33.52											
00:00	16650		5.02	33.57											
02:00	16770		5.04	33.59											
04:00	16890		5.06	33.61											
06:00	17010		5.09	33.64											
08:00	17130		5.13	33.68											
10:00	17250		5.16	33.71											
12:00	17370		5.16	33.71											
14:00	17490		5.17	33.72											
16:00	17610		5.17	33.72											
18:00	17730		5.14	33.69											

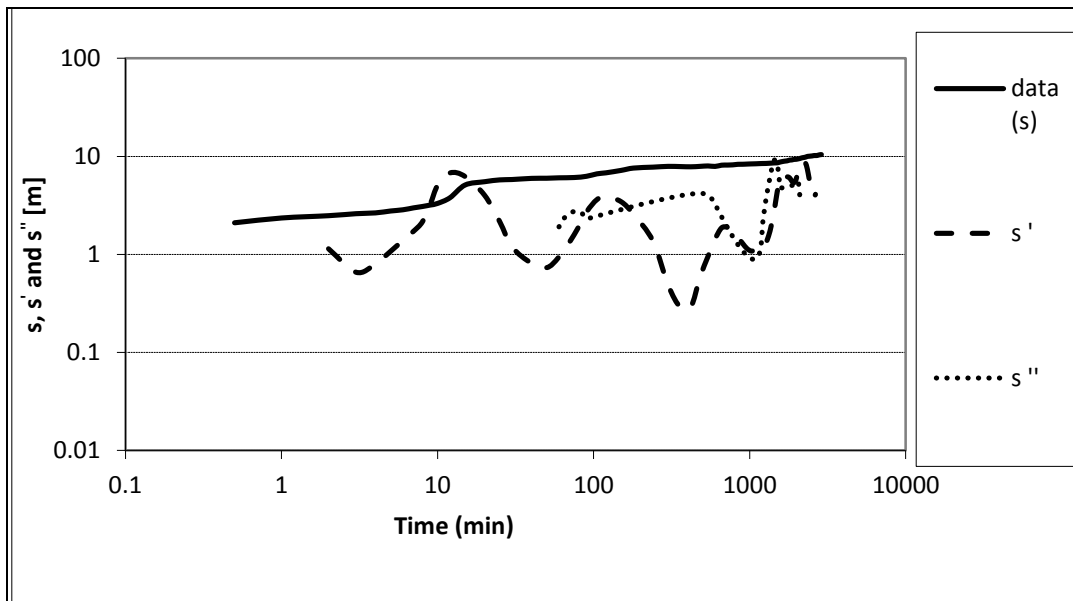
Test 2	Pumping BH3-39	CRT		RWL=28.55m			OBH- MH3-1	OBH- MH3-2	OBH- MH3-3	OBH- MH3-4	OBH- MH3-5	OBH- MH3-6B	OBH- MH3-8	BH- MH3-10	OBH- MH2-3
Real Time		Elapsed time (hr)	Drawdown BH3-9	W/ Level BH3-9			40 m W	40 m N	40 m E	40 m S	80 m E	80 m S	160 m W	260 m W	840 m W
20:00	17850		5.14	33.69											
22:00	17970		5.14	33.69											
00:00	18090		5.13	33.68											
02:00	18210		5.13	33.68											
04:00	18330		5.15	33.7											
06:00	18450		5.15	33.7											
08:00	18570		5.15	33.7											
10:00	18690		5.16	33.71											
12:00	18810		5.17	33.72											
14:00	18930		5.18	33.73											
16:00	19050		5.19	33.74											
18:00	19170		5.17	33.72											
20:00	19290		5.12	33.67											
22:00	19410		5.13	33.68											
00:00	19530		5.17	33.72											
02:00	19650		5.25	33.8											

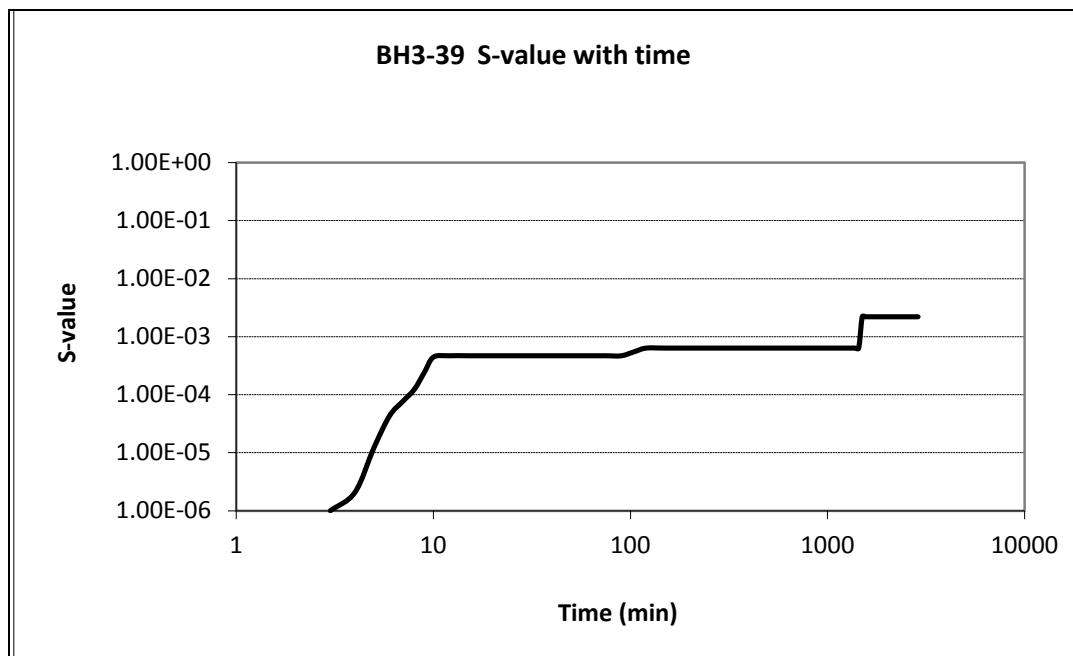
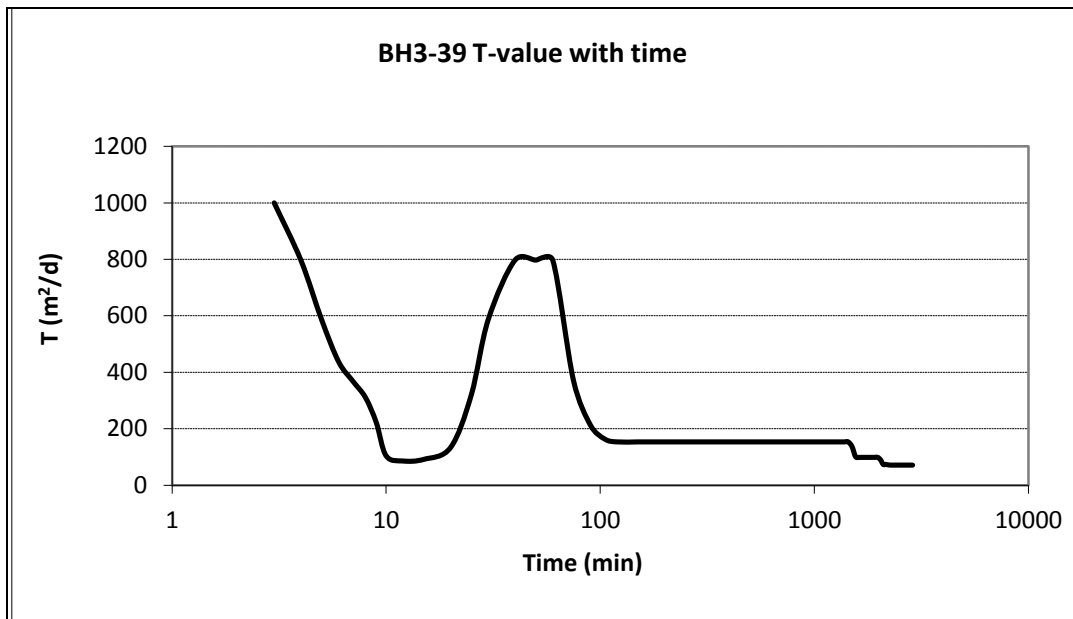
BH3-39 Diagnostic Plots





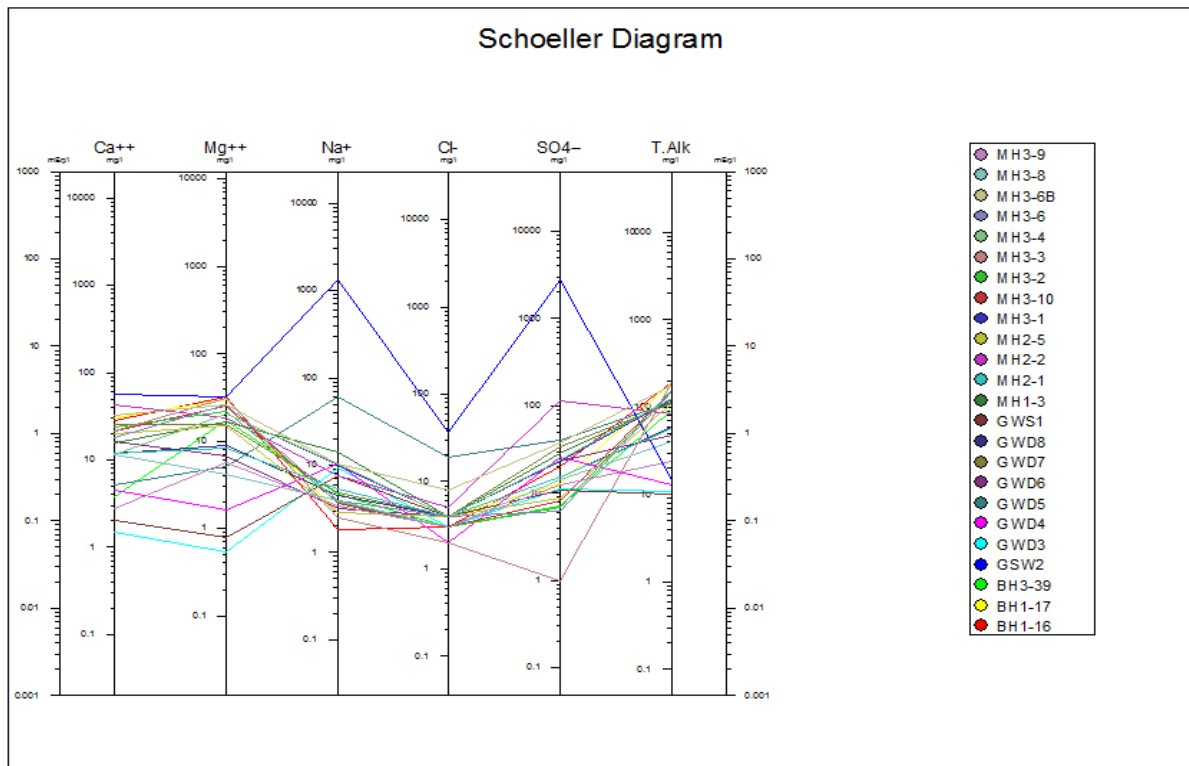
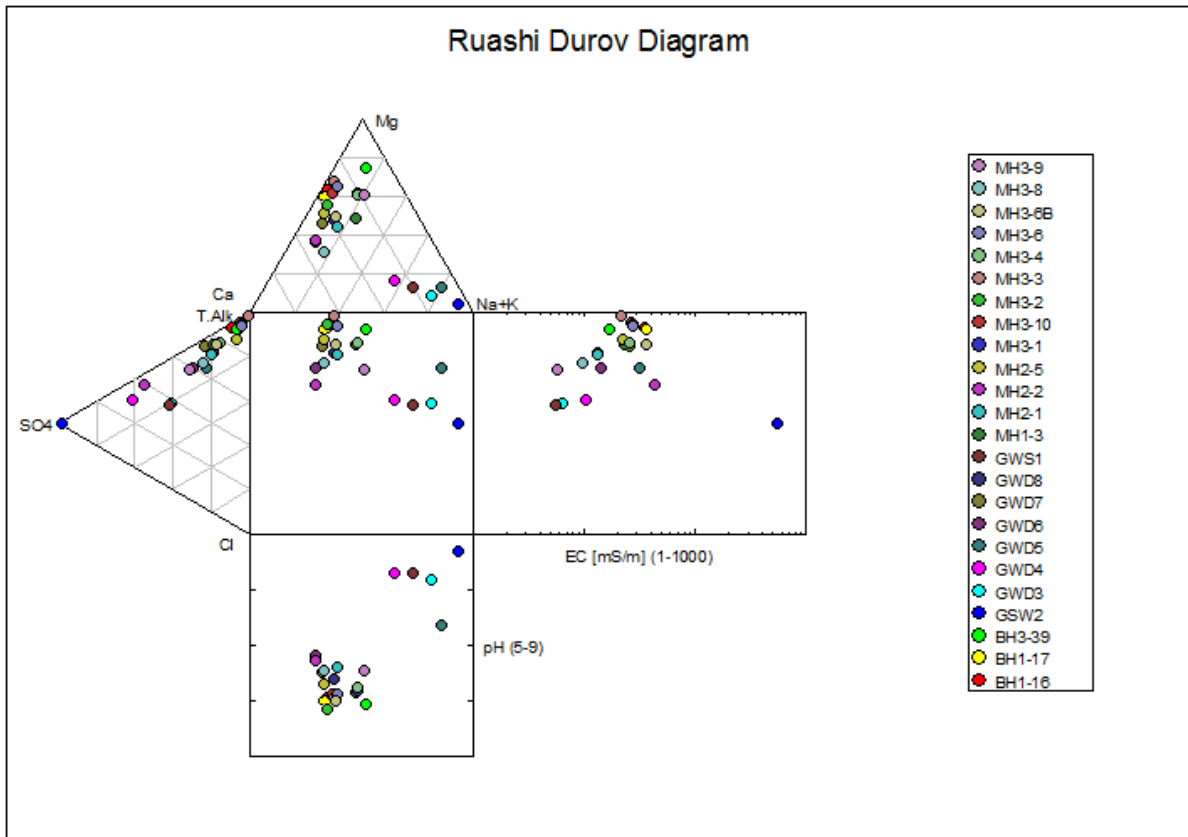
BH3-39 derivative Plots



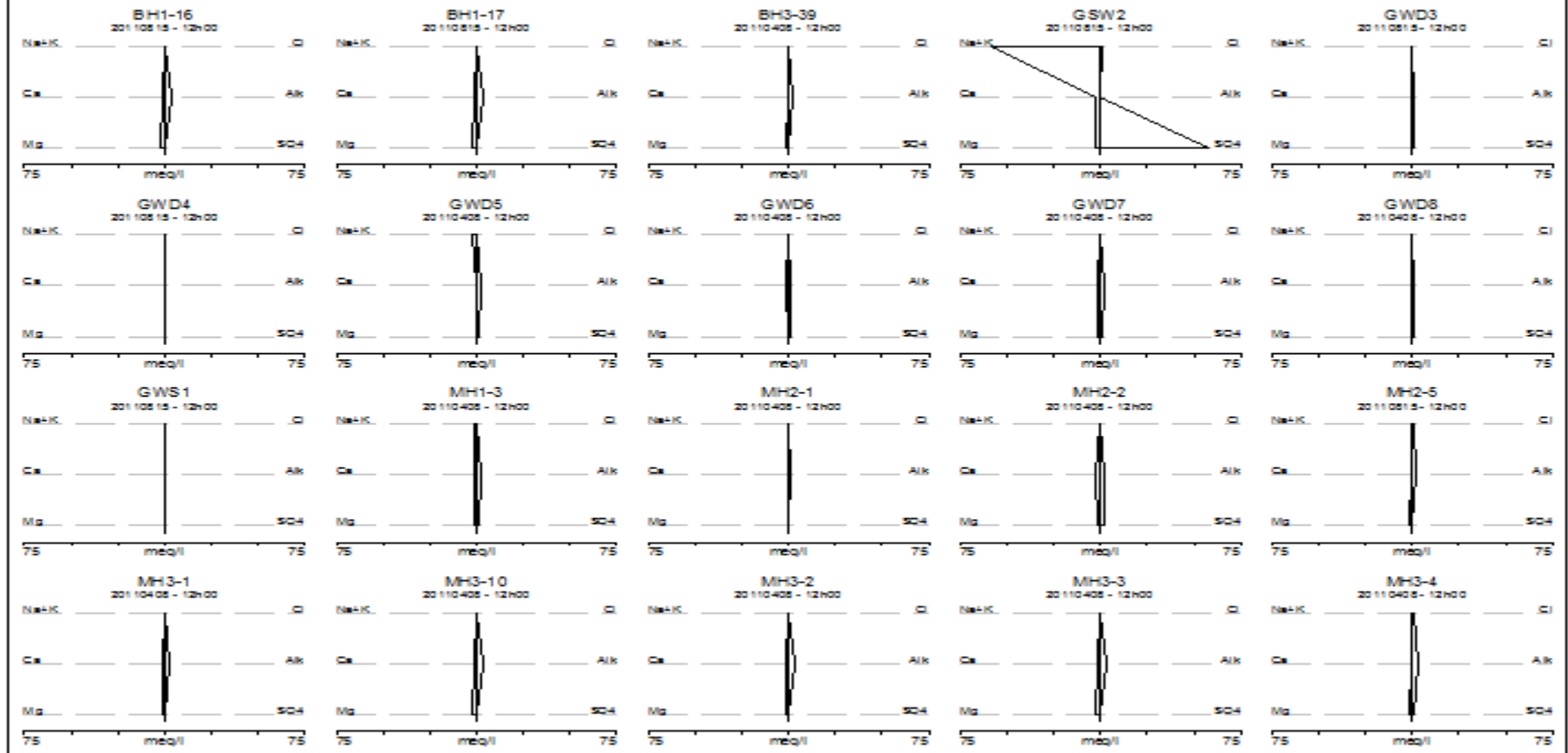


Appendix C

Hydrochemistry data



STIFF Diagrams



Appendix D

Numerical groundwater flow model data

Simulated vs. observed hydraulic heads

Date	MH1-14 modelled	MH1-14 observed	MH1-15 modelled	MH1-15 observed	MH1-16 modelled	MH1-16 observed
5-Jan-11	1228.431		1231.352		1229.63	1228.33
10-Jan-11	1228.842		1231.677		1230.04	1228.74
15-Jan-11	1228.84		1231.674		1230.03	1228.74
20-Jan-11	1228.747		1231.583		1229.94	1228.65
25-Jan-11	1228.635		1231.473		1229.83	1228.54
30-Jan-11	1228.523		1231.362		1229.71	1228.42
4-Feb-11	1228.418		1231.258		1229.61	1228.32
9-Feb-11	1228.324		1231.164		1229.51	1228.22
14-Feb-11	1228.238		1231.079		1229.43	1228.14
19-Feb-11	1228.16		1231.001		1229.35	1228.06
24-Feb-11	1227.93		1230.785		1229.12	1227.83
1-Mar-11	1227.792		1230.649		1228.98	1227.69
6-Mar-11	1227.988	1227.694	1230.817		1229.18	1227.89
11-Mar-11	1228.036	1227.94	1230.865		1229.22	1227.94
16-Mar-11	1228.045	1228.534	1230.874		1229.23	1227.95
21-Mar-11	1228.038	1227.734	1230.867		1229.23	1227.94
26-Mar-11	1228.028	1227.414	1230.856		1229.21	1227.93
31-Mar-11	1228.015	1227.287	1230.843		1229.20	1227.92
5-Apr-11	1227.125	1226.83	1230.006		1228.33	1227.03
10-Apr-11	1226.648	1226.97	1229.531		1227.85	1226.55
15-Apr-11	1226.305	1227.237	1229.189		1227.51	1226.21
20-Apr-11	1226.02	1225.08	1228.904		1227.22	1225.92
25-Apr-11	1225.776	1224.883	1228.66		1226.98	1225.68
30-Apr-11	1226	1224.908	1228.843		1227.20	1225.90
5-May-11	1226.014	1225.217	1228.856		1227.22	1225.91
10-May-11	1225.978	1225.3	1228.82		1227.18	1225.88
15-May-11	1225.927	1225.384	1228.769		1227.13	1225.83
20-May-11	1225.868	1225.467	1228.71		1227.07	1225.77
25-May-11	1225.803	1225.551	1228.646		1227.01	1225.70
30-May-11	1225.385	1225.698	1228.255		1226.59	1225.29
4-Jun-11	1225.165	1225.841	1228.035		1226.37	1225.07
9-Jun-11	1224.99	1225.935	1227.86		1226.19	1224.89
14-Jun-11	1224.84	1225.98	1227.71		1226.04	1224.74
19-Jun-11	1224.703	1225.957	1227.573		1225.91	1224.60
24-Jun-11	1224.575	1225.89	1227.446		1225.78	1224.48
29-Jun-11	1224.458	1225.824	1227.328		1225.66	1224.36
4-Jul-11	1224.345	1226.097	1227.215		1225.55	1224.25
9-Jul-11	1224.082	1226.169	1226.966		1225.05	1223.98
14-Jul-11	1223.925	1225.601	1226.809		1224.82	1223.83

19-Jul-11	1223.806	1224.863	1226.689	1227.067	1224.65	1223.71
24-Jul-11	1223.694	1224.891	1226.578	1227.031	1224.51	1223.59
29-Jul-11	1223.591	1224.207	1226.474	1226.824	1224.38	1223.49
3-Aug-11	1223.495	1223.797	1226.379	1226.624	1224.27	1223.40
8-Aug-11	1223.774	1223.737	1226.626	1226.582	1223.99	1223.67
13-Aug-11	1223.855	1223.663	1226.704	1226.557	1223.87	1223.76
18-Aug-11	1223.889	1223.558	1226.737	1226.566	1223.78	1223.79
23-Aug-11	1223.896	1223.485	1226.744	1226.577	1223.70	1223.80
28-Aug-11	1223.893	1223.58	1226.74	1226.598	1223.62	1223.79
2-Sep-11	1223.883	1223.674	1226.73	1226.619	1223.54	1223.78
7-Sep-11	1223.545	1223.559	1226.419	1226.555	1223.47	1223.45
12-Sep-11	1223.416	1223.387	1226.29	1226.469	1223.41	1223.32
17-Sep-11	1223.328	1223.214	1226.202	1226.383	1223.34	1223.23
22-Sep-11	1223.255	1223.042	1226.129	1226.296	1223.28	1223.16
27-Sep-11	1223.191	1222.869	1226.065	1226.21	1223.22	1223.09
2-Oct-11	1222.654	1222.697	1225.571	1226.124	1223.16	1222.55
7-Oct-11	1222.446	1222.577	1225.363	1225.984	1223.10	1222.35
12-Oct-11	1222.301	1222.277	1225.217	1225.774	1223.04	1222.20
17-Oct-11	1222.185	1222.31	1225.102	1225.961	1222.99	1222.09
22-Oct-11	1222.085	1222.216	1225.001	1225.93	1222.94	1221.99
27-Oct-11	1221.995	1222.037	1224.911	1225.728	1222.89	1221.90
1-Nov-11	1221.914	1221.837	1224.83	1225.483	1222.84	1221.81
6-Nov-11	1221.838	1221.844	1224.754	1225.362	1222.79	1221.74
11-Nov-11	1221.769	1221.902	1224.685	1225.271	1222.98	1221.67
16-Nov-11	1221.702	1221.961	1224.618	1225.18	1223.13	1221.60
21-Nov-11	1222.211	1222.015	1225.115	1225.096	1223.25	1222.11
26-Nov-11	1222.444	1222.07	1225.346	1225.012	1223.36	1222.34
1-Dec-11	1222.616	1222.216	1225.518	1224.913	1223.46	1222.52
6-Dec-11	1222.76	1222.33	1225.661	1225.789	1223.56	1222.66
11-Dec-11	1222.885	1222.422	1225.787	1225.803	1223.64	1222.79
16-Dec-11	1222.998	1222.514	1225.9	1225.817	1223.72	1222.90
21-Dec-11	1223.102	1222.605	1226.003	1225.832	1223.80	1223.00
26-Dec-11	1223.196	1222.697	1226.098	1225.846	1223.87	1223.10
31-Dec-11	1223.285	1222.788	1226.186	1225.86	1223.94	1223.19
5-Jan-12	1223.366	1222.88	1226.268	1225.875	1224.00	1223.27
10-Jan-12	1223.442	1222.972	1226.343	1225.889	1224.06	1223.34
15-Jan-12	1223.513	1223.315	1226.414	1226.111	1224.11	1223.41
20-Jan-12	1223.58	1223.557	1226.481	1226.065	1224.17	1223.48
25-Jan-12	1223.641	1223.643	1226.543	1226.281	1224.21	1223.54
30-Jan-12	1223.7	1223.138	1226.602	1225.893	1224.26	1223.60
4-Feb-12	1223.756	1223.241	1226.657	1226.021	1224.30	1223.66
9-Feb-12	1223.808	1223.344	1226.71	1226.15	1224.35	1223.71
14-Feb-12	1223.858	1223.447	1226.759	1226.278	1224.39	1223.76
19-Feb-12	1223.904	1223.551	1226.806	1226.407	1224.43	1223.80

24-Feb-12	1223.949	1223.516	1226.851	1226.244	1224.46	1223.85
29-Feb-12	1223.991	1223.732	1226.893		1224.50	1223.89
5-Mar-12	1224.032	1223.193	1226.934		1224.53	1223.93
10-Mar-12	1224.07	1223.298	1226.972		1224.56	1223.97
15-Mar-12	1224.106	1223.08	1227.009		1224.59	1224.01
20-Mar-12	1224.141	1223.073	1227.043		1224.62	1224.04
25-Mar-12	1224.174	1223.847	1227.077		1224.65	1224.07
30-Mar-12	1224.207	1223.543	1227.109		1224.67	1224.11
4-Apr-12	1224.237	1223.43	1227.139		1224.70	1224.14
9-Apr-12	1224.267	1223.717	1227.169		1224.72	1224.17
14-Apr-12	1224.295	1223.615	1227.197		1224.75	1224.20
19-Apr-12	1224.322	1223.514	1227.225		1224.77	1224.22
24-Apr-12	1224.348	1223.412	1227.251		1224.79	1224.25
29-Apr-12	1224.374	1223.311	1227.276		1224.81	1224.27
4-May-12	1224.398	1223.21	1227.301		1224.83	1224.30
9-May-12	1224.36	1223.9	1227.324		1224.29	1224.32
14-May-12	1224.444	1223.35	1227.347		1224.01	1224.34
19-May-12	1223.895	1223.18	1226.81		1223.79	1223.80
24-May-12	1223.613	1223.12	1226.529		1223.61	1223.51
29-May-12	1223.401	1223.04	1226.317		1223.44	1223.30
3-Jun-12	1223.216	1222.95	1226.134		1223.29	1223.12
8-Jun-12	1223.054	1222.78	1225.971		1223.16	1222.95
13-Jun-12	1222.906	1222.59	1225.824		1223.03	1222.81
18-Jun-12	1222.771	1222.52	1225.688		1222.91	1222.67
23-Jun-12	1222.644	1222.73	1225.561		1222.80	1222.54
28-Jun-12	1222.527		1225.444		1222.69	1222.43

Abstract

This dissertation describes the results of field based investigations on groundwater flow at Ruashi Mine located in Katanga Province of Democratic Republic of Congo (DRC). The core objectives of the study were to simulate groundwater flow, estimate flow into the pits and ultimately design a dewatering strategy for the mine. In order to understand how groundwater flows into and through the mine, a detailed conceptual hydrogeological model was constructed as framework for numerical groundwater flow modelling. The numerical model was used simulate groundwater flow and predict pit inflow volumes.

At the time of this research, mining at Ruashi was being carried out in three pits that are expected to reach terminal depth of 180 metres below ground level (mbgl) in 16 years of continued mining. The mine is located along a faulted overturned syncline composed of composed of Siltstones, Argillites, Sandstones and Shales and covered by Laterite. Based on aquifer hydraulic testing results, the transmissivity of the shallow aquifer was estimated to be $10 \text{ m}^2/\text{d}$. The specific yield for the deep aquifer was estimated to be 1×10^{-5} . The Chloride Mass Balance Method was used to estimate recharge to the groundwater system as 280 mm per annum (14% of Mean Annual Precipitation). Water levels vary from 1.02 to 62.5 mbgl. The general groundwater type was analysed to be calcium-magnesium-bicarbonate (Ca-Mg- HCO_3), typical of young groundwater.

The numerical groundwater flow model area is 15.7 km^2 and comprises 5 layers, 17 240 elements and 10 614 nodes. The model results indicated that groundwater flow to the pits is unlikely to exceed $42\,000 \text{ m}^3/\text{d}$. Using the pumping capacity ($15\,000 \text{ m}^3/\text{d}$) for year 2012, a maximum water level drawdown of 55 m was estimated. However, the numerical model demonstrated that the existing pumping boreholes can be augmented by an additional set of 16 boreholes pumping $2\,000 \text{ m}^3/\text{d}$ per borehole. This pumping rate can lower the groundwater level to about 1 188 mamsl which is about two meters below pit terminal elevation.

This study made significant contribution to understanding the hydrogeological properties of aquifers at the mine. The aquifer hydraulic testing data was used to estimate aquifer hydraulic parameters. However based on the field evidence, it is suggested that Packer testing could improve the estimates of aquifer hydraulic parameters for each aquifer. The numerical model demonstrated the typical aquifer response to different pumping scenarios. The different pumping scenarios were run in order to determine the optimum pumping rates to dewater the mine. **Keywords: Dewatering strategy, groundwater flow, conceptual hydrogeological model, recharge, numerical model.**

Opsomming

Die skripsie beskryf veldproewe om die grondwaterstelsel by die Ruashi-myn in die Katanga Provinsie van die Demokratiese Republiek van die Kongo (DRK) te bepaal. Die hoofdoelwitte van die studie was om 'n ontwateringstrategie vir die myn te berei wat afkomstig is van die veldproewedata. 'n Konsepuele grondwatermodel is opgestel om die grondwatergradiënt om die myn te bepaal en as onderbou te dien vir die numeriese vloei-model, wat grondwatervloei en volumes kan bepaal wat oor tyd in die oopgroefmyn invloei.

Gedurende die ondersoek het mynbou-aktiwiteite plaasgevind in drie oopgroefmynareas. Die finale diepte van die oopgroefareas gaan 180 m onder grondoppervlak wees na 16 jaar se ontginning. Die mynontwikkeling vind plaas oor 'n geologiese verskuiwing wat bestaan uit 'n omgevoerde sinklien wat bestaan uit moddersteen, gelaagde moddersteen, sandsteen en skalies wat bedek is met lateriete. Gebaseer op die akwifertoetse is die transmissiwiteit van die oppervlakakwifereer die hoogste ($10 \text{ m}^2/\text{d}$). Die spesifieke lewering (S_s) van die diep akwifereerstelsel is 1×10^{-5} . Die watertafelaanvulling is bepaal met behulp van die chloriedmetode en is ongeveer 280 mm per jaar of 14% van die gemiddelde jaarlikse reënval. Watervlakke varieer van 1.02 tot 62.5 m van die grondoppervlak. Die algemene grondwaterkarakter is kalsium-magnesiumbikarbonaat (Ca-Mg-HCO_3), wat verteenwoordigend is van 'n jonger grondwaterstelsel.

Die numeriese grondwatervloei-model beslaan 'n area van 15.7 km^2 en bevat vyf lae, 17 240 elemente en 10 614 nodusse. Die model se resultaat toon aan dat die invloei tempo in die oopgroefarea $42\,000 \text{ m}^3/\text{d}$ sal oorskrei. Die beskikbare pompkapasiteit op die mynarea is $15\,000 \text{ m}^3/\text{d}$ (2012) met 'n maksimum geprojekteerde verlaging in watervlak van 55 m. Die numeriese model het wel gedemonstreer dat die byvoeging van 'n verdere 16 ontwateringsgate ($2\,000 \text{ m}^3/\text{d}$) die gewenste effek sal behaal op die stelsel. Dit sal lei tot 'n watervlakverlaging tot en met 1 188 meter bo gemiddelde seevlak wat twee meter onder die finale oopgroefmynvloer sal wees.

Hierdie studie het 'n noemenswaardige bydrae gelewer tot die kennis van die gedrag van die grondwaterstelsel by die myn. Akwifereer-hidroliese toetse is uitgevoer, maar selektiewe toetse per akwifereerstelsel sou nuttig wees. Die numeriese model kan uitgebrei word om verskillende gevallestudies op die myn-akwifereer te doen, wat die optimalisering van ontwateringstrategieë tot gevolg kan hê.

Sleuteltermes: Ontwateringstrategie, grondwatervloei-model, konsepuele grondwatermodel, grondwateraanvulling, numeriese model.